SURFACE-TO-SUBSURFACE CORRELATION AND

LITHOSTRATIGRAPHIC FRAMEWORK OF THE

CANEY SHALE (INCLUDING THE "MAYES"

FORMATION) IN ATOKA, COAL, HUGHES,

JOHNSTON, PITTSBURG, AND PONTOTOC

COUNTIES, OKLAHOMA

By

PATRICK JOSEPH KAMANN

Bachelor of Science
The University of Findlay
Findlay, Ohio
2001

Master of Science
Wright State University
Dayton, Ohio
2004

Submitted to the Faculty of the
Graduate College of the
Okalahoma State University
in partial fulfillment for
the Degree of
MASTER OF SCIENCE
May, 2006

SURFACE-TO-SUBSURFACE CORRELATION AND

LITHOSTRATIGRAPHIC FRAMEWORK OF THE

CANEY SHALE (INCLUDING THE "MAYES"

FORMATION) IN ATOKA, COAL, HUGHES,

JOHNSTON, PITTSBURG, AND PONTOTOC

COUNTIES, OKLAHOMA

Thesis Approved:

Dr. Stan Paxton
_____
Thesis Advisor

Dr. Anna Cruse
_____

Dr. Darwin Boardman, II
_____

Dr. Jim Puckette
_____

Dr. William Coffey
_____

Dr. Gordon Emslie
_____
Dean of the Graduate College

ACKNOWLEDGEMENTS

TABLE OF CONTENTS

LIST OF TABLES

LIST OF FIGURES

xi

LIST OF PLATES

CHAPTER 1.0

INTRODUCTION

1.1 Purpose and Scope

The Caney Shale (Mississippian) is an organic-rich calcareous shale deposit

containing large carbonate concretions. This shale is located throughout much of

Oklahoma in the Arkoma, Ardmore, and Anadarko basins. Part of this organic-rich

deposit is equivalent to deposits in Arkansas (Fayetteville Shale) and North Texas

(Barnett Shale). The Caney Shale has been classified as a source rock by Weber (1992)

and Hendrick (1992), but because of expectations for conventional hydrocarbon

exploration, the formation was never considered a reservoir. As a result, few detailed

studies have been completed on the Caney Shale and little is documented about the

shale's sedimentary and stratigraphic nature.

The "Mayes" formation is a calcareous shale deposit found at the base of the

Caney Shale. This formation is recognized as a part of the lower Caney Shale formation

in outcrop by authors such as Elias and Branson (1959), however in the subsurface the

petroleum industry considers the "Mayes" to be independent from the Caney Shale. The

name "Mayes" is not a formal stratigraphic term, and therefore is written in quotation

marks. The "Mayes" is considered to be stratigraphically equivalent to the Sycamore

Limestone in Oklahoma (Elias, 1956; Champlin, 1959; Kleehammer, 1991). In this study

"Mayes" formation and the lower Caney Shale will be treated as the same stratigraphic unit. However, for clarity purposes the term "Mayes" formation will be used primarily to prevent confusion between the surface and subsurface terminology.

Recently, success in unconventional gas production from the Barnett Shale has increased industry interest in producing gas from the Caney Shale. Initial attempts at gas production from the shale have shown encouraging results. The Beebe #1, operated by New Dominion, had an initial production of 1.77 MMCF per day, and the Hammontree #1, operated by New Dominion, had and initial production of 1.09 MMCF per day. However, despite this encouraging early gas production from the Caney Shale, other wells have been less successful. The limited success in the Caney Shale is suspected to be a result of incorrect drilling and completion methods; a result of a lack of knowledge about sedimentology, stratigraphy, and rock properties.

In a gas-shale play there are several formation properties that need to be evaluated. These properties can be divided into two categories: prospective and performance-potential properties. Prospective properties include those properties of a formation that determine if it could be a successful shale-gas play. These properties include: the amount and type of organic matter content, maturity of the organic matter, prospective thickness, and depth of the shale formation. These properties should be evaluated in the initial stages of exploration in order to determine if the potential for a successful play is present. Organic content, maturity, and thickness are interdependent properties of a shale formation. A shale package with a low organic matter content my still source hydrocarbons of economic quantities if the package is thick enough and the borehole can contact a large surface area in the reservoir. In contrast, a thin organic-rich

shale with a thickness of only a few feet may be uneconomical. In addition to organic

content and thickness of a shale formation, a shale will only be economical if it is

thermally mature with respect to generation of gas. The depth of a shale formation is

another important consideration to prospectivity for two reasons. First, the depth has a

direct affect on the fluid pressures in the formation; the deeper the formation the higher

the pressures. Additionally, formations that are deeply buried will be costly to produce,

and potentially uneconomical if the drilling cost is not compensated by thickness or

organic content.

Performance-potential properties are those properties that dictate how a formation

will react when drilled and stimulated. These properties include: whole rock chemistry,

virgin porosity and permeability, natural fracture barriers in and around the formation,

faults, fractures, rock strength, and regional stress. These properties are used to

determine preferred drilling and completion practices, and are typically evaluated in

conjunction with prospective properties. Whole-rock chemistry is used to determine the

best stimulation fluids used to complete a shale-gas well. Certain clays and minerals

found within a formation react with stimulation fluids and can reduce permeability.

Therefore, formations need to be stimulated with the correct fluids in order to obtain

optimal permeability in the borehole. The volume of gas that flows into a borehole is a

reflection of the porosity and permeability of the formation. Choosing more porous and

permeable zones for well completions will result in production of larger volumes of

recoverable gas over shorter periods of time. The remaining rock properties dictate

stimulation fracture morphology. A technical understanding of these properties allows

for a drilling plan that will maximize the interconnected reservoir volume.

In the following investigation a detailed analysis of the Caney Shale is provided. The scope of this investigation is to develop a lithostratigraphic framework for the Caney Shale. With a new lithostratigraphic framework, one can then proceed to evaluating the prospective and performance-potential properties of the Caney Shale formation. An analysis of these properties will help to determine if the Caney Shale of southeast Oklahoma contains the elements to be a potential shale-gas play. To develop a lithostratigraphic framework of the Caney Shale, both sedimentological and stratigraphic techniques were employed. Specifics of these techniques include: the identification and description of lithostratigraphic units in surface outcrops and subsurface wells, establishment of gamma-ray profiles in outcrop, stratigraphic correlation and mapping of units from surface to subsurface using gamma-ray signatures, analysis of organic matter type and content of these units, and interpretation and discussion of depositional setting.

1.2 Location of Study Area

The study area for this investigation is located in portions of Atoka, Coal, Hughes, Johnston, Pittsburg, and Pontotoc Counties (Figure 1.1). Surface data collected for this study originated from outcrops off the southeastern flank of the Arbuckle Mountains in Section 11, T.2S., R.7E, from outcrops on the Lawrence Uplift in Sections 26 and 35, T.3N., R.6E., and on a thrust sheet of the Ouachita Mountains in Section 4, T.2N., R.15E. The subsurface data for this study came from wells located in the Arkoma Basin east of the Lawrence Uplift.

1.3 Stratigraphy

4
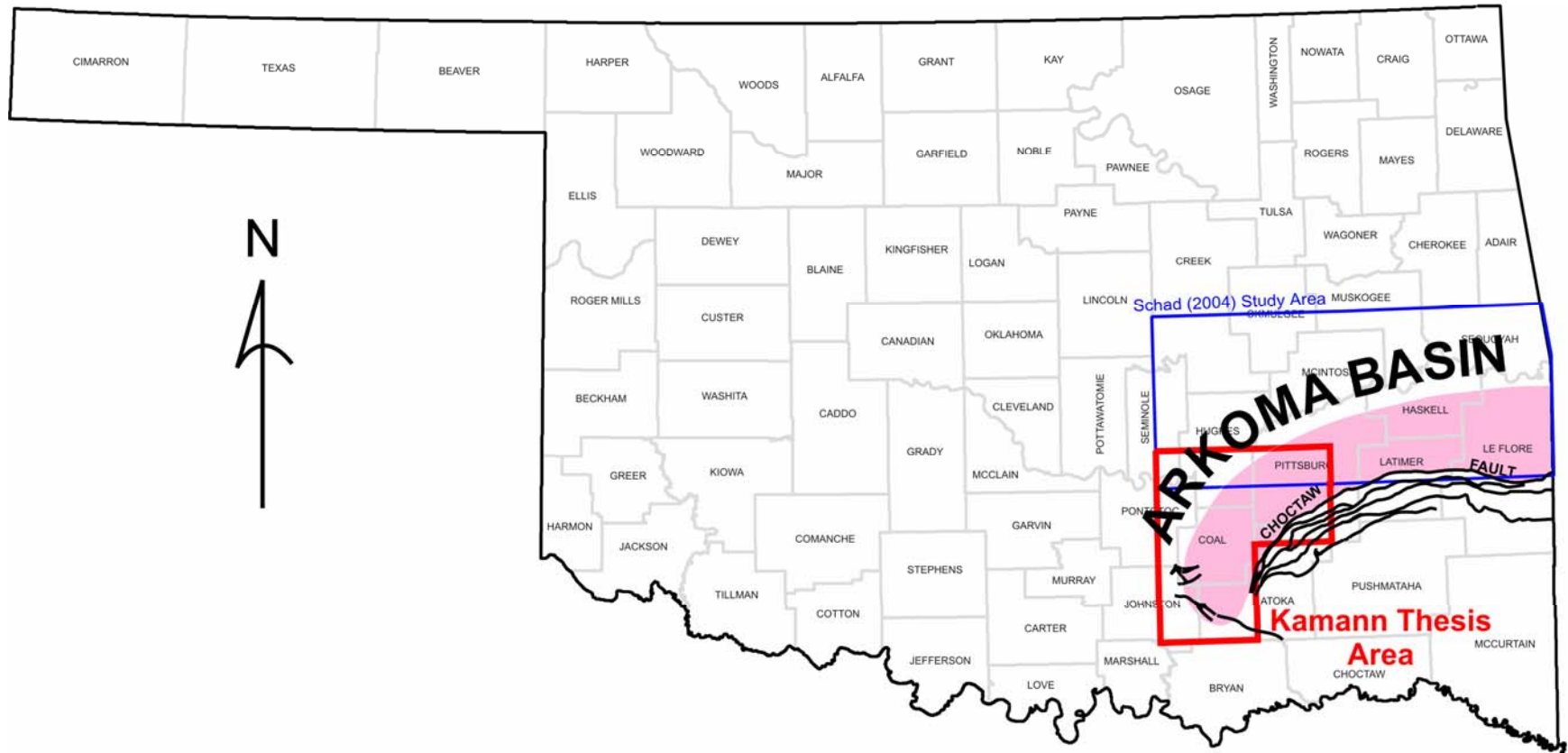
Figure 1.1 Map of Study Area Location. The study area is located in the Arkoma Basin of southeast Oklahoma, and encompasses portions of Atoka, Coal, Hughes, Johnston, Pittsburg, and Pontotoc Counties.

The Caney Shale is middle to late Mississippian in age (Figure 1.2). In terms of chronostratigraphy, Elias (1956) determined that the Caney corresponds to the Meramecian and Chesterian Stage. In the western Arkoma Basin and Eastern Arbuckle Mountains the Caney shale overlies (in order from oldest to youngest) the Woodford Shale, the pre-Welden Shale, the Welden Limestone, and the "Mayes" formation (lower Caney Shale). The Woodford is upper Devonian (Frasian) to early Mississippian (Kinderhookian). Sediments of the pre-Welden Shale were deposited in the remainder of the Kinderhookian Stage, and sediments of the Welden Limestone were deposited during much of the Osagean Stage (Haywa-Branch and Barrick, 1990). The lateral extent of both the pre-Welden Shale and the Welden Limestone is currently unknown. Typically, these formations are only identified in outcrops on the Lawrence Uplift, and are not identified in the subsurface. As stated earlier, the "Mayes" formation is considered the lower Caney Shale by authors such as Elias and Branson (1959), and it occupies the upper Osagean and lower Meramecian Stage (Elias, 1956 and Haywa-Branch and Barrick, 1990). The Caney Shale is overlain by the Rhoda Creek Formation in this study area. The Mississippian-Pennsylvanian boundary can be found within the Rhoda Creek Formation (Grayson et al., 1985). Other authors (Westheimer, 1956 and Lauden, 1958) refer to the Rhoda Creek formation as the Goddard Shale. In the lower section of the Goddard Shale there are commonly thin zones with a high gamma-ray response. These zones are often referred to as the "false Caney" by those in the petroleum industry. This interval is still a part of the Goddard Shale; Schad (2004) uses the term lower Goddard to replace the name "false Caney". This terminology is adopted in this study.

	STAGE		FORMATION
PENNSYLVANIAN	DESMOINESIAN	Krebs Group	Boggy Formation
			Savanna Formation
			McAlester Formation
			Harshorne Formation
	ATOKAN		Atoka Formation
	MORROWAN		Wapanucka Limestone
			Union Valley Formation
MISSISSIPPIAN	CHESTERIAN		Caney Shale
	MERAMECIAN		
	OSAGEAN		
	KINDERHOOKIAN		
DEVONIAN	UPPER		Woodford Shale
	LOWER	Hunton Group	Frisco Limestone / Bois d'Arc Limestone / Haragan Limestone
SILURIAN	UPPER		Henryhouse Formation
	LOWER		Chimney Hill Subgroup
ORDOVICIAN	UPPER	Viola Group	Sylvan Shale
			Welling Formation / Viola Springs Formation
	MIDDLE	Simpson Group	Bromide Formation / Tulip Creek Formation / McLish Formation / Oil Creek Formation / Joins Formation
	LOWER	Arbuckle Group	West Spring Creek Formation / Kindblade Formation / Cool Creek Formation / McKenzie Hill Formation / Butterly Dolomite
CAMBRIAN	UPPER		Signal Mountain Limestone / Royer Dolomite / Fort Sill Limestone
		Timbered Hills Group	Honey Creek Limestone / Reagan Sandstone
PRECAMBRIAN			Granite and rhyolite

PENNSYLVANIAN	Atokan	Atoka Formation
	Morrowan	Wapanucka Formation
		Union Valley Formation / Springer Formation
		Rhoda Creek
MISSISSIPPIAN	Chesterian	Caney Shale
	Meramecian	
		lower Caney "Mayes" / Sycamore Formation
	Osagean	Welden Limestone
	Kinderhookian	pre-Welden shale
		Woodford Shale

Figure 1.2 Generalized stratigraphic column of the units making up the chronostratigraphic framework of the Oklahoma Arkoma Basin and Lawrence Uplift (Modified from Sutherland, 1988).

1.4 Tectonic Setting

The Arkoma Basin is an important petroleum province in southeastern Oklahoma and west-central Arkansas (Figure 1.3). The sedimentary rock thickness in the Arkoma Basin ranges from 3,000 to 20,000 ft. The Arkoma Basin is bounded to the north by the Cherokee Platform and Ozark Uplift in Oklahoma and Arkansas, respectively. To the east the basin can be traced to the Black Warrior Basin with the Pascola "Arch" separating the two basins. To the south the Arkoma Basin is bounded by the Ouachita fold and thrust belt, and to the west the Arkoma Basin is bounded by the Arbuckle Uplift (Houseknecht and Kacena, 1983, and Perry, 1995).

The Arkoma Basin is considered to be a foreland basin that was created as the result of the formation of the Ouachita fold and thrust belt. The events that led up to the formation of the Arkoma Basin can be divided into four tectonic stages. These include a period of rifting, passive margin deposition, early Llanoria collision, and late Llanoria collision.

1.4.1 Stage 1: Rifting Stage

During the late Proterozoic to early Cambrian time it is believed that an upwelling of mantle plumes resulted in the uplift of the ancient craton in southern Oklahoma. This uplift resulted in a rift – rift – rift triple junction. Two of the rifting arms led to the opening of the proto-Atlantic Ocean basin. The third arm of this rift system failed to open and became what is known as the Southern Oklahoma Aulacogen (Figure 1.4). Rifting along the North American craton was not confined to the area of
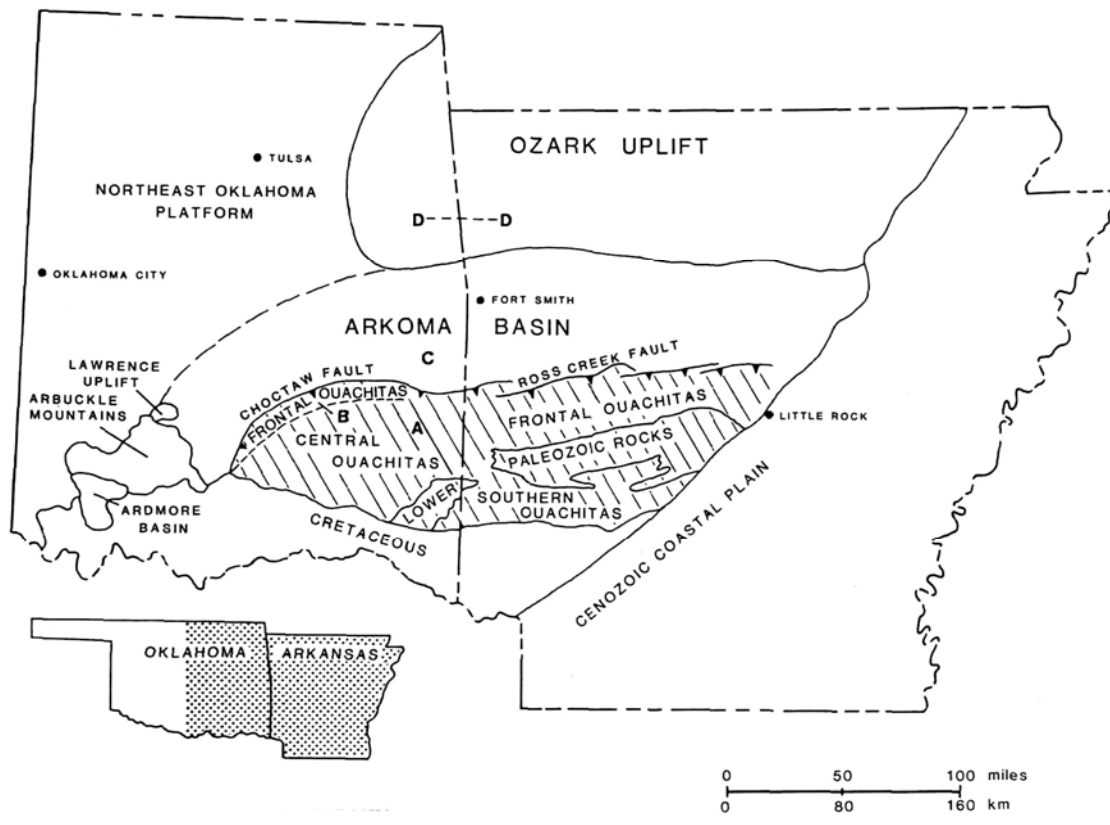
Figure 1.3 Location of Arkoma Basin and surrounding provinces in Oklahoma and Arkansas (From Sutherland, 1998)

9
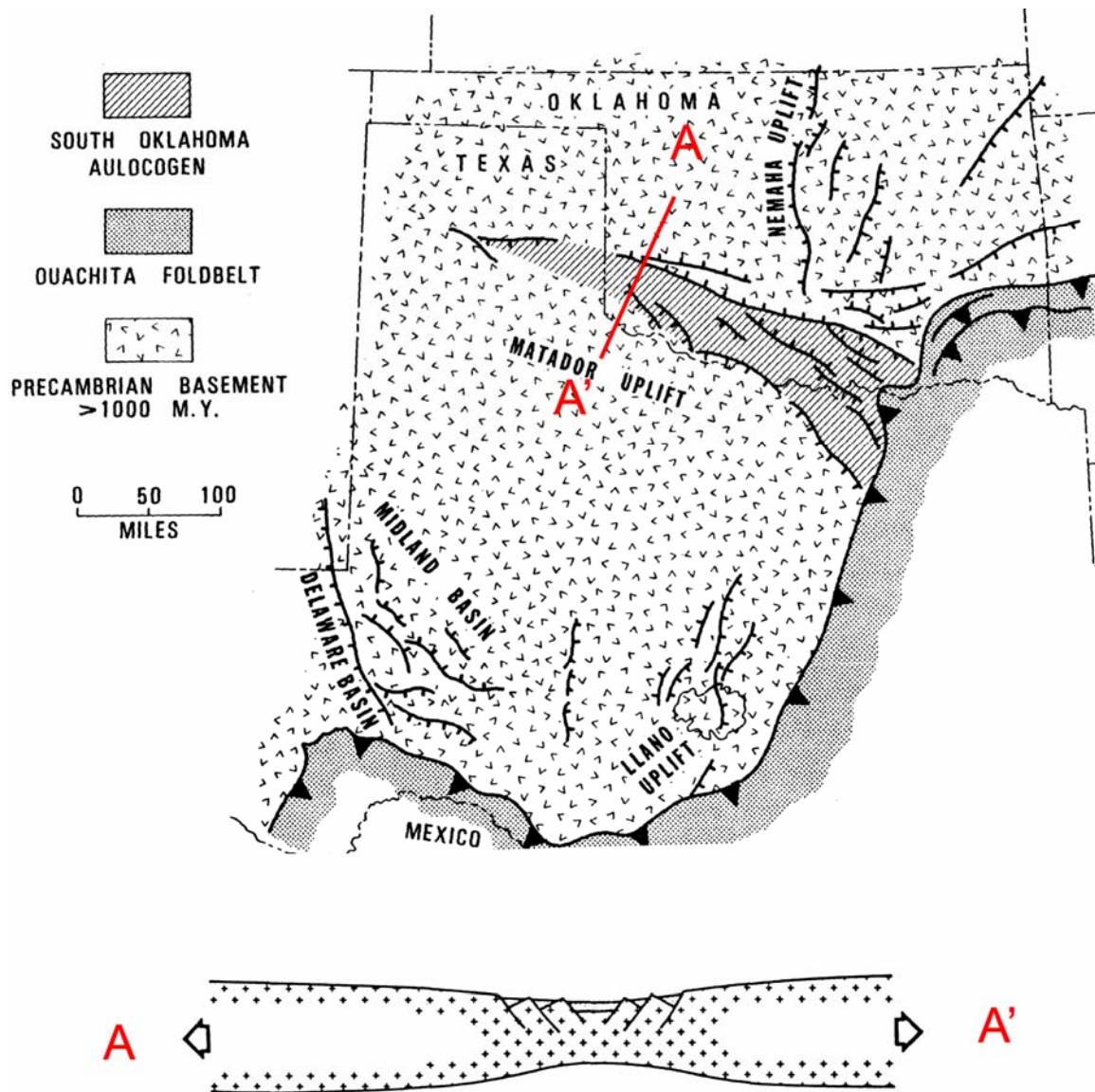
Figure 1.4 Location of Southern Oklahoma Aulacogen and generalized cross section across aulacogen (Modified from Housenecht and Kacena, 1983 and Wickham, 1978).

southern Oklahoma; rifting occurred all along the southern margin of North America

(Houseknecht and Kacena, 1983 and Wickham, 1978).

Evidence of this rifting stage can be found in the rocks. Cambrian granite,

rhyolite, gabbro, anorthosite, and troctolite can be found today in uplifted portions of the

aulacogen. These igneous rocks are interpreted to result from the intrusion of upwelling

magma at the rift locations. Also, positive gravity anomalies along with seismic data

indicate the presence of the aulacogen and what might be the former continental margin

(Wickham, 1978).

1.4.2 Stage 2: Passive Margin Deposition

After the rifting stage, the two active rifts continued to open the proto-Atlantic

ocean and the area of the present day Arkoma Basin became a passive margin (Figure

1.5). During this time period the continental margin and aulacogen were flooded as a

result of eustatic sea level rise, subsidence, or a combination of the two. Subsidence of

the continental margin likely resulted from cooling of the lithosphere as the mid-oceanic

ridge moved to the south. The flooding of the continental margin created a shelf-slope-

rise geometry with molasse deposits forming on the shelf and flysch deposits forming on

the lower slope and deep basin (Houseknecht and Kacena, 1983).

Molasse deposits on the shelf consisted of shallow water carbonates and

sandstones. The first of the shelf deposits was the Reagan Formation of Late Cambrian

age (Figure 1.2). The Reagan Formation is a well-washed mature sandstone. During the

Late Cambrian through Ordovician carbonate deposition continued on the shelf creating

the Arbuckle Group. Carbonate deposition kept pace with rising sea level, and thick

11
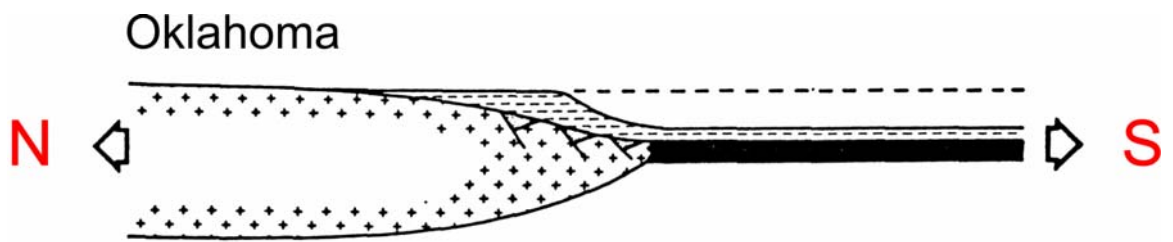
Figure 1.5 Generalized north-to-south cross section of passive margin (Modified from Wickham, 1978).

carbonate deposits formed across the area. The thickest portion of the Arbuckle Group

occurs in the Oklahoma Aulacogen as a result of continued subsidence of faults formed

during the initial rifting stage (Figure 1.6) (Houseknecht and Kacena, 1983 and

Wickham, 1978). During the Late Ordovician through Early Mississippian various

carbonates, sandstones, and shales continued to accumulate on the shelf. This package of

strata contains numerous unconformities representing large fluctuations in sea level.

Just south of the shelf, flysch type sediments were deposited on the slope and

deep ocean basin. Today, these deposits are exposed in the Central Ouachita Mountains.

From the Late Cambrian to the Early Devonian fine grained shale deposits commonly

formed in the deep basin, along with a few sandstones and limestones (Houseknecht and

Kacena, 1983).

1.4.3 Stage 3: Early Llanoria Collision

During the Early Mississippian or possible the Late Devonian the proto-Atlantic

ocean began to close, marking the beginning of the Ouachita Mountain Orogeny (Figure

1.7). The closing of the basin resulted from southern subduction under an approaching

landmass named "Llanoria". Subduction under Llanoria created a deep trough next to the

approaching landmass that transitions northwestward into a shallow shelf. The size of

Llanoria is uncertain, and ideas vary from island arc system, microcontinent, or a larger

continental mass (Graham et al., 1975 and Nelson et al., 1982). The closing of the

remnant proto-Atlantic ocean is believed to be from east to west as indicated by sediment

transport from the Ouachita orogenic belt at the southern edge of the Black Warrior Basin

(Graham et al., 1975).

13
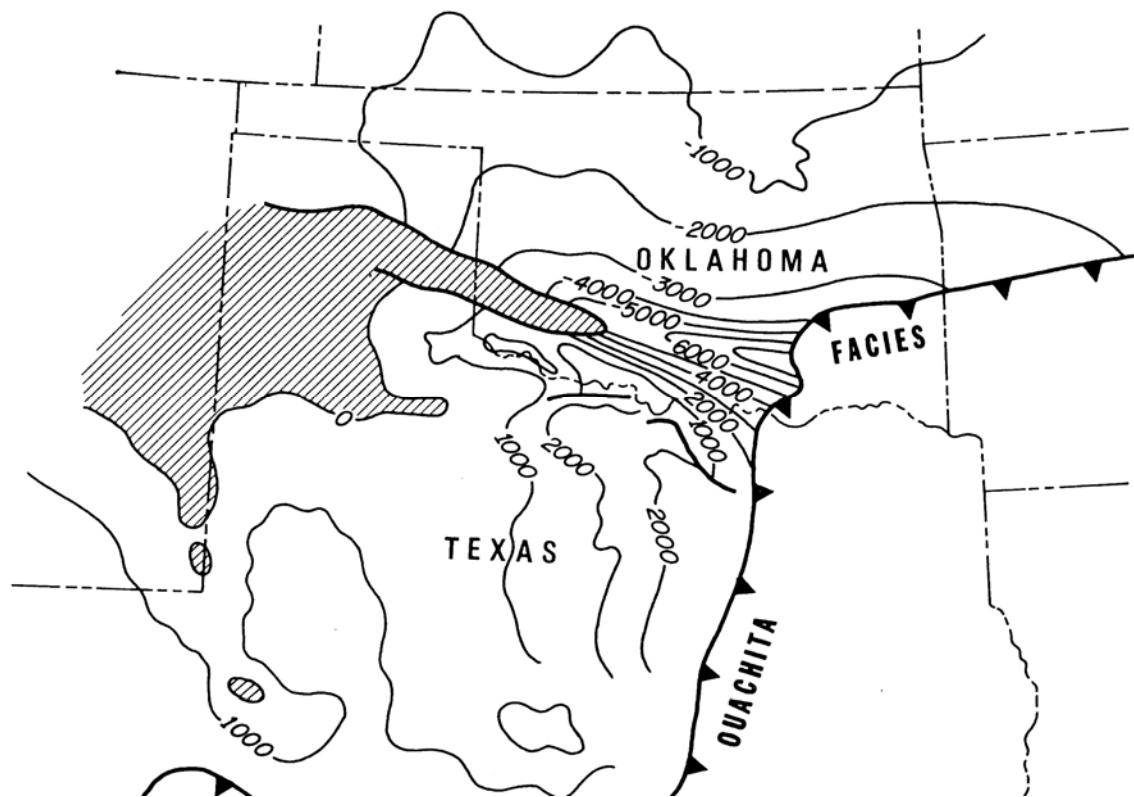
Figure 1.6 Isopach map of the Arbuckle Group showing a thickening in the area of the Oklahoma Aulacogen (From Wickham, 1978).
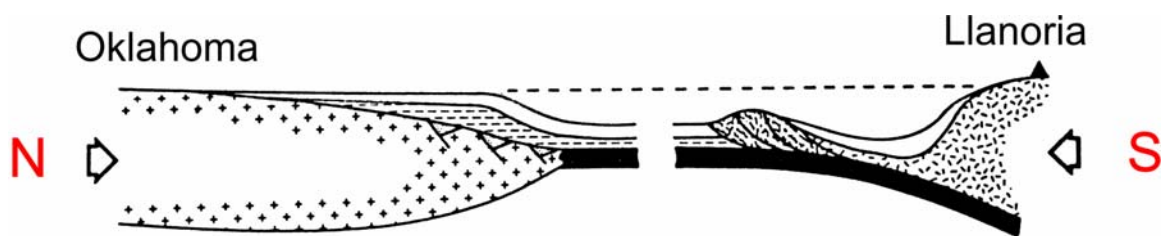
Figure 1.7 Generalized north-to-south cross section of Early Llanoria Collision
(Modified from Wickham, 1978).

One of the most convincing formations that provides evidence for the existence of a subduction zone would be the Stanley Group deposited during much of the Mississippian Period (Figure 1.8). The Stanley Group consists of mainly black shales, but sandstones and volcanic debris are also present. Volcanic debris includes tuffs and sands derived from the subduction complex. The Stanley Group is estimated to be around 3,300 m thick and thins quickly to the west and north, as illustrated from the stratigraphic cross section in Figure 1.9 (Sutherland, 1981). In the eastern sections the Stanley Group contains proximal submarine fan facies and in the western sections these submarine fan facies become distal and disappear. The thinning of the sediments and progradation of fan facies to the west indicates that much of the sediment was derived from the newly uplifted orogenic belt (Houseknecht and Kacena, 1983). As indicated in both Figure 1.8 and 1.9, the Stanley Group was deposited adjacent to the Caney Shale.

The Caney Shale is highly fossiliferous with bivalves, shark teeth, conodonts, cephalopods, fecal pellets, and woody material (Elias, 1954 and Schad, 2004). The preservation of organic material in the shale indicates an anoxic depositional environment. Anoxic waters develop in depositional environments containing a deep water column, a shallow water column that is restricted from current and wave energy, or a shallow water column with high biologic productivity depleting oxygen at depth. The water column during deposition of the Caney Shale is estimated by Schad (2004) to be moderately deep (from 100 to 600 ft). Geographically, these water depths could be reasonable, because the Stanley Group is thought to have been deposited in a deep trough created by the approaching Ouachita Mountain belt, while the Caney Shale is thought to have been deposited upon the shallower shelf areas adjacent to the deep trough
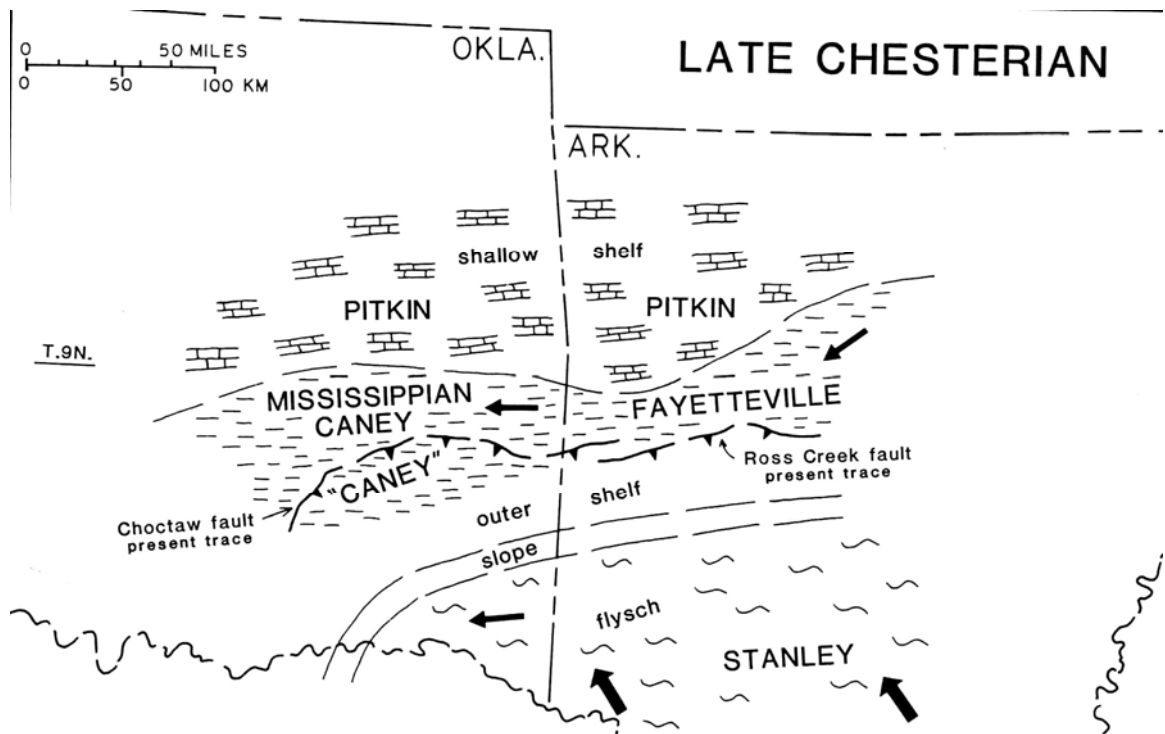
Figure 1.8 Facies map of Arkoma Basin during Chesterian Series (From Sutherland, 1988).
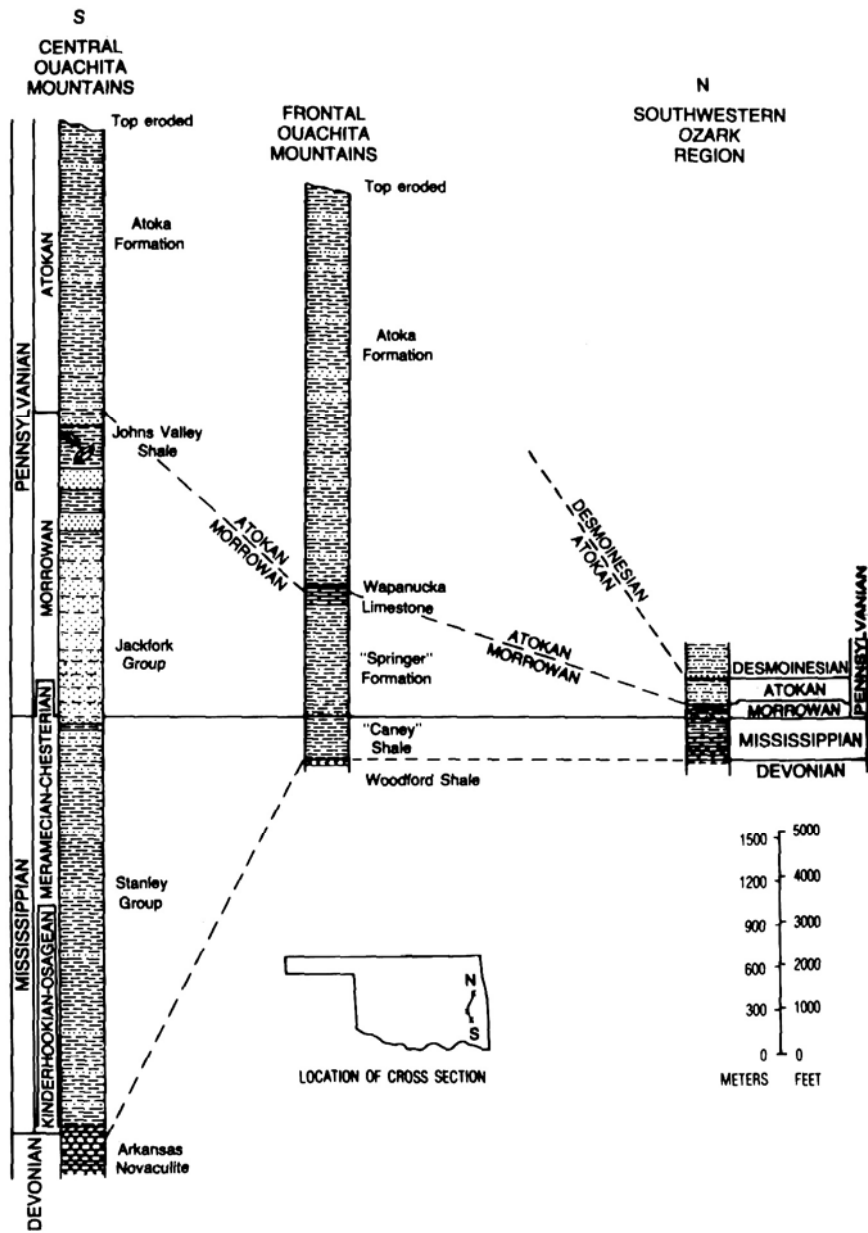
Figure 1.9 Stratigraphic cross section form the Central Ouachita Mountains north to the Ozark Uplift (From Sutherland, 1981).

(Sutherland, 1988). The approaching landmass (Llanoria) closing the proto-Atlantic ocean from east to west also likely provided additional restriction to the basin allowing anoxic waters to develop. A more detailed discussion on the depositional setting will be provided in the discussion and conclusions of this study.

By the Late Mississippian, deposition of Caney sediments is believed to have ended because of a withdrawal of the sea from the self areas. This withdrawal is thought to be a result of the rapidly sinking Ouachita trough and uplift of the Ozark Dome. The sea is thought to have only withdrawn from the shelf area, while sedimentation continued uninterrupted in the trough area. In the Early Pennsylvanian, the sea transgressed back onto the shelf and deposition of the Springer Group continued on the surface of the Caney Shale (Sutherland, 1988).

In the Ouachita trough during the Early Pennsylvanian, great volumes of sediment were shed into the remnant ocean basin and deposited mainly in submarine fan systems. The source for these sediments was possibly the Appalachian Mountains, Ouachita orogenic belt, and the Ozark Dome. The Units that represent these fan deposits are the Jackfork Group and Johns Valley Shale (Houseknecht and Kacena, 1983).

1.4.4 Stage 4: Late Llanoria Collision

By the Atokan time in the Middle Pennsylvanian, Llanoria had closed much of remnant proto-Atlantic Ocean, and began to collide with the rifted continental margin. This event marks the beginning of the formation of the Arkoma Basin as the shelf-slope-rise geometry is destroyed and flexural bending created a foreland basin (Figure 1.10). During this time, the sediments creating the Atoka Formation poured into the basin.
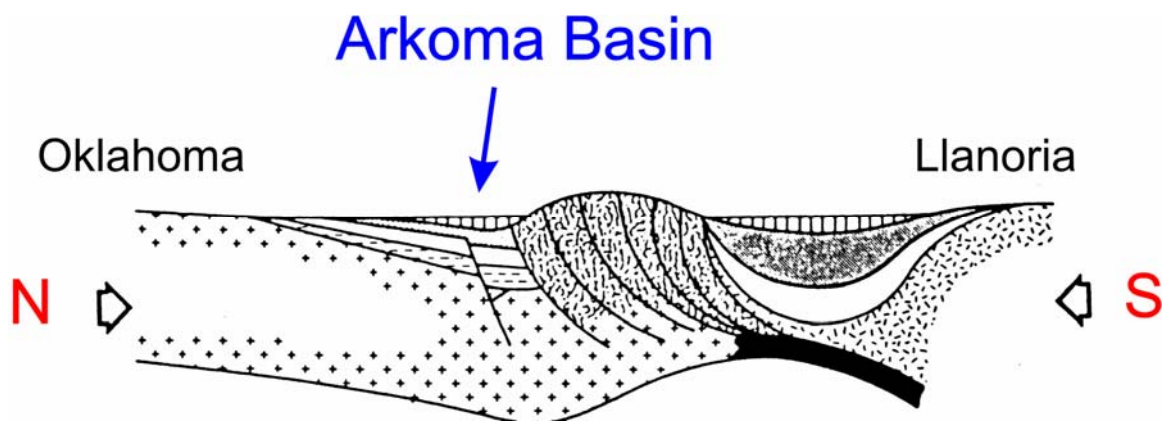
Figure 1.10 Generalized north-to-south cross section during late Llanoria collision (Modified from Wickham, 1978)

Finally, in the late Atokan to Desmoinesian Stage, the collision of Llanoria and uplift of the continental margin had ceased (Houseknecht and Kacena, 1983).

The formation of the Arkoma Basin with the addition of new sediments led to the burial of the Caney Shale. Sediments deposited during this time make up the Atoka Formation, the Krebs Group, the Cabaniss Group, and the Marmaton Group. These rocks are interpreted to be submarine fan deposits at the base to shallow water fluvial deltaic packages at the top. This package of rock represents a filling in of the Arkoma Basin. Burial of the shale during the collision of the two landmasses resulted in maturation of the Caney Shale (Houseknecht and Kacena, 1983).

The collision of Llanoria also activated normal faults in the Southern Oklahoma Aulacogen causing strike-slip movement. The movement of these faults created a series of uplifts and basins in southwestern Oklahoma (Figure 1.11). The first evidence for the movement of these faults is indicated by carbonate conglomerates in the Anadarko Basin formed during the Morrowan. Formation of the Arbuckle Mountains during this time caused rock units from the Proterozoic to the Pennsylvanian to be uplifted. As a result of this uplift, many of these rock units, including the Caney Shale, can be studied in outcrops throughout the area (Houseknecht and Kacena, 1983).

1.5 Previous Investigations

The Caney Shale was originally named by Taff (1901) and was thought to include dark bituminous shales lying above the Woodford Shale in the Arbuckle Mountain region and blue shales lying above the Jackfork Sandstone in the Ouachita Mountain region. He described the shale as being laminated and fissile with limestone concretions and septaria
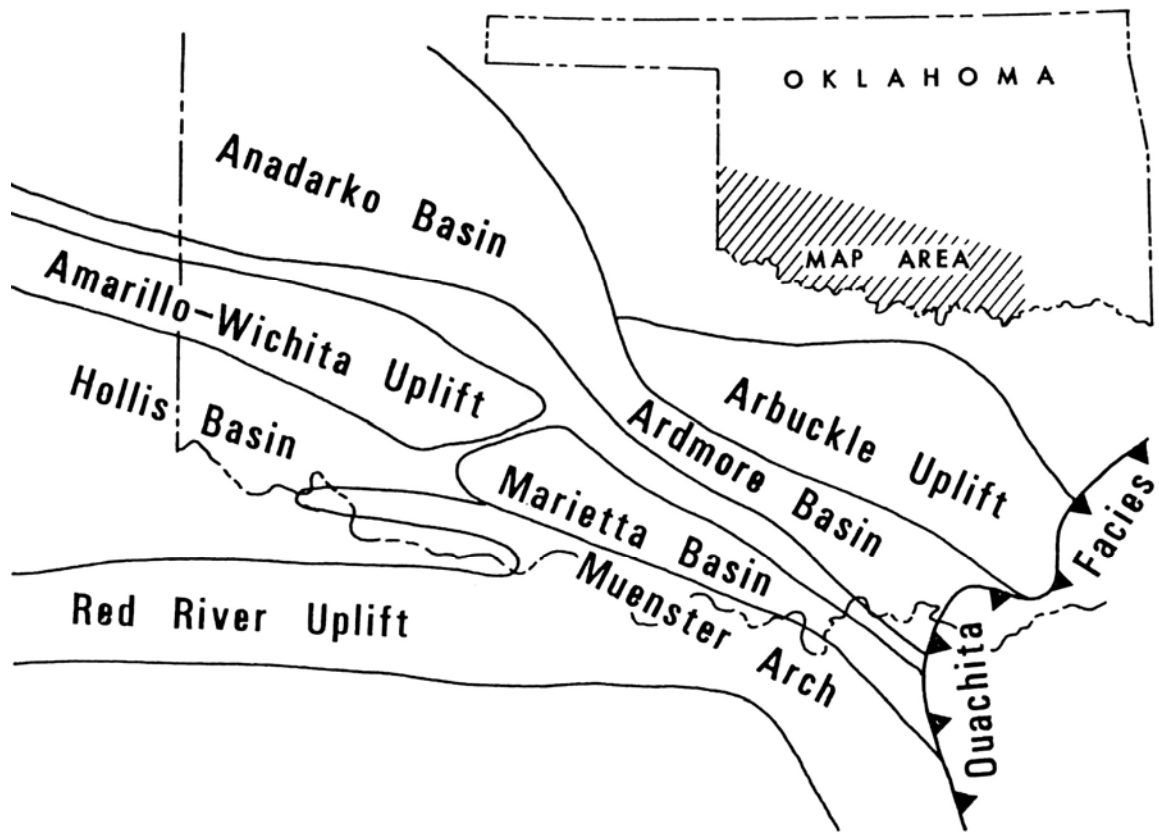
Figure 1.11 Basin and uplift locations in Southern Oklahoma as a result of the Ouachita Orogeny (From Wickham, 1978)

along with ironstone beds. Girty (1909) presented a detailed description of the fauna of the Caney Shale. Girty (1909) was not able to come to a concise conclusion about the age of the Caney Shale, and states "the problems presented by the Caney Shale are peculiarly baffling". He (ibid) had fossil evidence that the Caney Shale was late Mississippian in age, but because Mississippian fossils were found below the Caney Shale, he felt the Caney was possibly Pennsylvanian in age. So, he (ibid) assigned the age of the Caney Shale as Carboniferous.

Ulrich (1927), who worked with both Taff and Girty, concluded that the blue shale and black bituminous shales described in the Caney Shale were two different shale formations. He assigned the name Johns Valley Shale for the blue shales exposed in the Ouachita Mountains, and kept the name Caney Shale for the black bituminous shales. The two units were easily confused because the both contained limestone boulders. However, the boulders in the Caney Shale were carbonate concretions, while the boulders in the Johns Valley Shale were erratics from older carbonate formations.

Elias (1956) presented a study of the Mississippian and Pennsylvanian formations in south-central Oklahoma. In his work he describes the Caney Shale in both the northern and southern Arbuckle Mountains. Elias (1956) identified the fossils of the Caney Shale and determined the age of the shale to be Meramecian to Chesterian. Elias also divided the Caney Shale into three members. From oldest to youngest, these members are the Ahlosa, Delaware Creek, and Sand Branch.   The Ahlosa Member (also known as the "Mayes" or "Ada Mayes") is described as a light gray, calcareous shale. This member contains small carbonate concretions and is of a medium hardness. The Delaware Creek Member is described as gray, softer, and less calcareous than the Ahlosa

Member. Within the Delaware Creek large septarian carbonate concretions that are up to

12 ft. in diameter occur. Finally, the Sand Branch Member is a dark grey to black, non-

calcareous shale with high organic content. Within this member both apatite nodules and

carbonate septarian concretions are common (Elias, 1956). Elias determined that all three

members were present in the northern Arbuckles, but only the Delaware Creek and

possibly the Ahlosa were present in the southern Arbuckle Mountains.

Elias and Branson (1959) proposed a type section for the Caney Shale southwest

of Bromide, OK near the Viola Springs town site (W1/2 Sec. 13 and E1/2 Sec. 14, T2S-

R7E). In this publication they (ibid) amended the name of the Ahlosa Member to become

Ahloso. They (ibid) also presented detailed measured sections for the type section that

included the Woodford Chert and an interesting formation called the "Sycamore

Sandstone" under the Ahloso Member. They (ibid) also correlated the Delaware Creek

Member of the Caney Shale to the Johns Valley Shale, conflicting with evidence

presented by Ulrich (1927) that the Johns Valley Shale was of Pennsylvanian age.

Champlin (1959) completed a thesis on the Sycamore and related formations in

the eastern Arbuckle Mountains. In his work he confirmed work by Elias (1956) that the

Ahloso Member is Meramecian in age and is correlative to the upper part of the

Sycamore Limestone and lower part of the Caney Shale in the southern Arbuckle

Mountains. Champlin (1959) suspected that the facies change between these two units

was controlled by low relief islands.

Harris (1971) presented a study of the palynology of the Sand Branch Member of

the Caney Shale. In this work he (ibid) collected and analyzed samples from several

locations including the type section proposed by Elias (1959). Harris (1971) concluded

that erosion of Late Ordovician to Late Devonian strata contributed sediments to the Sand Branch Member of the Caney Shale. He (ibid) also determined that the Sand Branch Member was early to middle Chesterian in age and that this strata was correlative to the lower part of the Goddard Shale type section.

In more recent work, Monaghan (1985) studied the stratigraphy of Mississippian to Pennsylvanian shales in the Arbuckle Mountain region. In this work depositional environments for the Caney Shale were presented, but little descriptive detail and conclusive evidence was provided. Kleehammer (1991) studied the biostratigraphy of the Caney Shale. Kleehammer (1991) determined that dividing the Caney Shale into the members presented by Elias (1956) was unwarranted, as a result of not being based on lithologic differences. Kleehammer (1991) also determined that the Caney Shale in the northern Arbuckle Mountains was late Osagian to early Chesterian in age, while the Caney Shale in the southern Arbuckle Mountains was late Meramecian to early Chesterian in age.

Finally, Schad (2004) completed a subsurface study of the Caney Shale. In his study, the Caney Shale, excluding the "Mayes" (lower Caney Shale), was divided into six members based on log signatures and described using whole core. Schad (2004) also mapped the Caney Shale and surrounding formations, and presented thoughts on burial and maturation of the shale. The present study (Kamann, 2005) overlaps the study by Schad (2004) in townships T5N to T6N and R6E to R15E.

CHAPTER 2.0

METHODOLOGY

This study focuses on both surface and subsurface data from the Caney Shale. Gathering and analyzing data from both of these domains allows for better identification and correlation of sedimentary units, thus enabling a more detailed and rigorous lithostratigraphic framework to be constructed for the Caney Shale.

2.1 Surface

The main purpose of the surface study was to identify and quantify sedimentary units in outcrop. Ten outcrop locations were evaluated in this study. Procedures for evaluating each outcrop location are as follows. At each outcrop location the exposed section was measured to the nearest hundredth of a foot. On vertical outcrops it was easier to measure the thickness of the exposure from the top down. The section was then photographed and described in detail, noting characteristics such as color, grain size (if determinable), presence of apatite and carbonate, iron staining, jarosite precipitate, and bedding geometry. Silt-size quartz was identified at the outcrop location by crushing samples between ones teeth. Gritty samples were interpreted to contain silt. A grain size card and hand-lenses were also used to identify any larger sand-size grains present. After

the outcrop was photographed and described, gamma-ray measurements were taken at the outcrop.

Gamma-ray measurements were taken at each of the ten outcrop locations using a portable gamma-ray scintillometer (Exploranium GR-320, Figure 2.1). The gamma-ray scintillometer measures the amount of gamma rays emitted by potassium (K), uranium (U), and thorium (Th) in the measurement area. The instrument is able to quantify the amount of natural gamma rays received from each of these elements. By quantifying the amount of gamma rays received, the instrument is able to determine the amount of each of these elements in the measurement area. The total gamma-ray response for a measurement is quantified, in API units, with the equation,

$$GR = 4*Th + 8*U + 16*K,$$ (1)

where GR is equal to gamma-ray response, Th and U concentrations are expressed in ppm, and K concentrations are expressed in weight percent (Ellis, 1987). The radius of measurement of this unit is about 1.15 ft (35cm) into the Earth's surface (Richards, 2001), producing a hemisphere of measured rock volume.

Environmental conditions can affect gamma-ray scintillometer measurements. Ideally, measurements should be taken on large, fairly flat surfaces. Nearby boulders or cliffs will have an effect on the gamma-ray readings. Ten meters of air will only attenuate terrestrial radiation by 5-7%. Also, moisture tends to attenuate gamma rays. So, heavy rains can affect gamma-ray measurements by trapping radon particles or attenuating emitted gamma rays. Therefore, it is best to take measurements in dry environments. Additionally, soil and vegetation covering the outcrop can mask

Exploranium GR-320 Features

-256/512 channel operations: software selectable.
-One or two detector input: size range of 21 to 512 cu.ins.
-Automatic spectrum stabilization: internal or natural isotope
-8 regions of interest set from the keyboard.
-High linearity ADC with zero dead time.
-Choice of coincidence or anti-coincidence operation.
-Exposure rate mode for environmental data.
-Assay mode for geophysical data - %K, ppm eU, eTh.
-Input capability for GPS information with integrated data storage.
-717 full spectra or 4468 sets of ROI data in internal data storage.
-RS-232 serial digital output facilitates spectrum, ROI and GPS data output.
-Buffered output data for zero downtime during data transfer.
-Rechargeable or alkaline battery operation.
-Full remote control capability.
-User application programs supplied.
-Background, K, U and Th calibration using traceable test pads.

Figure 2.1 Portable gamma ray scintillometer (From the Exploranium GR-320 Manual).

gamma-ray measurements. Outcrop surfaces should be cleaned of weathered material before gamma-ray measurements are taken (Richards, 2001).

At each location, a single measurement was taken every 0.5 ft perpendicular to bedding planes. Occasionally, the spacing of these gamma-ray measurements was adjusted up or down at select locations in order to capture variations in lithology. These measurements were then plotted vertically with outcrop thickness to create a gamma-ray profile.

Finally, samples were taken at each section to capture additional sedimentological characteristics of the outcrop. The samples were used for a variety of lab analyses including; x-ray diffraction (XRD) analysis, thin section preparation and descriptions, and total organic carbon (TOC) analysis. Results from these analyses aid in the determination of a lithostratigraphic framework for the Caney Shale.

2.2 Subsurface

Information about the subsurface came from two wells in the study area. These wells are the Rogers Trust 1-24 and the Richardson 2-33. Mud logs from each of these wells were used to determine the general sedimentological character of the Caney Shale and "Mayes" formation (lower Caney Shale). Then, in each of these wells, sidewall cores of the Caney Shale and "Mayes" formation (lower Caney Shale) were collected to better define the lithologic properties of the formations. On each of the sidewall cores, XRD analysis, thin section preparation and description, TOC measurements, and thermal maturity measurements were performed. Additionally, borehole electrical image data

was collected in each of the wells in order to better characterize the sedimentology of the Caney Shale.

Wire-line gamma-ray logs from the subsurface were used to correlate to outcrop gamma-ray scans. This correlation allowed for the subsurface data collected in these two wells to be combined with the outcrop data. Combining the outcrop and subsurface data allowed for lithostratigraphic units within the Caney Shale and the depositional environment of the formation to be determined. More importantly, the combination of surface and subsurface data allows for the prospective and performance-potential properties of the Caney Shale to be evaluated in future studies.

CHAPTER 3.0

DESCRIPTION OF THE CANEY SHALE FORMATION IN SURFACE EXPOSURES

In the surface portion of this work 10 outcrops were evaluated. These ten

exposures include: Richard's Farm outcrop 1 (RF1), Richard's Farm outcrop 2 (RF2),

Jeff Luke shale pit (JL), Hass G outcrop (HG), Delaware Creek outcrop (DC), Little

Delaware Creek outcrop 1 (LDC1), Little Delaware Creek outcrop 2 (LDC2), Little

Delaware Creek outcrop 3 (LDC3), Little Delaware Creek outcrop 4 (LDC4), and the

Pine Top Mountain outcrop (PT). These outcrops vary in thickness from only a few feet

to hundreds of feet. Each section represents a portion of the "Mayes" formation (Lower

Caney Shale) and/or Caney Shale and no one section encompasses the entire thickness of

the units. This is suspected to be a result of a high susceptibility to weathering. Nine of

the ten exposures were located along streams and one section was exposed as a result of

quarrying operations.

A location map of the ten outcrops is shown in Figure 3.1. These ten outcrops can

be grouped into three general location areas. The first outcrop area evaluated in this

study is located on the Lawrence Uplift south of Ada, OK. The Lawrence Uplift outcrops

include: RF1, RF2, JL, and HG. The second outcrop area is located on the southeastern

flank of the Arbuckle Mountains near the town of Bromide, OK. This location will be

designated as the Bromide outcrop area and includes: DC, LDC1,
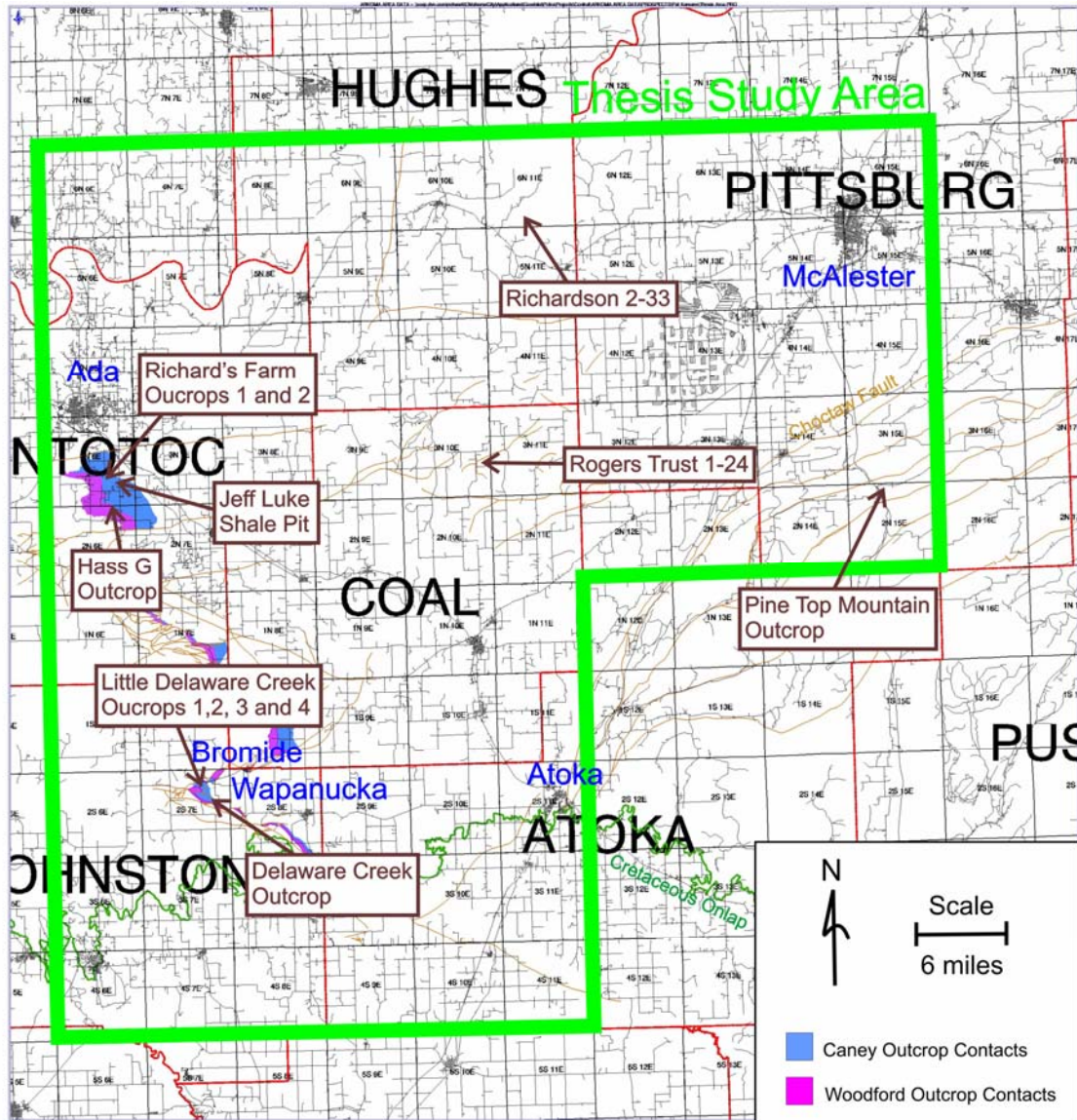
Figure 3.1 Map showing the general location of the ten outcrops and two subsurface wells evaluated in this research. More precise locations for these ten outcrops are provided in Appendix 1

LDC2, LDC3, and LDC4. The final outcrop, PT, is located near Pine Top, OK; this area is designated as the Pine Top Mountain outcrop area.

Each of the ten outcrops in this study were measured and described in detail. Only a summary of these measured sections is provided here. For a more detailed description of the ten outcrops, including their precise location, can be found in Appendix I.

The Richard's Farm outcrop 1 was measured to be 3.35 ft thick. The base of this outcrop contained a carbonate mudstone bed that was overlain by a bed of black calcareous fissile shale. This shale was then overlain by a thick dolomitic unit. The Richard's Farm outcrop 2 was measured to be 3.32 ft thick. This outcrop also contained a carbonate mudstone at the base and was overlain by a bed of calcareous fissile black shale. Above this shale a thin carbonate bed was present. This bed was then overlain by a non-calcareous black fissile shale.

The Jeff Luke shale pit is located to the east the Richard's Farm outcrops. The exposure at this location was measured to be 25.8 ft thick. This outcrop consisted of a black fissile shale. The bottom 4.4 ft of the section contained calcareous to slightly calcareous black shale. This shale was then overlain by a 21.4 ft of non-calcareous shale. This non-calcareous shale contained a large concentration of apatite nodules and laminations. These nodules and laminations were irregularly spaced throughout the outcrop. Jarosite precipitate and iron staining resulting from weathering were common on the shale exposure. Two carbonate nodules were noted in this non-calcareous unit. Above the non-calcareous shale a heavily weathered calcareous shale was present. This

shale contained abundant carbonate nodules. The shale was so poorly exposed due to weathering that it was not measured or sampled.

The Hass G outcrop was first described by Hass and Huddle (1965), and the section was given the name Hass G by Over and Barrick (1990). This outcrop contains the Woodford Shale, pre-Welden Shale, Welden Limestone, and "Mayes" formation (lower Caney Shale) contact. The Woodford Shale is composed of a black fissile shale and has a sharp contact with the pre-Welden shale. The pre-Welden Shale is characterized as a soft glauconite rich shale that contains apatite nodules. The contact between the pre-Welden Shale and the Welden Limestone is sharp. The Welden is composed of shaly wackstone and packstones. These limestones commonly contain glauconite and a component of silt. At this location the Welden Limestone is approximately 5.13 ft thick. The contact between the Welden Limestone and the "Mayes" formation (lower Caney Shale) again is sharp. The "Mayes" formation (lower Caney Shale) at this location is poorly exposed and only 2.85 ft of the unit was measured. This section contained a 1.55 ft of a tan calcareous shale and 1.3 ft of a blue green calcareous shale.

The Delaware Creek outcrop was measured to be 17.0 ft thick. This outcrop consisted of a black fissile shale. The shale was heavily weathered throughout most of the outcrop with jarosite and iron staining occurring on the weathered surfaces. At 4.0 ft apatite laminae were noted. These laminations were laterally adjacent to a large carbonate concretion in the outcrop. Plant fragments were noted in this outcrop at 10.9, 11.0, 12.0, 15.5, and 16.5 ft.

The Little Delaware Creek outcrop 1 was composed predominantly of a fissile black shale. There were many different facies variations to the fissile shale. Some shales were calcareous and/or silty. This outcrop contained a few carbonate nodules near the base. This outcrop was measured to be 12.7 ft thick

The second outcrop measured on the Little Delaware Creek, LDC2, was 11.2 ft thick. This outcrop was predominantly composed of a fissile black shale. The shale was variable like the LDC1 outcrop, with certain intervals containing carbonate and/or silt. Carbonate concretions were noted at the 6.4 and 8.4 ft from the top of the outcrop. Brachiopod and mollusk shell impressions were noted at the base of the outcrop

The Little Delaware Creek outcrop 3 was measured to be 9.2 ft thick. This outcrop was composed of black fissile shales. Again like the other outcrops exposed along Little Delaware Creek this outcrop contains facies variations. Some facies contain a component of carbonate and/or silt. Again at this section carbonate concretions were noted along with mollusk and brachiopod impressions.

The final outcrop measured on the Little Delaware Creek, LDC4, was 7.8 ft thick. The base of the exposure consisted of a slightly calcareous shale. This shale was black and fissile. Above the black shale a carbonate mudstone bed occurred. This mudstone bed was 0.6 ft thick and had wavy upper and lower boundaries with the black shale. Above this carbonate bed the outcrop contained a fissile black shale with thin discontinuous apatite laminations. Finally, the top of the outcrop consisted of 1.05 ft of blackish-brown shale with abundant apatite nodules.

The final outcrop evaluated in this study was the Pine Top Mountain outcrop. This outcrop was first described by Hendricks and Gardner (1947) and then was later

35

visited by Siy (1988) and Suneson and Campbell (1990). The original location given by Hendricks and Gardner (1947) differs from that given by Suneson and Campbell (1990). Suneson and Campbell's (1990) location differs slightly from the one given in Appendix 1. The location for this outcrop given in Appendix 1 is an accurate outcrop location, but it is possible that the location is not the same as that described by Hendricks and Gardner (1947). Their (ibid) location describes units and thicknesses not observed in this study.

This outcrop is interpreted to be a slump block of Caney Shale that was latter upthrusted during the Ouachita Orogeny. The exposed shale in this location is more brittle and resistant than Caney Shale viewed in outcrops to the west. At first glance the section appears to contain mainly Woodford Shale lithology. However, after detailed investigation the outcrop was determined to be "Mayes" (lower Caney Shale) and Caney on the basis of gamma-ray response and lithologic content. The difference in lithology between this outcrop and the other "Mayes" (lower Caney Shale) and Caney outcrops studied probably indicates a facies change between the outcrop locations, and perhaps higher thermal maturity (rock more consolidated because of temperature-related diagenesis). The use of this outcrop in this research is somewhat problematic, because the outcrop is no longer in its original stratigraphic position and the lithology of the Caney and "Mayes" (lower Caney Shale) is different than that viewed at the outcrops at the eastern Arbuckle Mountains.

The measured thickness of the PT outcrop was 207.8 ft. The base of the outcrop is composed of 29.5 ft of black fissile shale. This shale is more resistant than the shales exposed at the other outcrop locations and appeared to be slightly siliceous. Above this resistant shale a series of less resistant shales are exposed. The total thickness of these

36

shales was measured to be 42.9 ft thick. These shales commonly contained a carbonate component and shales are silty. A small interval in this section contains a more resistant fissile shale. However, this shale quickly transitions back into a less resistant shale. Also, in this interval three carbonate beds are noted. These carbonate beds are described as dolomitic silty mudstones. Above this less resistant interval to the top of the outcrop the exposed section transitions back into a more siliceous resistant shale. The shale is fissile, non-calcareous, and black. Also, within this shale apatite nodules can be found scattered throughout. The top 6.5 ft of this outcrop is composed of a silty to sandy, non-calcareous shale. This shale is very resistant and forms a small ridge at the outcrop location.

CHAPTER 4.0

OUTCROP GAMMA RAY CHARACTERIZATION

Gamma-ray measurements were taken at each of the ten outcrop locations. At each location, a single measurement was taken every 0.5 ft perpendicular to bedding planes. Occasionally, the spacing of these gamma-ray measurements was adjusted up or down at select locations in order to capture variations in lithology. These measurements were then plotted vertically with outcrop thickness to create a gamma-ray profile. This profile is briefly compared to the outcrop lithologies below. These outcrop gamma-ray scans were also used to correlate from surface to subsurface, results of which are discussed in Chapter 5.

4.1 Richard's Farm Outcrop 1

This outcrop has gamma-ray measurements that range between approximately 50 and 105 API units. A gamma-ray profile is plotted in conjunction with the outcrop photograph in Figure 4.1. This profile indicates that Unit 3 at 0.5 ft has the highest gamma-ray measurement at 102.0 API units. This unit is characterized as a brownish-black, calcareous, fissile shale. Gamma-ray measurements increase again at the top of the section with Unit 5 having a measurement of 80.4 API units.
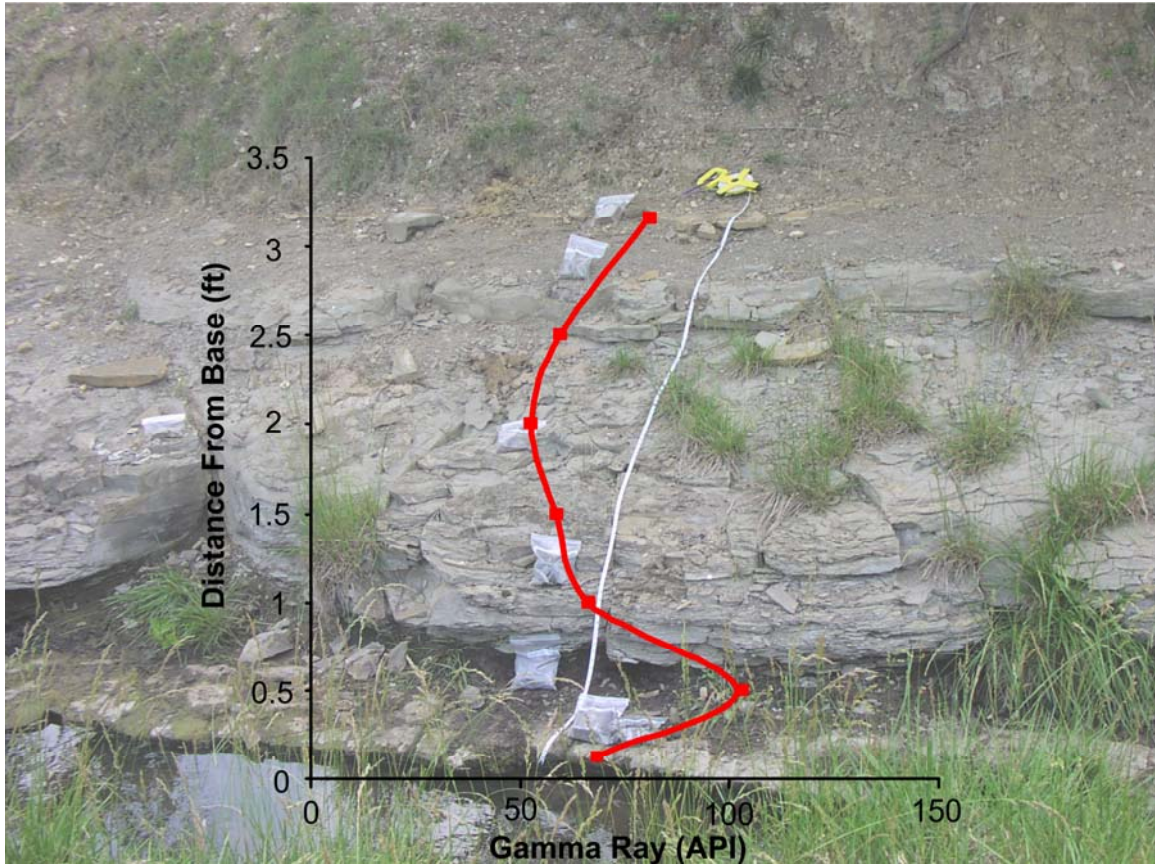
Figure 4.1 Photograph of Richard's Farm outcrop 1 with overlay of gamma-ray profile. Gamma-ray measurements, indicated by red squares, were taken approximately every 0.5 ft.

4.2 Richard's Farm Outcrop 2

The gamma-ray readings of this outcrop are considerably higher than those at RF1. The gamma-ray measurements range between approximately 190 and 265 API units. A gamma-ray profile is plotted in conjunction with the outcrop in Figure 4.2. At this outcrop gamma-ray response decrease from highest in Unit 1 (shaly carbonate mudstone) to lowest at the base of Unit 2 (grayish-black fissile shale). In the middle of Unit 2 gamma-ray readings increase back up to 243.5 API units, and then level off at around 200 API units in the top half of the outcrop.

4.3 Jeff Luke Shale Pit

The gamma-ray readings from each of the five Jeff Luke sections are plotted in Figures 4.3 to 4.7. This section containes continuously highest gamma-ray readings throughout the majority of the outcrop. Gamma-ray measurements range from 155 to 390 API units. The "hottest" part of this outcrop occurs at the top of JL2 and the base of JL3. Apatite nodules and laminae are very prevalent in the majority of this outcrop, and the outcrop has a very "hot" gamma-ray signature relative to other locations. However, there does not appear to be a direct correlation between apatite beds and hot gamma-ray signatures.

There are some possible sampling errors in the gamma-ray measurements at this location. Measurements in section JL1A and those at the base of JL1B were taken in trenched areas. Therefore, these measurements are suspected to be anomalously high. The top of JL1B and the bottom of JL2 overlap each other for 1.0ft. The top of JL1B has gamma-ray measurements that are lower than those at the base of JL2. This difference in

40
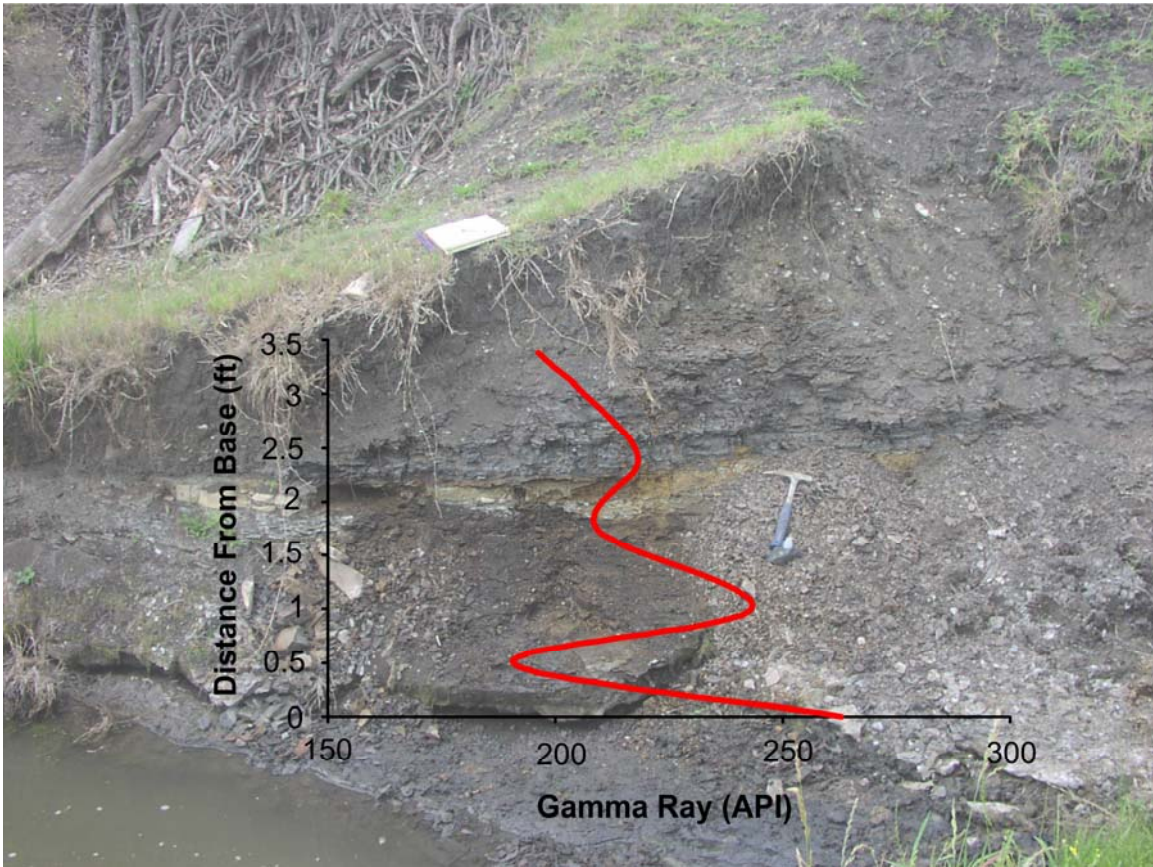
Figure 4.2 Photograph of Richard's Farm outcrop 2 with overlay of gamma-ray profile. Gamma-ray measurements were taken every 0.5 ft.
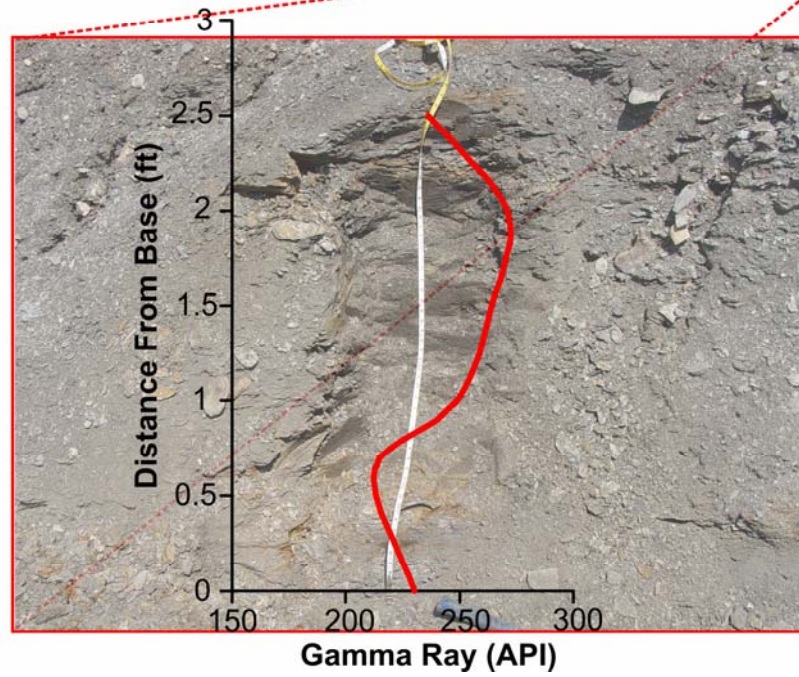
Figure 4.3 Photograph of Jeff Luke shale pit Section 1A with overlay of gamma-ray profile. Gamma-ray measurements were taken every 0.5 ft.

Figure 4.4 Photograph of Jeff Luke shale pit Section 1B with overlay of gamma-ray profile. Gamma-ray measurements were taken every 0.5 ft.
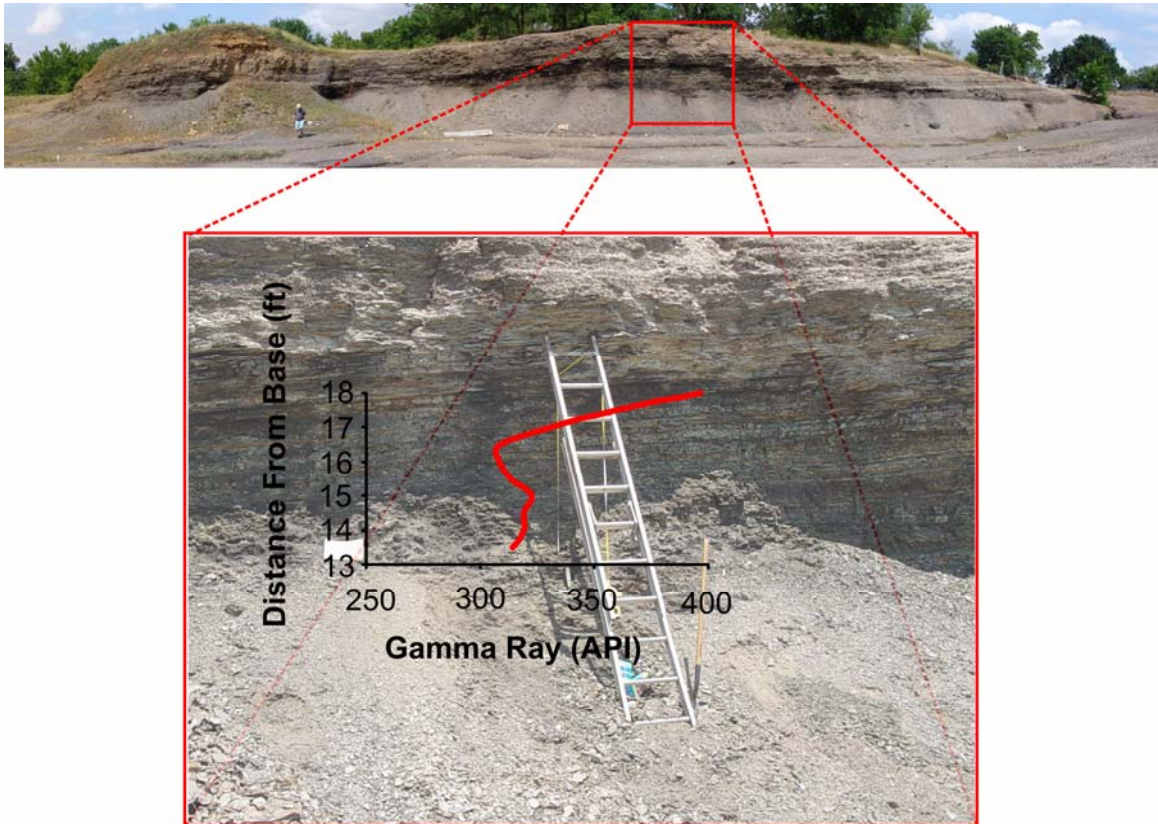
Figure 4.5 Photograph of Jeff Luke shale pit Section 2 with overlay of gamma-ray profile. Gamma-ray measurements were taken every 0.5 ft.
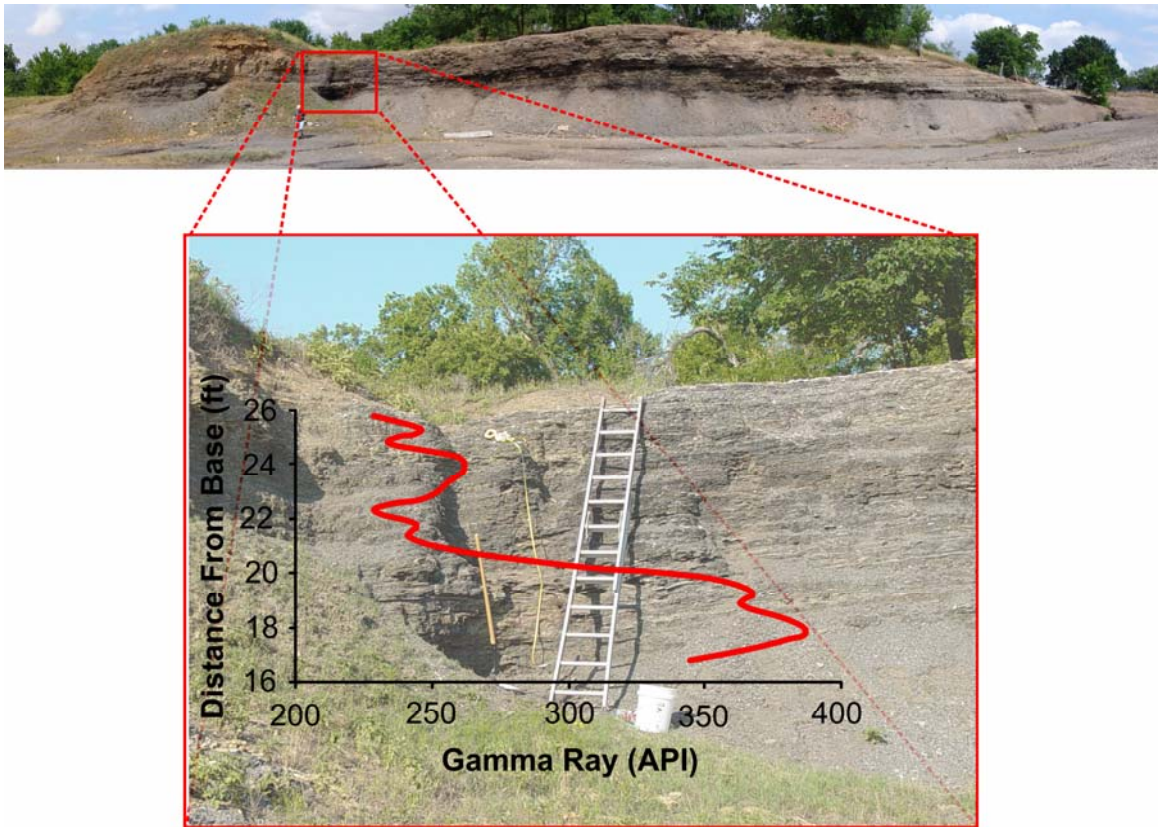
Figure 4.6 Photograph of Jeff Luke shale pit Section 3 with overlay of gamma-ray profile. Gamma-ray measurements were taken every 0.5 ft.
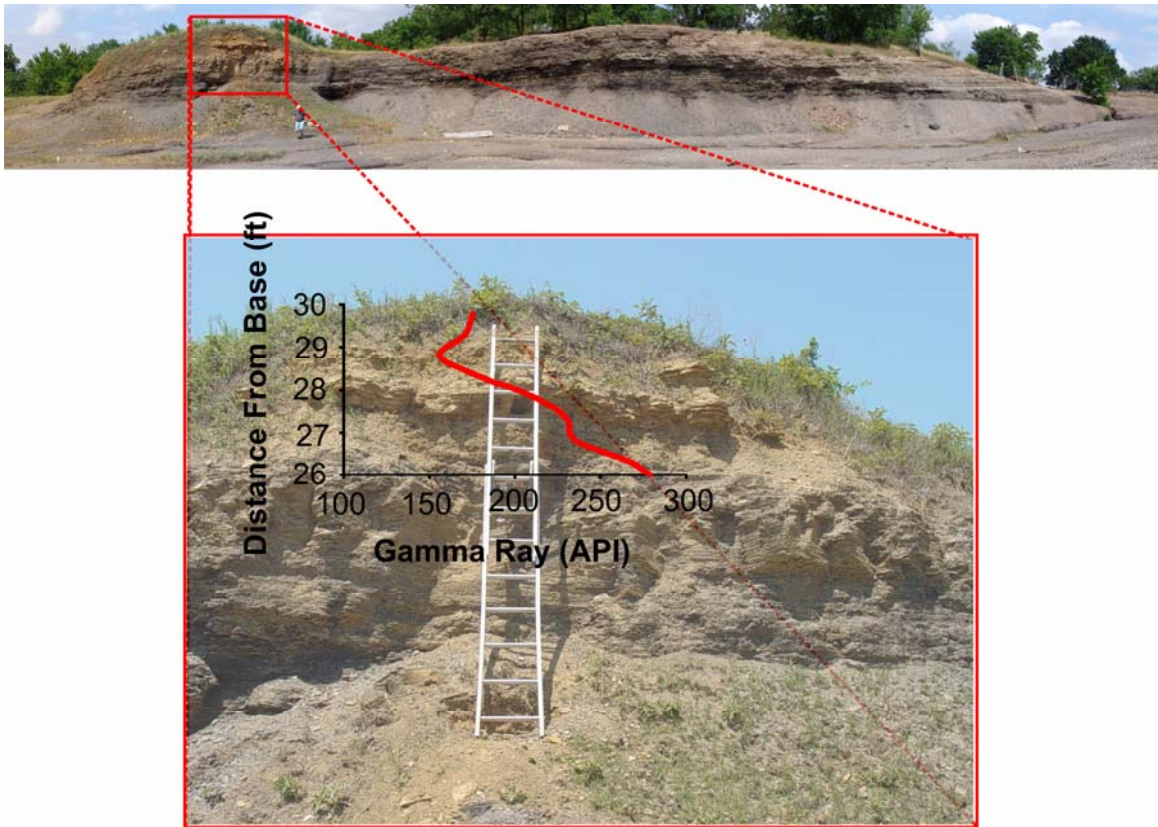
Figure 4.7 Photograph of Jeff Luke shale pit Section 4 with overlay of gamma-ray profile. Gamma-ray measurements were taken every 0.5 ft.

gamma-ray readings in interpreted to be a result of weathering at the top of JL1B. In addition, section JL4 consists of a heavily weathered soily shale. According to Olson (1982) weathering of shale tends to decrease uranium content, but he (ibid) did not attempt to quantify by how much uranium was reduced. As a result, gamma-ray measurements at the top of JL1B and at JL4 are considered to be lower due to weathering.

4.4 Hass G Outcrop

The Hass G outcrop covers the boundary between the Woodford shale, pre-Welden Shale, Welden Limestone, and the "Mayes" formation (lower Caney Shale). A picture of this outcrop with the gamma-ray response superimposed on the photo is contained in Figure 4.8. As noted in the figure, the Woodford Shale has high gamma-ray readings that peak to 380 API units at the boundary of the Woodford Shale and pre-Welden shale. From the pre-Welden Shale into the Welden Limestone gamma-ray readings decrease to 50-to-60 API units. The gamma-ray response increases to 180-to-200 API units in the "Mayes" formation (lower Caney Shale). Gamma-ray response in the "Mayes" formation (lower Caney Shale) at this locality may be reduced as a result of weathering. Most of the "Mayes" (lower Caney Shale) required excavation to uncover shale that was slightly weathered. This weathering according to Olson (1982) reduces the amount of total uranium in the rock.

4.5 Delaware Creek Outcrop
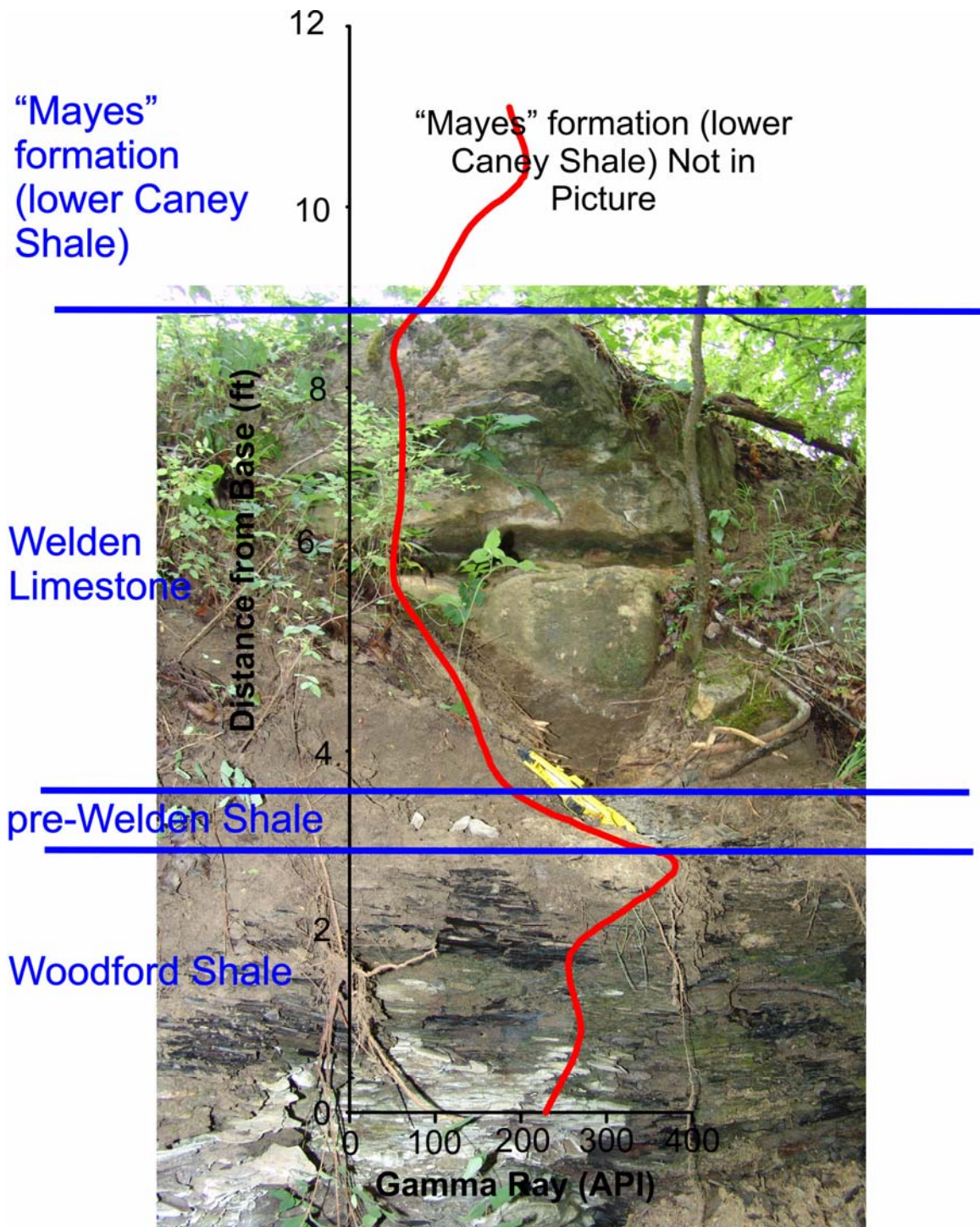
Figure 4.8 Photograph of Hass G outcrop with overlay of gamma-ray profile. This outcrop contained the contacts between the Woodford Shale, pre-Welden Shale, Welden Limestone and "Mayes" (lower Caney Shale). Gamma-ray measurements were taken every 0.5 ft.

A picture of this outcrop with the gamma-ray response superimposed on the photo is contained in Figure 4.9. At this outcrop there was a high gamma-ray response at the base (Unit 1), but the majority of the outcrop, comprised in Unit 2, has an average response of approximately 140 API units. The large gamma-ray response at the base of the outcrop peaks at 424.8 API units. This peak occurs about 1.0 ft from the base of the outcrop and correlates to a non-calcareous shale with abundant apatite nodules located at this point. Apatite nodules are also noted at 1.4 ft from the base, but the gamma-ray measurement at 1.5 ft has a much lower gamma-ray response of 241.2 API units.

4.6 Little Delaware Creek Outcrop 1

This first outcrop on Little Delaware Creek has a high gamma-ray response at the base similar to the Delaware Creek outcrop. The gamma-ray curve is superimposed on top of a photo of this outcrop in Figure 4.10. The top of the outcrop, Units 1-3, has a gamma-ray response that is generally between 200 and 220 API units. The remaining outcrop down to Unit 9 has a gamma-ray response generally between 180 and 170 API units. The base of the outcrop has a response of 341.2 API units and corresponds to the base of Unit 9. Unit 9 is a non-calcareous black shale with silt.

4.7 Little Delaware Creek Outcrop 2

The second outcrop exposure along Little Delaware Creek has a similar gamma-ray pattern as DC and LDC1.   This outcrop again has the highest gamma-ray response (281.8 API units) at the base of the exposure. A photo of this outcrop with the gamma-ray curve superimposed on it is contained in Figure 4.11. This hot peak at the base
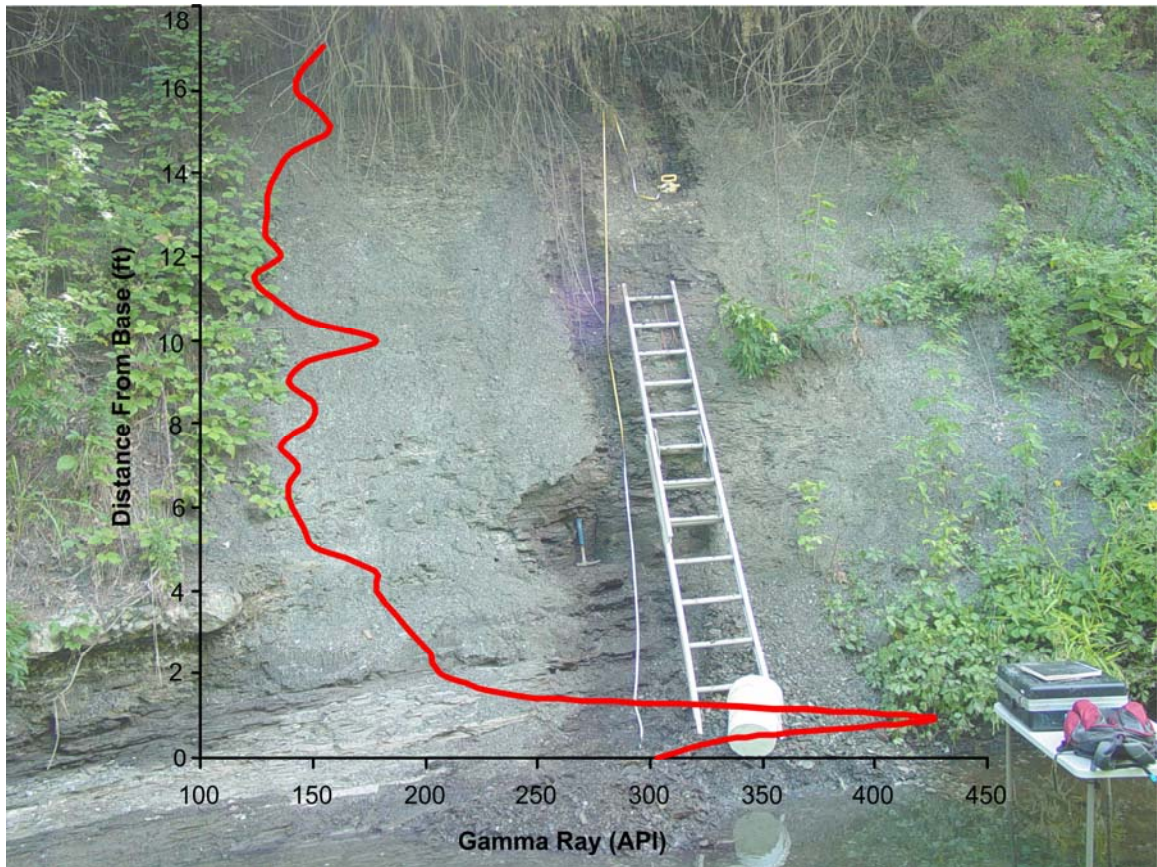
Figure 4.9 Photograph of Delaware Creek outcrop with overlay of gamma-ray profile. Gamma-ray measurements were taken every 0.5 ft.
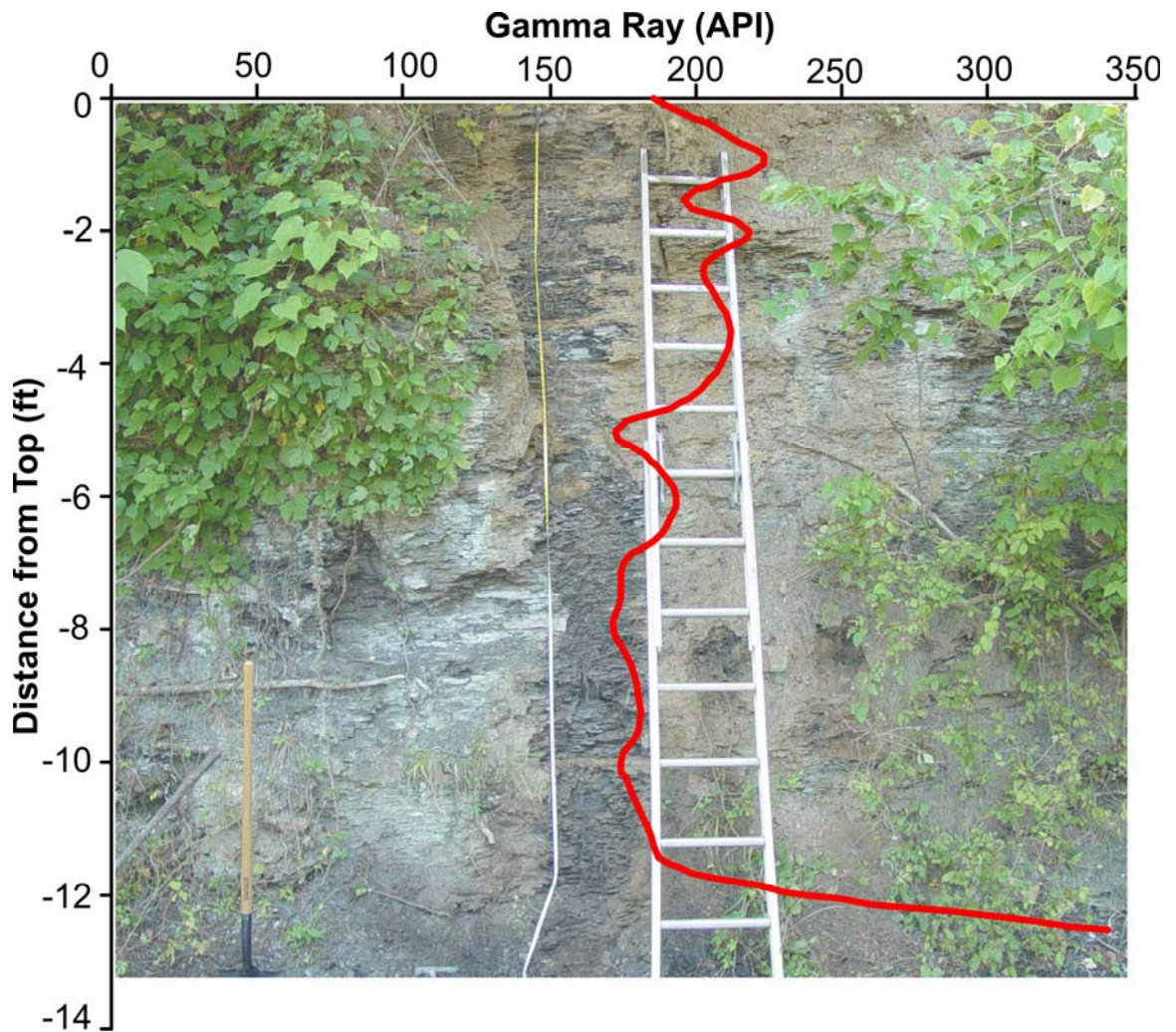
Figure 4.10 Photograph of Little Delaware Creek outcrop 1 with overlay of gamma-ray profile. Gamma-ray measurements were taken every 0.5 ft.
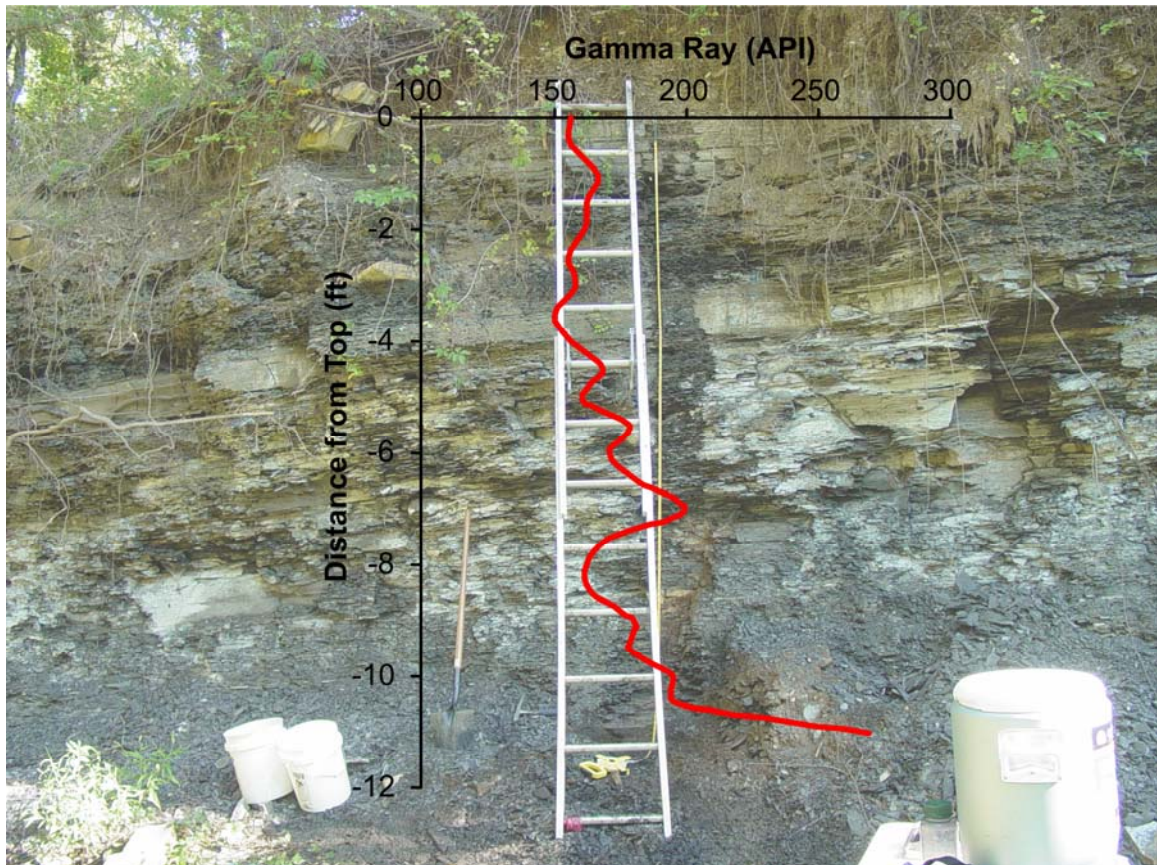
Figure 4.11 Photograph of Little Delaware Creek outcrop 2 with overlay of gamma-ray profile. Gamma-ray measurements were taken every 0.5 ft.

corresponds to Unit 6 in the outcrop. Unit 6 is non-calcareous, contains no silt, and has

brachiopod and mollusk impressions (Figure 4.12). The remaining outcrop has a gamma-

ray response between 150-180 API units, and there is a slight peak to 199.2 API units at

7.0 ft from the top of the outcrop.

The occurrence of a larger gamma-ray spike at the base of the section multiple

times could possibly indicate that these hotter shales are more resistant to weathering.

The shales at each of these three locations, DC, LDC1, and LDC2, are all non-calcareous.

However, other shales in these exposures are also non-calcareous and are not as resistant

to weathering. So, carbonate content does not seem to be the controlling factor.

4.8 Little Delaware Creek Outcrop 3

The third outcrop exposure along Little Delaware Creek did not have a large

gamma-ray spike at the base of the exposure. A photo of this outcrop with the gamma-

ray curve superimposed on it is contained in Figure 4.13. The gamma-ray response was

fairly consistent throughout this section. All of the gamma-ray measurements ranged

between approximately 150 and 200 API units.

4.9 Little Delaware Creek Outcrop 4

A photo of the fourth exposure along Little Delaware Creek with the gamma-ray

curve superimposed on it is contained in Figure 4.14. The gamma-ray response at this

outcrop was again fairly consistent. The top of the outcrop in Unit 1 has a slight gamma-

ray peak of 236.0 API units, but then drops quickly down to approximately 200 API units

in the rest of the Unit 1. This outcrop contained a carbonate concretionary bed between

Figure 4.12 Fossil impressions found in Unit 6 at the base of the Little Delaware Creek outcrop 3.
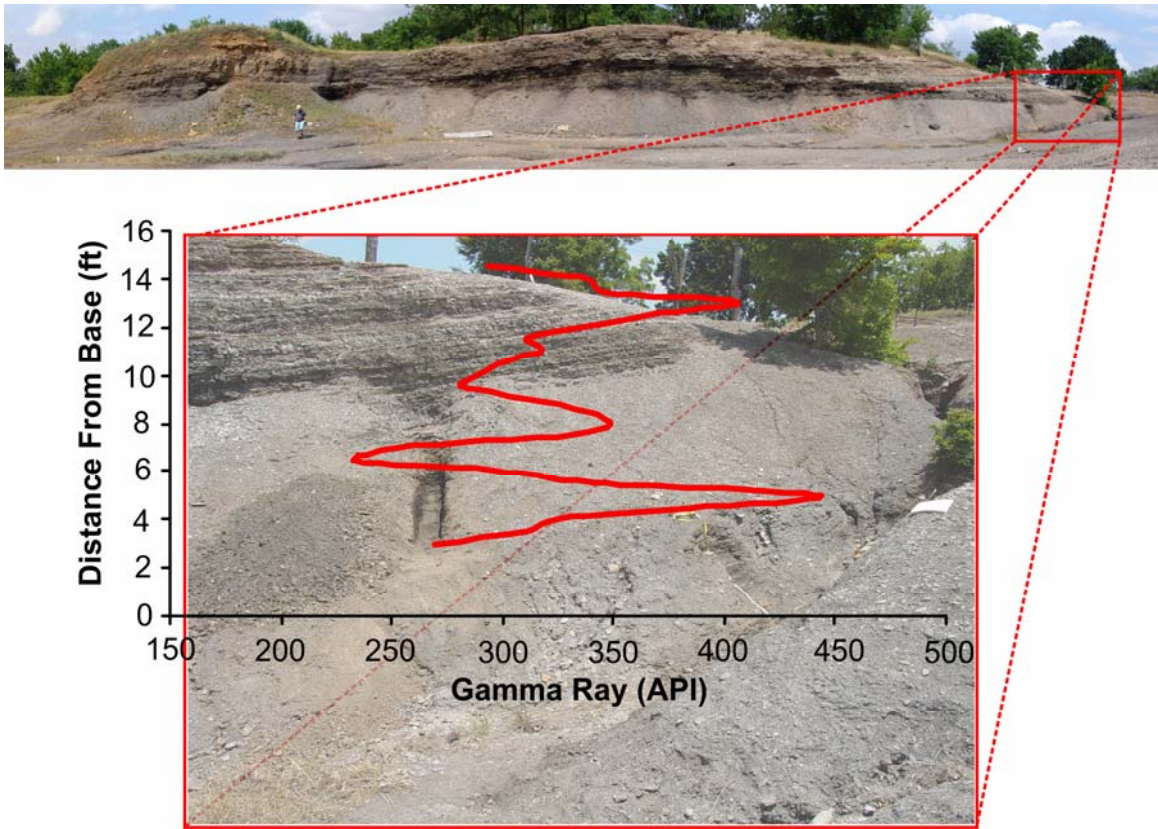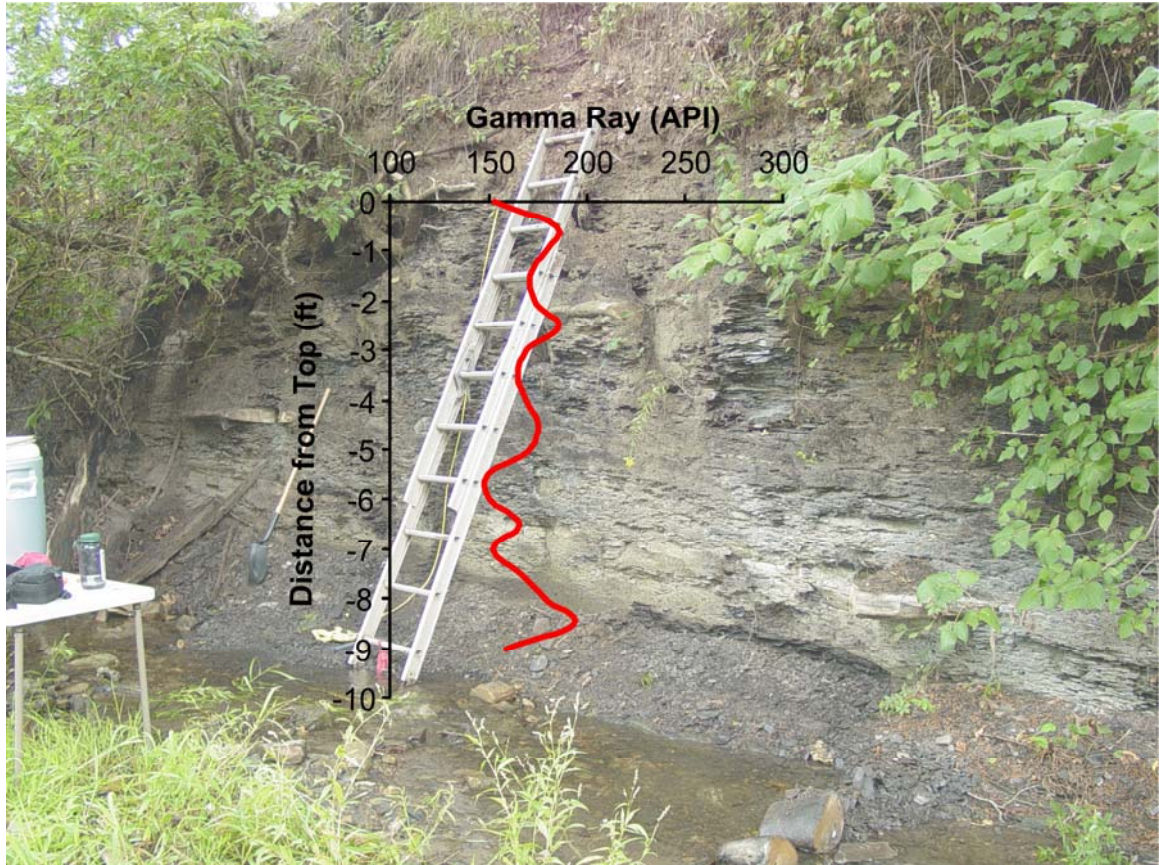
Figure 4.13 Photograph of Little Delaware Creek outcrop 3 with overlay of gamma-ray profile. Gamma-ray measurements were taken every 0.5 ft.
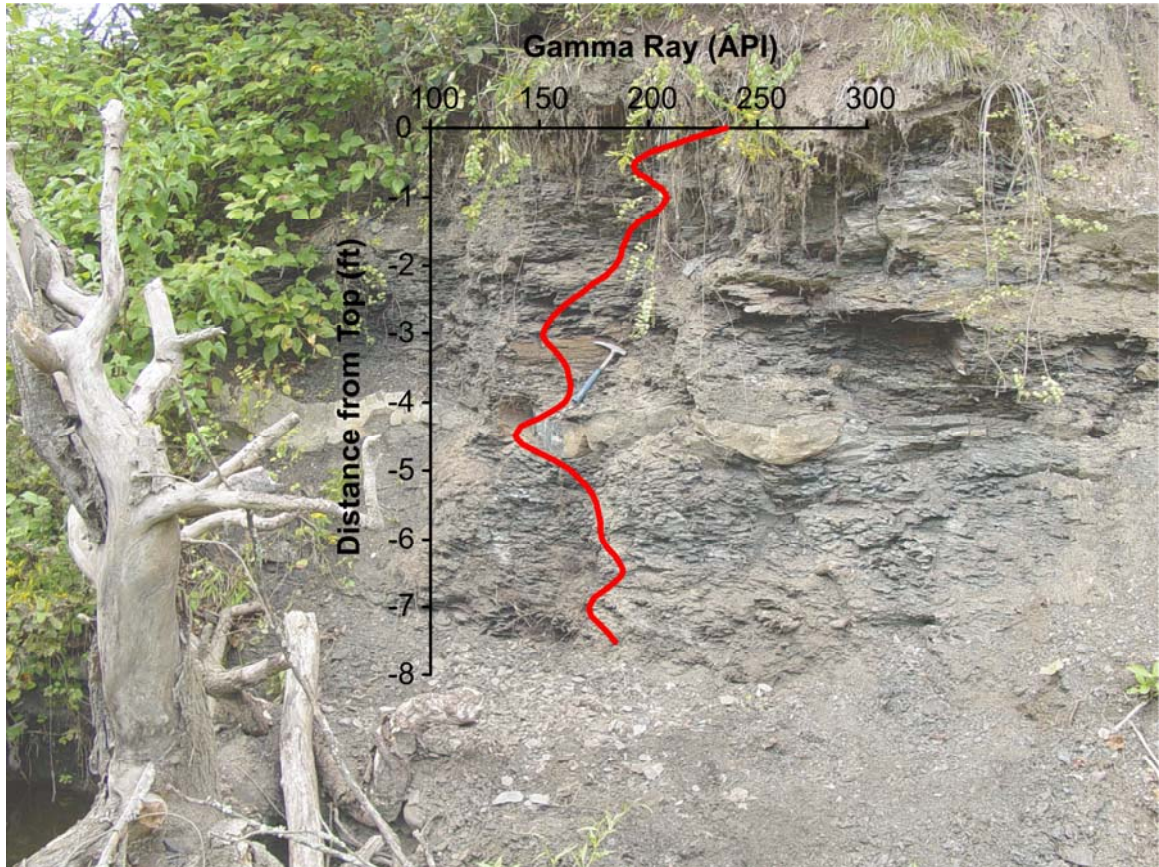
Figure 4.14 Photograph of Little Delaware Creek outcrop 4 with overlay of gamma-ray profile. Gamma-ray measurements were taken every 0.5 ft.

4.1 and 4.7 ft from the top of the outcrop. This bed had the lowest gamma-ray response

at 139.2 API units. Gamma-ray response increases over 160 API units above and below

this bed.

4.10 Pine Top Mountain Outcrop

The Pine Top Mountain outcrop is divided up into seven sections. The divisions

for these sections are based on field equipment and topography limitations, and do not

necessarily represent lithologic changes. However, because the seven sections are

discussed independently in Appendix I, they are discussed independently here.

4.10.1 Pine Top Mountain Section 1

This section consists of a resistant shale that resembles Woodford Shale lithology

at first glance. However, the gamma-ray response for this section is much lower than the

typical gamma-ray response of Woodford Shale. The Woodford Shale typically has a

gamma ray reading that averages around 360 API units (Krystyniak, 2005). Figure 4.15

contains a picture of this section with the gamma-ray profile superimposed on the photo.

The gamma-ray response for this section ranges between 110 and 190 API units. The

section appears fairly uniform throughout, but there is variation in the gamma-ray

response. Carbonate nodules were noted to occur at 14.9-to-15.6 ft and 23.5-to-24.0 ft.

There is a decrease in the gamma-ray response at both of these intervals, but it is difficult

to distinguish them from other decreases in gamma-ray response that are not associated

with nodules.
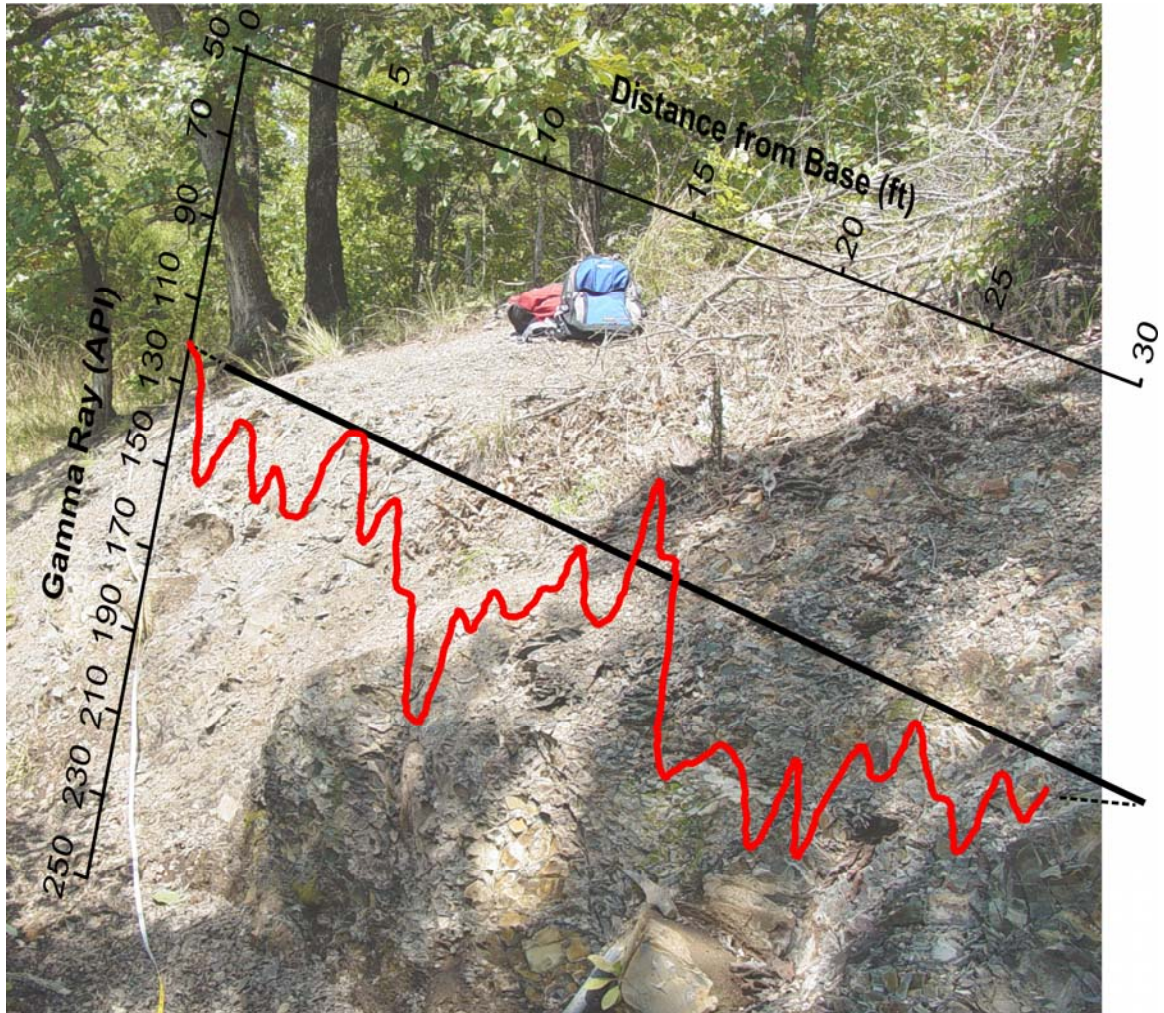
Figure 4.15 Photograph of Pine Top Mountain outcrop Section 1 with overlay of gamma-ray profile. At this location, the distance away from the outcrop that a picture could be taken was limited by vegetation and topography. As a result, this picture is skewed to the left. Gamma-ray measurements were taken every 0.5 ft.

4.10.2 Pine Top Mountain Section 2

Figure 4.16 contains a photo of this section with the gamma-ray profile

superimposed on it. This section has a gamma-ray profile that generally increases from

bottom to top. At the top of the section this trend changes to a large decrease in gamma-

ray response. In this section gamma-ray response varies from 80 to 215 API units.

Within the section there are dolomitic silty mudstone beds at 5.6-6.4 ft, 16.75-17.16 ft,

and 41.7-42.9 ft. The gamma-ray response at each of these locations is depressed from

the responses above and below them. However, it is difficult to distinguish these

depressions from other gamma-ray lows in the section. Apatite nodules were recorded at

the contact between this section and PT1; however, there is no notable response in the

gamma ray at this location that could be attributed to apatite.

4.10.3 Pine Top Mountain Section 3

This small section shows a gamma-ray response that has a decreasing upward

trend. Figure 4.17 contains a photo of this section with the gamma-ray profile

superimposed on it. The gamma-ray response in this section varies from approximately

210 to 140 API units. Apatite nodules were recorded at 4.6 and 6.0 ft; however, there is

no identifiable response in the gamma ray at these locations.

4.10.4 Pine Top Mountain Section 4

A photo of this section with the gamma-ray profile superimposed on it is

contained in Figure 4.18. This section has a fairly uniform appearance in outcrop, but the

gamma-ray profile does not have a uniform character. The gamma-ray response in this
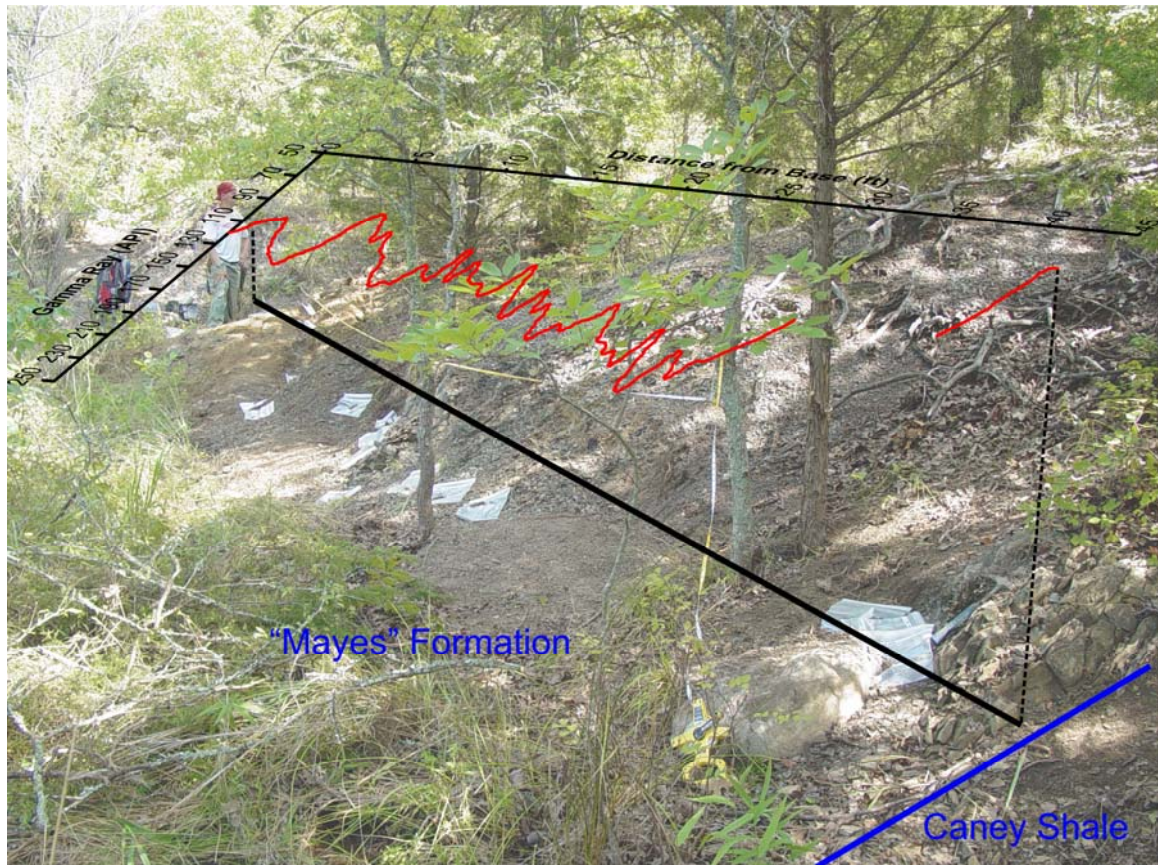
Figure 4.16 Photograph of Pine Top Mountain outcrop Section 2 with overlay of gamma-ray profile. At this location, the distance away from the outcrop that a picture could be taken was limited by vegetation and topography. As a result, this picture is skewed to the left. The top of this section marks the contact between the "Mayes" Formation and Caney Shale. Gamma-ray measurements were taken every 0.5 ft.
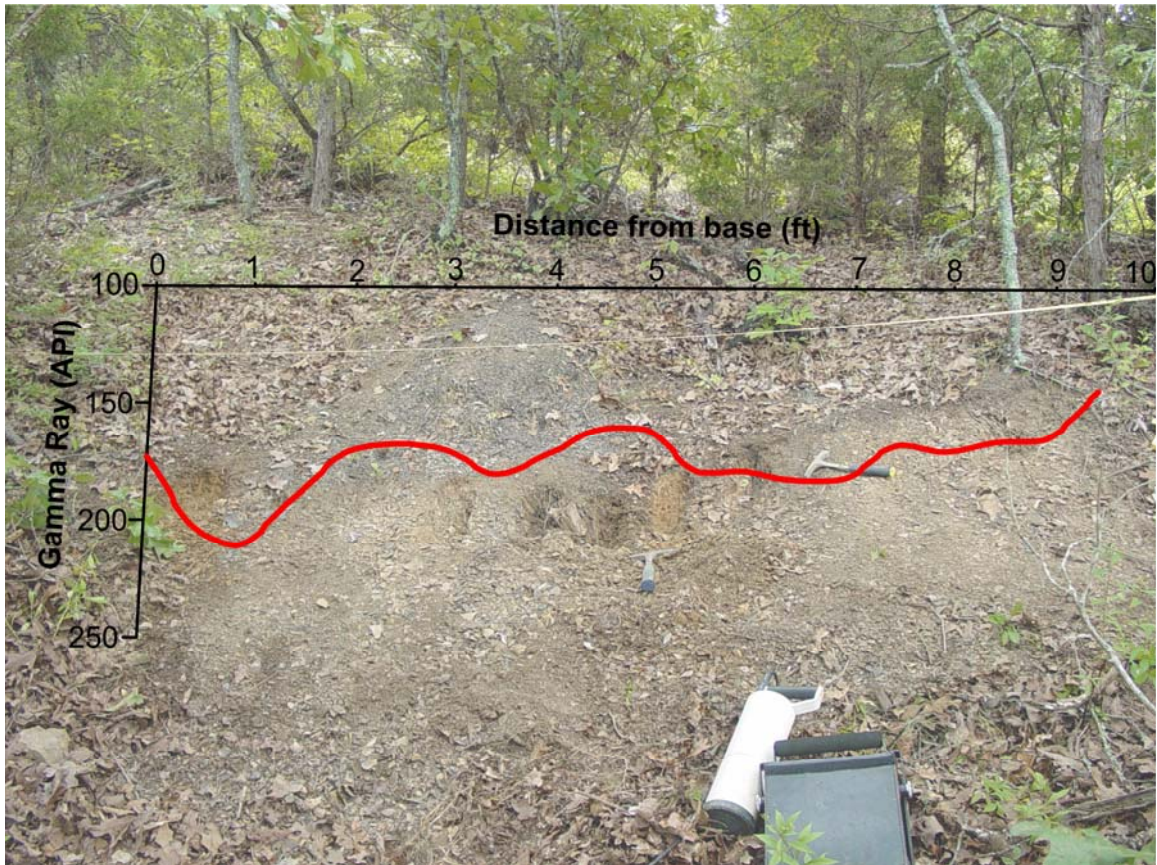
Figure 4.17 Photograph of Pine Top Mountain outcrop Section 3 with overlay of gamma-ray profile. Gamma-ray measurements were taken every 0.5 ft.
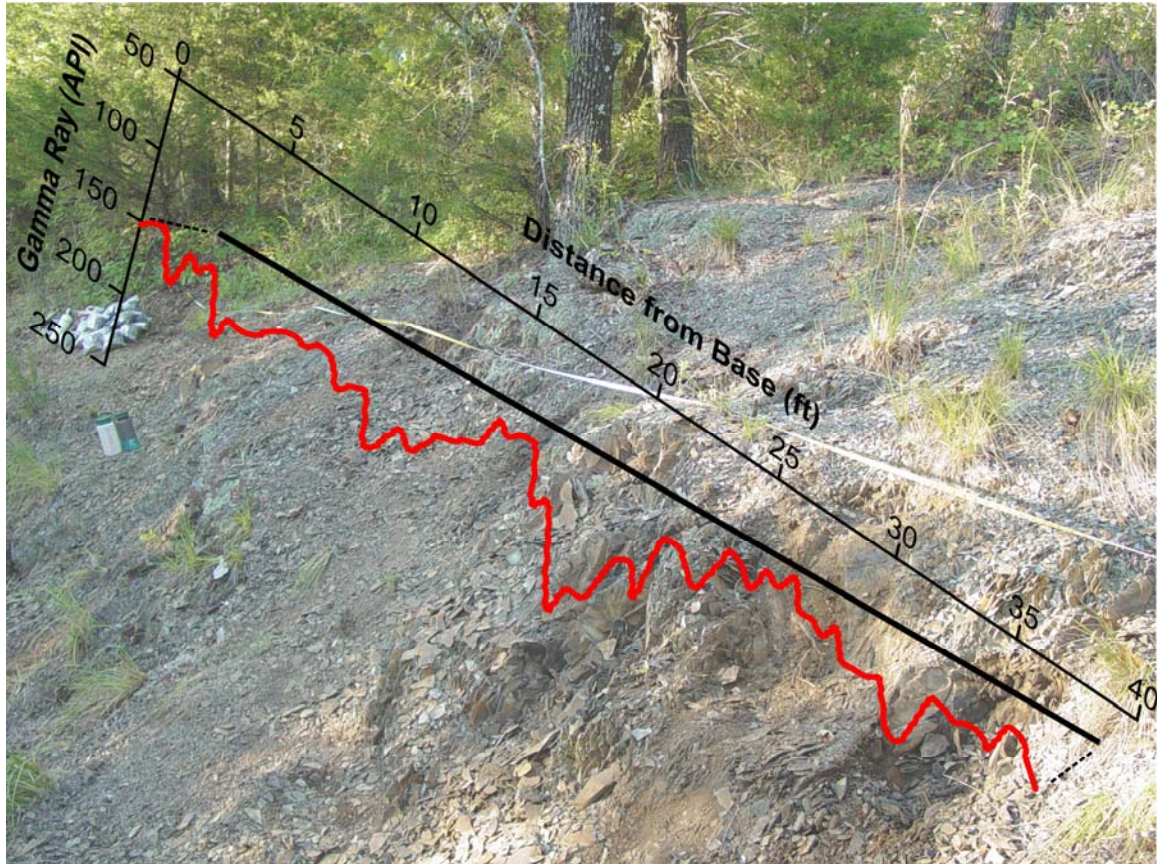
Figure 4.18 Photograph of Pine Top Mountain outcrop Section 4 with overlay of gamma-ray profile. At this location, the distance away from the outcrop that a picture could be taken was limited by vegetation and topography. As a result, this picture is skewed to the left. Gamma-ray measurements were taken every 0.5 ft.

section ranges from approximately 100 to 220 API units. Several gamma-ray peaks are present with the largest occurring at 18.0 ft from the base of the section. In this section apatite nodules were recorded at 6.1, 6.5, 9.95, 11.0, 11.8, 14.4, 15.0, 15.8, 16.2, 23.8, 24.7, and 33.6 ft; however, there was no identifiable response in the gamma ray at these locations, suggesting that apatite is not sequestering uranium.

4.10.5 Pine Top Mountain Section 5

Figure 4.19 contains a photo of this section with the gamma-ray profile superimposed on the photo. This section has a very uniform lithology that is very similar in lithology to PT4. However, the gamma-ray response is less variable and more uniform than the response in PT4. Gamma-ray response varies between approximately 130 and 170 API units. In this section, apatite nodules were recorded at 4.1, 10.5, 15.0, 15.5, 17.2, and 20.5 ft, and a carbonate concretion at 2.95 ft; however, there is no identifiable response in the gamma ray at these locations.

4.10.6 Pine Top Mountain Section 6

This small section has a gamma-ray response that varies between approximately 120 and 190 API units. Figure 4.20 contains a photo of this section with the gamma-ray profile superimposed on the photo. An apatite nodule was recorded at 2.8 ft from the bottom of the section, but does not correlate to any particular response in the gamma ray.

4.10.7 Pine Top Mountain Section 7

63
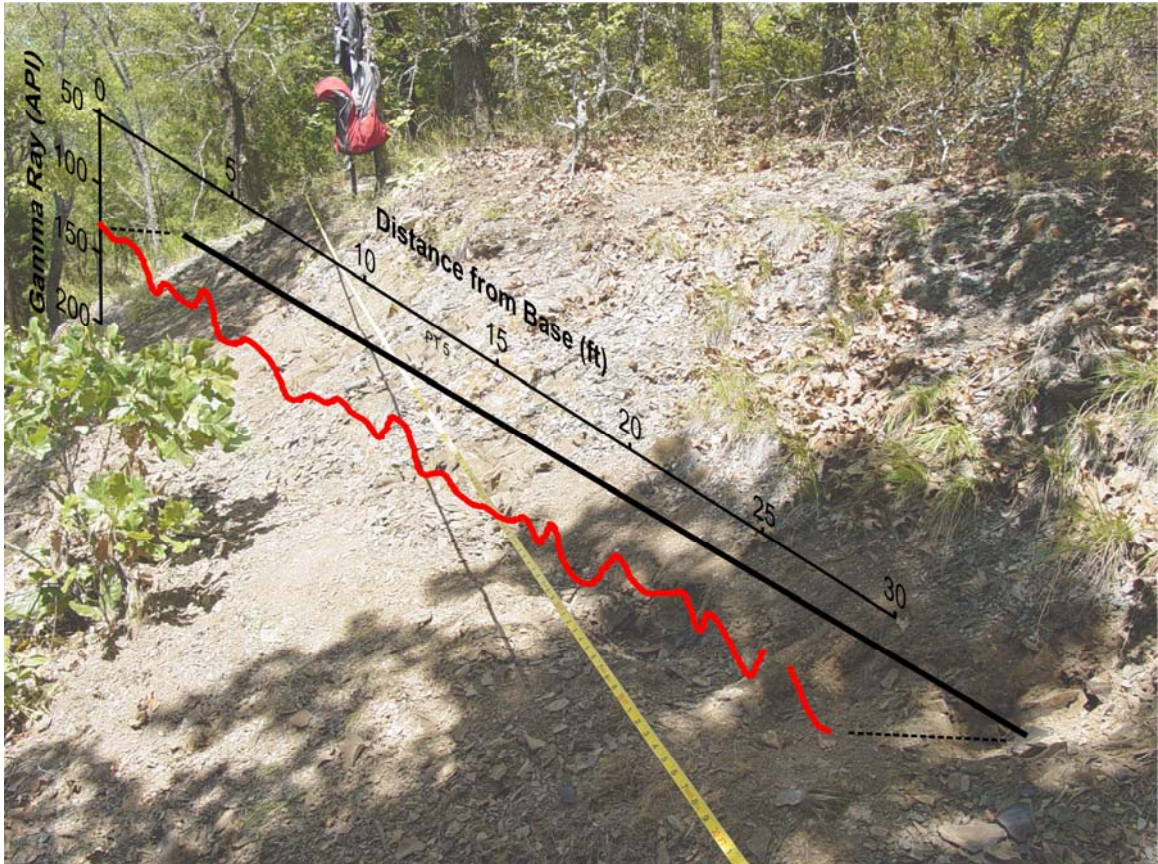
Figure 4.19 Photograph of Pine Top Mountain outcrop Section 5 with overlay of gamma-ray profile. At this location, the distance away from the outcrop that a picture could be taken was limited by vegetation and topography. As a result, this picture is skewed to the left. Gamma-ray measurements were taken every 0.5 ft.

64
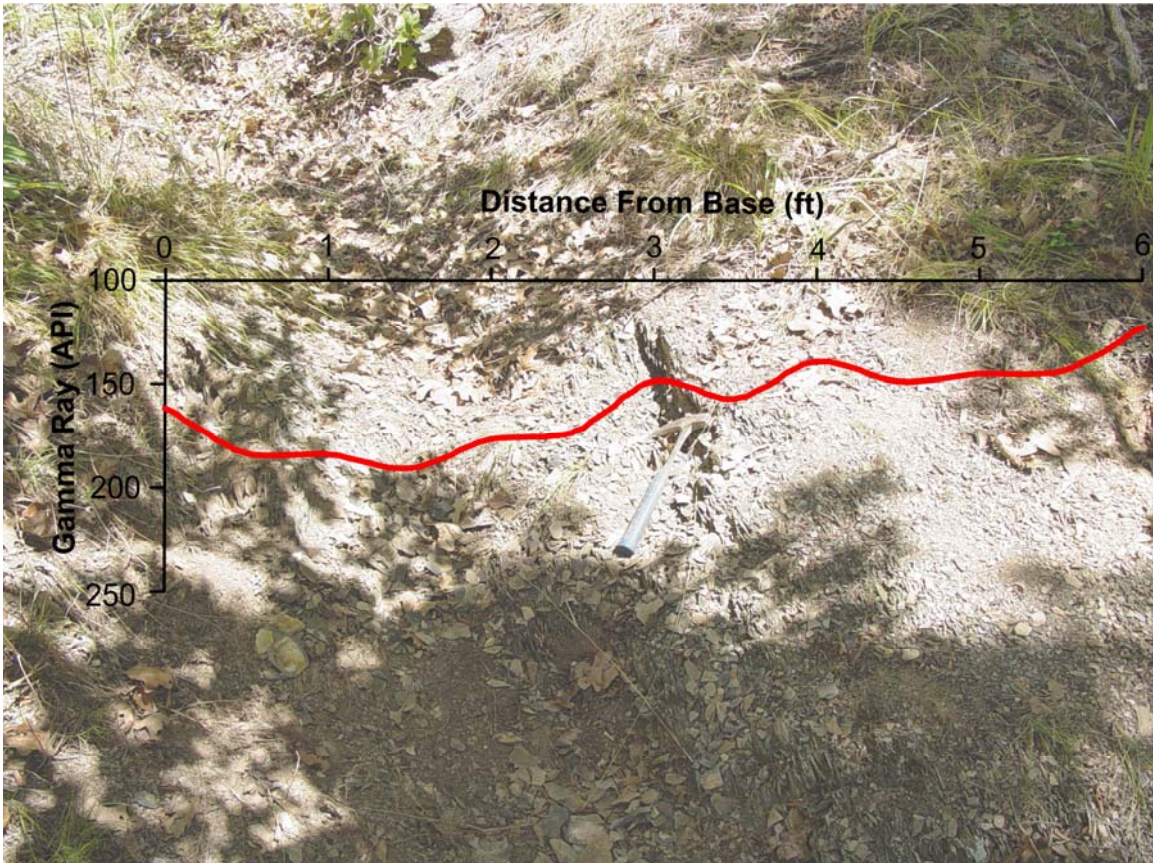
Figure 4.20 Photograph of Pine Top Mountain outcrop Section 6 with overlay of gamma-ray profile. Gamma-ray measurements were taken every 0.5 ft.

This last section has a gamma-ray response that varies between approximately 85 and 150 API units. A photo of this section with the gamma-ray profile superimposed on it is contained in Figure 4.21. This section shows a general increasing upward trend.
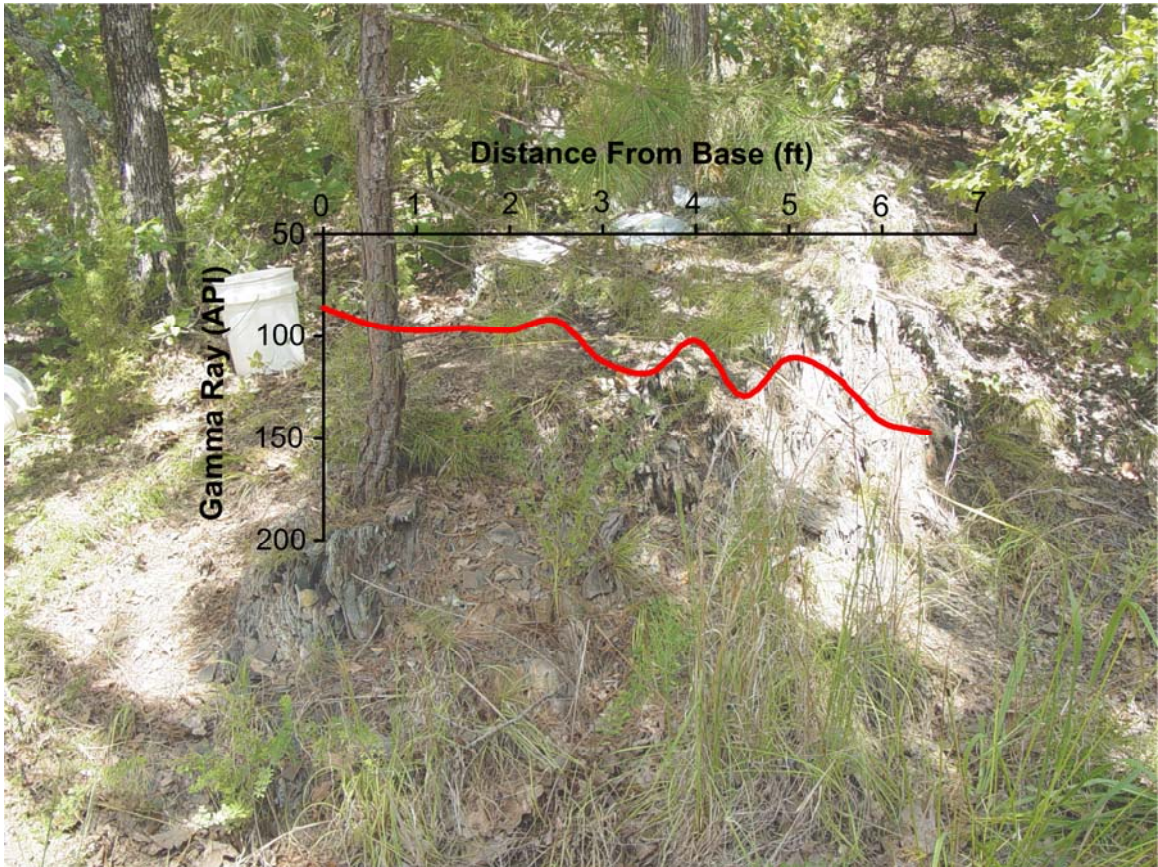
Figure 4.21 Photograph of Pine Top Mountain outcrop Section 7 with overlay of gamma-ray profile. Gamma-ray measurements were taken every 0.5 ft.

CHAPTER 5.0

SURFACE TO SUBSURFACE OUTCROP CORRELATION

The gamma-ray scans from the outcrops studied in this work were correlated to gamma-ray logs from closest subsurface wells. In these correlations the gamma-ray pattern from the outcrops were matched the gamma-ray pattern from the subsurface. The exact measured API values from the surface and subsurface generally did not match in any of the wells. This is possibly a result of a weathering, instrument calibrations, and radiation received by secondary sources. As a result, the gamma-ray reading by the scintillometer used to measure outcrops are generally higher than those from the subsurface. Since weathering and radiation received from secondary sources is variable at each outcrop location, quantifying how much higher the scintillometer measurements are expected to be at outcrop is difficult. Despite these higher gamma-ray readings by the scintillometer, Krystyniak (2005) was able to show that pattern matching between surface and subsurface gamma-ray readings was possible. In the figures discussed below, which show the correlation between surface and subsurface gamma rays, it is important to note that the outcrop gamma-ray scans have been plotted over the subsurface gamma-ray measurements in order to establish a pattern match. The gamma-ray measurements from the outcrops are not directly relatable to the API scale for each subsurface log shown on the x-axis in the figures.

5.1 Lawrence Uplift Outcrop Area

Two of the four outcrops exposed on the Lawrence Uplift (JL and HG) were combined in a composite section and correlated to the nearest well (Rollow #1) in Figure 5.1). This well is located in section 29 of Township T3N, R6E, and is approximately 4 miles east of the outcrops. The two outcrops exposed on Richard's Farm were both small exposures. Outcrop 1 was 3.35 ft thick and outcrop 2 was 3.32 ft thick. These small outcrops were difficult to fit to the gamma-ray log from the Rollow #1 well. As a result, a direct correlation to the subsurface could not be made. However, according to the geologic map by Johnson (1990), the Richard's Farm locality is near the contact between the Woodford and the "Mayes" (lower Caney Shale). From this map and descriptions of the "Mayes" formation (lower Caney Shale) by Elias (1956), Elias and Branson (1959), and Champlin (1959) the outcrops exposed at the Richard's Farm locality are indeed those of the "Mayes" (lower Caney Shale).

The Jeff Luke shale pit provided a thick well exposed section of the Caney Shale. This section had gamma-ray readings well over 150 API units and was easily correlated to the Rollow #1 well (Figure 5.1). This section correlates to the upper section of the Caney Shale on the log that is more radioactive than the rest of the formation. The correlation between the outcrop and subsurface gamma rays was very good, and the author is confident that stratigraphic location of this section is accurate.

The Hass G outcrop gamma-ray scan was easily matched to the subsurface gamma ray from the Rollow #1 well (Figure 5.1). This outcrop was only 11.38 ft thick and so only a small gamma-ray curve composite was available for the correlation. The
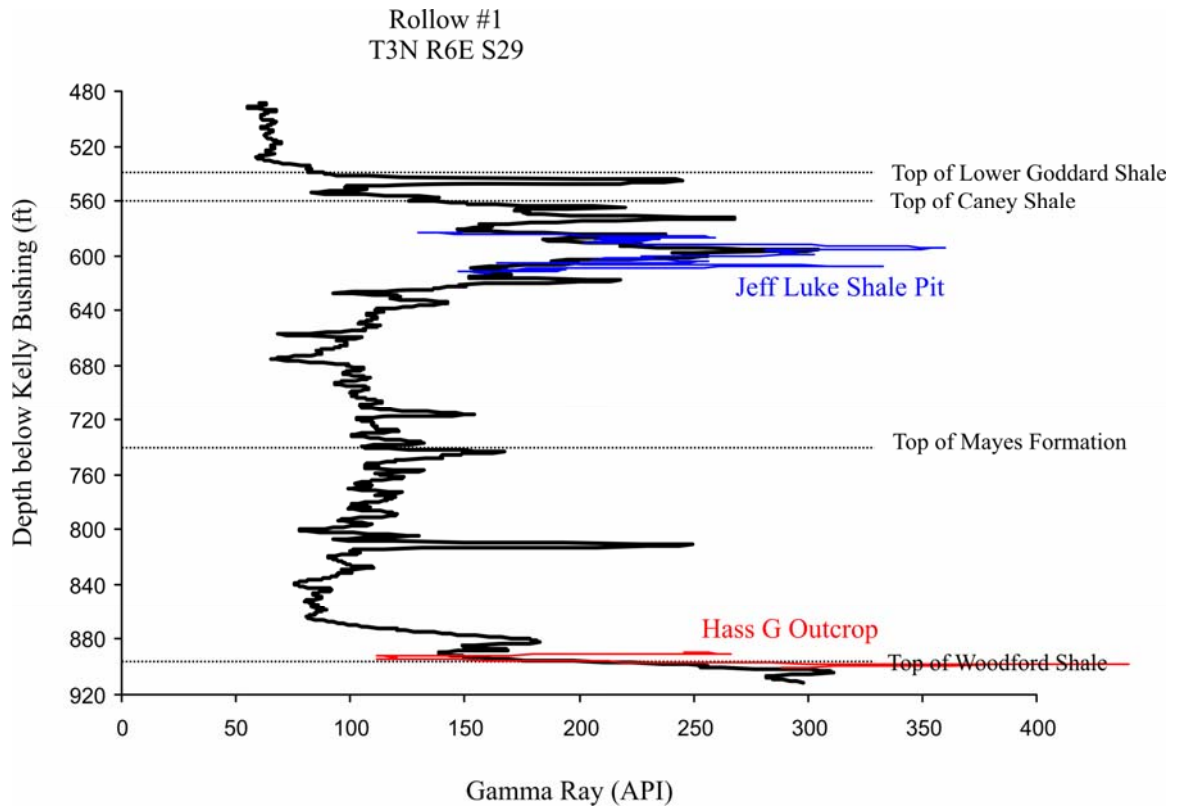
Figure 5.1 Gamma-ray correlation from the outcrops exposed on the Lawrence Uplift to the gamma ray log from the Rollow #1 well. This well is located about four miles east of the outcrops. The Jeff Luke shale pit and the Hass G outcrop both match the subsurface gamma ray well. The two outcrops exposed at Richard's Farm were too small to be accurately matched the subsurface gamma ray.

match for this gamma-ray section was further reinforced by the coincidence of the top of the Woodford Shale, which has a distinctively high gamma-ray signature, in both the surface and subsurface.

5.2 Bromide Outcrop Area

The Delaware and Little Delaware Creek outcrops were combined into a composite section and correlated to the Jobe 1-17 well. This well is located in section 17 of township T2S, R8E, and is approximately 3 miles east of the outcrops. Strike and dip measurements were taken in this outcrop area in order construct a composite section of the five outcrops measured. After reconstruction, the gamma-ray responses from the outcrops could not be matched accurately to the gamma-ray response in the subsurface. The geologic map by Johnson (1990) indicates that faults do exist at the outcrop location; thus, making a construction of a composite section from strike and dip measurements possibly inaccurate. Therefore, the gamma-ray readings were matched to the gamma-ray from the nearby well independently of one another.

The Delaware Creek outcrop correlated to the boundary between the Caney Shale and lower Goddard Shale (Figure 5.2). According to the correlation, this boundary occurs approximately 5 ft from the base of the measured section. In this correlation the outcrop gamma ray mimics the well gamma ray closely, and so the correlation from surface to subsurface is thought to be accurate.

The first outcrop exposed along Little Delaware Creek is correlated the subsurface gamma ray in Figure 5.2. According to this correlation, the outcrop is stratigraphically higher than the Delaware Creek outcrop, and slightly overlaps the
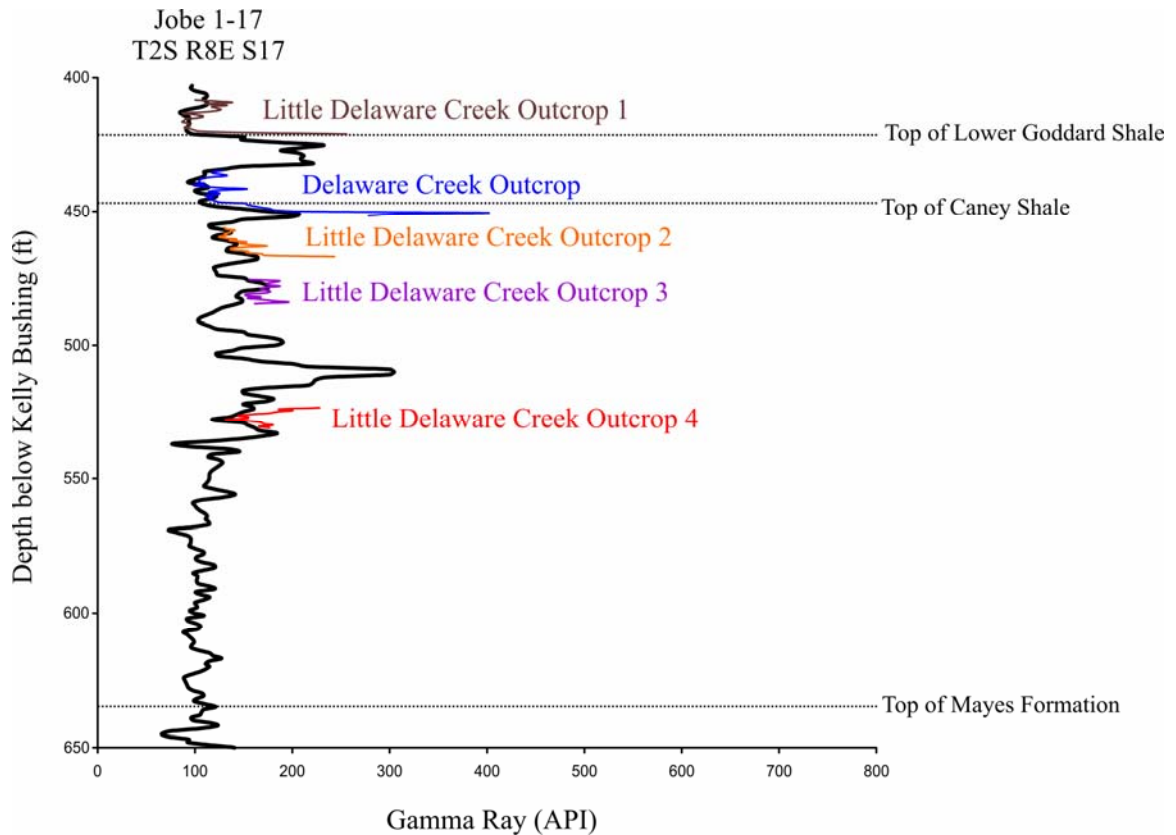
Figure 5.2 Gamma-ray correlation from the outcrops exposed near Bromide, OK to the gamma ray log from the Jobe 1-17 well. This well is located about three miles east of the outcrops. The outcrops exposed on the Delaware Creek and Little Delaware Creek all match the subsurface gamma ray well.

boundary between the lower Goddard and upper Goddard. This contact is referred to as the "false Caney" by geologists in the petroleum industry. The boundary between these two intervals occurs approximately 0.5 to 1 ft above the base of this outcrop. As before, this gamma-ray correlation is good with the outcrop gamma ray mimicking the subsurface gamma ray well.

The Little Delaware Creek outcrops 2, 3, and 4 all correlate to the upper half of the Caney Shale (Figure 5.2). Outcrop 2 is the highest stratigraphically and outcrop 4 is the lowest.   These three outcrops are fairly small, and hence, the profiles are difficult to correlate with. However, the outcrop gamma-ray profiles have a good pattern match with the subsurface.

5.3 Pine Top Mountain Outcrop Area

The Pine Top Mountain outcrop was correlated to the Blue Creek 1-7 well located in section 7 of township T2N, R14E. This well is approximately 8 miles west, southwest of the outcrop. This outcrop provided the largest continuous gamma-ray scan that could be correlated to the subsurface. These correlations are in Figure 5.3 below. The Caney Shale and "Mayes" formation (lower Caney Shale) are both thinner in the Pine Top Mountain outcrop than the Blue Creek 1-7 well. To compensate for this thinning the 7 sections exposed in at this outcrop were pattern matched independently of the measured thickness between the outcrops.

The gamma-ray correlations according to pattern matching for this well are not as good as those correlations at the other outcrop locations discussed above. However, overall the gamma ray of the outcrop matches fairly well to the gamma ray in the

73
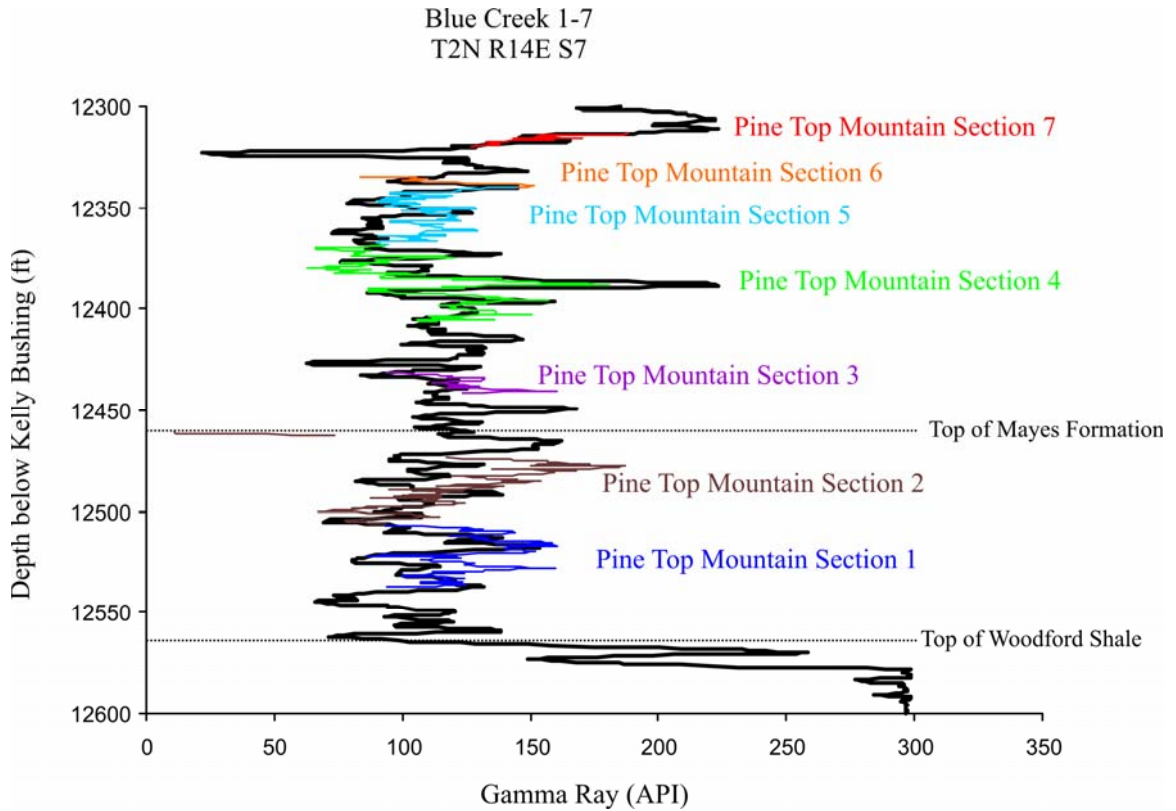
Figure 5.3 Gamma-ray correlation from the outcrop exposed at the Pine Top Mountain outcrop area to the gamma ray log from the Blue Creek 1-7 well. This well is located about eight miles west of the outcrop. All seven sections of the Pine Top Mountain outcrop match the subsurface gamma ray fairly well.

subsurface. The differences between the two gamma rays may be a result of this section being emplaced by thrusting during the Ouachita Orogeny. Therefore, the original distance between this outcrop section and the Blue Creek Well may be much larger than the present day distance.

Section 1 exposed at the Pine Top Mountain outcrop had a gamma-ray response that correlated to the lower to middle of the "Mayes" formation (lower Caney Shale). This section was identified as Woodford Shale by Hendricks and Gardner (1947), Siy (1988), and Suneson and Campbell (1990). However, as illustrated in the gamma-ray correlation this section does not matches the gamma-ray response of the Woodford Shale in the Blue Creek 1-7 well. Moreover, an analysis of U and Th, from the same gamma-ray scintillometer, for the Woodford vs. Caney Shales indicates that the proportion of U to Th is different in each of the two shales (Figure 5.4). The Pine Top Mountain outcrop has U and Th ratios that are similar to that of the Caney Shale and not the Woodford Shale.

The Pine Top Mountain Section 2 correlates to the upper "Mayes" formation (lower Caney Shale). The upper part of this correlation does not match the gamma-ray response as well as the lower half, with the upper part of the section displaying a gamma-ray response that is considerably lower than observed in the nearby well. This large difference may be a result of weathering, improper correlations, or a facies difference between the well and the outcrop. According to this correlation, the top of the measured section represents the boundary between the "Mayes" formation (lower Caney Shale) and the Caney Shale.
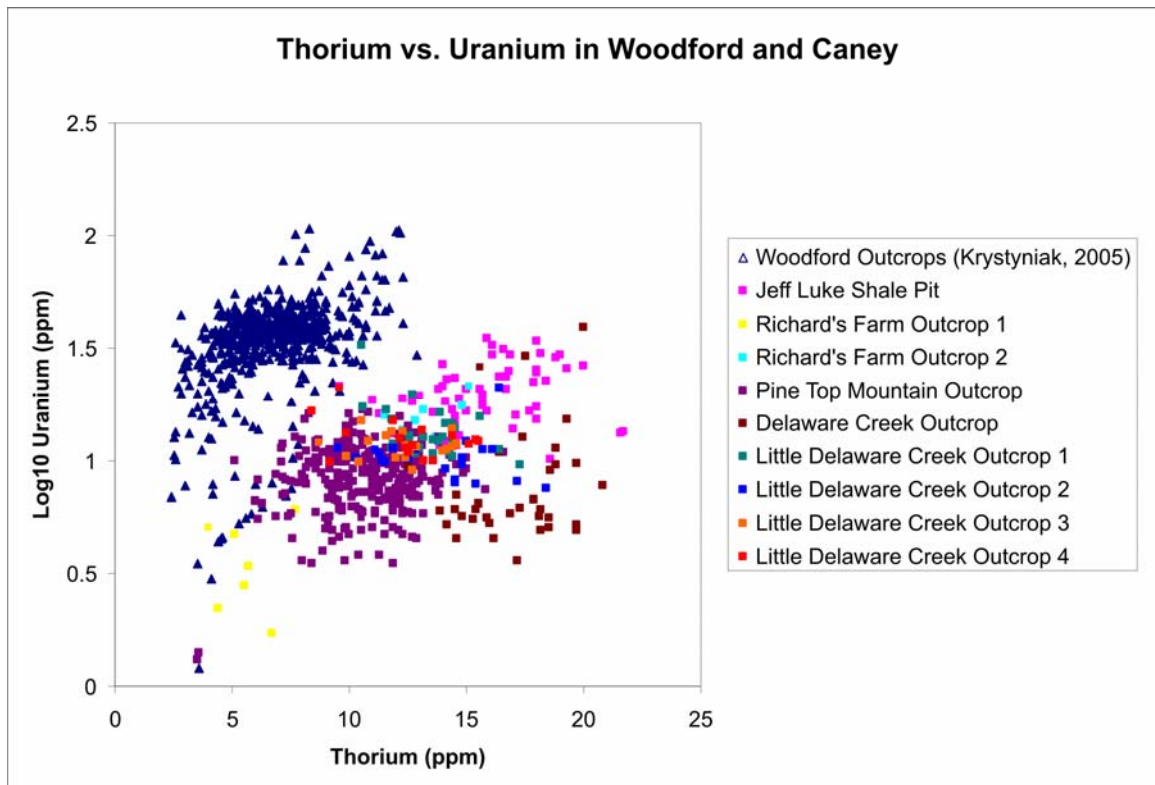
Figure 5.4 Proportion of uranium to thorium measured at Woodford Shale (Krystyniak, 2005), "Mayes" formation (lower Caney Shale), and Caney Shale outcrops by a gamma-ray scintillometer. Analysis shows that the Pine Top Mountain outcrop has Uranium and thorium proportions similar to Caney Shale and "Mayes" outcrops and dissimilar to Woodford Shale outcrops.

Sections 3, 4, 5, 6, and 7 at Pine Top Mountain correspond to the lower two-thirds of the Caney Shale. The gamma ray from these outcrop sections match nicely with the subsurface gamma ray. The gamma-ray pattern in Section 5 deviates slightly from the gamma ray in the nearby well; however, this deviation is slight and overall the correlation is considered acceptable.

Plate 1 represents a cross section of the outcrop gamma-ray scans and the subsurface Rogers Trust 1-24 and Richardson 2-33 wells. In this figure the Hass G outcrop and Jeff Luke outcrop were combined into a composite section for the Lawrence Uplift outcrop area and the Delaware Creek and Little Delaware Creek sections were combined into a composite section for the Bromide outcrop area. As illustrated in the cross section, the outcrops studied in this work represent a majority of the Caney through "Mayes" (lower Caney Shale) interval, including the upper and lower contacts of this stratigraphic interval. Recall that, a facies change and possibly a thermal maturity change are believed to exist between the Pine Top Mountain outcrop and the other outcrop locations. As a result of this facies change, the use of this outcrop to characterize the lithology of the Caney Shale maybe less reliable.

CHAPTER 6.0

DESCRIPTION OF THE CANEY SHALE FORMATION IN THE SUBSURFACE

FROM MUD LOGS

For the subsurface analysis of the sedimentology of the Caney Shale two wells

were analyzed. These wells are the Rogers Trust 1-24 and the Richardson 2-33. Figure

3.1 shows the general location of these wells in the study area. Both of these wells were

exploratory wells drilled in the study area in order to evaluate the gas potential of the

Caney Shale. A suite of data was collected at each of the well locations. This data

includes mud logs, wire-line logs, and sidewall cores. The sidewall cores from each of

the wells were then used for XRD, TOC, and thin section analyses. In this chapter, a

gross analysis of the Caney Shale based on the mud logs is reviewed.

6.1 Rogers Trust 1-24

The Rogers Trust 1-24 well is located in Coal County, Oklahoma, section 24 of

township T3N, R10E. The well was spud on October 14th, 2004 and was drilled to a

depth of 8,010 ft. The elevation of the kelly bushing at this location was 735 ft above

MSL. This hole was slightly directional with a 7.8 to 2.5 degree dip in the Caney to

"Mayes" (lower Caney Shale) interval. The mud log for this well was prepared by Serge

Nkoghe-nze of Horizon Well Logging, Inc., and is contained in Figure 6.1. All of the depths from this log are depths according to the driller.

The top of the Woodford Shale was determined to be at 7128 ft on the mud log. Above the Woodford a platey shale with calcite laminae was logged. This unit is 16 ft thick. Overlaying this shale unit is a dark brown limestone. The limestone is approximately 12 ft thick and is described as a finely crystalline shale limestone with 10 to 20% sandstone inclusions. From the mud log descriptions it is possible that these two units correlate to the pre-Welden Shale and Welden Limestone observed in the Hass G outcrop.

From 7018 to 7100 ft the "Mayes" formation (lower Caney Shale) was logged. The bottom of this formation contained small limestone beds that possibly indicate a gradational boundary between the lower limestone unit and the "Mayes" (lower Caney Shale). The "Mayes" (lower Caney Shale) is characterized as a brownish-black fine textured shale. The shale is interpreted as very silty with some very fine-grained sand. The unit is very calcareous with occasional calcite and pyrite present in the cuttings. Dark brown hard siderite was also noted. In the upper portions of the "Mayes" (lower Caney Shale), translucent calcite laminated with shale was noted along with fossil fragments.

According to the mud log, the Caney Shale is present between 6746 and 7100 ft. At the base of the section the Caney is described as a gray to light gray shale with a very fine to fine texture. The shale is calcareous with pyrite inclusions. Moving up section the shale gradually becomes dark gray-to-black in appearance. The shale is commonly calcareous, with limestone beds noted. At approximately 6810 ft the fossil fragments
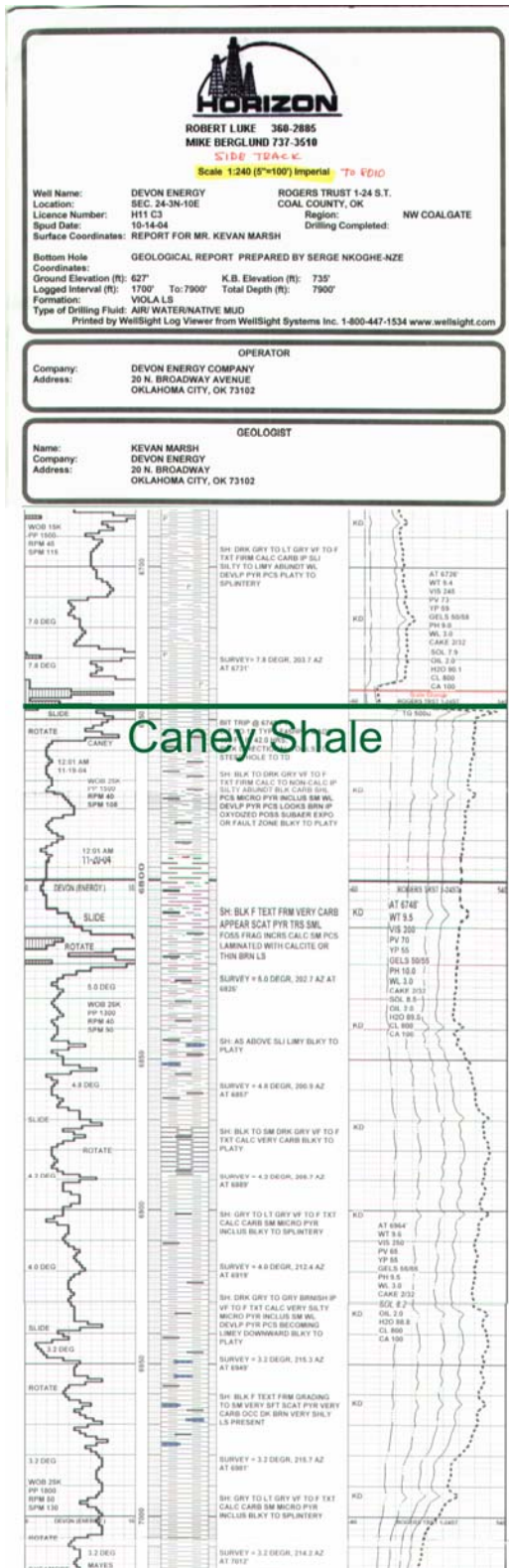
Figure 6.1 Mud log for the Rogers Trust 1-24 well. This mud log as prepared by Serge Nkoghe-nze of Horizon Well Logging, Inc.

were noted in the cuttings, and at approximately 6770 ft a possible subareal exposure or fault was noted from brown, oxidized shale fragments.

6.2 Richardson 2-33

The Richardson 2-33 is located in Hughes County, Oklahoma; section 24 of T6N, R11E. The spud date for this well was April 30th, 2005. The total depth of the well was 6540 ft. The elevation of the kelly bushing was 840 ft above MSL. The mud log was prepared by Bud Walker at Horizon Well Logging, Inc., and is contained in Figure 6.2. All of the depths from this log are depths according to the driller.

The top of the Woodford was logged at 6235 ft in this well. The lithology above the Woodford is described as a white to tan to light brown limestone. The limestone is very finely crystalline and dense, and is approximately 45 ft thick. Similar to the Rogers Trust 1-24 well, this limestone possibly correlates to the Welden Limestone at the Hass G outcrop. This limestone is also noted into the upper 55 ft of the Woodford Shale. The appearance of the limestone in the Woodford is interpreted as a mistake by the mud logger.

Above this limestone from 6110 to 6190 ft the "Mayes" formation (lower Caney Shale) was logged. This formation is described as a gray to gray/green shale. The shale is silty and calcareous in locations. Pyrite was also noted in some of the cuttings. The base of the shale contains carbonate layers that possibly indicate a gradational boundary between the "Mayes" (lower Caney Shale) and the lower carbonate unit.

The Caney Shale was logged from 5880-to-6120 ft. The base of the Caney is marked by approximately 5 ft of light brown to tan gray limestone (Figure 5.2). The
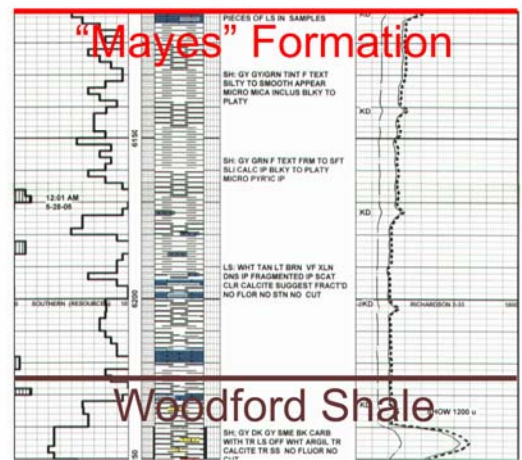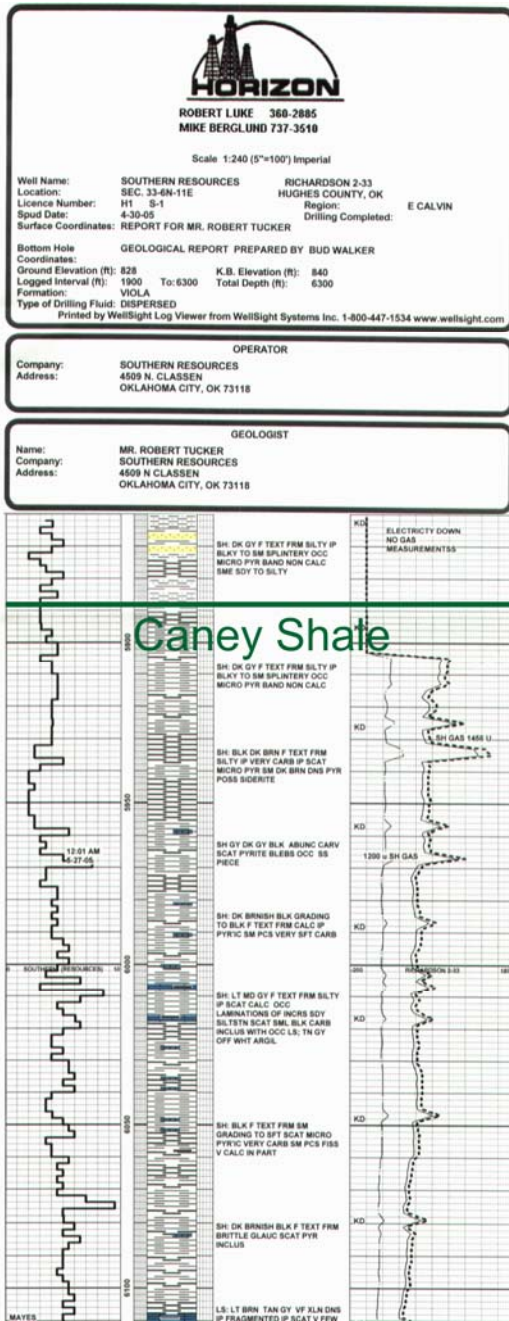
Figure 6.2 Mud log for the Richardson 2-33 well. This mud log as prepared by Bud Walker of Horizon Well Logging, Inc.

limestone was very finely crystalline and dense. Above the small limestone the Caney is described as a brownish-black, black-to-gray shale. The color of the Caney changes to dark gray or dark brown-to-black in the upper half of the formation. Some glauconite is noted in the shale at the base. Limestone fragments are common in the cuttings from 5960 ft to the base of the section, and most of the shale is calcareous. The upper 20 to 30 ft of the section is the only section noted to be non-calcareous. Pyrite is commonly noted throughout. Silt, sand, and siderite are occasionally noted in the cuttings.

CHAPTER 7.0

SUBSURFACE WIRE-LINE LOG CHARACTERIZATION

A suite of wire-line logs was run in both the Rogers Trust 1-24 and Richardson 2-33 wells. These logs include the gamma ray, shallow induction, medium induction, deep induction, photoelectric, neutron porosity, density porosity, and electrical image. The logs for the Rogers Trust 1-24 and Richardson 2-33 are shown in Figures 7.1 and 7.2 respectively. Because the wire-line log data for these two wells is digital, summary statistics of the wire-line readings of each formation were calculated (Table 7.1). A discussion of the general characteristics of each of these logs follows.

7.1 Gamma-Ray Log

The gamma-ray log is the most important log used to correlate the Caney Shale. As illustrated in Figures 4.3 and 4.4, the characteristics of the gamma-ray curve are distinctive. The Woodford Shale has a very high gamma-ray count and is typically identified by the thick package of strata with gamma-ray readings greater than 150 API units and commonly greater than 250 API units. According to Krystyniak (2005), the Woodford Shale in outcrop exposures has an average gamma-ray reading of 360 API units. The average gamma ray for the Woodford Shale in the Rogers Trust 1-24 and Richardson 2-33 is 413 API units (Table 7.1). Moving up the section the boundary
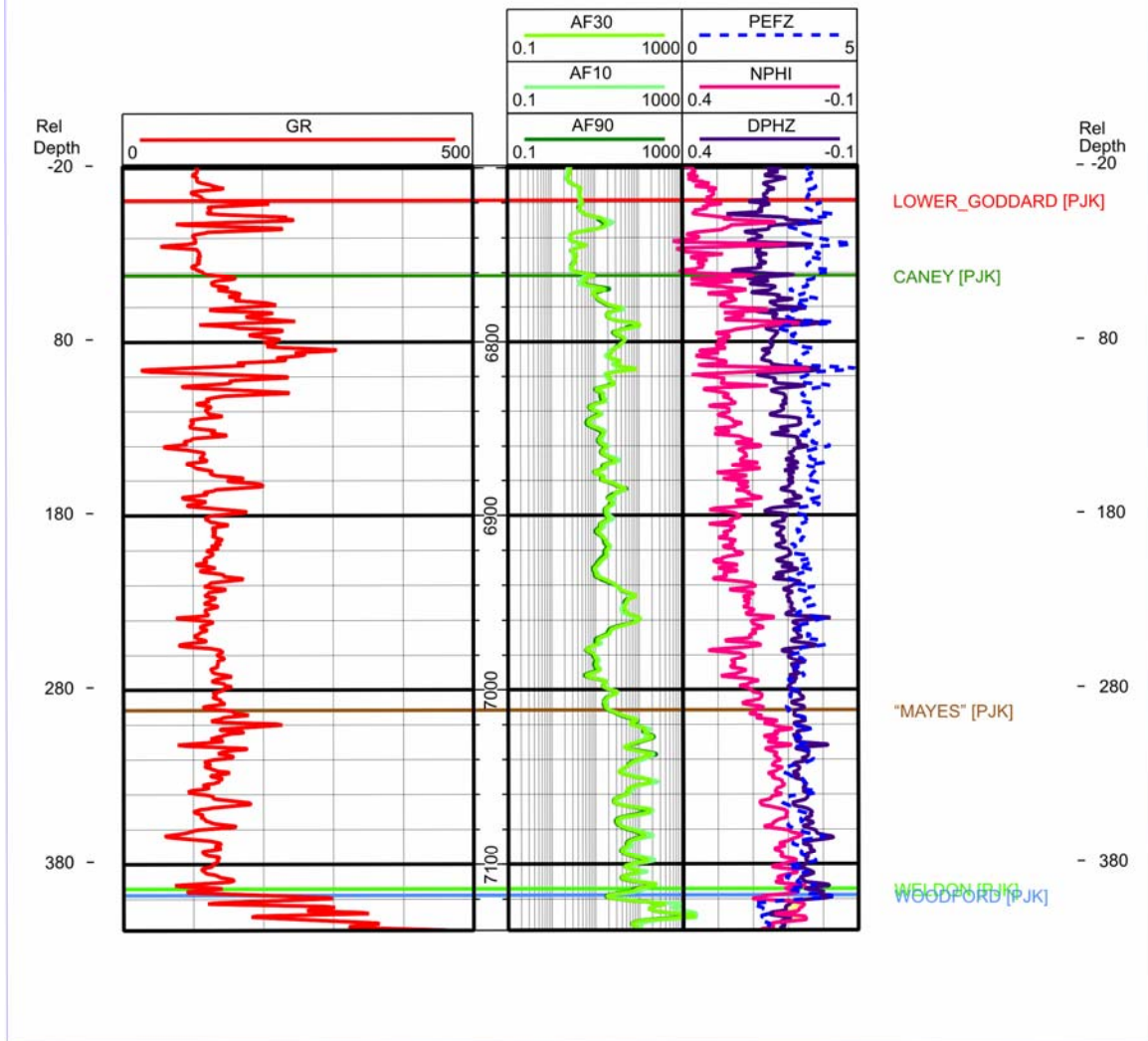
Figure 7.1 Rogers Trust 1-24 well log, where GR equals gamma ray, AF10 equals shallow induction log, AF30 equals medium induction log, AF90 equals deep induction log, PEFZ equals photoelectric log, NPHI equals neutron porosity log, and DPHZ equals density porosity log.
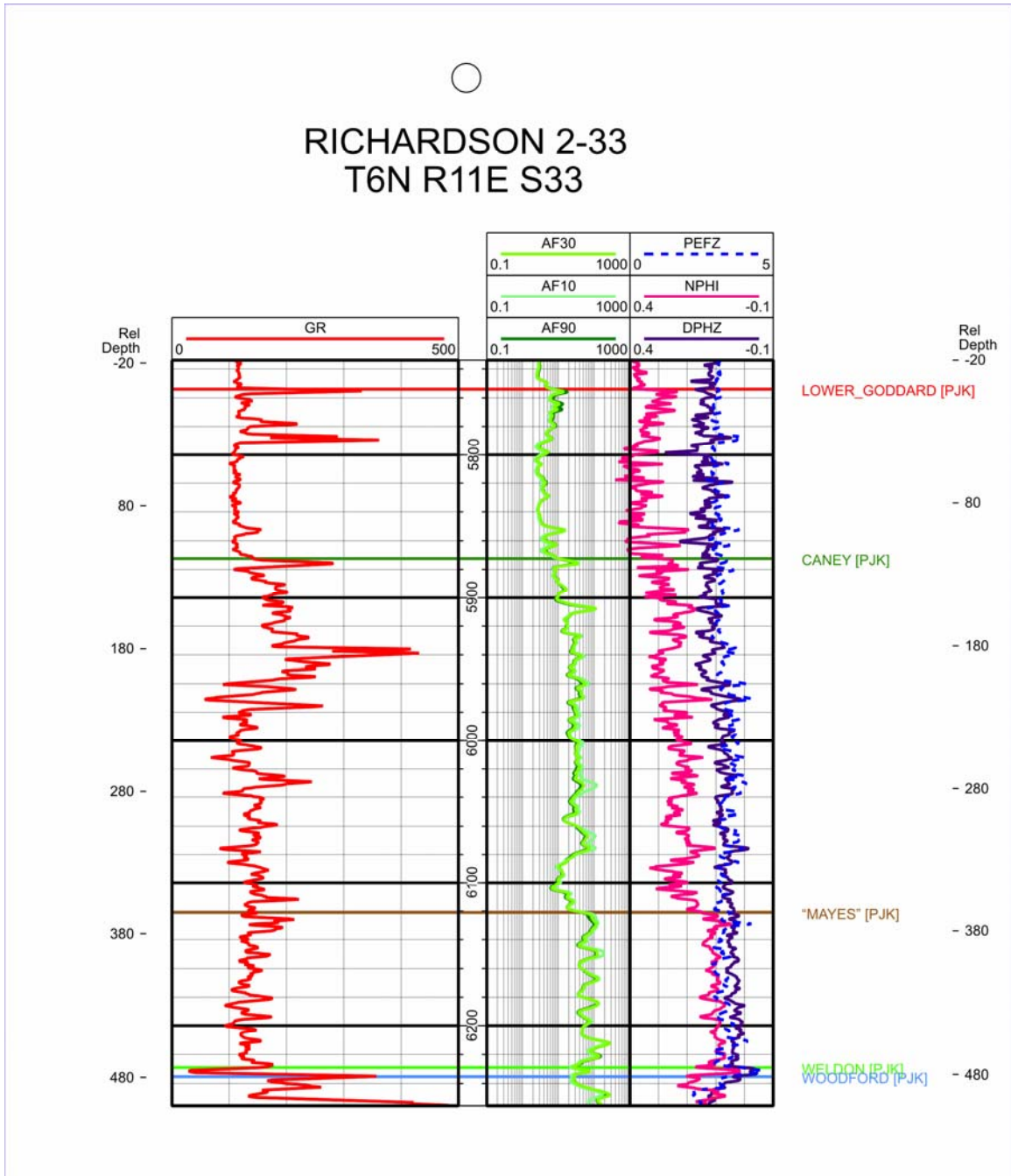
Figure 7.2 Richardson 2-33 well log, where GR equals gamma ray, AF10 equals shallow induction log, AF30 equals medium induction log, AF90 equals deep induction log, PEFZ equals photoelectric log, NPHI equals neutron porosity log, and DPHZ equals density porosity log.

Table 7.1 Wire-line log summary statistics for the Wooford Shale, "Mayes" formation (lower Caney Shale), and Caney Shale; where PE is equal to photoelectric log, Neutron is equal to neutron porosity log, Density is equal to density porosity log, GR is equal to gamma ray log, and Resistivity is equal to resistivity log. Data was derived from of the Rogers Trust 1-24 and Richardson 2-33 wells.

Upper Caney Shale

	Average	Std	min	max
PE	3.34	0.28	2.68	4.04
Neutron	0.26	0.04	0.17	0.38
Density	0.12	0.03	0.06	0.17
GR	192.12	48.10	100.89	390.31
Resistivity	22.49	19.99	4.97	188.22

Lower Caney Shale

	Average	Std	min	max
PE	3.40	0.28	2.82	4.23
Neutron	0.20	0.06	0.06	0.33
Density	0.07	0.03	-0.03	0.15
GR	128.74	27.30	27.56	238.21
Resistivity	43.01	48.68	4.16	683.95

"Mayes" Formation

	Average	Std	min	max
PE	3.16	0.41	1.98	4.61
Neutron	0.13	0.05	0.02	0.25
Density	0.07	0.05	-0.04	0.16
GR	130.43	25.85	27.03	227.06
Resistivity	195.89	292.47	12.28	1950.00

Woodford Shale

	Average	Std	min	max
PE	3.24	0.51	2.18	4.93
Neutron	0.19	0.05	0.01	0.30
Density	0.07	0.07	-0.14	0.23
GR	413.38	130.11	97.89	786.19
Resistivity	157.37	211.38	4.66	1615.94

between the Woodford and the overlying formation is typically marked where the gamma-ray curve drops and predominantly stays below 150 API units.

The pre-Welden Shale and Welden Limestone are difficult to map in the subsurface and are typically not recognized by those in the petroleum industry. These formations are usually considered to be apart of the "Mayes" (lower Caney Shale). However, there is a large gamma ray decrease just above the Woodford Shale. This decrease in gamma ray is typically lower than 75 API units and could represent the Welden Limestone.

The "Mayes" formation (lower Caney Shale) has a much lower gamma-ray reading that averages 130 API units (Table 7.1). In some intervals of the "Mayes" (lower Caney Shale), the gamma ray increases over 150 API units, but quickly drops back to about 130 API units. The top of the "Mayes" (lower Caney Shale) is usually marked by a small group of gamma-ray spikes greater than 150 API units. However, the top is difficult determine with the gamma-ray curve alone and is typically identified with the help of the resistivity curves.

Based off of the gamma-ray signature, the Caney Shale can be divided into two distinct units. The lower two-thirds of the Caney Shale has a gamma-ray signature commonly less than 150 API units; while, the upper one-third of the Caney Shale has a gamma-ray signature commonly greater than 150 API units. Based off of these two gamma-ray responses the Caney Shale is initially divided into the middle Caney and the upper Caney Shale (Recall, the term lower Caney refers to the section occupied by the "Mayes" formation.) In Chapter 9.0 the Caney Shale is divided further into

lithostratigraphic units, but for the sections leading up to Chapter 9.0 the Caney will be referred to in terms of middle and upper.

The middle Caney Shale has an average gamma-ray signature of 128 API units (Table 7.1). In the middle Caney there are some rare spikes that are greater than 150 API units. The average gamma-ray measurement for the upper Caney is computed to be 192 API units (Table 7.1). The top of the Caney is typically identified where the gamma-ray curve drops and stays below 150 API units consistently.

7.2 Induction Logs

The shallow, medium, and deep induction logs track each other through most of the Caney and "Mayes" (lower Caney Shale) intervals. The tracking of the three logs indicates that there in no invasion of the drilling fluids into the formations, and hence the formations are not permeable. Despite the lack of separation between the curves, the resistivity logs can be used to identify formation changes. The Woodford Shale typically has a resistivity between 5 and 1600 ohm-m, with an average resistivity of 157 ohm-m (Table 7.1). This resistivity drops downs to approximately 15 to 20 ohm-m at the top of the Woodford Shale. In the Welden through "Mayes" (lower Caney Shale) sections the resistivity curve oscillates regularly between 10 and 2000 ohm-m with an average resistivity of 196 ohm-m. The high resistivity in the "Mayes" (lower Caney Shale) is probably because of the carbonate content of the formation. The resistivity curve does display an increase at the possible location of the Welden Limestone, but this resistivity increase is not differentiable from the rest of the "Mayes" formation (lower Caney Shale). The top of the "Mayes" formation (lower Caney Shale) is identified mainly by the

resistivity curve. The resistivity curve drops down to approximately 15 ohm-m at the top of the "Mayes" (lower Caney Shale), and continues to drop to about 5 ohm-m in the middle Caney. The resistivity of the middle Caney Shale varies between 4 and 700 ohm-m, with and average resistivity of 49 ohm-m. The upper Caney with the high gamma-ray response also has a resistivity that varies between 5 and 190 ohm-m, with and average resistivity of 22 ohm-m. The top of the Caney is marked by a decrease in resistivity down to approximately 3 ohm-m.

7.3 Photoelectric Log

The photoelectric (PE) curve is used to help determine the lithology present within the formation. A photo electric value of 1.81 barns/electron indicates quartz, a value of 5.08 barns/electron indicates calcite, a value of 3.14 barns/electron indicates dolomite, and value of 3.42 barns/electron indicates shale (Rider, 2002). By looking at the photoelectric curve an interpretation about the lithology can be made. The Woodford Shale has an average PE measurement of 3.24 barns/electron (Table 7.1). Above the top of the Woodford Shale the PE curve peaks at about 4.5 barns/electron. This peak, along with the low gamma ray and high resistivity, suggests that a limestone is present in this interval. The presence of a limestone above the Woodford Shale suggests that this interval would likely correlate to the Welden Limestone viewed at the Hass G outcrop.

In the "Mayes" formation (lower Caney Shale) the PE curve varies between 2.0 and 4.8 barns/electron and averages about 3.16 barns/election (Table 7.1). This indicates that the lithology in the "Mayes" (lower Caney Shale) could be sand, shale, dolomite, calcite, or any mixture of the four lithologies. The lower and upper Caney Shale has an

average PE response of 3.4 and 3.3 barns/electron respectively. These averages for the

Caney Shale indicate that the Caney is more shale rich than the "Mayes" formation

(lower Caney Shale). However, there are small intervals within the Caney that have PE

measurements indicating the presence of quartz and calcite rich facies.

7.4 Density Porosity and Neutron Porosity Logs

The density and neutron porosity logs run in the Rogers Trust 1-24 and

Richardson 2-33 were run assuming a limestone matrix. According to these logs, the

average density porosity for the Woodford formation is 7% and the average neutron

porosity is 19% (Table 7.1). The density porosity log determines a negative porosity in

the Welden Limestone, while the neutron porosity log determines a porosity of about two

percent. Recall that, the density porosity for these units was determined under the

assumption that the formation is limestone. Under this assumption, the formation must

have a higher density than limestone in order to determine a porosity value less than 0.

The density porosity and neutron porosity logs read average porosities of 7% and 13% in

the "Mayes" (lower Caney Shale) interval respectively.

The neutron porosity is higher in the Caney Shale than it is in the "Mayes"

formation (lower Caney Shale), with an average porosity of 20% in the middle Caney and

26% in the upper Caney. This large increase in porosity estimate is possibly due to the

clay content in the Caney Shale. The bound water, free water, and organic matter

contained in the shale have high hydrogen indexes and can cause higher neutron porosity

results. The density porosity measured in the middle Caney is similar to the

measurements in the "Mayes" formation (lower Caney Shale) with the average porosity

determined to be 7%. In the upper Caney the average density porosity increases slightly to 12%. This increase in porosity is possibly a result of high organic matter content or the presence of gaseous hydrocarbons. Note that at locations were the PE curve drops below 3 the density porosity and neutron porosity curves start to converge. These curve characteristics help argue that siltier or sandier intervals exist within the formation.

7.5 Electrical Image Logs

Electrical image logs were run in both the Rogers Trust 1-24 and the Richardson 2-33. A detailed analysis of an electrical image log enables an interpretation about the lithology, bedding, formation boundaries, faults, fracture system, and present-day regional stress. A complete analysis of an electrical image log would be lengthy and does not fit the scope of this work. This work is focused on the lithostratigraphic framework of the Caney and "Mayes" formations (lower Caney Shale), and so, the electrical image logs will be used to briefly analyze the lithology and bedding of these formations.

In a formation image logs the brighter the image color the more resistive the lithofacies. Limestones are typically more resistive than shales and should be easily identified in the formation image log, with the help of the conventional logs discussed above. At the base of the "Mayes" formation (lower Caney Shale) and top of the Woodford Shale, both of the formation image logs for these wells indicate a resistive rock layer. These rock layers appear to be separated by a thin, more conductive lithology. Comparing the image to the PE curve and the gamma-ray curve these resistive layers are interpreted to be limestone. As discussed above it is possible that this interval correlates to the Welden Limestone viewed at the Hass G outcrop.

In the "Mayes" formation (lower Caney Shale), the image logs indicate a parallel laminated lithology. These laminations are continuous in the borehole (Figure 7.3). Also, note that the "Mayes" (lower Caney Shale) contains calcareous thin beds and abundant pyrite blebs. In both the Rogers Trust 1-24 and the Richardson 2-33 wells, carbonate nodules that disturb the bedding plans were noted to occur approximately 10 ft from the top of the formation (Figure 7.3). The occurrence of nodules at the same location in both wells appears to indicate that the geochemical conditions at the sea floor to precipitate these nodules were possibly widespread.

The formation image of the middle Caney Shale is very similar to that of the "Mayes" formation (lower Caney Shale). Again this formation consists of continuous parallel laminations. Like the "Mayes" formation (lower Caney Shale) carbonate nodules and thin beds are present in the formation (Figure 7.4). The Caney Shale contains pyrite blebs like the "Mayes" (lower Caney Shale); however, in the image log these blebs are generally less pronounced in the Caney. The pyrite blebs that are present in the formation appear to be more abundant in the middle Caney.

In the upper Caney Shale, where the gamma-ray readings are the highest in the formation, small less resistive nodules and slightly discontinuous laminae are present in the shale (Figure 7.5). The nodules are more pronounced than the pyrite nodules viewed in other areas of the image and the nodules appear to be in the same layer as the less resistive horizontal laminae. Nodules and laminations of apatite were noted in the Jeff Luke outcrop that are similar in appearance to these nodules and laminations (Figure 7.6). An electron microprobe analysis of nodules from the JL indicates that these nodules and laminae are apatite with the presence of iron (Figure 7.7). Iron is a conductive metal and

93
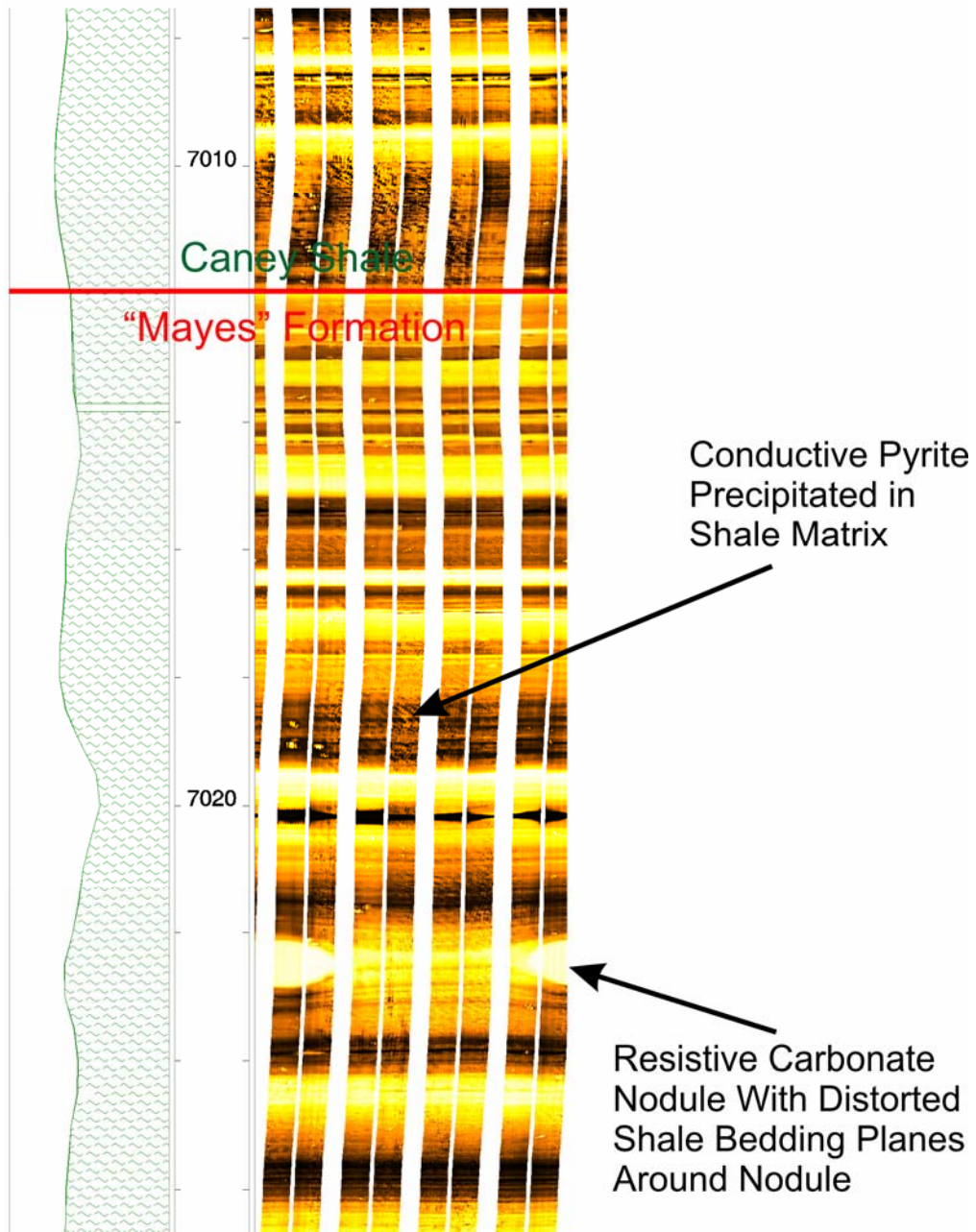
Figure 7.3 Electrical image log of the top of the "Mayes" formation in the Rogers Trust 1-24 well. A Carbonate nodule that disturbs the bedding planes is present approximately 10 ft below the top of the "Mayes". Also, conductive pyrite blebs are noted in the log.
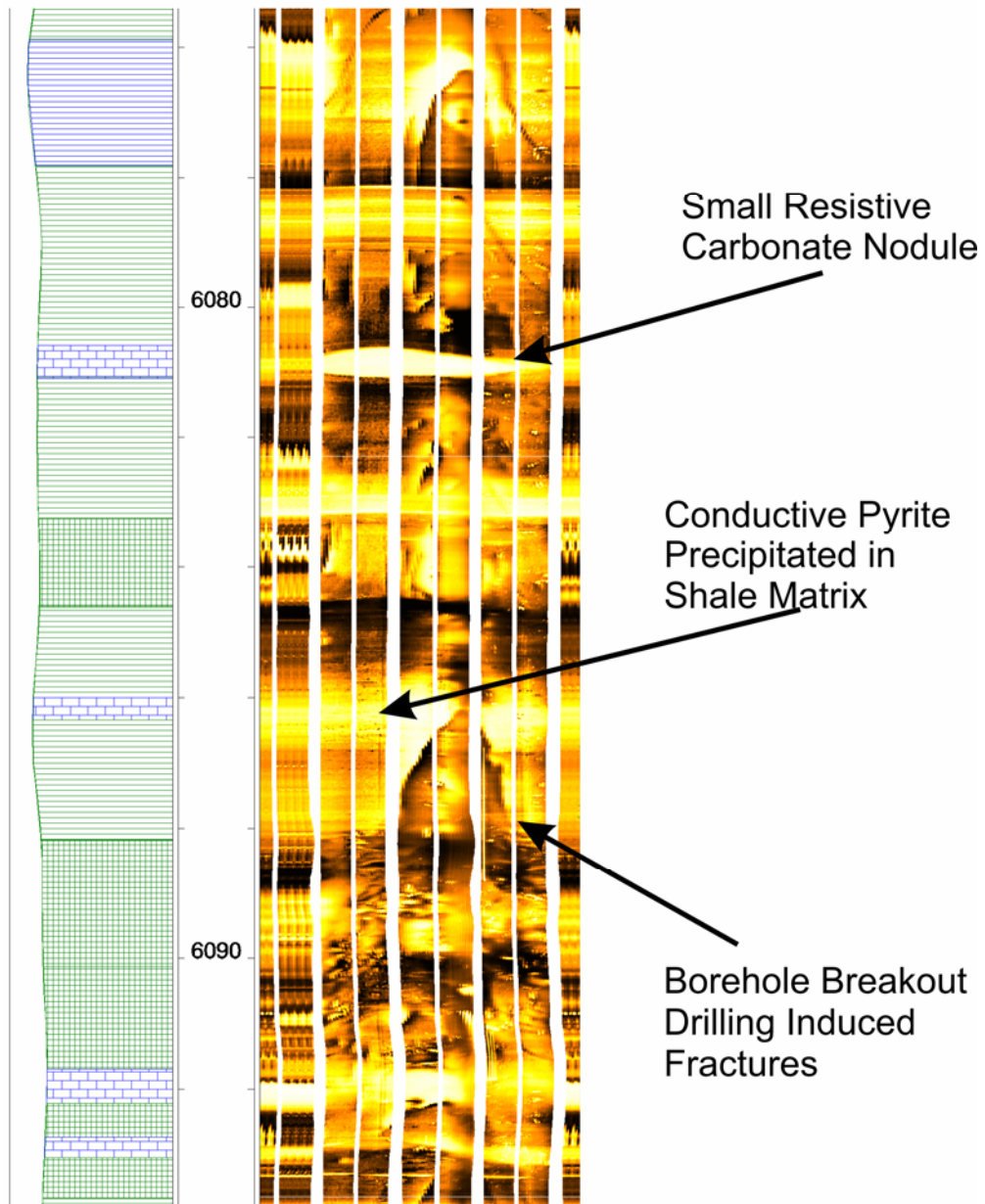
Figure 7.4 Electrical image log of the Caney Shale in the Richardson 2-33 well. The image log shows the presence of drilling induce fractures, pyrite, and carbonate nodules.
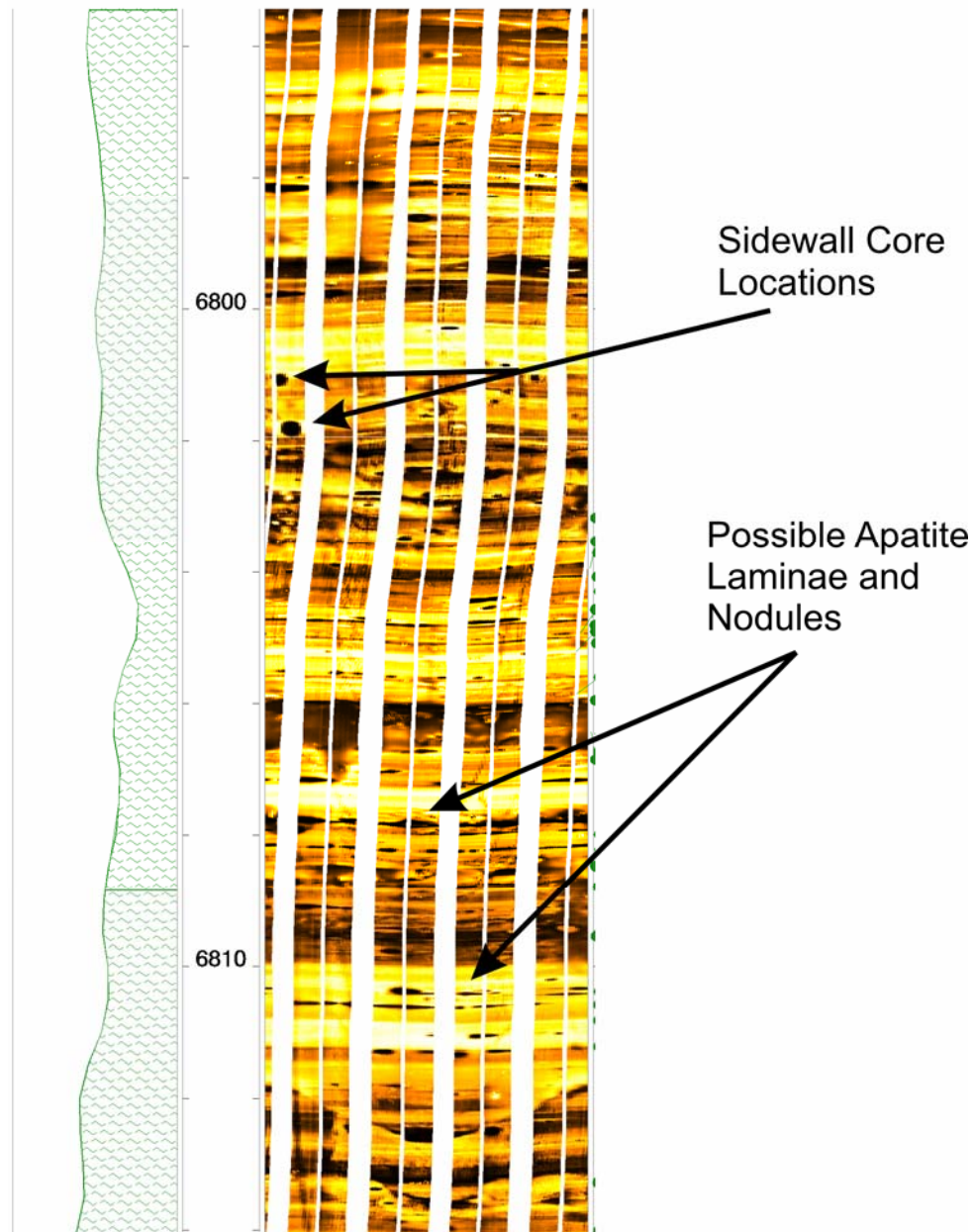
Figure 7.5 Electrical image log of the upper Caney Shale in the Rogers Trust 1-24 well. This electrical image logs indicates the presence of possible apatite laminations and nodules. Note, that the location of sidewall cores can also be determined in the log.

Figure 7.6 Apatite laminae and nodule photographed in the Jeff Luke shale pit. This photograph was taken at the top of Section 3, and is approximately 24.5 ft above the base of the exposure.
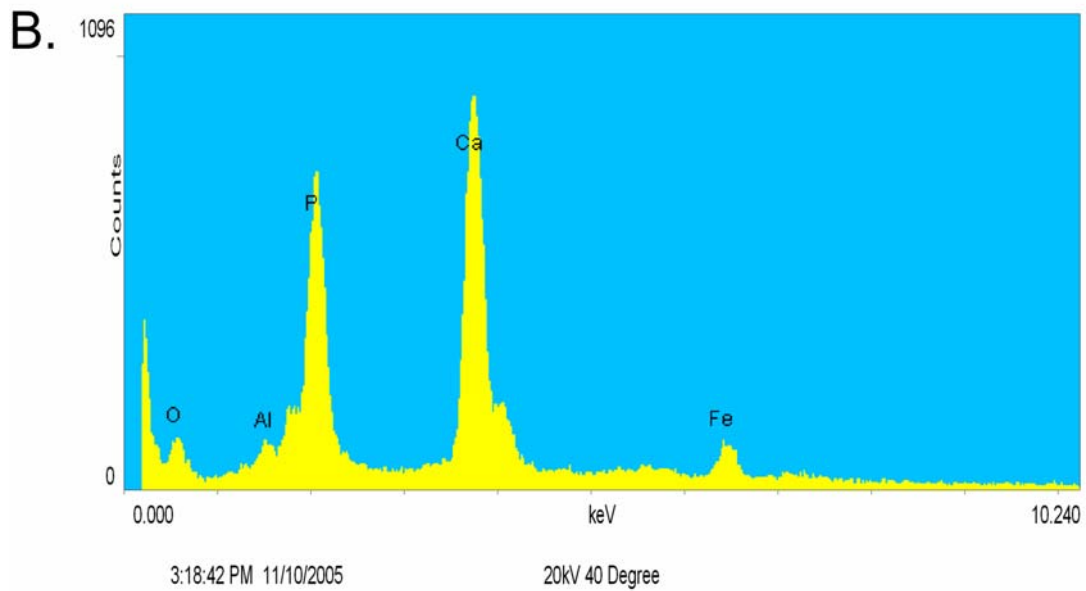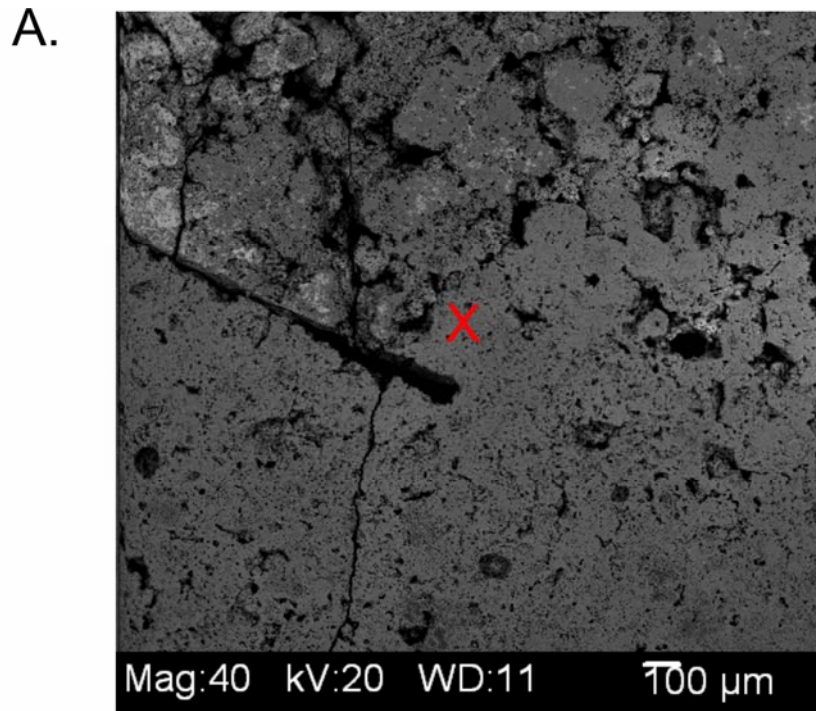
Figure 7.7 A.) Scanning electron microscope image of a nodule from the Jeff Luke shale pit. B.) X-ray spectrum of the nodule in A; measurement point is marked by the letter X. According to the spectrum this nodule is calcium apatite, with traces of iron and aluminum.

is believed to be why the nonconductive apatite nodules and laminae appear conductive in the electrical image log.

An east west cross section from the Jeff Luke shale pit to the Rogers Trust 1-24 Well is given in Plate 2. This cross section indicates that the Jeff Luke shale pit is correlative to the upper part of the Rogers Trust 1-24 where the apatite nodules are seen on the electrical image log. Therefore, it is very likely that the less resistive nodules and laminations in the electrical image log are also apatite.

The top of the Caney Shale is possibly marked by an erosional surface (Sutherland, 1988). However, there are no erosional surfaces visible above and below the top of the Caney Shale as selected on the basis of the gamma ray. At the top of the Caney Shale there is a change in the bedding that is visible in the electrical image log. The top of the Caney Shale is identified in the electrical image log where the parallel laminations of the Caney Shale become disrupted and discontinuous (Figure 7.8). These disrupted laminations are interpreted to be a result of bioturbation during deposition of the Goddard Shale (Savrda and Bottjer, 1989). This evidence indicates that sedimentation between the Caney and Goddard Shale is continuous, and the boundary between the two formations represents a change in environmental conditions. Also, note that carbonate nodules and beds are more common near the top of the Caney Shale. These nodules exist on both sides of the contact between the Caney Shale and the Goddard Shale, and therefore the chemical environmental conditions to promote the precipitation of the carbonate did not change with time. Therefore, the carbonate nodules can not be used to distinguish the boundary between the two formations in all cases.
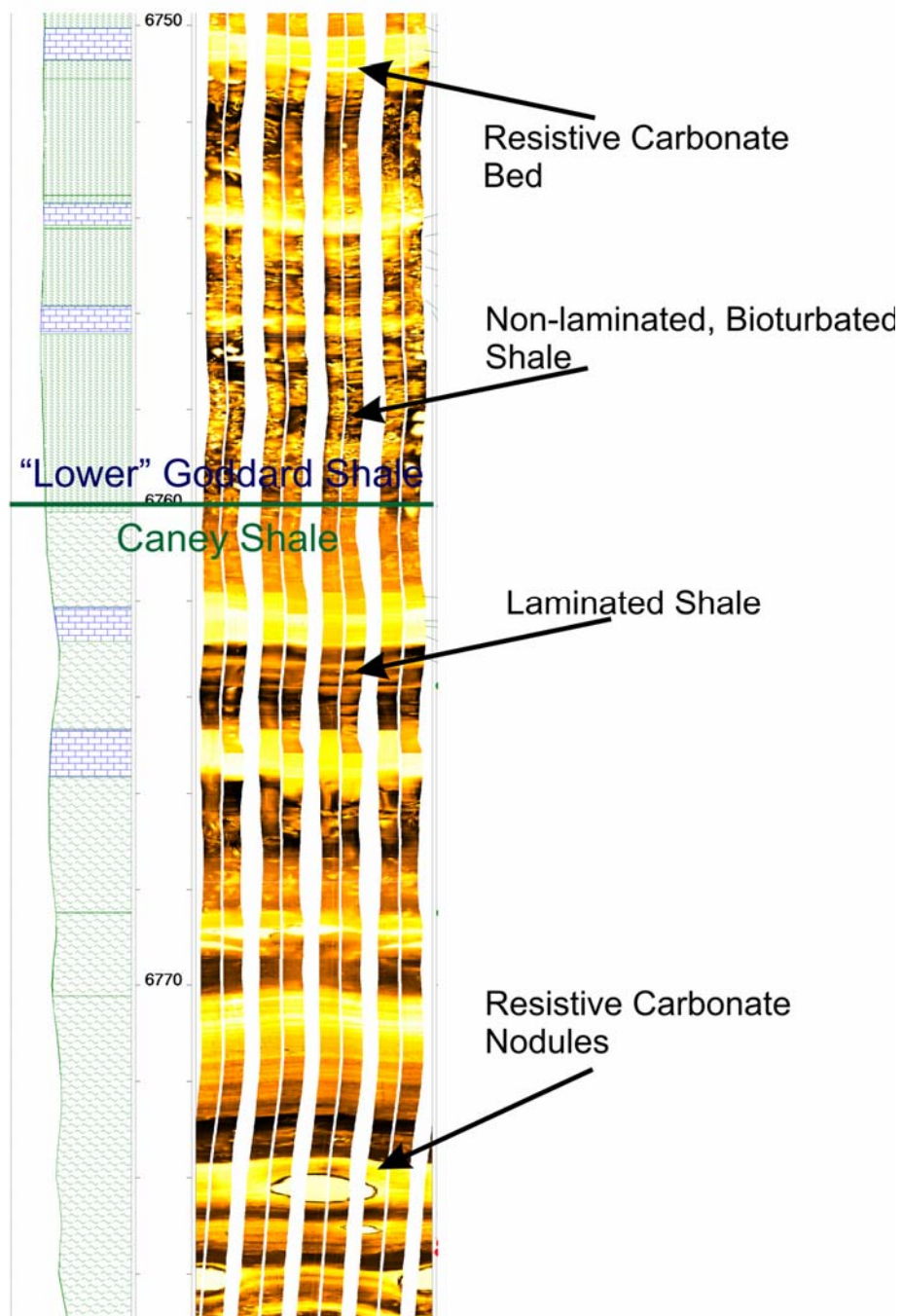
Figure 7.8 Electrical image log of the contact between the Caney Shale the lower Goddard Shale in the Rogers Trust 1-24 well. This electrical image logs indicates the Caney Shale is laminated while the lower Goddard Shale is non-laminated, bioturbated.

CHAPTER 8.0

PETROLOGY OF SURFACE AND SUBSURFACE SAMPLES

Samples collected from each of the 10 outcrop locations and sidewall cores from

the Richardson 2-33 and Rogers Trust 1-24 were petrographically analyzed through thin

sections. Detailed descriptions of each of the thin sections collected in this study are

presented in Appendix A.   In addition, TOC and XRD analyses were collected for the

rock samples. These three types of analyses allow for the Caney Shale and "Mayes"

formation (lower Caney Shale) to be further evaluated for their physical and chemical

properties that can not be determined from hand sample inspection alone. Detailed shale

petrography allows for the identification of facies variations. These variations can then

be used to assist in the development of larger scale lithostratigraphic units within the

formation.

The location of outcrop hand samples and subsurface sidewall cores in relation to

their stratigraphic position is illustrated in Plate 1 above. These sample locations were

selected in order to capture the lithologic variability viewed in outcrops and subsurface.

8.1 Thin Sections

Samples of the "Mayes" formation (lower Caney Shale) were collected at the

Richard's Farm outcrops, the lower part of the Pine Top Mountain outcrop, and in the

Rogers Trust and Richardson wells. Thin sections of samples form Richard's Farm and the Richardson 2-33 indicate that the "Mayes" (lower Caney Shale) is a very calcareous formation. Thin sections indicate the "Mayes" (lower Caney Shale) contains shaly silty dolomites, dolomitic silty carbonates, and shaly muddy dolomites. The quartz present in the thin sections is silt to fine sand in size and is angular. Within the thin sections, mollusk and brachiopod fragments are common. These fragments are whole to abraided (Figure 8.1). Some samples of shale contain abundant pyrite blebs possibly precipitated in algal Tasmanites. In more dolomitic facies, ghost structures of fossil fragments are common.

In addition to the carbonate dominated facies noted in thin section, clay-rich facies were also noted in thin sections collected in outcrop of the "Mayes" formation (lower Caney Shale). At Richards Farm outcrop 2, a weakly laminated to non-laminated brown shale is noted to be clay-rich and carbonate poor (Figure 8.1). This shale contains Tasmanites algal cysts that are replaced by microquartz or bitumen. These cysts are commonly compacted; however, some cysts replaced by pyrite are not compacted, suggesting pyrite formed prior to major mechanical compaction. This shale also contain mollusk fragments consisting of calcite. Some of the mollusk fragments are dissolved away or are replaced by dolomite.

Thin sections of a shale facies in the "Mayes" formation (lower Caney Shale) were also evaluated at the Pine Top Mountain outcrop. The shale was different than the Richard's Farm shale. This lithofacies consists of a brown-to-black shale that is laminated to weakly laminated (Figure 8.2). The shale contains abundant Tasmanites cysts. These cysts are again replaced by microquartz and bitumen. Within this facies
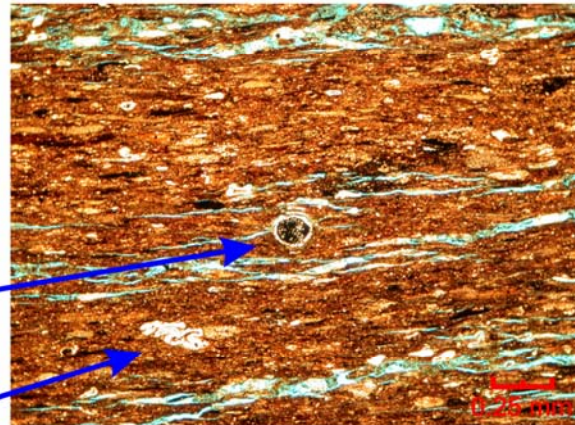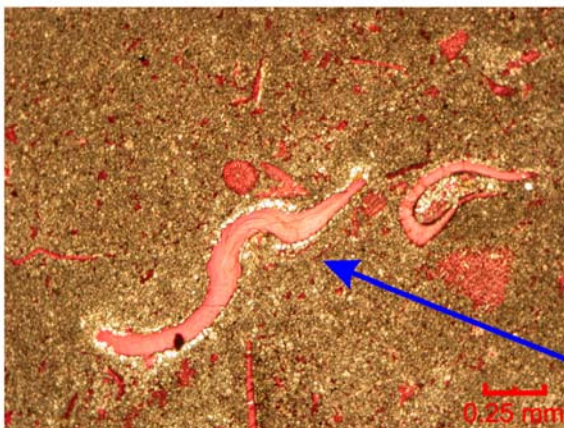
Figure 8.1 Thin sections of the "Mayes" formation (lower Caney Shale) from Richard's Farm Outcrops 1 and 2.
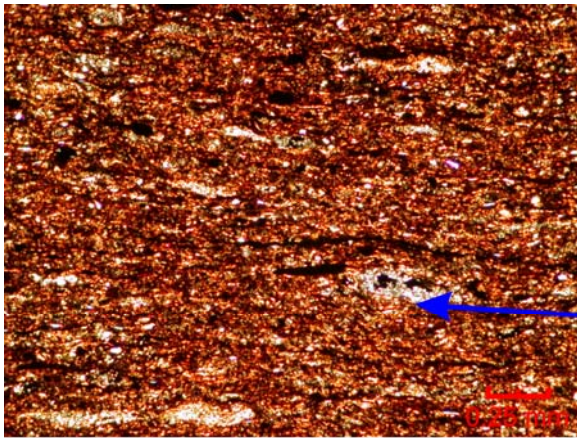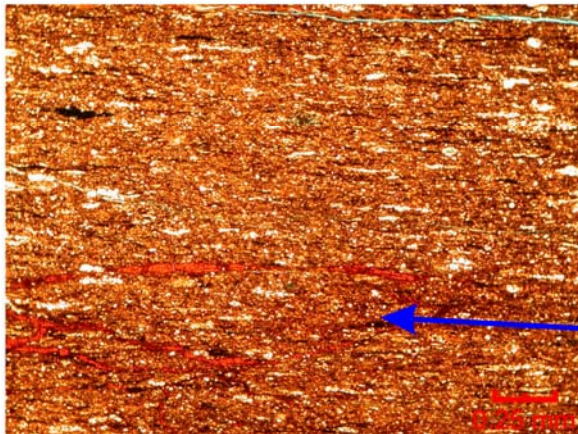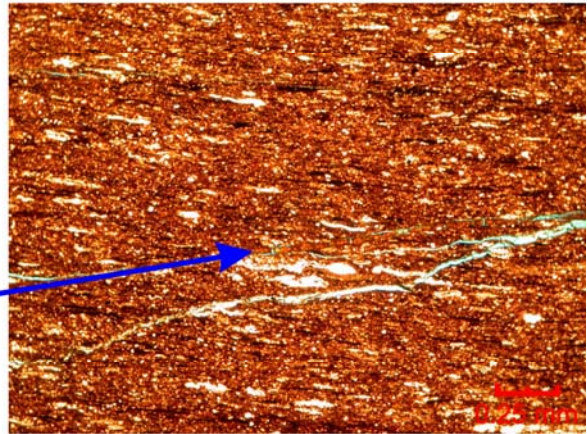
Figure 8.2 Thin sections of the "Mayes" formation (lower Caney Shale) from the Pine Top Mountain Outcrop.

angular silt-size quartz grains are dispersed within the shale matrix along with well-rounded, spherical grains. These spherical grains are interpreted to be replaced radiolarians. One thin section from this facies contained apatite laminations that were stained with iron.

The majority of the thin sections collected in the Caney Shale came from the upper, more radioactive portion of the member. Only a few thin sections from the lower, less radioactive zone were studied. The thin sections from the less radioactive part of the section came from the Pine Top Mountain outcrop and from the subsurface wells. At the Pine Top Mountain outcrop, the middle Caney is weakly laminated to non-laminated (Figure 8.3). Tasmanites cysts are commonly found within the thin sections. These cysts are typically compacted and replaced with microquartz and bitumen. Some of the cysts are non-compacted and replaced by pyrite. Pyrite is interdispersed within the thin sections. Radiolarians and small angular silt-size quartz are also present in thin sections.

In thin sections prepared from samples taken from the subsurface, the middle Caney Shale has a different appearance than observed for samples from the Pine Top Mountain outcrop. Subsurface thin sections from the middle Caney Shale are more calcareous than those from Pine Top Mountain. In the Richardson 2-33 well the thin section collected 5996 ft below the kelly bushing is of a non-laminated tan to brown shale (Figure 8.4). This shale contains abundant bivalve fragments and gastropod shells. Silt-size carbonate and quartz grains are very common. Only a few Tasmanites cysts are noted. These cysts are compacted and replaced with mircroquartz and bitumen. Pyrite blebs are also common in the thin section. Recall that the subsurface Caney Shale samples are from wells in the northwest corner of the study area while the Pine Top
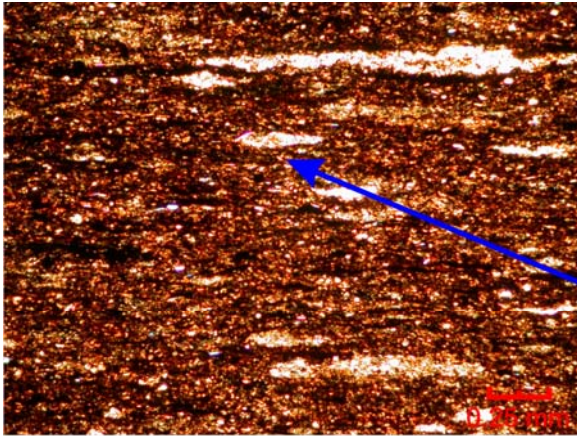
A. 6.5 Pine Top Section 4

Weakly Laminated Brown/Black Shale

Compacted Tasmanites Cyst
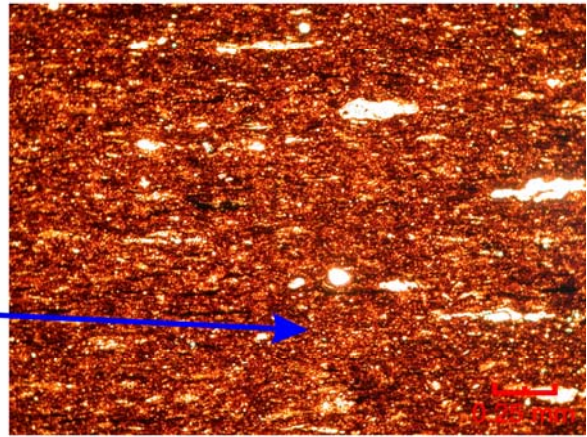
B. 11.0 Pine Top Section 5

Weakly Laminated Brown Shale

Silt Size Quartz Grain
Possible Radiolarian
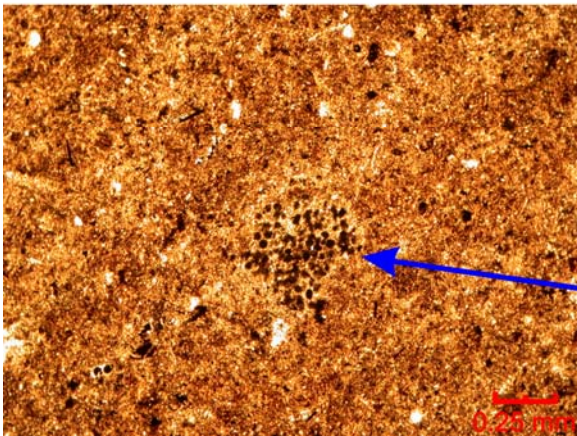
C. 6.0 Pine Top Section 7

Non-Laminated Brown Shale

Pyrite Blebs

Figure 8.3 Thin Sections of the middle Caney Shale exposed at the Pine Top Mountain outcrop.
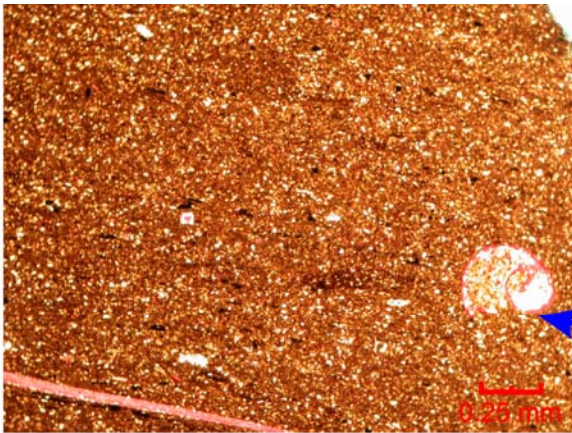
A. 5996 f. Richardson 2-33

Non-Laminated Brown Shale

Gastropod

0.25 mm

B. 6846 ft Rogers Trust 1-24

Weakly Laminated Black/Brown Shale

Bivalve Fragment
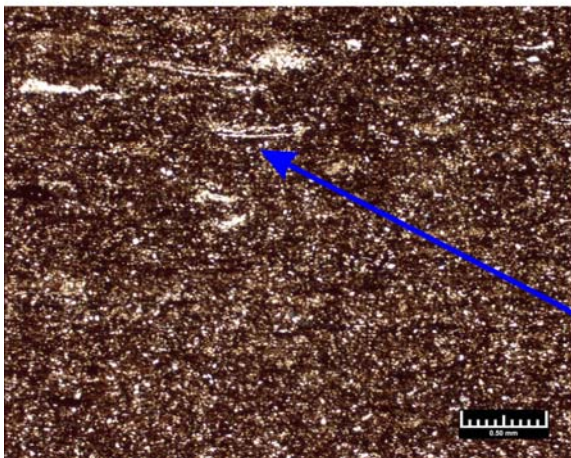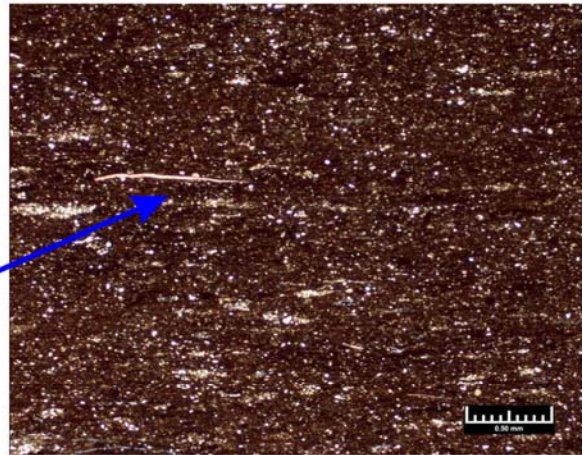
C. 7001 ft Rogers Trust 1-24

Weakly Laminated Black/Brown Shale

Compacted Tasmanites Cyst

Figure 8.4 Thins sections of the middle Caney Shale from the Rogers Trust 1-24 and Richardson 2-33.

Mountain outcrop is interpreted to be a slump block that was emplaced by thrusting during the Ouachita Orogeny. Therefore the lateral distance (palinspastic reconstruction) between these two areas is probably large.

The upper, more highly radioactive, Caney Shale was well sampled in both outcrop and the subsurface. The lithology of the upper Caney is variable at different depths and from location to location. However, most of the thin sections contain apatite. The apatite in thin sections is well developed in laminations to weakly developed and scattered throughout the sample (Figure 8.5). The apatite occurs as nodules that are non-compacted to slightly compact. These nodules are possibly stained with iron in some thin sections. Glauconite is common to many of the slides from the upper Caney, and is generally associated with or near apatite nodules.

Also, in the upper Caney, <u>Tasmanites</u> cysts are noted in most of the thin sections (Figure 8.6). These cysts varied from abundant to sparse. The cysts are mostly compacted and replaced by microquartz and bitumen. Some cysts are replaced by pyrite and are non-compacted. Mollusk shells and fragments are present in many of the thin sections. Silt-size quartz grains are also present in all of the thin sections from the upper Caney. These grains were commonly angular and are sometimes concentrated in laminations (Figure 8.6).

One thin section from the Richardson 2-33 wells is very different from the other thin sections collected from the upper Caney. This thin section, from 5932 ft below the kelly bushing, contains no apatite nodules or glauconite (Figure 8.7). The thin section is composed of silt-size calcite fragments and quartz grains. The calcite fragments are predominately abraded with only a few large fragments that are not broken. All of the
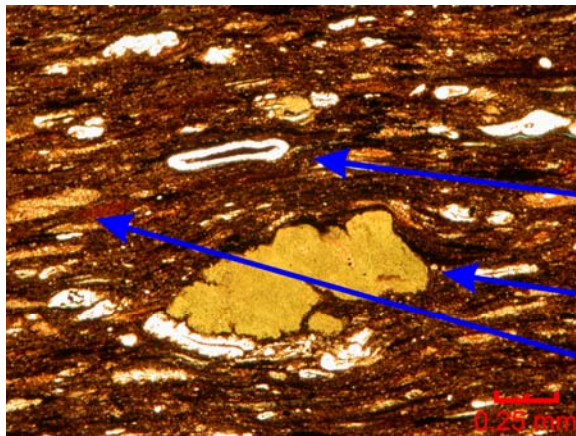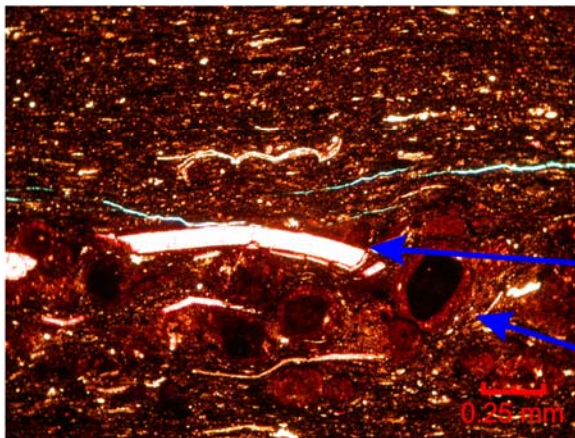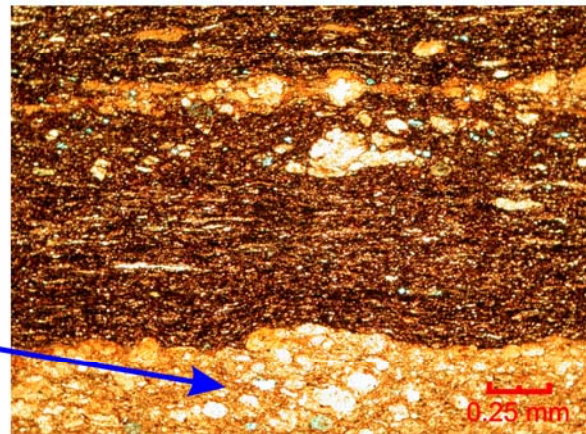
Figure 8.5 Thin sections of the upper Caney Shale from the Delaware Creek outcrop, the Jeff Luke shale pit, and the Richardson 2-33 well.
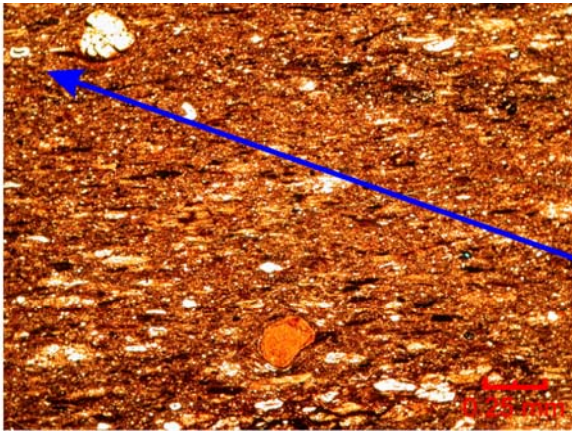
A. 8.0 ft Jeff Luke Shale Pit 1B

Slightly Laminated Brown Shale

Tasmanites Cyst

B. 5881.5 ft Richardson 2-33

Non-Laminated Brown Shale

Large Bivalve Fragments
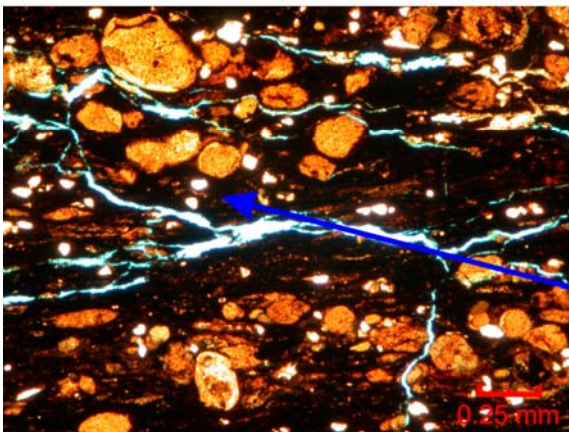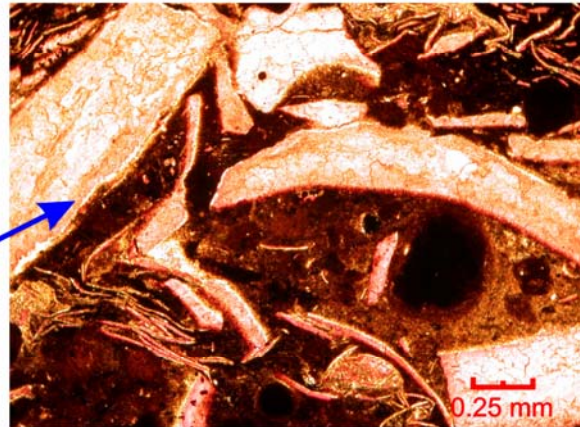
C. 4.0 ft Delaware Creek

Slightly Laminated Black Shale

Silt Size Angular Quartz

Figure 8.6 Thin sections of the upper Caney Shale from the Jeff Luke shale pit, the Richardson 2-33 well, and the Delaware Creek outcrop.

110
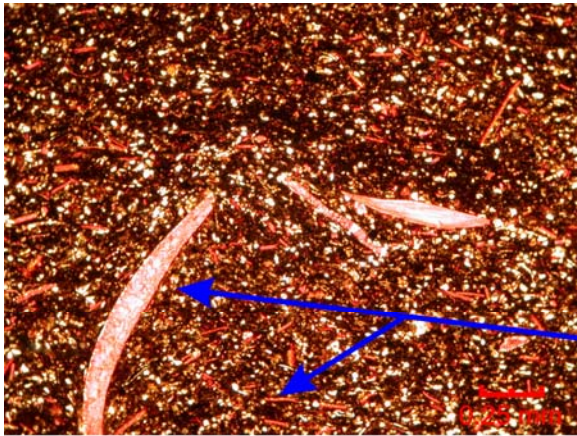
A. 5932 ft Richardson 2-33

Non-Laminated Brown Shale

Abraided to Whole Bivalve Fragments

B. 5932 ft Richardson 2-33

Non-Laminated Brown Shale

Silt Size Angular Quartz
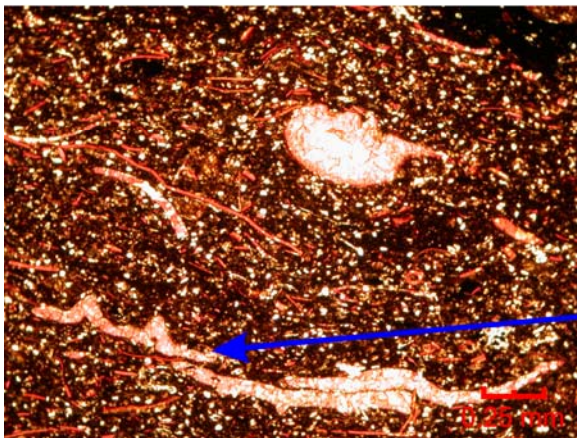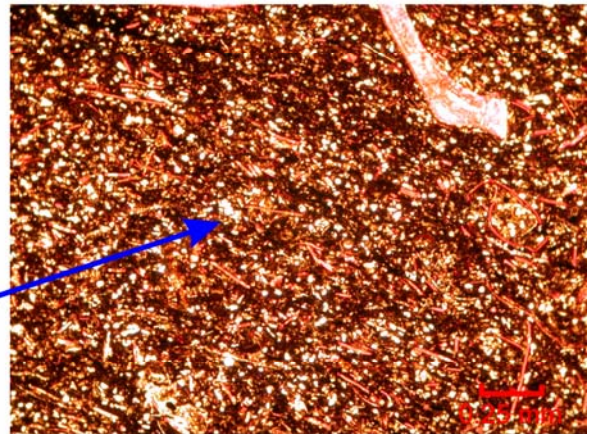
C. 5932 ft Richardson 2-33

Non-Laminated Brown Shale

Brachiopod Fragment

Figure 8.7 Thin section of a sidewall core from a depth of 5932 ft in the Richardson 2-33 well. This thin section shows abundant fossils fragments, silt size quartz, and clay.

quartz grains are angular and are suspended in a clay matrix. A few algal cysts are identified in this thin section.

Two samples were collected from the lower Goddard Shale formation. Thin sections of these samples resemble many of the features viewed in the upper Caney. At the Delaware Creek outcrop the thin sections from the lower Goddard are of a laminated brown shale (Figure 8.8). The thin sections contain Tasmanites cysts but no apatite nodules or quartz grains. Thin sections from the Little Delaware Creek outcrop are of a laminated dolomitic to calcareous shale (Figure 8.8). The thin section contains apatite laminations and glauconite nodules.

8.2 X-Ray Diffraction

Outcrop samples and sidewall cores from the Richardson 2-33 and Rogers Trust 1-24 wells were sent away for x-ray diffraction (XRD) analyses. The Omni Laboratories, Inc. performed the XRD analysis of the sidewall cores, and Mineralogy, Inc. performed the XRD analysis of the outcrop samples. The results from the both of these analyses are shown in Tables 8.1 and 8.2. As illustrated in the table, the analysis by Mineralogy, Inc. estimates the amount of amorphous organic matter found in each of the samples. In addition, Mineralogy, Inc. documents trace amounts of minerals that are not documented in the subsurface. These minerals are all products of outcrop weathering and they include: jarosite, gypsum, and goethite, (Hurlbut and Klein, 1977).

In Figure 8.9 the average mineralogical constituents for the Caney and "Mayes" formations (lower Caney Shale) are plotted. According to the data, there is a large mineralogical difference between the Caney and the "Mayes" (lower Caney Shale). The
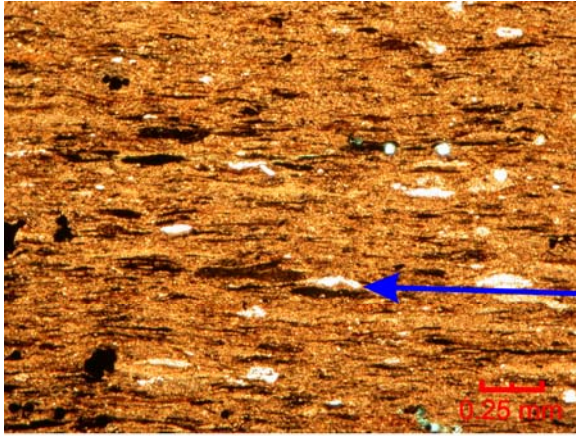
A. 11.0 ft Delaware Creek

Laminated Brown Shale

Tasmanites Cysts

0.25 mm

B. 12.0 ft Little Delaware Creek 1

Laminated Brown Dolomitic Shale

Glauconite and Apatite Laminae

0.25 mm
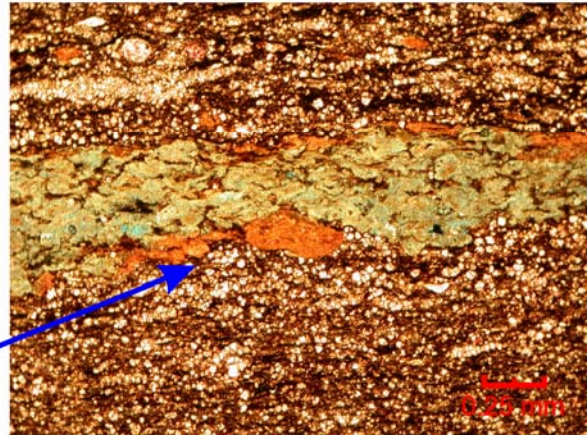
Figure 8.8 Thin sections of the lower Goddard Shale from the Little Delaware Creek outcrop 1 and the Delaware Creek outcrop.

Table 8.1 X-ray diffraction data for sidewall cores taken from the Rogers Trust 1-24 and the Richardson 2-33 wells. Results were calculated by Omni Laboratories, Inc.

Caney Shale �
"Mayes" Formation ▰

Richardson 2-33

Sample	CLAYS				CARBONATES			OTHER MINERALS					SUM		
Depth (ft)	Chlorite	Kaolinite	Illite	Mx I/S*	Calcite[1]	Dol/Ank**	Siderite	Quartz	K-spar	Plag.	Pyrite	Apatite	Clays	Carbonates	Other Minerals
5908.0	4	3	13	1	1	trc	2	61	1	3	1	10	21	3	76
5927.0	2	7	29	2	1	1	3	33	2	5	2	13	40	5	55
5996.0	3	4	20	9	28	4	0	27	1	2	2	0	36	32	32
6142.0	1	0	3	trc	14	66	Tr	11	2	3	trc	Tr	4	80	16
6208.0	1	1	14	3	14	7	Tr	50	3	6	trc	1	19	21	60

Rogers Trust 1-24

Sample	CLAYS				CARBONATES			OTHER MINERALS					SUM		
Depth (ft)	Chlorite	Kaolinite	Illite	Mx IS*	Calcite[1]	Dol/Ank**	Siderite	Quartz	K-spar	Plag.	Pyrite	Apatite	Clays	Carbonates	Other Minerals
6778.00	trc	10	16	18	4	5	0	31	1	4	2	9	44	9	47
6826.00	trc	6	19	16	10	2	0	36	0	5	4	2	41	12	47
6846.00	4	trc	22	25	13	3	0	25	trc	4	4	trc	51	16	33
7059.00	0	0	17	4	12	21	0	40	trc	3	3	trc	21	33	46

*Ordered interstratified mixed-layer illite/smectite, with 35% expandable interlayers for samples with abundant mixed-layers
**Includes dolomite and iron-bearing dolomites (i.e., Fe-dolomite and ankerite)
***No mixed illite, all smectite
[1]Includes the Fe-rich varieties

Table 8.2 X-ray diffraction results for samples collected from outcrops studied in this thesis. Results were calculated by Mineralogy, Inc.

Caney Shale
"Mayes" Formation

Outcrops

Sample Depth (ft)	CLAYS				CARBONATES			OTHER MINERALS									SUM		
	Chlorite	Kaolinite	Illite	Mx IS*	Calcite[1]	Dol/Ank**	Siderite	Quartz	K-spar	Plag.	Pyrite	Apatite	Jarosite	Gypsum	Goethite	Amorphous	Clays	Carbonates	Other Minerals
JL1A 0.65	1	3	16	21	32	1	0	15	0	trc	1	0	0	0	0	10	41	33	26
JL1B 3.5	3	4	25	32	trc	0	0	20	trc	1	3	0	0	trc	0	12	64	0	36
JL1B 5.0	trc	10	33	18	0	0	0	19	1	2	2	0	trc	1	0	14	61	0	39
JL1B 7.0	2	2	22	31	0	0	trc	26	trc	1	0	0	2	0	0	14	57	0	43
JL1B 11.0	trc	4	28	19	0	0	trc?	31	trc	2	0	0	3	0	0	13	51	0	49
JL2 4.0	trc	2	33	17	0	0	0	29	trc	3	0	trc	1	0	0	15	52	0	48
JL3 8.0	trc	2	30	23	0	0	0	24	1	5	0	2	1	trc	0	12	55	0	45
PT1 24.0	1	1	28	24	0	0	0	34	1	2	0	1	trc	0	0	8	54	0	46
PT2 32.5	1	2	26	37	0	0	0	24	1	1	0	trc?	trc	trc	0	8	66	0	34
PT3 9.0	1	3	24	28	0	0	0	32	1	4	0	trc?	trc	0	0	7	56	0	44
PT4 34.5	1	2	24	27	0	0	0	35	trc	2	0	trc	1	0	0	8	54	0	46
PT5 11.0	trc	3	24	34	0	0	0	31	trc	1	0	0	1	0	0	6	61	0	39
PT6 6.0	trc	2	30	28	0	0	0	31	trc	1	0	0	0	0	1	7	60	0	40
PT7 6.0	trc	1	17	21	0	0	0	53	0	trc	0	0	trc	0	1	7	39	0	61
LDC1 3.0	trc	2	22	34	1	0	0	29	1	2	0	4	trc	0	0	5	58	1	41
LDC1 6.0	trc	2	18	28	1	16	0	24	trc	2	0	1	0	trc	0	7	48	17	34
LDC1 12.0	1	5	24	31	trc	0	trc	22	1	3	1	0	0	0	0	12	61	0	39
LDC2 2.3	trc	2	7	38	13	0	0	29	trc	2	0	2	0	0	0	7	47	13	40
LDC2 3.5	trc	1	4	38***	3	19	0	28	trc	1	1	1	0	0	0	4	5	22	35
LDC2 6.0	1	2	6	47	trc	0	0	30	2	3	trc	1	0	trc	0	8	56	0	44
LDC2 11.0	1	4	11	44	3	0	0	20	1	2	1	6	0	trc	0	7	60	3	37
LDC3 3.0	1	2	10	37	3	0	0	33	1	2	0	1	trc	0	0	10	50	3	47
LDC3 5.0	1	5	7	44***	2	0	0	29	trc	2	trc	0	0	0	0	10	13	2	41
LDC3 8.5	1	3	8	39	5	0	0	26	1	2	1	2	0	0	0	12	51	5	44
LDC4 0.5	1	3	8	46	0	0	0	26	1	2	0	trc	0	trc	0	13	58	0	42
LDC4 7.0	trc	2	6	43	3	0	0	27	trc	2	1	4	0	0	0	12	51	3	46
DC 1.0	trc	2	7	32	0	0	0	20	trc	trc	4	22	0	1	0	12	41	0	59
DC 4.0	1	2	6	35	trc	0	0	18	trc	trc	1	21	0	1	0	15	44	0	56
DC 9.0	6	8	4	47	0	0	0	20	trc	trc	0	0	0	trc	0	15	65	0	35
DC 11.0	5	7	3	51	0	0	0	18	trc	1	0	0	1	trc	0	14	66	0	34
DC 15.5	3	5	3	55	0	0	0	17	1	trc	0	0	4	trc	0	12	66	0	34
RF1 3.25	trc	2	10	6	32	35	0	14	trc	1	0	0	0	0	0	0	18	67	15
RF1 2.0	trc	1	11	5	3	66	0	13	trc	1	0	0	0	0	0	0	17	69	14
RF2 0.6	2	4	17	21	28	trc	0	15	0	1	2	0	0	0	0	10	44	28	28
RF2 0.1	trc	1	5	15	65	0	0	6	0	0	3	0	0	0	0	5	21	65	14
RF2 2.0	2	2	23	18	0	0	0	22	0	1	0	17	0	0	0	15	45	0	55

*Ordered interstratified mixed-layer illite/smectite, with 35% expandable interlayers for samples with abundant mixed-layers
**Includes dolomite and iron-bearing dolomites (i.e., Fe-dolomite and ankerite)
***No mixed illite, all smectite
[1]Includes the Fe-rich varieties
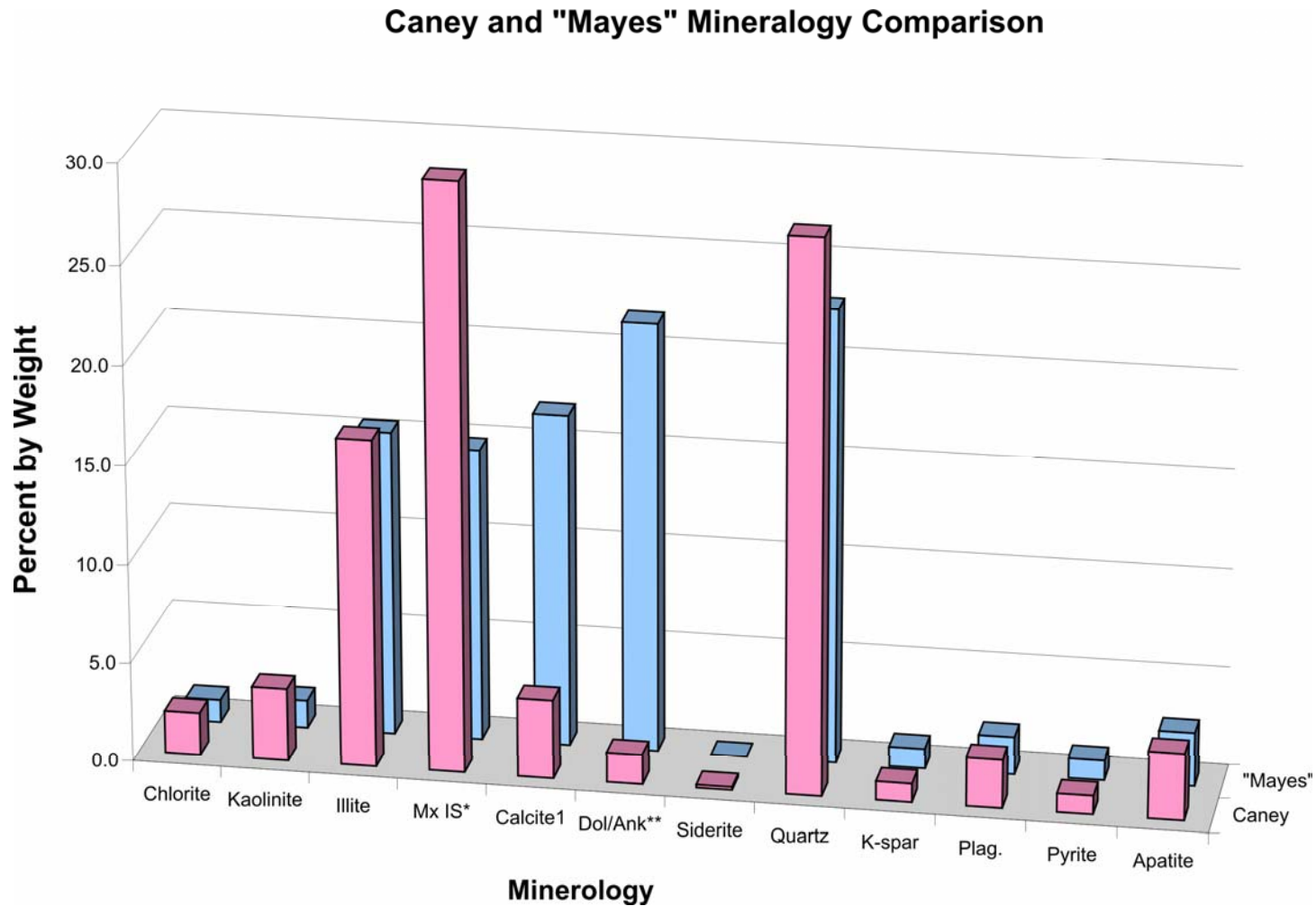
Figure 8.9 Bar chart showing the average mineralogy of the Caney Shale and "Mayes" Formation. The data for this chart came from computing the averages of each mineral constituent in Tables 8.1 and 8.2

"Mayes" (lower Caney Shale) contains far more calcite and dolomite than the Caney Shale. This agrees with the outcrop and subsurface thin section descriptions of the formation. The Caney is slightly more quartz rich, contains more illite, and significantly more mixed layer illite-smectite.

8.3 Total Organic Carbon

Outcrop samples and subsurface samples from the Richardson 2-33 and Rogers Trust 1-24 wells were analyzed for total organic carbon (TOC) and kerogen type by Humble Geochemical Services. The results of these analyses are shown in Tables 8.3 and 8.4. According to the data, the Caney Shale and "Mayes" formations (lower Caney Shale) have TOC values that range form 0.5% to 11.0%. In Figure 8.10 the TOC values are plotted against the remaining hydrocarbon potential of the shales. As one can see from the data, the subsurface samples indicate that the organic matter type in the Caney Shale is Type III woody. In contrast the outcrop data indicate that the organic matter type is predominantly Type II with some mix of Type II and III. In Figure 8.11 the thermal maturity of the samples is illustrated. According to the data, the outcrops studied in this work all have a similar thermal maturity. The outcrop samples are thermally immature, while subsurface samples are mainly in the oil to dry gas window.

Table 8.3 Table of total organic carbon and maturity results from the Rogers Trust 1-24 and Richardson 2-33 wells. Results were calculated by Humble Geochemical Services.

"Mayes" Formation ▮ (blue)
Caney Shale ▮ (magenta)

Well Name	Top Depth (ft.)	Bottom Depth (ft.)	Median Depth (ft.)	Formation Name	Sample Type	TOC	S1	S2	S3	Tmax (oC)		Cal. %Ro	Meas. %Ro	HI	OI	S2/S3	S1/TOC	PI	Notes Checks	Notes Pyrogram
Richardson 2-33	5881.0		5881	Caney	swc	0.55	0.13	0.14	0.04	320	*	-1.00	1.64	25	7	4	24	0.48	c	n
Richardson 2-33	5908.5		5908.5	Caney	swc	4.83	1.56	3.03	0.10	473		1.35		63	2	30	32	0.34		n;ltS2p
Richardson 2-33	5926.5		5926.5	Caney	swc	4.75	1.28	2.78	0.09	474		1.37	1.68	59	2	31	27	0.32		n
Richardson 2-33	5932.0		5932	Caney	swc	1.20	0.22	0.45	0.06	485	*	1.57		37	5	7	18	0.33		n
Richardson 2-33	5951.0		5951	Caney	swc	7.26	1.49	4.52	0.09	478		1.44		62	1	50	21	0.25		n
Richardson 2-33	6208.0		6208	Mayes	swc	0.67	0.12	0.16	0.00	481	*	1.50		24	0	-1	18	0.43		n

Well Name	Top Depth (ft.)	Bottom Depth (ft.)	Median Depth (ft.)	Formation	Sample Type	TOC	S1	S2	S3	Tmax (oC)	Cal. %Ro	Meas. %Ro	HI	OI	S2/S3	S1/TOC	PI	Notes Checks	Notes Pyrogram
Rogers Trust 1-24	6800	6810	6805	Caney	cuttings	2.75	0.60	1.77	0.28	455	1.03	1.19	64	10	6	22	0.25		n
Rogers Trust 1-24	7000	7010	7005	Caney	cuttings	2.03	0.50	1.15	0.19	453	0.99	1.18	57	9	6	25	0.30		na
Rogers Trust 1-24	7130	7140	7135	Base Mayes & Top WDFD	cuttings	1.46	0.20	0.89	0.11	460	1.12	1.23	61	8	8	14	0.18		na

Note: "-1" indicates not measured or meaningless ratio

* Tmax data not reliable due to poor S2 peak

TOC = weight percent organic carbon in rock
S1, S2 = mg hydrocarbons per gram of rock
S3 = mg carbon dioxide per gram of rock

Tmax = °C

HI = hydrogen index = S2 x 100 / TOC
OI = oxygen index = S3 x 100 / TOC
S1/TOC = normalized oil content = S1 x 100 / TOC
PI = production index = S1 / (S1+S2)
Cal. %Ro = calculated vitrinite reflectance based on Tmax
Measured %Ro = measured vitrinite reflectance

Notes:
c = Rock-Eval analysis checked and confirmed
lc = Leco TOC analysis checked and confirmed

Pyrogram:
n=normal
ltS2sh = low temperature S2 shoulder
ltS2p = low temperature S2 peak
htS2p = high temperature S2 peak
f = flat S2 peak
na = printer malfunction pyrogram not available

118

Table 8.4 Table of total organic carbon and maturity results from the outcrops studied in this thesis. Results were calculated by Humble Geochemical Services.

"Mayes" Formation
Caney Shale

Client ID 1	Formation Name	Sample Type	Leco TOC	S1	S2	S3	Tmax (°C)	Cal. %Ro	Meas. %Ro	HI	OI	S2/S3	S1/TOC	PI	Notes Checks	Pyrogram
RF2 0.6	"Mayes" For	outcrop	4.38					* -1.00								
RF2 2.0	"Mayes" For	outcrop	10.93	0.85	41.11	4.58	425	0.49		376	42	9	8	0.02	c	n;ltS2p
JL 1A	Caney shale	outcrop	2.81	0.31	11.00	0.28	428	0.54		391	10	39	11	0.03		n
JL 1B 2	Caney shale	outcrop	5.17	0.45	19.71	1.63	419	0.38		381	32	12	9	0.02		n;ltS2p
JL 1B 9	Caney shale	outcrop	6.41	1.16	23.88	0.74	416	0.33		373	12	32	18	0.05		n;ltS2p
JL 1B 17	Caney shale	outcrop	6.24					* -1.00								
JL 3 4.0	Caney shale	outcrop	6.06					* -1.00								
JL 2 4.0	Caney shale	outcrop	7.43					* -1.00								
JL 1B 5	Caney shale	outcrop	6.05	0.73	24.89	0.41	420	0.40		411	7	61	12	0.03		n
JL 3 8.0	Caney shale	outcrop	9.79	1.32	44.08	2.59	416	0.33		450	26	17	13	0.03		n
PT1 24.0	"Mayes" For	outcrop	7.34	2.41	37.99	0.40	429	0.56		518	5	95	33	0.06		n;ltS2p
PT2 32.5	"Mayes" For	outcrop	5.92					* -1.00								
PT3 9.0	Caney shale	outcrop	3.01	0.06	1.69	2.67	436	0.69		56	89	1	2	0.03		n
PT4 34.5	Caney shale	outcrop	7.02	1.64	29.96	1.38	427	0.53		427	20	22	23	0.05	c	n;ltS2p
PT5 24.0	Caney shale	outcrop	6.02					* -1.00								
PT6 6.0	Caney shale	outcrop	1.72					* -1.00								
PT7 6.0	Caney shale	outcrop	8.54	3.49	34.31	2.24	428	0.54		402	26	15	41	0.09		n;ltS2p
LDC1 3.0	Caney shale	outcrop	5.37					* -1.00								
LDC1 6.0	Caney shale	outcrop	4.09					* -1.00								
LDC1 12.0	Caney shale	outcrop	4.31	0.61	22.03	0.49	419	0.38		511	11	45	14	0.03		n;ltS2p
LDC2 2.3	Caney shale	outcrop	9.48					* -1.00								
LDC2 3.5	Caney shale	outcrop	1.70	0.43	15.00	0.86	419	0.38		882	51	17	25	0.03		n;ltS2p
LDC2 6.0	Caney shale	outcrop	3.85					* -1.00								
LDC2 11.0	Caney shale	outcrop	3.72	0.37	12.71	0.36	424	0.47		342	10	35	10	0.03		n
LDC3 3.0	Caney shale	outcrop	5.24					* -1.00								
LDC3 5.0	Caney shale	outcrop	3.16	0.23	8.80	0.93	425	0.49		278	29	9	7	0.03		n
LDC3 8.5	Caney shale	outcrop	4.68					* -1.00								
LDC4 0.5	Caney shale	outcrop	5.22	0.19	13.11	3.47	431	0.60		251	66	4	4	0.01		n
LDC4 7.0	Caney shale	outcrop	5.38					* -1.00								
DC1 1.0	Caney shale	outcrop	5.43	0.18	11.22	0.61	424	0.47		207	11	18	3	0.02		n
DC1 4.0	Caney shale	outcrop	3.95					* -1.00								
DC1 9.0	Caney shale	outcrop	2.08					* -1.00								
DC1 11.0	Caney shale	outcrop	2.87	0.11	2.22	0.80	428	0.54		77	28	3	4	0.05	c	n
DC1 15.5	Caney shale	outcrop	2.60					* -1.00								

Note: "-1" indicates not measured or meaningless ratio

* Tmax data not reliable due to poor S2 peak

TOC = weight percent organic carbon in rock
S1, S2 = mg hydrocarbons per gram of rock
S3 = mg carbon dioxide per gram of rock
Tmax = °C

HI = hydrogen index = S2 x 100 / TOC
OI = oxygen index = S3 x 100 / TOC
S1/TOC = normalized oil content = S1 x 100 / TOC
PI = production index = S1 / (S1+S2)
Cal. %Ro = calculated vitrinite reflectance based on Tmax
Measured %Ro = measured vitrinite reflectance

Notes:
c = Rock-Eval analysis checked and confirmed
lc = Leco TOC analysis checked and confirmed

Pyrogram:
n=normal
ltS2sh = low temperature S2 shoulder
ltS2p = low temperature S2 peak
htS2p = high temperature S2 peak
f = flat S2 peak
na = printer malfunction pyrogram not available

Figure 8.10 Plot of total organic carbon vs. remaining hydrocarbon potential. Chart indicates that outcrops samples are mainly Type II and Type II/III mixed kerogen, while subsurface samples are Type III kerogen.
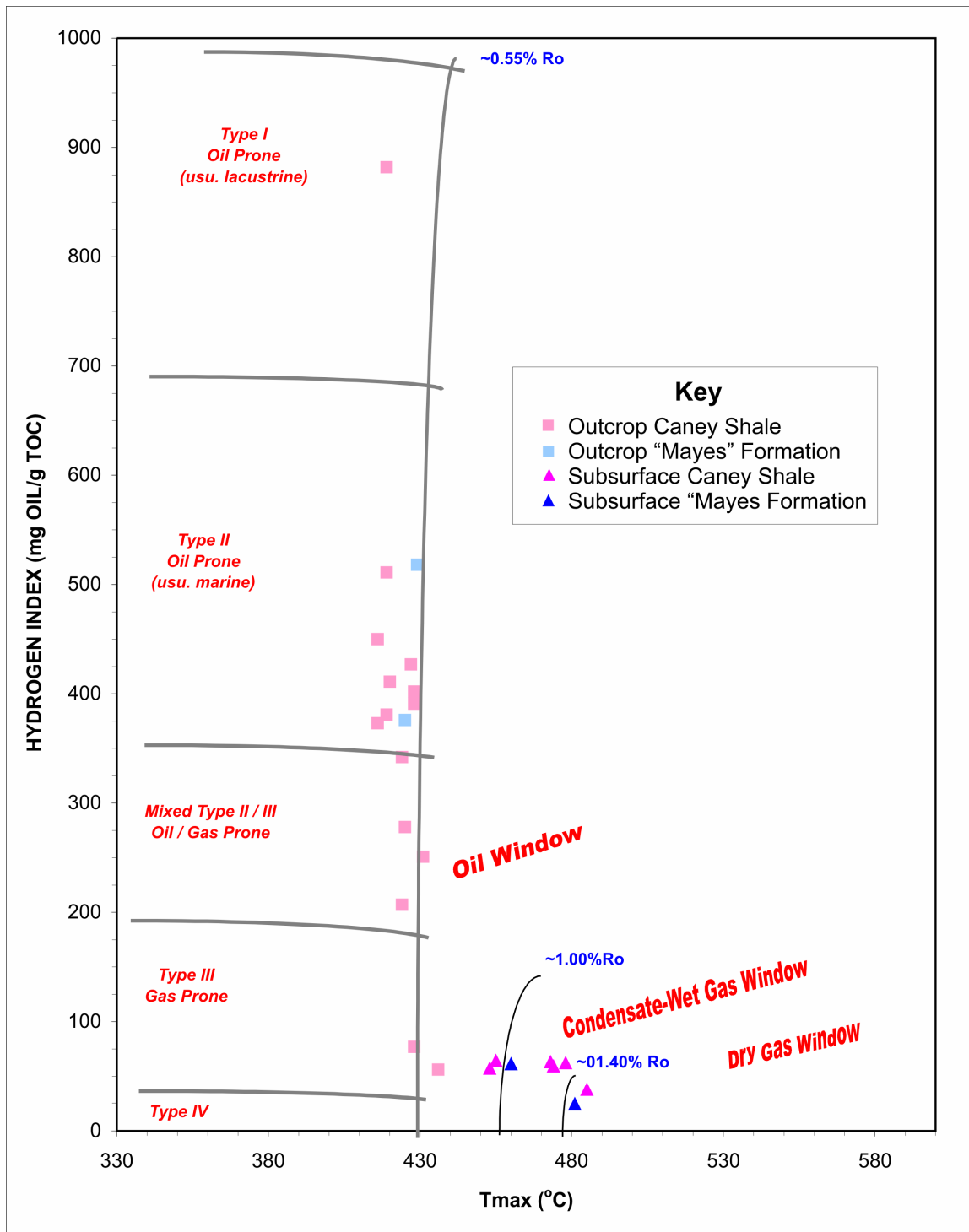
Figure 8.11 Plot of temperature max vs. hydrogen index. Plot indicates that subsurface samples are mature for gas, while outcrop samples are immature.

CHAPTER 9.0

LITHOSTRATIGRAPHIC UNIT DIVISIONS

Based on results in this study, the Caney Shale and "Mayes" formation (lower

Caney Shale) are two distinct lithostratigraphic units. These lithostratigraphic units are

large enough in scale to be mapped and correlated in both the subsurface and surface.

Whether the "Mayes" formation (lower Caney Shale) is part of the Caney Shale

formation, or it should be classified as an independent formation will not be discussed

here. However, in this work the "Mayes" (lower Caney Shale) is considered to be an

independent lithostratigraphic unit based on the data presented in this thesis.

The "Mayes" formation (lower Caney Shale) and Caney Shale each consist of

several smaller-scale lithostratigraphic units that are identifiable in outcrops or core.

These smaller units either consist of 1) a different lithology or 2) a lithologic variation of

the parent lithology. For the purpose of this work, the "Mayes" formation (lower Caney

Shale) is not broken down into smaller lithostratigraphic units, but the Caney Shale is

broken down into four lithostratigraphic units; Caney C1, C2, C3, and C4. These

lithostratigraphic units were identified by differences in lithologic character viewed in

outcrops, subsurface data, and wire-line logs presented above. An ideal or type wire-line

log with each of the four units identified is presented in Figure 9.1 below. Because

outcrop exposures were limited, some divisions rely more heavily on subsurface data.
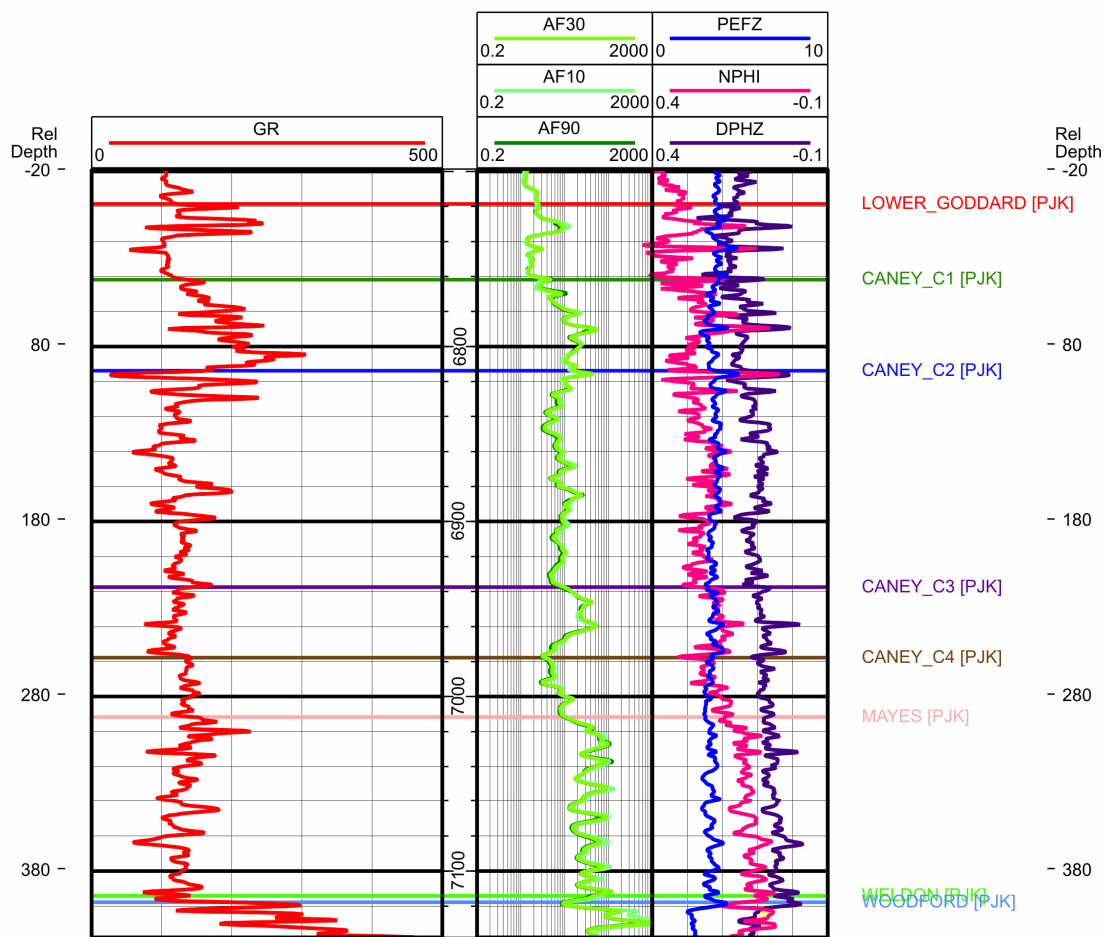
Figure 9.1 Caney Shale Type Log showing the lithostratigraphic divisions of the Caney Shale, C1, C2, C3, and C4, where GR equals gamma ray, AF10 equals shallow induction log, AF30 equals medium induction log, AF90 equals deep induction log, PEFZ equals photoelectric log, NPHI equals neutron porosity log, and DPHZ equals density porosity log.

Additionally, these lithostratigraphic units were chosen based on large scale lithostratigraphic characteristics and not small scale facie changes. As more outcrops and subsurface cores are studied of the Caney Shale these lithostratigraphic units will likely be modified. Further research may indicate that the Caney Shale needs to be divided and evaluated on a more refined level.

The Caney C4 unit is the lowest lithostratigraphic unit found within the Caney Shale formation. This unit rest upon the "Mayes" formation (lower Caney Shale). The contact between these two intervals appears to be sharp in the outcrop exposed at Pine Top Mountain, however, this outcrop is heavily weathered and the contact is poorly exposed. In electrical image logs this contact also appears to be sharp. At the Pine Top Mountain outcrop (Section 3) the Caney C4 unit is composed of a black fissile shale that is non-calcareous. A thin section of a sidewall core was taken from this interval at 7001 ft in the Rogers Trust 1-24 well. In this thin section, the C4 unit is composed of a slightly laminated to non-laminated shale with angular silt-size quartz grains. A few Tasmanites were present in the unit indicating some algal organic component. In the electrical image logs a few limestone beds occur within the unit. Pyrite and some bioturbated intervals are possibly present in the unit. This lithostratigraphic unit was mostly covered in the Pine Top Mountain outcrop, and so it was difficult to accurately determine the lithology. Therefore, the description for this lithology comes from mud logs, thin sections, and interpretations of borehole image logs.

In wire-line logs the Caney C4 unit typically has an average gamma-ray reading of 140 API units (Table 9.1). The PE curve falls between 2.9 and 4.0 barns/electron, which indicates silty shales and calcareous shales in the interval. The neutron porosity

Table 9.1 Wire-line log summary statistics for the four lithostratigraphic divisions of the Caney Shale, C1, C2, C3, and C4; where PE is equal to photoelectric log, Neutron is equal to neutron porosity log, Density is equal to density porosity log, GR is equal to gamma ray log, and Resistivity is equal to resistivity log. Data was derived from of the Rogers Trust 1-24 and Richardson 2-33 wells.

Caney C1

	Average	Std	min	max
PE	3.34	0.28	2.68	4.04
Neutron	0.26	0.04	0.17	0.38
Density	0.12	0.03	0.06	0.17
GR	192.12	48.10	100.89	390.31
Resistivity	22.49	19.99	4.97	188.22

Caney C2

	Average	Std	min	max
PE	3.44	0.27	2.95	4.23
Neutron	0.22	0.05	0.09	0.33
Density	0.08	0.03	-0.02	0.15
GR	127.31	31.56	27.56	238.21
Resistivity	34.84	33.54	4.16	271.22

Caney C3

	Average	Std	min	max
PE	3.38	0.30	2.82	3.93
Neutron	0.16	0.04	0.10	0.28
Density	0.06	0.02	-0.01	0.11
GR	122.43	18.20	75.59	175.26
Resistivity	62.45	53.06	12.16	348.67

Caney C4

	Average	Std	min	max
PE	3.26	0.23	2.92	4.03
Neutron	0.19	0.06	0.01	0.33
Density	0.05	0.02	-0.03	0.11
GR	140.29	12.71	113.38	191.05
Resistivity	50.07	73.75	5.20	683.95

for this unit averages around 19% and the density porosity averages around 5%. Figure 9.1 illustrates the ideal wire-line log signature for this interval. Using the wire-line logs the contact between the "Mayes" formation (lower Caney Shale) and the Caney C4 unit is marked by a decrease in gamma ray below 150 API units and a decrease in resistivity from 100 ohm-m to 8 ohm-m. Additionally, at this contact the neutron porosity increases over 20%.

The Caney C3 unit is found stratigraphically above the Caney C4 unit. This lithostratigraphic unit was not exposed in the outcrops evaluated above and sidewall cores were not taken in this interval. Lithologic descriptions of this unit come from mud log descriptions and interpretations of wire-line logs and electrical image logs. The contact between C4 and C3 appears to be sharp in the borehole image logs, with the top of the C4 unit being bioturbated and the base of the C3 unit being laminated. The Caney C3 unit is differentiated from the C4 unit by the presence of calcareous shale. This unit also contains carbonate beds and/or nodules. In between the carbonate beds the shale is typically laminated and contains pyrite.

The typical wire-line log signature of the C3 unit is shown in Figure 9.1. The gamma-ray response for this unit averages approximately 122 API units (Table 9.1) The PE curve falls between 2.8 and 3.9 barns/electron, which indicates shales that contain little to very abundant carbonate. The neutron porosity for this interval averages around 16% and the density porosity averages around 6%. The boundary between the Caney C4 and C3 lithostratigraphic units is marked by a decrease in gamma-ray response from approximately 140 to 75 API units. The resistivity begins to increase at this contact toward 50 ohm-m, and the neutron porosity decreases toward the density porosity.

The Caney C2 unit is found stratigraphically about the Caney C3 unit. The contact between these two units is unknown in outcrop. The contact is covered in the Pine Top Mountain outcrop and is not present at any of the other outcrop locations. In the borehole electrical image logs this contact appears to be sharp. At Pine Top Mountain this unit is characterized as a fissile black shale that is non-calcareous. In borehole electrical image logs from the northwestern part of the study area this unit contains both calcareous and non-calcareous shales. This unit also contains interbedded carbonate concretions and thin carbonate beds. Despite the presence of calcareous shales and carbonate beds and/or concretions, this unit is believed to be less calcareous than the Caney C3 lithostratigraphic unit. Pyrite and apatite are common within the shale matrix. Apatite also occurs as nodules in the unit. In thin sections from the Rogers Trust and Richardson wells, this section is characterized as a laminated to non-laminated black shale. Large fossil fragments are common to rare, and angular silt-size quartz grains are abundant. Compacted Tasmanites cysts were present in small quantities in these thin sections. At top of the unit, two carbonate beds separated by a "hot" shale is typical. The top of the uppermost carbonate unit marks the boundary between the C2 and C1 lithostratigraphic unit. This carbonate bed was exposed in Little Delaware Creek outcrop 4. This carbonate bed is characterized as a mudstone with no visible fossils. The bed had wavy irregular upper and lower boundaries. The upper and lower carbonate beds also have wavy irregualar boundaries in electrical image logs.

The average gamma-ray reading in the Caney C2 unit is 127 API units (Table 9.1). Most of the interval has gamma-ray readings below 150 API units; however several spikes over 150 API units commonly occur. The top of the unit is characterized by two

low gamma-ray spikes separated by high (over 200 API units) gamma-ray spike. The PE curve for this unit ranges between 3 and 4.2 barns/electron, which indicates calcareous and non-calcareous shales. The neutron porosities for this unit vary between 9 and 33%, and density porosities vary between 0 and 15 %. The contact between the Caney C2 and C3 lithostratigraphic units is marked by a gamma-ray spike over 150 API units and a decrease in resistivity to approximately 5 ohm-m. Additionally, neutron porosity increases to 25 to 30% and density increases slightly from 7% to 15%.

The Caney C1 unit is the youngest lithostratigraphic unit identified. This unit lies conformably above the C2 unit. Again, the contact between this unit and the one below is believed to be exposed at the Little Delaware Creek outcrop 4. The borehole image log for this interval shows a wavy irregular contact, which agrees with the contact viewed in this outcrop. The C1 unit was well exposed in the Lawrence Uplift and Bromide outcrop areas. This unit is composed predominately of a fissile black silty shale that has a high gamma-ray response. The shale is generally non-calcareous, laminated, and contains abundant apatite. These characteristics make the Caney C1 unit significantly different than the C2 unit which does not contain well developed apatite, is more calcareous, and has a lower gamma-ray response. The apatite in the C4 unit commonly occurs in concretions and laminae. Some concretions and laminae are large enough to be seen in outcrop, others are only visible in thin section. These laminae are slightly discontinuous and can contain concretions. In the Lawrence Uplift outcrop area apatite concretions and laminae are large enough to be seen in outcrop. However, in the Bromide outcrop area apatite concretions and laminae are predominantly visible only in thin section. Pyrite, carbonate concretions and beds, and fossil impressions have been noted to occur in this

section. Schad (2004) noted plant fragments in this interval. Also, a thin section from 6786.0 ft in the Rogers Trust 1-24 well contained a possible plant fragment. Carbonate beds and concretions are more abundant in the Bromide outcrop area where apatite is less pronounced. Also, within this unit there are calcareous shale intervals. These more calcareous shales appear to weather more quickly in outcrop.

The Caney C1 unit has the highest gamma-ray readings throughout the section. The gamma ray is generally well above 150 API units and averages about 192 API units (Table 9.1). The intervals that contain abundant apatite coincide with the intervals having high gamma-ray readings. The PE curve for this section ranges between 3.0 and 4.2 barns/electron, which indicates both quartz and carbonate rich shales. The neutron porosity for this interval is generally high with ranges between 9 and 33% porosity. A few calcareous intervals to carbonate beds have the lowest neutron porosities. The density porosity for this interval is ranges between 0 and 15%; with the lowest porosities again occurring in the carbonate-rich intervals. The contact between the C1 and C2 lithostratigraphic units is marked by a sharp increase in gamma-ray response from approximately 35 API units to over 150 API units. Additionally, there is a sharp increase in neutron porosity from approximately 4% to 35%, and density porosity from approximately 1% to 15%. The contact between the lower Goddard Shale and Caney Shale is marked by a constant gamma-ray decrease below 150 API units and a decrease in resistivity below approximately 2 ohm-m. Also, at this contact the neutron porosity increases to approximately 40% and the density porosity increases to approximately 25%.

CHAPTER 10.0

DEPOSITIONAL ENVIRONMENT

Few depositional environment interpretations for the Caney Shale and "Mayes"

formations (lower Caney Shale) have been proposed. Champlin (1959) hypothesized that

the "Mayes" formation (lower Caney Shale) was deposited in a low energy environment

with water depths similar to those of the Sycamore Formation. He (ibid) interpreted the

Caney Shale to be a deep marine deposit that resulted from a relative sea level rise at the

end of the "Mayes" (lower Caney Shale). Sutherland (1988), summarizing work from

several authors, indicates that the Caney Shale was deposited on the shelf with sediment

transport from the east (Figure 1.9). During the deposition of the Caney Shale, the

Stanley Shale was deposited off the shelf in the deep ocean basin.

Schad (2004) attempted to construct paleo-water depths at the time of deposition

of the "Mayes" formation (lower Caney Shale) and Caney Shale, but did not provide a

detailed depositional environment interpretation. Paleo-water depths were determined by

decompacting the Caney Shale in water depths at the start of the Mississippian. Water

depths at the start of the Mississippian were estimated from a paleostructure map of the

top of the Arbuckle Group by Byrnes and Lawyer (1999). Byrnes and Lawyer (1999)

estimated the top of the Arbuckle Group at the start of the Mississippian to be 1300 ft

subsea in Schad's (2004) area of calculation. To this depth, Schad (2004) added the

present day thickness of the Sylvan Shale and Hunton Limestone and decompacted the

Woodford Shale to get water depths during deposition of "Mayes" formation (lower

Caney Shale) sediments. He then added to the present thickness of the "Mayes"

formation (lower Caney Shale), assuming no compaction, to determine water depths at

the start of deposition of Caney Shale sediments. In these calculations, the thickness of

the "Mayes" (lower Caney Shale) and original thickness of the Caney were greater than

sea level as determined from Brynes and Lawyer (1999), so Schad (2004) added sea level

rises into the calculation. Because the basis for these sea level rises was purely

speculative, the water depths estimated by Schad (2004) are likely incorrect.

In the following paragraphs an interpretation of the depositional environment of

the Caney Shale and "Mayes" formation (lower Caney Shale) will be provided. The

evidence used for this interpretation comes from sedimentary and stratigraphic

observations viewed in the study area. As a result this interpretation of the depositional

environment, like all other interpretations before it, will likely be modified as more

information is learned about these formations in future studies.

At the Pine Top Mountain outcrop the "Mayes" formation (lower Caney Shale)

was primarily composed of organic rich siliceous shales. In addition to this lithofacies

non-organic rich shales (calcareous to non-calcareous) along with dolomitic carbonate

beds were present. The Richard's Farm outcrops on the Lawrence Uplift and sidewall

cores from the northwestern part of the study area show a much different "Mayes"

formation (lower Caney Shale). At these locations organic rich shales, silty dolomitic

carbonates, and shaly silty dolomites were present. However, there were no siliceous

shales viewed in this area. Authors such as Elias (1956) and Champlin (1959) have not described the "Mayes" (lower Caney Shale) as a siliceous shale.

The difference in lithology observed in the "Mayes" formation (lower Caney Shale) is interpreted to be a result of facies changes across the basin. Recall, that the Pine Top Mountain outcrop is interpreted to be a slump block emplaced by thrusting during Ouachita Orogeny. As a result, the original stratigraphic location of this section is unknown, but was potentially farther basinward. The siliceous shale in this outcrop represents a deeper depositional environment. In the siliceous shale intervals, deposition is well below wave base and there is little to no influx of silt and sand. This environment is interpreted to be anoxic with the preservation of organic matter. A large drop in relative sea level resulted in the dolomitic carbonate beds and non-siliceous calcareous shales found at the Pine Top outcrop. With a drop in sea level the environment became more oxidizing.

In the western portion of this study area the "Mayes" (lower Caney Shale) was deposited in a much shallower water environment. This is indicated by the presence of sandy to silty dolomitic carbonates along with shaly silty dolomites. Thin sections of this formation do not show any bedding structures and clays and carbonate mud support larger grains. Fossils are present in the thin section, but are not abundant. The environment for this deposit is interpreted to be an environment just below normal wave base. Here, the influx of larger grains is possible as waves and currents carry larger grains offshore, but energy is low enough to keep fine clays and carbonate mud from washing out. A rise in sea level may result in the deposition of the organic rich shale deposits measured at the Richard's Farm outcrop.

Based on the work by Elias (1956), Champlin (1959) and Kleehammer (1991), the Sycamore Limestone is chronostratigraphically equivalent and laterally adjacent to the "Mayes" formation (lower Caney Shale). The Sycamore Limestone, described by Champlin (1959) and Coffey (2000), is a packstone containing quartz silt and sand. This indicates a moderate energy environment with an influx of siliciclastic material. The Sycamore limestone represents a slightly restricted depositional environment such as a lagoon with possibly less siliciclastic input than the "Mayes" (lower Caney Shale). Carbonate fossils and grains produced in this environment could have easily been transported basinward and deposited in the "Mayes" (lower Caney Shale).

The formation of carbonate concretions in the "Mayes" formation (lower Caney Shale) indicates that sulfate reduction and pyrite precipitation occurred during early diagenesis. These processes increase the alkalinity and cause supersaturation with respect to calcite (Curtis and Coleman, 1986). Sulfate reduction occurs when sulfate is present and oxygen levels are reduced through organic matter decay.

The top of the "Mayes" formation (lower Caney Shale)/base of the Caney Shale (Caney C4 lithostratigraphic unit) is interpreted to be a result of an increase in relative sea level. Evidence for this sea level increase is provided by the finer grained shale deposit of the Caney Shale overlying the coarser carbonate sediments of the "Mayes" formation (lower Caney Shale). Thin sections from the C4 unit indicate a black fissile shale that is non-calcareous. The nature of this deposit indicates water deeper environment than the carbonate dominated deposit of the "Mayes" formation (lower Caney Shale).

As in the "Mayes" formation (lower Caney Shale), the Caney Shale in the Pine Top Mountain outcrop is more siliceous than the Caney observed at the other outcrop locations in this study. This more siliceous shale is believed to be a result of silica input from the dissolution and replacement of radiolarians and <u>Tasmanites</u> cysts with microquartz. A more siliceous Caney Shale has also been noted by Elias (1956) and this author (outcrop reconnaissance for this study) on the southern flank of the Arbuckle Mountains. Initial interpretation of the outcrops on the southern flank is that they too might represent deeper-water deposition than locations to the north.

Deposition of the Caney Shale is believed to have occurred during the Early Llanoria Collision tectonic stage discussed above. During this stage, the approaching landmass begins to override the continental margin creating a flexural moat and a peripheral bulge, i.e. a foreland basin. Evidence for the existence of a flexural moat is provided by a deposit of thick Stanley Group sediments containing volcanic debris to the south of the Caney Shale (Figure 1.9). The Caney Shale is believed to have been deposited on the slope between the peripheral bulge and flexural moat. As discussed above, the boundary between the Caney and "Mayes" formations (lower Caney Shale) is believed to have resulted from an increase in relative sea level. This increase in sea level possibly resulted from the early formation of a slope and bulge.

The Caney C3 lithostratigraphic unit is believed to represent a decrease in relative sea level. The electrical image logs indicate carbonate beds are present within the formation. The shale beds within this unit are both laminated and disturbed. This is possibly an indication of an environment that fluctuates between oxic and anoxic conditions. These fluctuations could be a result of minor fluctuations in sea level.

The Caney C2 lithostratigraphic unit appears to be less calcareous than the C3 lithostratigraphic unit. Thin sections from this interval show a laminated to non-laminated black shale. Carbonate fossil fragments are common in the unit along with abundant angular silt-size quartz. Algal _Tasmanites_ cysts were also noted in small quantities in the thin sections. Electrical image logs in this unit indicate that carbonate beds and concretions are common in much of the unit. The formation of the carbonate concretions are a result of sulfate reduction and pyrite precipitation during early diagenesis. The depositional environment includes a deep-water environment with the preservation of organic matter and little to no bioturbation in this interval. Short periods of oxidation result in bioturbation of sediment. Silt is transported into the depositional environment by either wind or water currents.

The top of the Caney C2 interval is marked by two carbonate layers separated by hot shales. These two layers are relatively continuous across the basin and might represent uniform geochemical conditions in the basin at the time of deposition. One of these carbonate beds was present in the Little Delaware Creek 4 outcrop. This carbonate bed was classified as a mudstone that contained a component of clay in the matrix. The upper and lower boundaries of the unit were wavy. These carbonate bed may be a product of basin wide sulfate reduction of the organic matter in the neighboring hot shales. However, it seems unlikely that geochemical conditions that promote the precipitation of carbonate would be uniform across the basin. It may be possible that waters were clear and shallow enough for carbonate mud to be organically precipitated in the area. A thin section of one of these carbonate beds would help to answer this question.

The Caney C1 lithostratigraphic unit is characterized as a black laminated shale. A few intervals within the unit contain abundant abraided fossil fragments and are non-laminated. Glauconite is commonly present with abundant apatite precipitated in the unit, and silt-size quartz is found throughout the shale matrix. The shales are predominantly non-calcareous with some calcareous intervals. Plant fragments were noted within this interval with the organic matter being Type II or a mix of Type II and III. These characteristics of the C1 unit indicate an environment that is below wave base with occasional large storms or currents increasing energy at the base of the section. Upwelling currents increase the input of phosphate and cause high biological productivity. As a result the sea floor becomes anoxic due to the abundant organic matter falling to the sea floor. Sedimentation rates appear to be slow with formation of glauconite. A constant supply of silt-size quartz grains suggest either a windblown source or water transported source in the area of deposition. The presence of woody plant material and a mix of type II and III organic matter indicates that a continental landmass is close to the depositional area.

The Caney C1 lithostratigraphic unit contains the highest gamma-ray response in the study area and the greatest concentration of apatite. At the Jeff Luke shale pit, apatite laminations and nodules were abundant and visible. These features were also noted on the FMI images from the Richardson 2-33 and the Rogers Trust 1-24. The presence of apatite in an marine shale is often interpreted to be a result of upwelling from the deep ocean basin. One geologic setting were Ziegler (1979) determined coastal upwelling to be possible was east-west coasts on continents at about 15° latitude. According to a paleogeography reconstruction by Blakey (2004), Oklahoma was in a position ideal for

coastal upwelling (Figure 10.1).   According to Demaison and Moore (1980), upwelling

can originate from water depths as shallow as 200 meters. Water depths of this

magnitude or greater are likely possible in the deeper waters south of the area of Caney

Shale deposition as the encroaching Llanoria landmass creates the flexural moat

(Sutherland, 1988).

The outcrop exposures along Little Delaware Creek and Delaware Creek

represented the same stratigraphic section as the Jeff Luke outcrop. However, exposures

in this area contained mainly small scale apatite nodules and laminations, and the unit is

less radioactive. The presence of apatite in the Bromide outcrop area indicates that

upwelling was widespread across the basin. However, the smaller amount of apatite

deposits appears to indicate that the upwelling was less concentrated at this location.

Another explanation is that sedimentation rates at the Bromide outcrop area are higher

than sedimentation rates at the Lawrence Uplift outcrop area. Higher sedimentation rates

could possibly dilute the amount of phosphate accumulating in the sediment.

Demaison and Moore (1980) and Swanson (1961) state that uranium is substituted

for calcium in carbonate fluorapatite. Thus, explaining why apatite-rich shale units can

have a high gamma-ray response. In this study, the higher gamma-ray readings of the

Caney Shale were found to also occur in the more apatite rich intervals. However, in

outcrop measurements higher gamma-ray readings did not correlate directly with higher

concentrations of apatite. Thus, suggesting that there is no direct correlation between the

apatite and uranium content.

Swanson (1961) also suggests that slower sedimentation rates allow more

uranium to diffuse into and be concentrated in shale deposits. Slower sedimentation rates

Figure 10.1 Paleogeography reconstruction of Oklahoma and surrounding area during the Late Mississippian (340 Ma). Reconstruction is taken from Blakey (2004).

may also allow for more phosphatic rich grains to accumulate in the sediment. Slow

sedimentation rates are indicated by the presence of glauconite in thin sections of the

Caney Shale. Therefore, the increase in gamma-ray response and increase in apatite in

the C1 unit of the Caney Shale may be a direct consequence of slower sedimentation

rates and not deeper water or uranium substitution for calcium in apatite.

Deposition of the Caney Shale ended with a drop in sea level and a stop in coastal

upwelling of phosphate rich water. The Goddard Shale was deposited in a restricted

water environment. The water was well oxygenated and bioturbation was common in

bottom sediments. The hot streaks marking the top of the lower Goddard Shale represent

brief periods of upwelling and anoxic conditions returning to the shelf.

CHAPTER 11.0

CONCLUSIONS AND FUTURE STUDIES

11.1 Conclusions

In this research, the "Mayes" (lower Caney Shale) and Caney Shale Formations were evaluated in both the subsurface and in surface outcrops. The scope of this work was to develop a lithostratigraphic framework for the Caney Shale. With a lithostratigraphic framework developed, one can then begin to evaluate the prospective and performance-potential properties of the Caney Shale. An analysis of these properties will help to determine if the Caney Shale of southeast Oklahoma contains the elements to be a potential shale-gas play. To develop a lithostratigraphic framework of the Caney Shale, both sedimentology and stratigraphy techniques were employed. An analysis of the data from this work has led to the following significant conclusions:

(1) During the outcrop reconnaissance, the Caney Shale type section, proposed by Elias (1959) and studied by Harris (1971), was investigated. The author has concluded that very little to virtually no shale is exposed in the tributaries to Delaware Creek in the W1/2 of section 14 and E1/2 of section 14, of township T2S, R7E. Soil covers much of the bottom and banks of the streams in the area, with exposed rock generally being Woodford Shale or older. Exposures of Caney

Shale were so thin that no conclusive evidence about the sedimentology and stratigraphy of the "Mayes" (lower Caney Shale) and Caney could be drawn. As a result, a new type section should be assigned for the Caney Shale.

(2) For the most part, gamma-ray correlations from outcrop to subsurface were successfully achieved in this work. Eight of the ten outcrops were successfully correlated to the subsurface. The two outcrops, Richards Farm outcrops 1 and 2, that were not correlated into the subsurface were a little over 3 ft thick. These outcrops were too small to establish a convincing gamma-ray correlation.

(3) The "Mayes" formation (lower Caney Shale) contains shaly silty dolomites, dolomitic silty carbonates, shaly muddy dolomites, and siliceous shales. The "Mayes" (lower Caney Shale) in the western and northwestern part of the study area is dominated by coarse dolomitic deposits, and in the southeastern part of the study area this formation is dominated by siliceous shales. The difference between the two formations is believed to represent a facies change in the formation between these two locations, and not a difference in thermal maturity; as the thermal maturity at all outcrop locations is similar. This facie change in the "Mayes" formation (lower Caney Shale) across the study area is believed to be a result of increasing water depths to the south.

(4) Shale exposed at the Pine Top Mountain outcrop was identified as Woodford Shale by Hendricks and Gardner (1947), Siy (1988), and Suneson and Campbell

(1990). However, this entire section has a gamma-ray response that correlates to the gamma-ray response of the "Mayes" formation (lower Caney Shale) in a nearby well. Additionally, proportions of uranium and thorium measured at the Pine Top Mountain outcrop are similar to the uranium/thorium ratios measured in the Caney Shale at other locations, and dissimilar to uranium and thorium proportions measured by Krystyniak (2005) for the Woodford Shale. Therefore, the Pine Top Mountain outcrop appears to represent the "Mayes" formation (lower Caney Shale) and Caney Shale.

(5) The "Mayes" formation (lower Caney Shale) was not subdivided into separate lithostratigraphic units in this work. Instead is considered a large-scale lithostratigraphic unit. The "Mayes" (lower Caney Shale) is lithologically different from the Caney Shale formation and can be correlated and mapped across the basin. As a result this lithostratigraphic unit should not be considered to be a member of the Caney Shale, but considered to be a separate recognized formation. Using the term lower Caney Shale for the "Mayes" formation exposed in outcrops is confusing and illogical.

(6) The Caney Shale can be divided into four distinct lithostratigraphic units, Caney C4, C3, C2, and C1. The Caney C4 lithostratigraphic unit is the oldest and the Caney C1 lithostratigraphic unit is the youngest. Each lithostratigraphic unit has different lithologic characteristics that can be easily identified in wire-line logs.

(6a) The Caney C4 lithostratigraphic unit is composed of a black fissile

shale that is non-calcareous. In thin section, the C4 unit is composed of a

slightly laminated to non-laminated shale with angular silt-size quartz

grains. A few Tasmanites cysts are present in the unit indicating an algal

organic component. In the electrical image logs a few limestone beds

occur within the unit. Pyrite and some bioturbated intervals are present in

the unit. The contact between this unit and the "Mayes" formation (lower

Caney Shale) is sharp.

(6b) The Caney C3 lithostratigraphic unit is characterized as a calcareous

shale unit with carbonate beds and/or nodules. In between the carbonate

beds the shale is typically laminated and contains pyrite. The contact

between C4 and C3 appears to be sharp in the borehole image logs, with

the top of the C4 unit being bioturbated and the base of the C3 unit being

laminated.

(6c) The Caney C2 lithostratigraphic unit is characterized as a laminated

to non-laminated black shale. The contact between the C2 and C3 unit is

appears to be sharp. The Caney C2 unit contains interbedded carbonate

concretions and thin carbonate beds. Pyrite and apatite are common

within the shale matrix, large fossil fragments are common to rare, and

angular silt-size quartz grains are abundant. Apatite also occurs as

nodules in the unit. Compacted <u>Tasmanites</u> cysts are present in small

quantities in these thin sections. At the top of the unit two carbonate beds

separated by a "hot" shale are typically present. This carbonate bed is

characterized as a mudstone with no visible fossils; the unit has wavy

parallel upper and lower boundaries. The top of the uppermost carbonate

unit marks the boundary between the C2 and C1 lithostratigraphic unit.

(6d) Finally, the Caney C1 lithostratigraphic unit is composed

predominately of a fissile black silty shale. The shale is generally non-

calcareous, laminated, and contains glauconite and abundant apatite. This

apatite commonly occurs in concretions and laminae within the unit.

Some concretions and laminae are large enough to be seen in outcrop,

others are only visible in thin section. The upper boundary between the

Caney C1 unit and the Goddard shale is sharp, non-erosional, and marked

by a change from laminated shale to bioturbated, non-laminated shale.

The occurrence of carbonate concretions can not be used to distinguish the

Caney Shale from the Goddard Shale

(7) The apatite rich C1 unit has the highest gamma-ray response. Demaison and

Moore (1980) and Swanson (1961) believe that uranium is substituted for calcium

into the apatite. However, there is not a direct correlation between outcrop

gamma-ray measurements and apatite. It is believed that uranium may have been

concentrated in this unit as a result of slow sedimentation rates and not elemental substitution within the apatite.

(8) The "Mayes" formation (lower Caney Shale) was deposited on a continental shelf. This shelf dipped to the south southeast. In the west to northwest part of the study area the sediments of the "Mayes" (lower Caney Shale) were deposited just below normal wave base. The "Mayes" (lower Caney Shale) was deposited laterally adjacent to the Sycamore Limestone and received sediment input from this shallower carbonate dominated deposit. To the south and southeast the water depths were deeper and siliceous shales were predominantly deposited with little carbonate input.

(9) Deposition of the Caney Shale occurred during the early stages of the Ouachita Orogeny. The Caney is envisioned to have been deposited in a shelf environment between the peripheral bulge and flexural moat created by the approaching landmass. Early deposition of the Caney (lithostratigraphic units C2, C3, and C4) occurred below wave base in a dominantly anoxic water environment. The anoxic conditions were probably setup by high biologic productivity and restricted, below-wave-base water depths. Occasional fluctuations in environmental conditions lead to brief periods of oxidation of bottom sediments resulting in bioturbated, non-laminated shales. Silt-size quartz is deposited throughout the Caney. This silt was transported into the basin by wind or water.

(10) An increase in water depth and upwelling of phosphate rich water form the deep ocean basin resulted in the deposition of the upper Caney Shale (lithostratigraphic unit C1). The increase in phosphate stimulated biologic activity and an increase in organic matter accumulating on the sea floor. Degradation of organic matter resulted in anoxic water conditions. During this time, sedimentation rates were slow and glauconite accumulated on the sea floor. Slow sedimentation rates also allowed for thick accumulations of phosphate and for more uranium to diffuse into the muddy sediment bottom. Deposition of the Caney Shale ended with a drop in sea level and the end of upwelling deep ocean waters. This resulted in a more oxygenated system and less organic mater being preserved.

11.2 Future Studies

The lithostratigraphic framework of the Caney Shale developed in this study is based on limited surface exposures and data from two subsurface wells. Future studies should take the information learned here and expand the coverage with additional outcrops and more subsurface data. Evaluation of a continuous core of the "Mayes" formation (lower Caney Shale) and Caney Shale would provide a complete section of the two formations that can not be viewed in outcrop. Upon learning more data about the Caney Shale, the lithostratigraphic framework developed here will likely be modified and adjusted to more properly represent the additional lithologic changes in the formation.

The reason for developing a lithostratigraphic framework was to enable the evaluation of prospective and performance-potential properties of the Caney Shale. With an initial lithostratigraphic framework clearly established, future studies should now attempt to quantify prospective and performance-potential properties of each of these units. Analysis of these properties will help to determine if the lithostratigraphic units of the Caney Shale contain all the elements required to make a viable shale-gas play.

REFERENCES

Blakey, R. 2004. Global Plate Tectonics and Paleogeography. 10 June 2004. 18 October
    2005. < http://jan.ucc.nau.edu/~rcb7/>.

Byrnes, A. P. and G. Lawyer, 1999. Burial, Maturation, and Petroleum Generation
    History of the Arkoma Basin and Ouachita Foldbelt, Oklahoma and Arkansas.
    Natural Resources Research, 8, no. 1, pp. 3-26.

Champlin, S. C., 1959. A Stratigraphic Study of the Sycamore and Related Foramations
    in the Eastern Arbuckle Mountains. Master of Science Thesis, 66 pp. The
    University of Oklahoma, Norman, Oklahoma.

Coffey, W. S., 2000. The Diagentic History and Depositional System of the Sycamore
    Formation (Mississippian), Carter-Knox Field, Grady and Stephens Counties,
    Oklahoma. Doctorate of Philosophy dissertation, 167 pp. Oklahoma State
    University, Stillwater, Oklahoma.

Curtis, C. D. and M. L. Coleman, 1986. "Controls on the Precipitation of Early
    Diagenetic Calcite, Dolomite, and Siderite Concretions in Complex Depositional

Sequences". Roles of Organic Matter in Sediment Diagenesis. Society of
Economic Paleontologists and Mineralogists, Special Publications, 38, pp. 23-33.

Demaison, G. J. and G. T. Moore, 1980. Anoxic Environments and Oil Source Bed
Genesis. The American Association of Petroleum Geologists Bulletin, 64, no. 8,
pp. 1179-1209.

Elias, M. K., 1956. Upper Mississippian and lower Pennsylvanian formations of south-
central Oklahoma. Petroleum geology of southern Oklahoma 1, The American
Association of Petroleum Geologists, pp. 56-134.

Elias, M. K. and C. C. Branson, 1959. Type Section of the Caney Shale. Oklahoma
Geological Survey Circular, 52, 24 pp.

Ellis, D. V., 1987. Well logging for Earth Scientists. Elsevier, New York, 532 pp.

Girty, G. H., 1909. The Fauna of the Caney Shale of Oklahoma. United States
Geological Survey Bulletin, 377, 106 pp.

Graham, S. A., R. V. Ingersoll, and W. R. Dickinson, 1975. Himalayan-Bengal model for
flysch dispersal in the Appalachian – Ouachita System. Geological Society of
America Bulletin, 86, pp. 273-286.

Grayson, R. C. Jr., W. T. Davidson, E. H. Westgaard, S. C. Atchely, J. H. Hightower, P. T. Monaghan, and C. D. Pollard, 1985. Mississippian-Pennsylvanian (Mid-Carboniferous) boundary conodonts from the Rhoda Creek Formation: *Homoceras* equivalent in North America. in Lane H. R. and W. Ziegler, 1985. Toward a Boundary in the Middle of the Carboniferous; Stratigraphy and Paleontology. Courier Forschungsinstitut Senckenberg, 74, pp 149-179.

Harris, R. W. Jr., 1971. Palynology of the Sand Branch Member of the caney Shale Formation (Mississippian) of Southern Oklahoma. Doctor of Philosophy Dissertation, 169 pp. The University of Oklahoma, Norman, Oklahoma.

Hass, R. W. and J. W. Huddle, 1965. Late Devonian and Early Mississippian Age of the Woodford Shale in Oklahoma, as Determined From Conodonts. U. S. Geological Survey Professional Paper 525-D, pp D125-D132.

Haywa-Branch, J. N. and J. E. Barrick, 1990. Conodont Biostratigraphy of the Weldon Limestone (Osagean, Mississippian), Lawrence Uplift, Southern Oklahoma. Oklahoma Geological Survey Guidebook, 27, pp. 75-84.

Hendrick, S. J., 1992. Vitrinite reflectance and deep Arbuckle maturation at Wilburton Field, Latimer County, Oklahoma: Source rocks in the southern midsontinent, 1990 symposium. Oklahoma Geological Survey Circular, 93, pp. 176-184.

Hendricks, T. A. and L. S. Gardner, 1947. Guide Book, Tulsa Geological Society field

    conference in western part of the Ouachita Mountains in Oklahoma, May 8-10,

    1947. Tulsa Geological Society.

Houseknecht, D. W. and J. A. Kacena, 1983. Tectonic and sedimentary evolution of the

    Arkoma foreland basin. SEPM Midcontinent Section 1, pp. 1-33.

Hurlbut, C. S. Jr., and C. Klein, 1977. <u>Manual of Mineralogy (after James D. Dana)</u>. 19th

    Edition. John Wiley and Sons, 532 pp.

Kleehammer, R. S., 1991. Conodont Biostratigraphy of Late Mississippian Shale

    Sequences, South-Central Oklahoma. Master of Science Thesis, 134 pp. The

    University of Oklahoma, Norman, Oklahoma.

Krystyniak, A. M., 2005. Outcrop-Based Gamma-Ray Characterization of the Woodford

    Shale of South-Central Oklahoma. Mater of Science Thesis, 142 pp. Oklahoma

    State University, Stillwater, Oklahoma.

Laudon, R. B., 1958. Chesterian and Morrowan Rocks in the McAlester Basin of

    Oklahoma. Oklahoma Geological Survey Circular, 46. 29 pp.

Monaghan, P. T., 1985. The Stratigraphy of the Mississippian-Pennsylvanian Shale
   Sequence of Southern Oklahoma. Mater of Science Thesis, 52 pp. Baylor
   University, Waco, Texas.

Nelson, K. D., R. J. Lillie, B. deVoogd, J. A. Brewer, J. E. Oliver, S. Kaufman, L.
   Brown, and G. W. Viele, 1982. COCORP seismic reflection profiling in the
   Ouachita Mountains of western Arkansas: Geometry and geologic interpretations:
   Tectonics 1, pp. 413-430.

Neman, R. L., 2002. Guidebook for Geological Field Trips in South-Central Oklahoma.
   Arbuckle Geosciences, 140 pp.

Olson, R. K., 1982. Factors Controlling Uranium Distribution in Upper Devonian-Lower
   Mississippian Black shales of Oklahoma and Arkansas. Doctor of Philosophy
   Dissertation, 208 pp. The University of Tulsa, Tulsa, Oklahoma.

Over, J. D. and J. E. Barrick, 1990. "The Devonian/Carboniferous Boundary in the
   Woodford Shale, Lawrence Uplift, South-Central Oklahoma". Early to Middle
   Paleozoic Conodont Biostratigraphy of the Arbuckle Mountains, Southern
   Oklahoma. Oklahoma Geological Survey Guidebook, 27, pp 63-73.

Perry, W. J., 1995. Arkoma basin Province (062): Central energy team assessments of
energy resources 1995 geologic report. National Oil and Gas Assessment, United
States Geologic Survey, 17pp.

Richards, D., 2001. "Calibration and Use of Portable Gamma-Ray Spectrometers: Part 2
– Field Procedures and Calculations of Ground Concentrations." Gamma-Ray
Spectrometers. SAIC Exploranium, pp. 23-25.

Rider, M, 2002. The Geological Interpretation of Well Logs. Sutherland, Scotland.
Rider-French Consulting Ltd., 280 pp.

Savrda, C. E. and D. J. Bottjer, 1989. Trace-fossil model for reconstructiong oxygenation
histories of ancient marine bottom waters; application to Upper Cretaceous
Niobrata Formation, Colorado. Palaeogeography, Palaeoclimatology,
Palaeoecology, 74-1-2, pp. 49-74.

Schad, S. T., 2004. Hydrocarbon potential of the Caney Shale in southeastern Oklahoma.
The University of Tulsa, Copyright 2004, 128 pp.

Suneson, N. H. and J. A. Campbell, 1990. "Stop 8: Pinetop Section." Geology and
Resources of the Frontal Belt of the Western Ouachita Mountains, Oklahoma.
Oklahoma Geological Survey Special Publications, 90-1. pp. 50-54.

Sutherland, P. K., 1981. Mississippian and lower Pennsylvanian stratigraphy in

Oklahoma. Oklahoma Geological Survey Oklahoma Geology Notes, 41, pp. 3-22.

Sutherland, P. K., 1988. Late Mississippian and Pennsylvanian depositional history in the

Arkoma basin area, Oklahoma and Arkansas. GSA Bulletin, 100, pp. 1787-1802.

Swanson, V. E., 1961. Geology and Geochemistry of Uranium in Marine Black Shales: A

Review. Geological Survey Professional Paper 356-C. 112 pp.

Taff, J. A., 1901. Description of the Coalgate quadrangle (Indian Territory). United States

Geological Survey Geologic Atlas, 74, 6 pp.

Ulrich, E. O., 1927. Fossiliferous Boulders in the Ouachita "Caney" Shale and the Age of

the Shale Containing Them. Oklahoma Geological Survey Bulletin, 45, 48 pp.

Weber, J. L., 1992. Organic matter content of outcrop samples from the Ouachita

Mountains, Oklahoma: Source rocks in the southern midsontinent, 1990

symposium. Oklahoma Geological Survey Circular, 93, pp.347-352.

Westheimer, J. M., 1956. The Goddard Formation. Petroleum Geology of Southern

Oklahoma – a symposium. Ardmore Geological Society, 1, pp. 392-396.

Wickham, J., 1978. The Southern Oklahoma Aulacogen: Field guide to structure and

    stratigraphy of the Ouachita Mountains and the Arkoma basin. 1978 annual

    meeting of the AAPG, pp. 1-35.

Ziegler, P. A., 1979. Factors controlling North Sea Hydrocarbon Accumulations. World

    Oil, 189, no. 6, p. 111-124.

APPENDIX I

OUTCROP DESCRIPTIONS

Outcrop 1 – Richard's Farm Outcrop 1 (RF1)

This small outcrop is exposed along the west bank of a small tributary to Welden Creek. This tributary is located a little over a ½ mile west of Clear Boggy Creek on EW 1590 (Neman, 2002). The outcrop is just south of Ada, OK in Section 27, T.3N., R.6E. (Figure AI.1). Two shale exposures were evaluated at this location. The outcrop described here is the closest exposure south of the road. The coordinate marked location for this outcrop is N34.70877^o and W96.65451^o (Datum WGS 84). The Outcrop was measured from the bottom up. Total thickness was measured to be 3.35 ft. A geology strip log and photograph of this outcrop are contained in Figures AI.2 and AI.3 respectively below.

Unit 1 – Thickness unknown

This unit consists of a brownish black fissile shale. This shale is calcareous and contains no apparent silt. The total thickness of the shale is unknown as a result of the base of the shale being under water.

Unit 2 – 0.0 to 0.25 ft
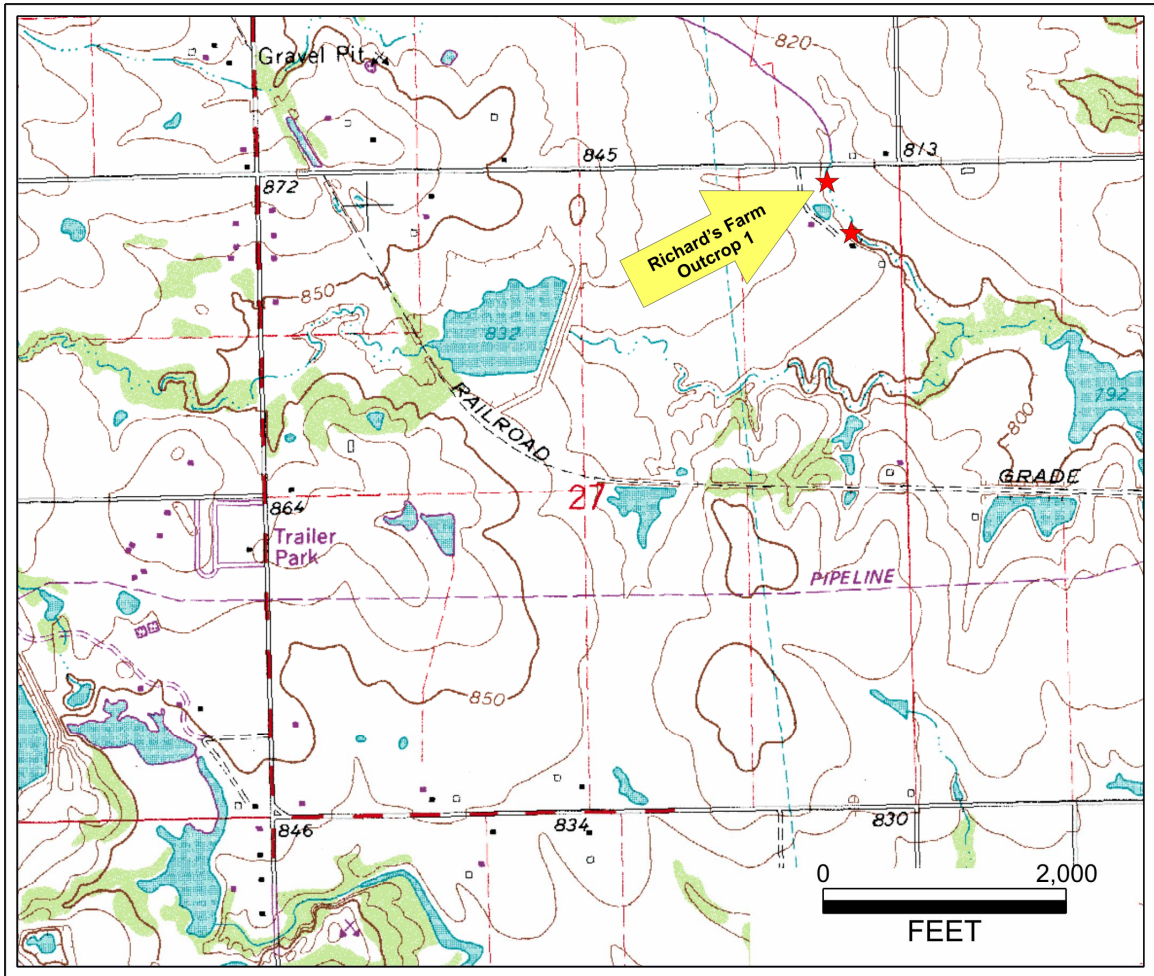
Figure AI.1 Location map for Richard's Farm outcrop 1

Figure AI.2 Geology strip log of Richard's Farm outcrop 1

Figure AI.3 Photograph of Richard's Farm outcrop 1

This unit consists of a carbonate mudstone. This mudstone has a dark gray color that weathers light gray to white. This unit contains no visible fossils or carbonate grains. The mudstone appears to be very resistant. The upper and lower boundaries of this unit are straight parallel.

Unit 3 – 0.25 to 0.54 ft

This thin unit consists of a brownish black fissile shale. This shale contains no apparent silt and is calcareous. The shale is not very resistant and weathers easily in outcrop.

Unit 4 – 0.54 to 3.16 ft

This unit consists of a sandy, silty, calcareous, shaly, dolomite. The exact composition of the member is difficult to determine in outcrop. This interval is light olive gray to olive gray in color. The base of the unit is more fissile and contains laminae that are 0.04 to 0.12 inches thick. These beds thicken upward to 0.4 to 0.7 inches.

Unit 5 – 3.16 to 3.35 ft

This unit consists of a muddy, silty, sandy, dolomitic carbonate. This member is brown to tan in color and appears very resistant. At one section in the exposure a small vertical fracture in Unit 4 is filled with this sandy unit.

Outcrop 2 – Richard's Farm Outcrop 2 (RF2)

This small outcrop is exposed along the west bank of a small tributary to Welden Creek. This tributary is located a little over a ½ mile west of Clear Boggy Creek on EW 1590 (Neman, 2002). The outcrop is just south of Ada, OK in Section 27, T.3N., R.6E. (Figure AI.4). Again, two shale exposures were evaluated at this location. This outcrop is the first exposure south of RF1. The coordinate marked location for this outcrop is N34.70772^o and W96.65383^o (Datum WGS 84). The outcrop was measured from the bottom up. Total thickness was measured to be 3.32 ft. Figures AI.5 and AI.6 below contain a geology strip log and photograph of this outcrop respectively.

Unit 1 – 0.0 to 0.17 ft

This unit consists of a blackish-gray carbonate mudstone. The mudstone weathers light gray in color. This unit contains no apparent fossils or grains, and is possibly shaly. The upper and lower boundaries of this unit are straight parallel.

Unit 2 – 0.17 to 1.42 ft

This unit consists of a grayish black fissile shale. The bottom 0.25 ft of the shale is very calcareous as it reacts vigorously with dilute acid. The upper portion of the unit reacts mildly with acid. The upper 1.0 ft of this unit contains iron staining on weathered surfaces

Unit 3 – 1.42 to 1.65 ft
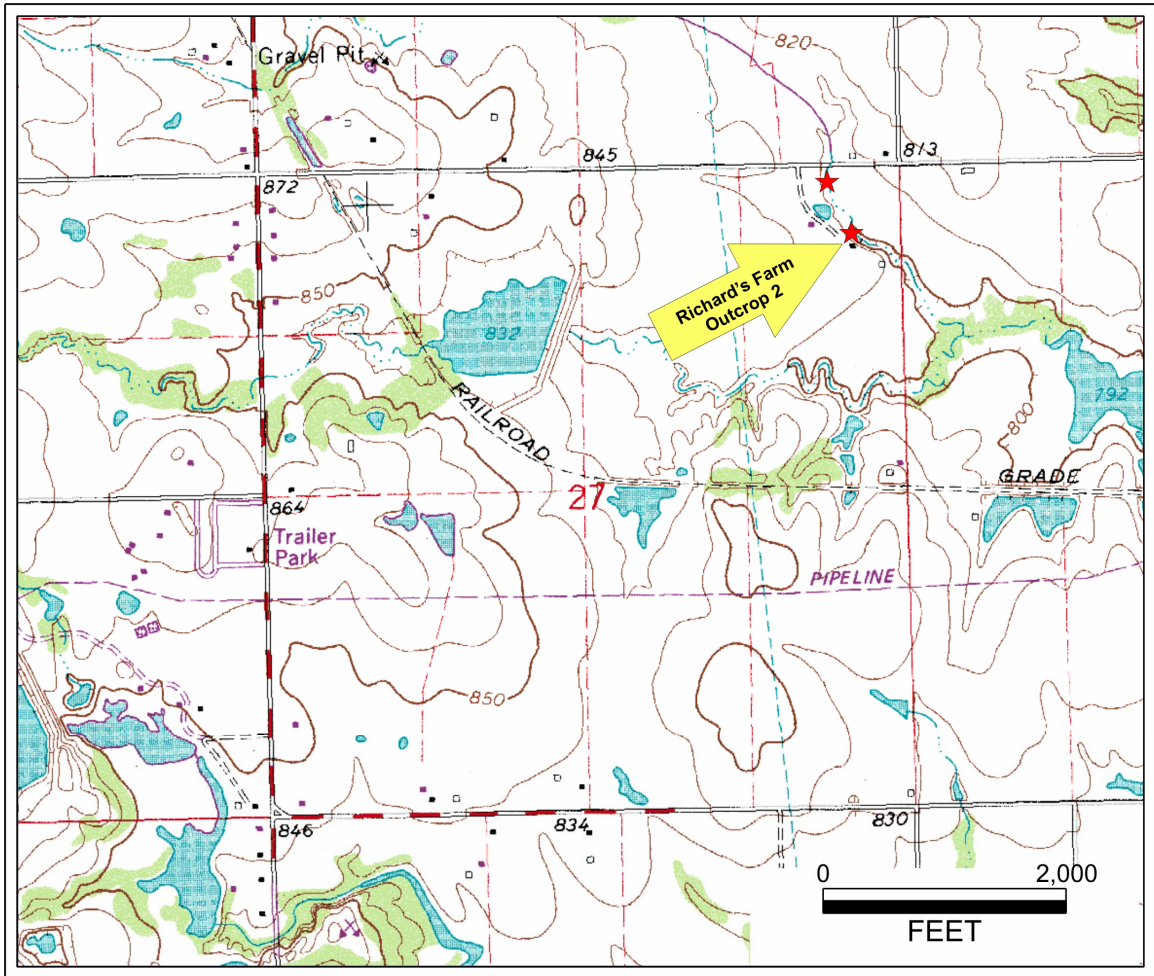
Figure AI.4 Location Map for Richard's Farm outcrop 2.

Figure AI.5 Geology strip log for Richard's Farm outcrop 2

Figure AI.6 Photograph of Richard's Farm outcrop 2

This unit is heavily weathered in outcrop, and so it is difficult to make an accurate assessment of the lithology. It appears that this layer consists of a carbonate mudstone that weathers to a calcareous yellowish tan clayey layer.

Unit 4 – 1.65 to 3.32 ft

This unit consists of a grayish black fissile shale that weathers gray. The bottom 0.9 ft of the unit has a coaly appearance. Iron staining is common on weathered surfaces, with the heaviest staining occurring at the base. This unit in non-calcareous and contains no apparent silt.

Outcrop 3 – Jeff Luke Shale Pit (JL)

This outcrop is an abandoned shale pit on the property of Mr. Jeff Luke in Section 26, T.3N., R.6E. This outcrop is just southeast of the Richards' Farm outcrops, and is located just east of a dam on Welden Creek (Figure AI.7). The coordinates for this location are N34.70280^o and W96.64357^o (Datum WGS 84). The total thickness of the measured section was 25.8 ft. This exposure is laterally extensive with a shallow dip and could not be measured as one continuous section. As a result the outcrop was divided up into five sections. These sections are Jeff Luke 1A, 1B, and 2 through 4. Figure AI.8 contains a geologic strip log of the Jeff Luke Shale Pit. Figure AI.9 contains a photograph of the outcrop with the marked locations of the five measured sections.

Jeff Luke Section 1A (JL1A)

The total measured thickness of this section was 2.8 ft.
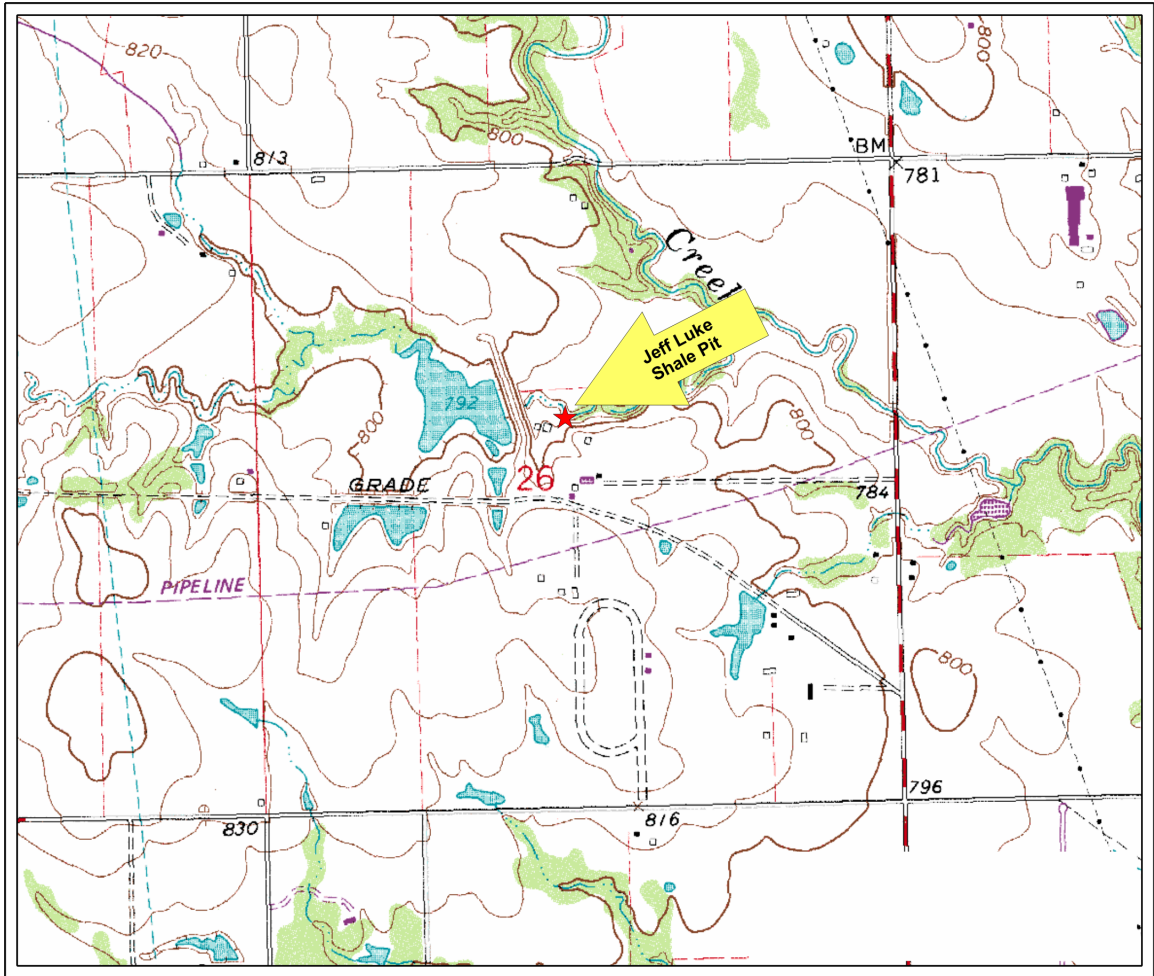
Figure AI.7 Location map for the Jeff Luke shale pit
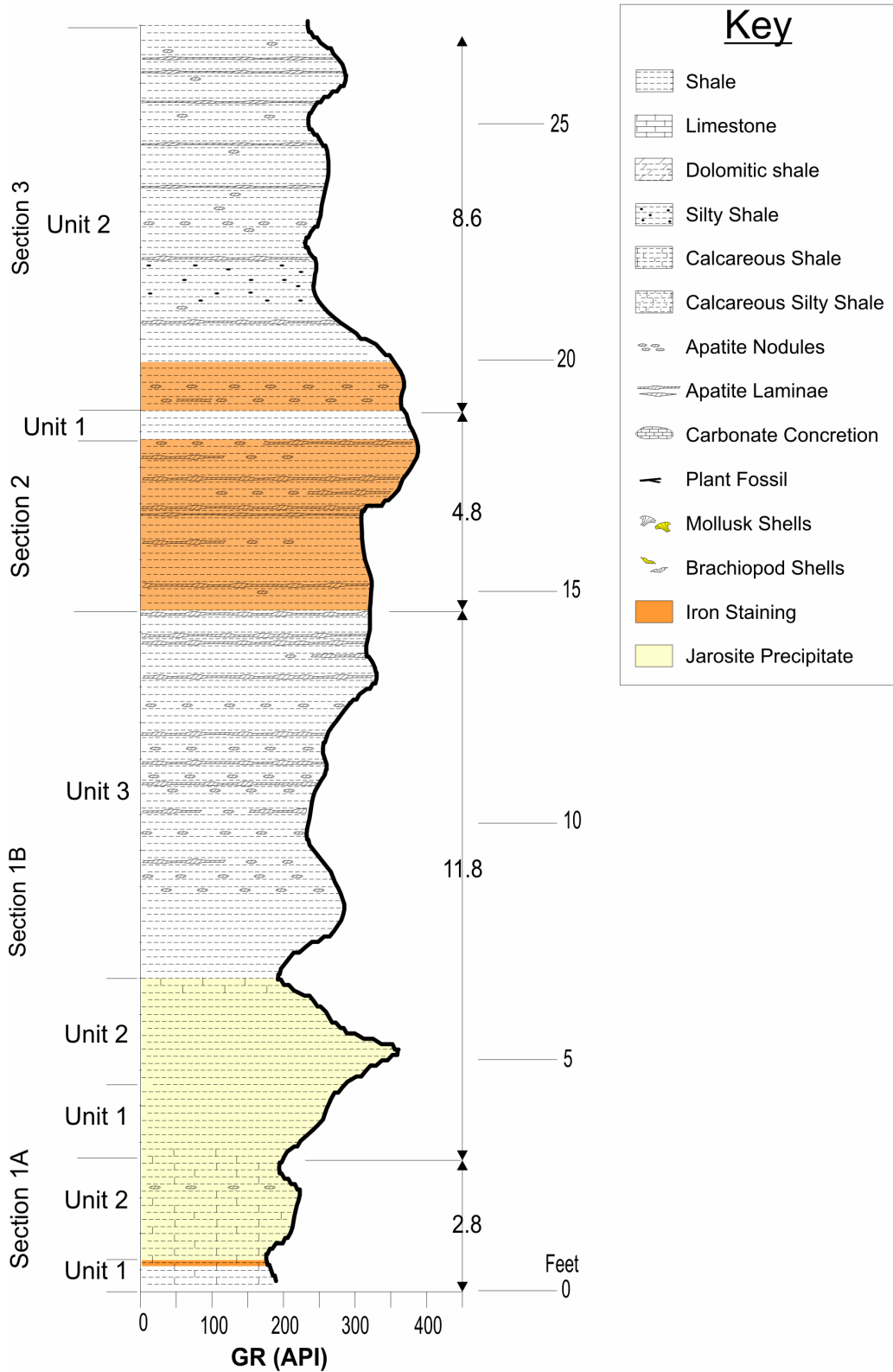
Figure AI.8 Geology strip log for the Jeff Luke shale pit
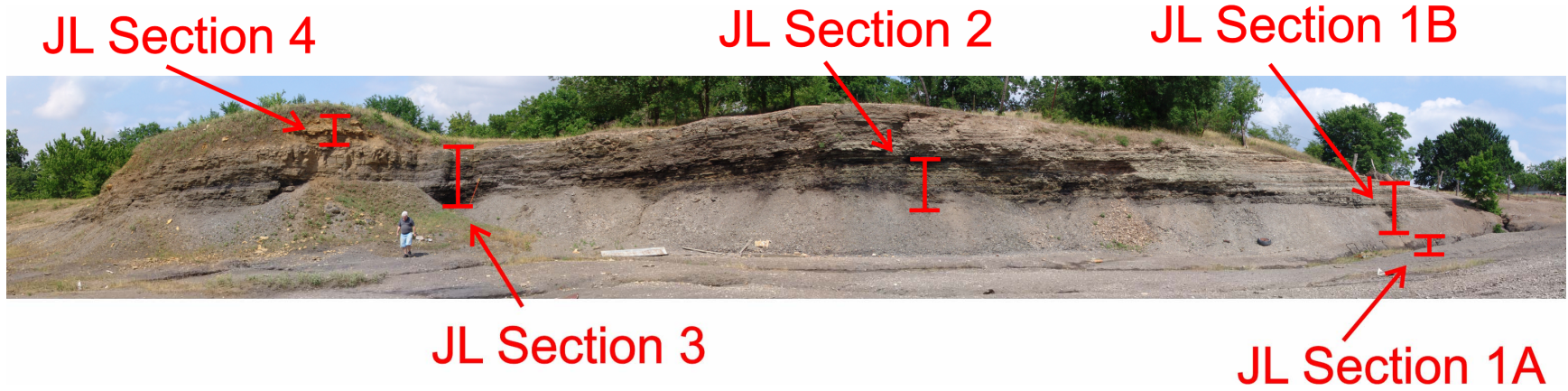
Figure AI.9 Photograph of the Jeff Luke shale pit with the measured sections marked

Unit 1 – 0.0 to 0.65 ft

The bottom 0.65 ft is composed of grayish black thinly laminated shale. This shale is more resistant than the upper part of the section, and forms a bench. The resistant shale reacts vigorously with dilute HCl and this high concentration of $CaCO_3$ my result in its more resistant nature. Iron from weathering is precipitated in a 1 in. shaly bed at the interface between this section and the one above.

Unit 2 – 0.65 to 2.8 ft

The upper 2.15 ft is composed of a black fissile shale that is less resistant than the unit below. The shale in this section reacts mildly with dilute HCl indicating a lower concentration of $CaCO_3$ than the unit below. Iron staining and a yellow precipitate from weathering are common within this section. Apatite nodules occur approximately 2.3 ft from the base of the section.

Jeff Luke Section 1B (JL1B)

The total thickness of this section was 11.8 ft. (Section starts approximately at the top of JL1A.)

Unit 1 – 0.0 to 1.6 ft

The bottom 1.6 ft is composed of dark grey to black thinly laminated shale. The shale has a more resistant blocky nature than the other shales in the transect. The shale reacts slightly with dilute HCL. The resistant nature of this shale may be a result of the being a fresh unweathered section. Some iron staining occurs in this section.

Unit 2 – 1.6 to 4.0 ft

The middle 2.4 ft is composed of dark grey to black fissile shale. The shale does not react with dilute HCl. Iron staining occurs in section along with a yellow precipitate. Iron staining appears to occur in layers, but these layers are highly discontinuous. A thin laminae of calcareous shale occurs approximately 3.5 ft from the base of this transect. However, this bed does not appear to be continuous. There are not nodules or layers of apatite or carbonate visible in this section.

Unit 3 – 4.0 to 11.8 ft

The upper 7.8 ft is composed of a dark gray to black fissile shale. This shale weathers to a light gray to brown color, and does not react with dilute HCl. At approximately 5.6 ft from the base of Transect 1B the first nodules of apatite occur in this unit. This nodular layer is slightly discontinuous. Apatite layers occur from this first layer to the top of the transect at intervals that are anywhere from 0.1 ft to 1.0 ft apart.. At approximately 7.9 ft from the base of Transect 1B apatite layers become more continuous. The consistent layers are made up of nodules that are connected by an apatite bed that is 0.01 to 0.03 ft thick.

A strike and dip measurement was taken at the top of this outcrop above section JL1B. This outcrop has a strike of N65^{o}W with a dip of 6° to the NE.

Jeff Luke Section 2 (JL2)

The total thickness of this section is 4.8 ft. (Section starts approximately 1.0 ft below JL1B.)

This transect is composed of a blocky, thinly laminated, black shale that is slightly fissile. The shale has a coaly type appearance and commonly has a yellow precipitate along with iron precipitate on the surface. Application of dilute HCl to the shale shows no reaction. Apatite beds are common throughout transect. Beds again consist of nodules connected by what appears to be thin beds of apatite. Apatite nodules are spherical to elongate. Apatite beds are continuous to slightly discontinuous. Apatite beds were noted to occur at 0.5, 1.o, 1.7, 2.7, 3.0, 3.25, 3.35, 3.6, and 4.2 ft. from the base.

Jeff Luke Section 3 (JL3)

The total thickness of this section is 8.6 ft. (Section starts approximately 1.2 ft below JL2.)

Unit 1 – 0.0 to 1.6 ft

The bottom 1.6 ft is composed of blocky, thinly laminated, black shale that is slightly fissile. Apatite nodules occur at 1.0 and 1.2 ft from the base. Yellow precipitate along with iron staining from weathering is common in this section. Application of dilute HCl to the shale shows no reaction.

Unit 2 – 1.6 to 8.6 ft

The upper 7.0 ft is composed of black shale that is more fissile in nature than the bottom section of this transect. Shale does not react with dilute HCl, apatite beds containing nodules are present in the shale. These beds are 0.025 to 0.05 ft thick, and are spaced 0.3 to 1.0 ft. apart. apatite nodules also occur in-between apatite beds. These nodules are particularly concentrated at approximately 4.6 ft from the base. A more resistant layer was noted in this section at approximately 2.9 to 3.4 ft from the base of the transect. The layer appeared slightly silty.

Jeff Luke Section 4 (JL4)

The total thickness of this section is 4.0 ft. (Section starts approximately at the top of JL3.) This transect was composed of a heavily weathered calcareous shale. Weathering was so severe that only weathered shale fragments could be identified along with carbonate concretions. The majority of the section consisted of a brownish tan, calcareous, soily clay material. Within the transect large travertine deposits formed from weathering and precipitation were noted. Because this transect was so heavily weathered the section was not sampled. Gamma-ray measurements were collected, however these measurements are suspect because of weathering.

Outcrop 4 – Hass G Outcrop (HG)

The Hass G Section was first described by Hass and Huddle (1965), and the section was given the name Hass G by Over and Barrick (1990). This section is located along the South Fork of Jack Fork Creek in Section 35, T.3N., R.6E. This exposure is located ¾ of a mile west of Highway 99 on EW 1610 (Figure AI.10). The coordinates for
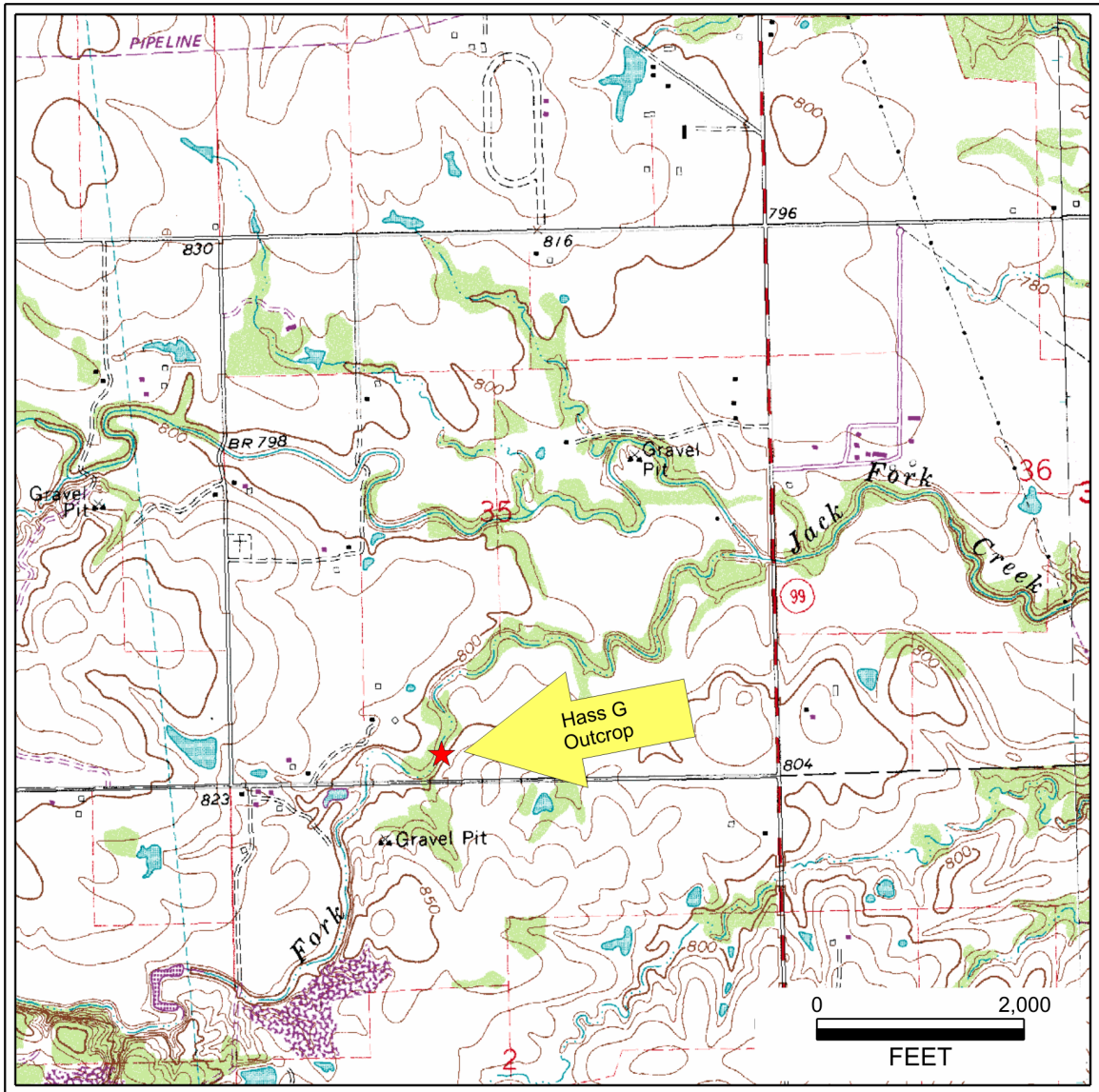
Figure AI.10 Location map for the Hass G outcrop.

this location are N34.68042o and W96.64566° (Datum WGS 84). The total thickness of the measured section was 10.38 ft. Figures AI.11 and AI.12 below contain a geology strip log and photograph of this outcrop respectively.

Woodford Shale – 0.0 to 2.69 ft

The Woodford section is composed of black fissile shale. There are no concretions present in the shale. The upper boundary of the shale is sharp and parallel to bedding planes. A disturbed zone is present within this section of the shale. The zone is located 0.85 ft from the base of the measured section.

Pre-Welden Shale – 2.69 to 3.4 ft

The Pre-Welden shale is a calcareous thinly laminated blue green shale. Blue green color is suspected to originate from glauconite in the shale. Apatite nodules are present in the section at the top, along with a 0.06 ft carbonate laminae. This carbonate laminae contains clear large calcite crystals and is possibly made of ploikiotopic cement.

Welden Limestone – 3.4 to 8.53 ft

Unit 1 – 2.6 ft thick

This unit is composed of a massive limestone. The limestone is classified as a wackestone in hand sample and the limestone contains glauconite.

Unit 2 – 0.45 ft thick

This unit is composed of a calcareous thinly laminated silty shale.
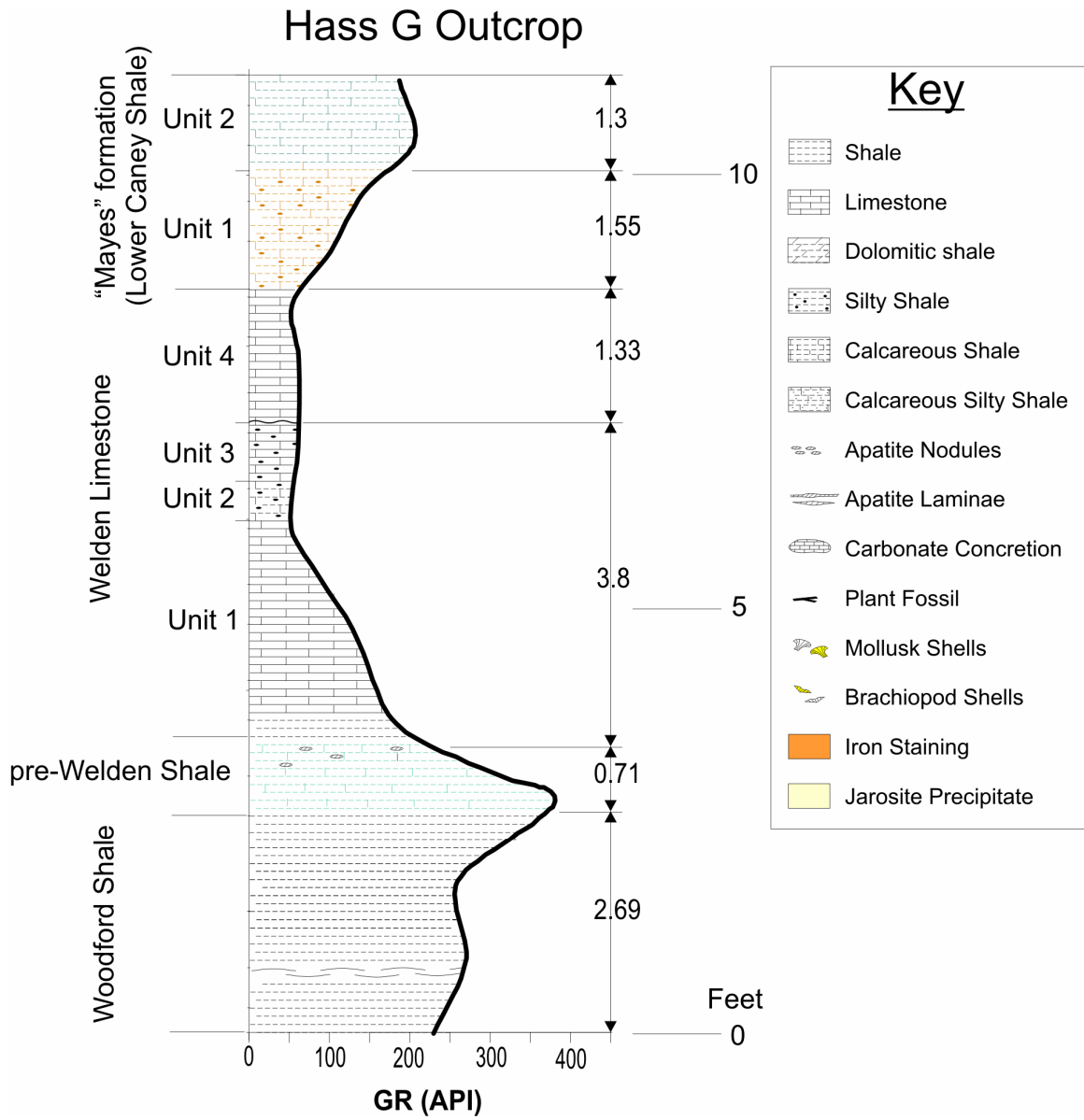
Figure AI.11 Geology strip log for the Hass G outcrop.

Figure AI.12 Photograph of the Hass G outcrop

Unit 3 – 0.75 ft thick

This unit consists of a dirty, grainy limestone. The limestone is classified as a packstone to possible grainstone. The top 0.1 to 0.15 ft of the section appears to be wavy bedded.

Unit 4 – 1.325 ft thick

This unit consists of a dark gray limestone. The limestone is classified as a packstone and contains some glauconite.

"Mayes" Formation (also known as lower Caney Shale) – 7.53 to 11.38 ft

Unit 1 – 1.55 ft thick

This unit is composed of a tan-to-brown calcareous silty shale. The shale is thinly laminated.

Unit 2 – 1.3 ft thick

This unit is composed of a blue green slightly calcareous shale. The shale again appears thinly laminated, but no silt is apparent.

Outcrop 5 – Delaware Creek Outcrop (DC)

This small outcrop is exposed on the west bank of the Delaware Creek, south of mouth of the Little Delaware Creek. The outcrop is located southwest of the town of Bromide, OK in Section 11, T.2S., R.7E. (Figure AI.13). The coordinate marked location for this section is N 34.39400^o and W 96.53884^o (Datum WGS 84). The Section was
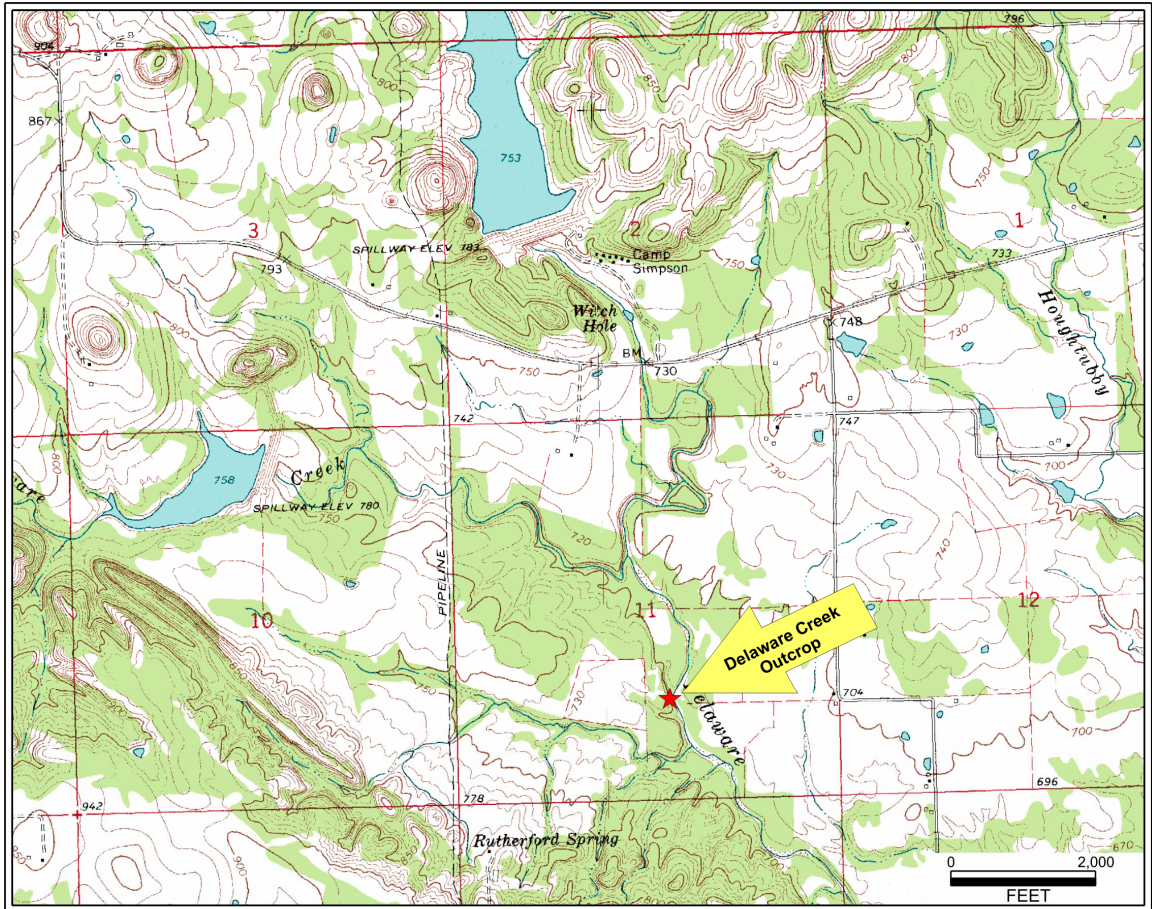
Figure AI.13 Location map for the Delaware Creek outcrop.

measured from the bottom up. Total thickness of the measured section was 17.0 ft. Figures AI.14 and AI.15 below contain a geology strip log and photograph of this outcrop respectively.

Unit 1 – 0.0 to 1.5 ft

This unit contains black, finely laminated, non-calcareous shale. The shale weathers blackish-gray to light gray. The shale is more resistant and less weathered than shale above. This may be a result of water flowing more often at this level. Apatite nodules were noted at 1.0 and 1.4 ft.

Unit 2 – 1.5 to 17.0 ft

This unit contains black, finely laminated, non-calcareous shale. Shale weathers blackish-gray to light gray in color. All shale is moderately fissile and heavily weathered. Red iron staining is common on exposed surfaces and beddings planes. This staining is more prevalent 4.0 to 6.0 ft from the base and again from 10.3 to 11.0 ft. Iron concentrations are highest in this upper layer creating a more resistant interval. Apatite concretions were noted at 9.0, 9.5, 10.0, 11.5, and 12.5 ft from the base. These nodules are spherical to flat elliptical in shape. Thin silty phosphatic lenses were noted at 3.5 to 4.0 ft. At 4.0 ft. shale beds are laterally adjacent to a large carbonate concretion to the south. Above 4.0 ft a yellow precipitate, probably jarosite, is common on the weathered surface of the shale. This precipitate is most prevalent from 13.0 t0 17.0 ft. Plant fossils were noted at 10.9 to 11.0 ft, 12.0 ft, 15.5ft, and 16.5 ft.
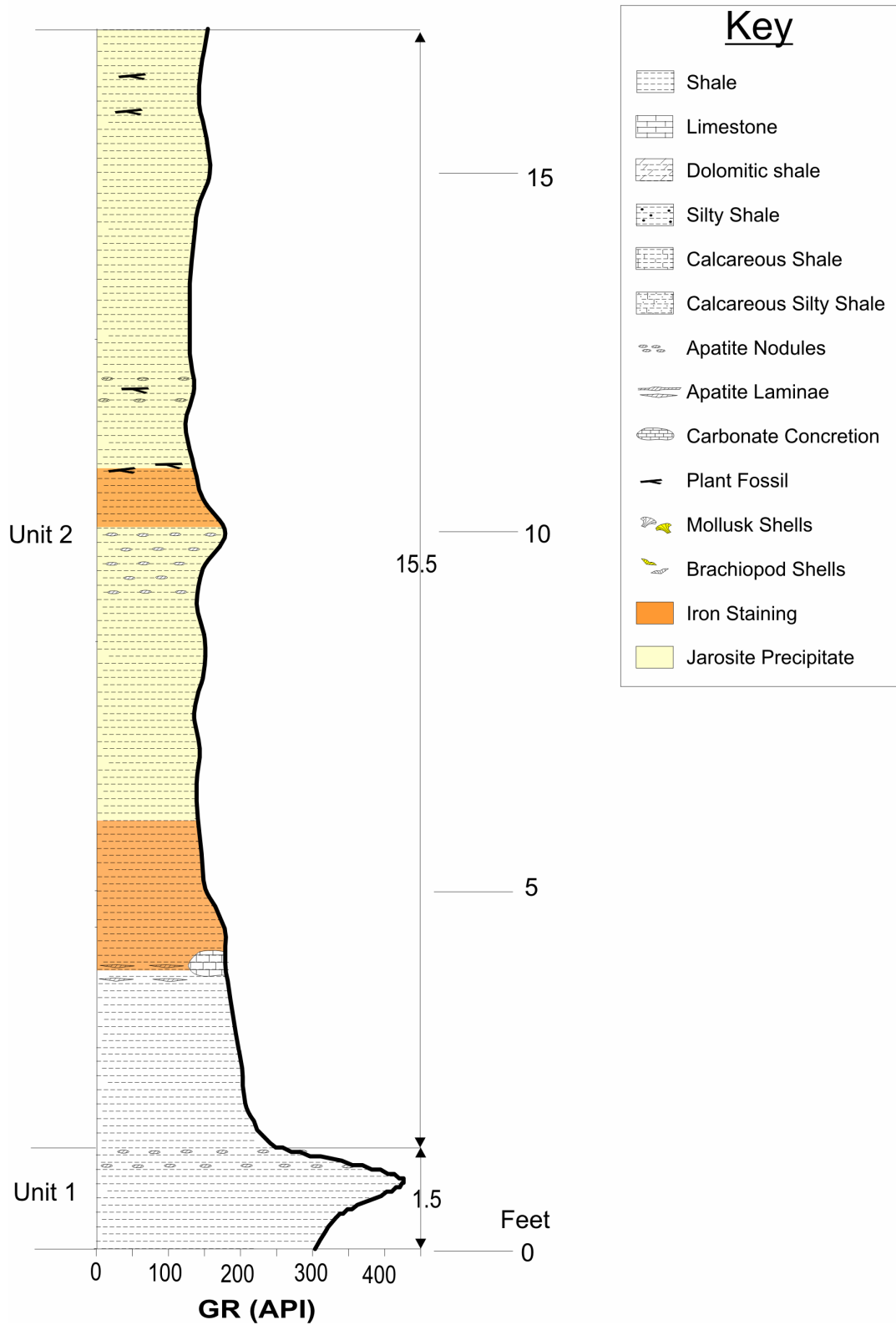
Figure AI.14 Geology strip log for the Delaware Creek outcrop.

Figure AI.15 Photograph of the Delaware Creek outcrop

Outcrop 6 – Little Delaware Creek Outcrop 1 (LDC1)

This outcrop is a part of a series of four outcrops exposed along the Little Delaware Creek. This small outcrop is exposed in the south bank of the Little Delaware Creek. The Section is located southwest of Bromide, OK in Section 11, T.2S., R.7E. (Figure AI.16). The coordinate marked location for this section is N 34.40019^o and W 96.54449^o (Datum WGS 84). This section, like all other sections on the Little Delaware Creek, was measured from the top down. These four sections are the only sections in this study that were measured from the top down. The total thickness of this measured section was 12.7 ft. Figures AI.17 and AI.18 below contain a geology strip log and photograph of this outcrop respectively.

Unit 1 – 0.0 to 2.9 ft

This unit is composed of grayish-black fissile shale. The shale weathers to a light gray. The shale contains no apparent silt, and is non-calcareous to slightly calcareous at the base. The shale is slightly weathered.

Unit 2 – 2.9 to 3.7 ft

This unit is composed of grayish-black fissile shale that weathers to a light gray. The shale is silty, slightly calcareous, and resistant. Shale is slightly weathered at the surface.

Unit 3 – 3.7 to 4.2 ft
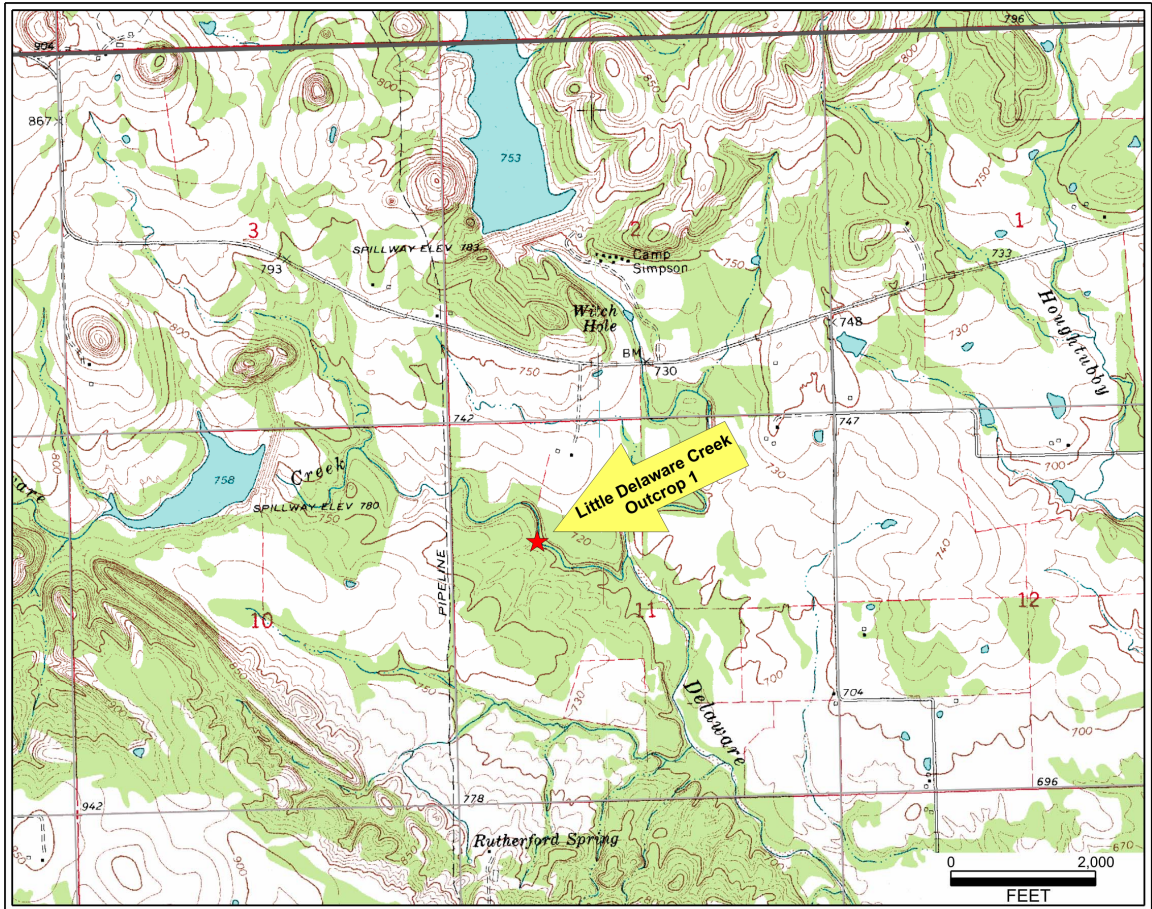
Figure AI.16 Location map for Little Delaware Creek outcrop 1.

183
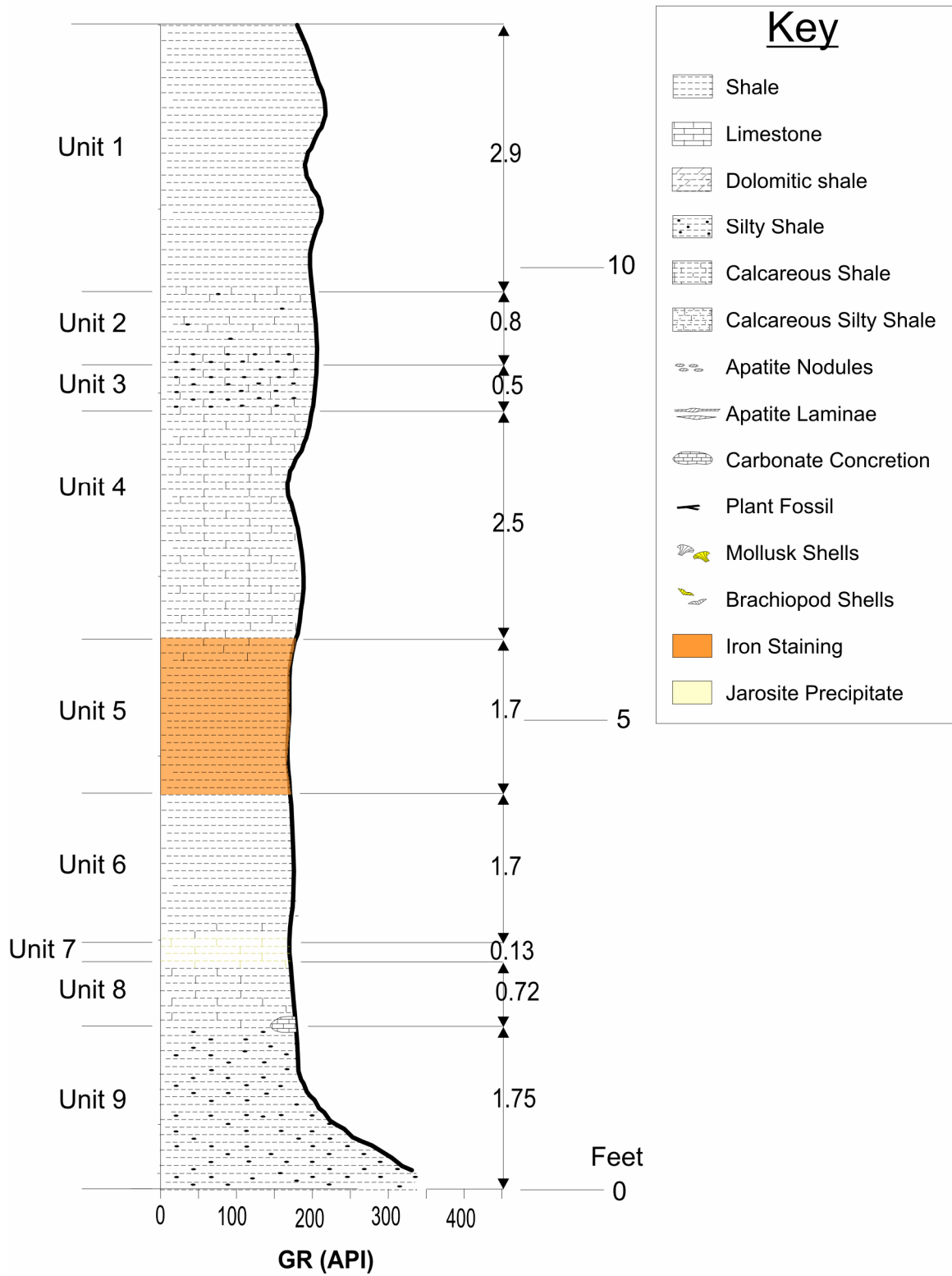
Figure AI.17 Geology Strip log for Little Delaware Creek outcrop 1

Figure AI.18 Photograph of Little Delaware Creek outcrop 1

This unit is composed of a grayish-black silty shale. The shale weathers to a light gray, and is blocky in nature. This unit is calcareous as it reacts strongly with dilute HCL. The shale is slightly weathered at the surface.

Unit 4 – 4.2 to 6.7 ft

This unit is composed of a grayish-black shale. The shale weathers to a light gray, and is blocky in nature. The shale contains no apparent silt and is calcareous. The unit is less resistant than the unit noted above.

Unit 5 – 6.7 to 8.4 ft

This unit is composed of a grayish-black shale that weathers to a light gray. The shale is slightly calcareous at the top to non-calcareous at the bottom. This unit is less blocky and more fissile. Iron staining is common along weathered surface and bedding planes.

Unit 6 – 8.4 to 10.1 ft

This unit is composed of a grayish-black shale that weathers to a light gray. This shale is very hard and resistant. It contains no apparent silt and is non-calcareous above 9.7 ft and calcareous below 9.7 ft.

Unit 7 – 10.1 to 10.23 ft

This unit is composed of a calcareous shale. The shale is whitish tan in color. The small unit is heavily weathered and weakly consolidated.

Unit 8 – 10.23 to 10.95 ft

This unit is composed of a grayish-black shale that weathers to a light gray. The unit is calcareous and contains no apparent silt. A carbonate concretion is laterally adjacent to shale at 10.9 ft.

Unit 9 – 10.95 to 12.7 ft

This unit is composed of a grayish-black shale that weathers to a light gray. The shale is fissile to slightly blocky. The unit is non-calcareous and contains silt. The shale is very resistant to weathering and appears more resistant between 12.0 and 12.7 ft. The shale is also grittier between 12.0 and 12.7 ft indicating a larger concentration of silt.

Outcrop 7 – Little Delaware Creek Outcrop 2 (LDC2)

This outcrop is the second of four outcrops exposed along the Little Delaware Creek. This small outcrop is exposed on the south bank of the Little Delaware Creek. This outcrop is located to the southwest of Bromide, OK in Section 11, T.2S., R.7E. (Figure AI.19). The coordinate marked location for this outcrop is N 34.39928^o and W 96.54340^o (Datum WGS 84). This outcrop was measured from the top down. The total thickness of this measured section was 11.2 ft. Figures AI.20 and AI.21 below contain a geology strip log and photograph of this outcrop respectively. Two bedding plane strike and dip measurements were taken at this location. The measurements were: strike, N1^{o}E and dip, 3.5^o E; strike, N11^{o}E and dip, 3.5^{o}E. The strike and dip of joints in the outcrop
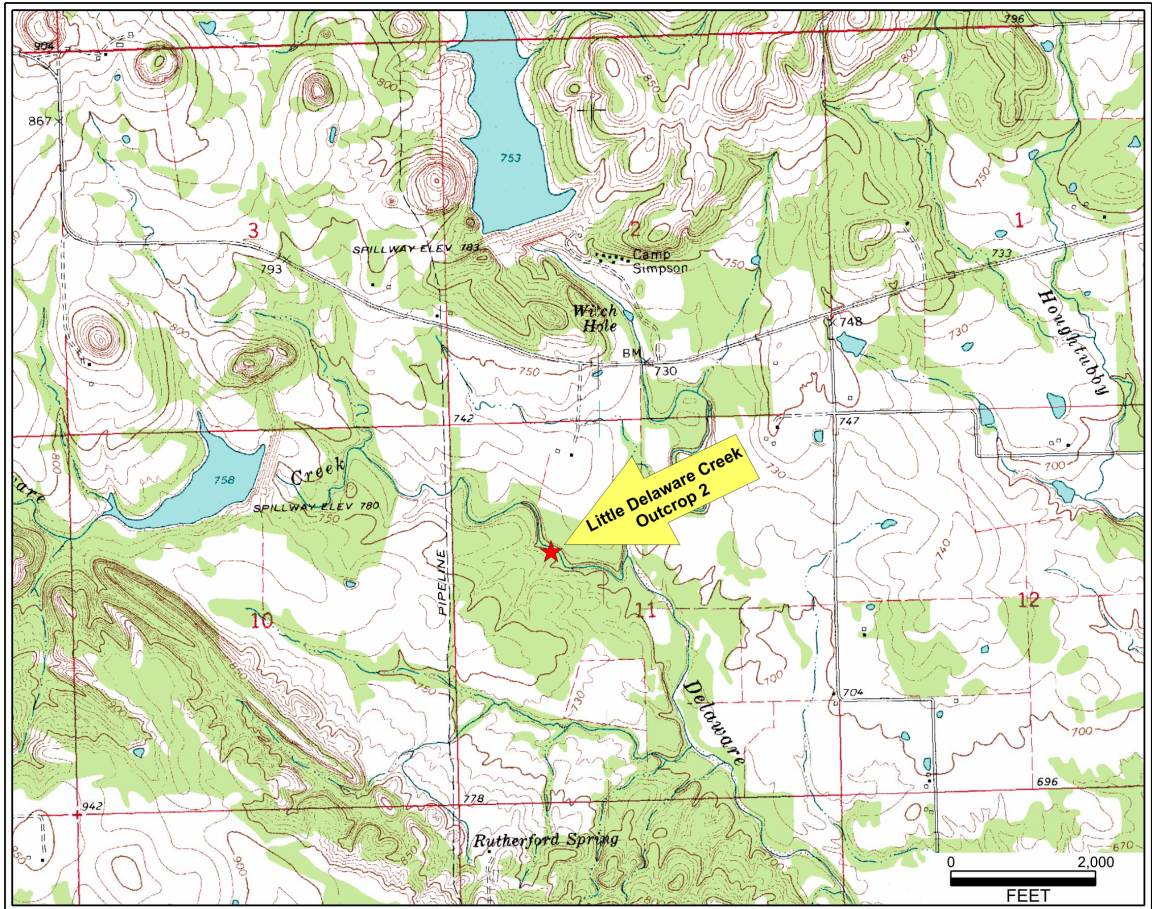
Figure AI.19 Location map for Little Delaware Creek outcrop 2
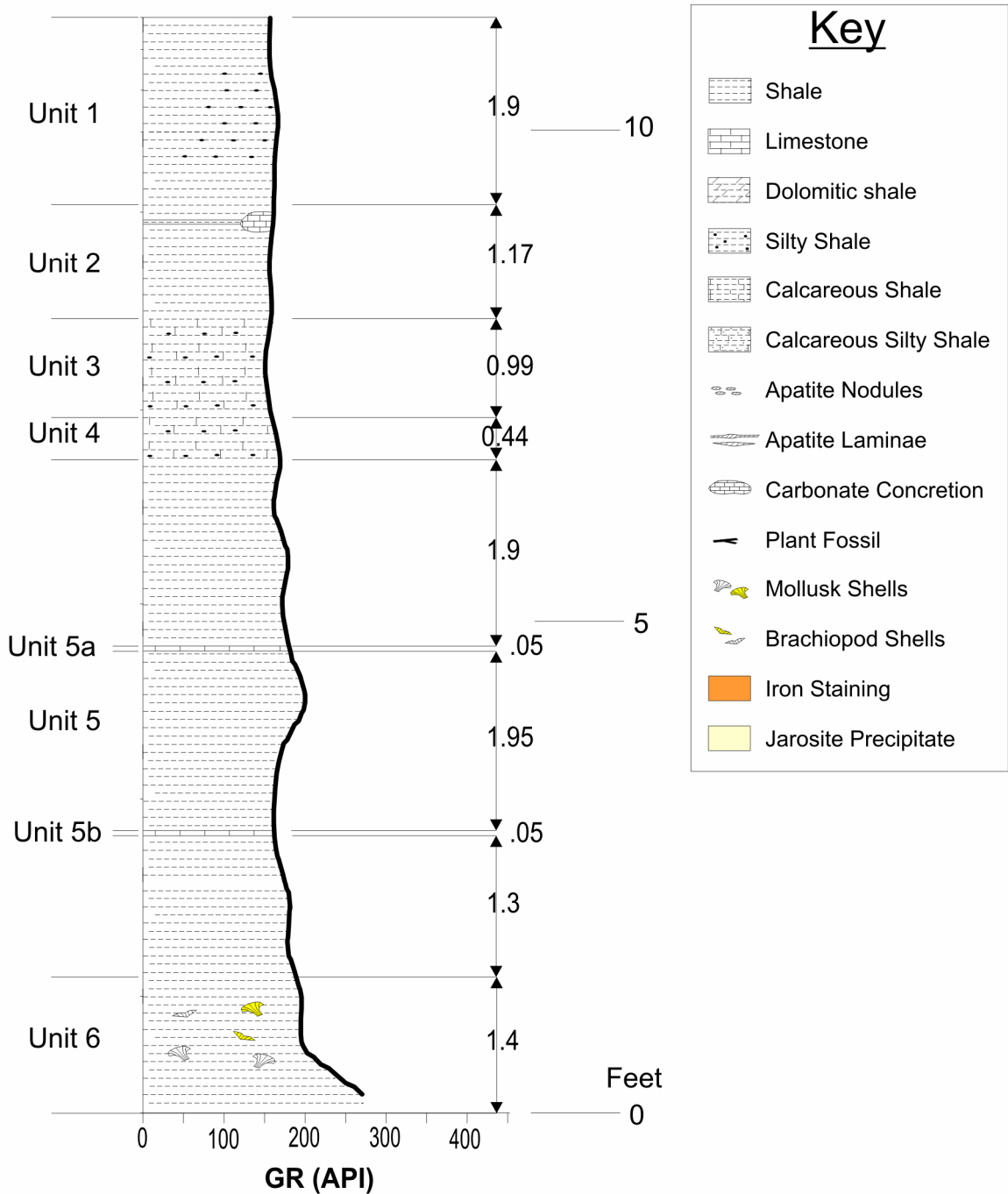
Figure AI.20 Geology strip log for Delaware Creek outcrop 2
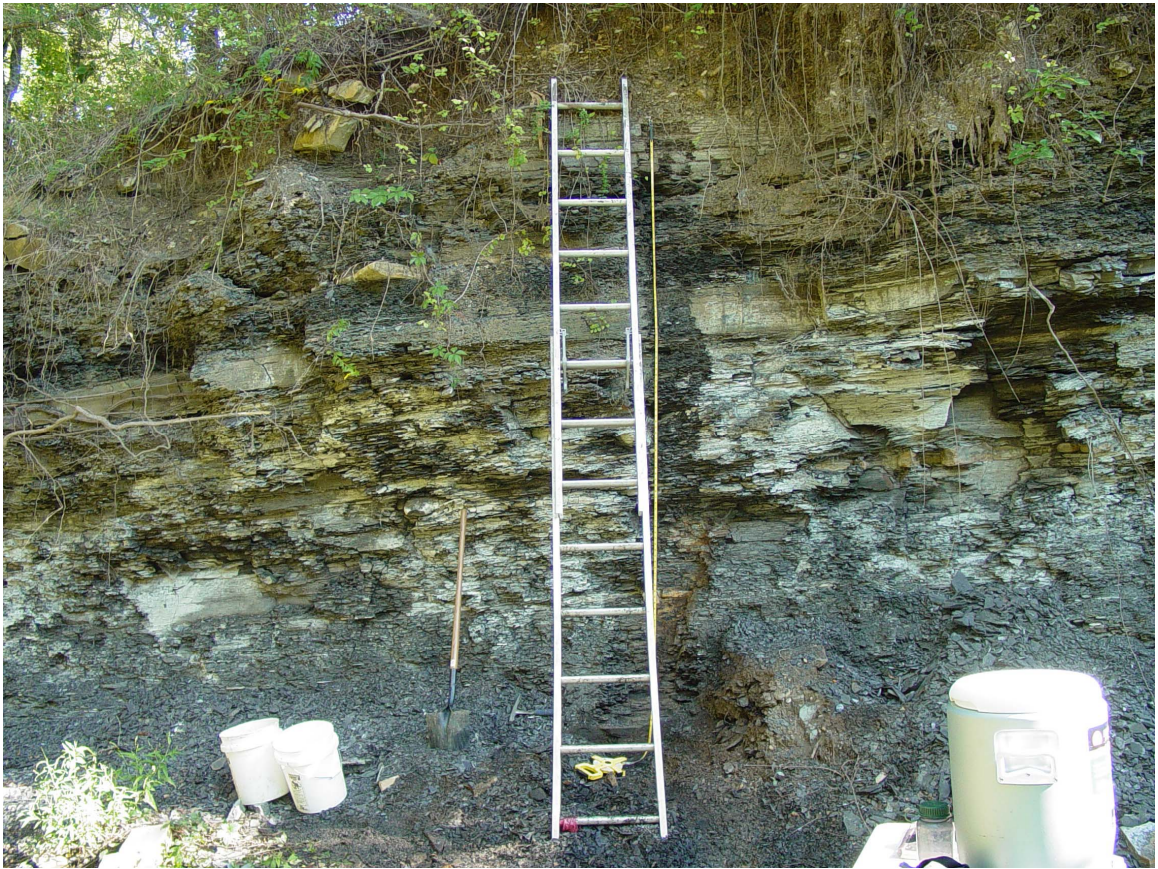
Figure AI.21 Photograph of Little Delaware Creek outcrop 2

were also measured. These measurements were: strike, N21°E and dip, 60°NW; strike, N25°W and dip, 76°NE.

Unit 1 – 0.0 to 1.9 ft

This unit is composed of a grayish-black shale that weathers to light gray. The shale contains a very small amount of silt and is non-calcareous. The shale is thinly bedded and blocky, and the unit is slightly resistant to weathering.

Unit 2 – 1.9 to 3.07 ft

This unit is composed of a grayish-black shale that weathers to a light gray. The shale contains no apparent silt and is non-calcareous. The shale is less blocky than shale above and slightly fissile. Within this unit at 2.3 to 2.37 ft a thin calcareous shale bed is present. This bed can be traced laterally where it thickens into a carbonate concretion.

Unit 3 – 3.07 to 4.06 ft

This unit is composed of a blackish-gray shale that weathers to a light gray. This shale is silty and calcareous. The unit is the most resistant unit in the outcrop giving a massive bedded appearance. The unit is very resistant to weathering and has a blocking character.

Unit 4 – 4.06 to 4.5 ft

This unit is composed of a grayish-black shale that weathers to light gray. The shale is slightly calcareous and silty. It has a fissile to blocky nature and is resistant to weathering, however it is less resistant than the layer above.

Unit 5 – 4.5 to 9.8 ft

This unit is composed of a grayish-black shale that weathers to light gray. The shale contains no apparent silt and is non-calcareous. The shale is fissile with a slight blocky nature.

Unit 5a – 6.4 to 6.45 ft

This small unit contains two laminated calcareous shale layers that are separated by non-calcareous shales. These two calcareous layers pass laterally into carbonate concretions.

Unit 5b – 8.4 to 8.5 ft

This interval contains a gray carbonate concretion that weathers to a brownish yellow color. Laterally adjacent to this concretion are two laminated calcareous shale layers that are separated by non-calcareous shales.

Unit 6 – 9.8 to 11.2 ft

This unit is composed of a grayish-black shale that weathers to a light gray. The shale contains no apparent silt and is non-calcareous. This unit is more resistant to

weathering than the unit above. This unit also contains brachiopod and mollusk shell impressions, some impressions are pyritized.

Outcrop 8 – Little Delaware Creek Outcrop 3 (LDC3)

This outcrop is the third of four outcrops exposed along the Little Delaware Creek. This small outcrop is exposed on the north bank of the Little Delaware Creek. This outcrop is located to the southwest of Bromide, OK in Section 11, T.2S., R.7E. (Figure AI.22). The coordinate marked location for this outcrop is N 34.39939^o and W 96.54195^o (Datum WGS 84). This outcrop was measured from the top down. The total thickness of this measured section was 9.2 ft. Figures AI.23 and AI.24 below contain a geology strip log and photograph of this outcrop respectively.

Unit 1 – 0.0 to 2.3 ft

This unit contains a grayish-black weakly fissile shale that weathers to a light gray. The unit is slightly resistant, contains no apparent silt, and is non-calcareous.

Unit 2 – 2.3 to 2.6 ft

This unit contains a grayish-black shale that weathers to a light gray. The shale unit is silty, calcareous, and resistant. It has a slightly laminated appearance, and it laterally adjacent to a carbonate concretion.

Unit 3 – 2.6 to 5.3 ft
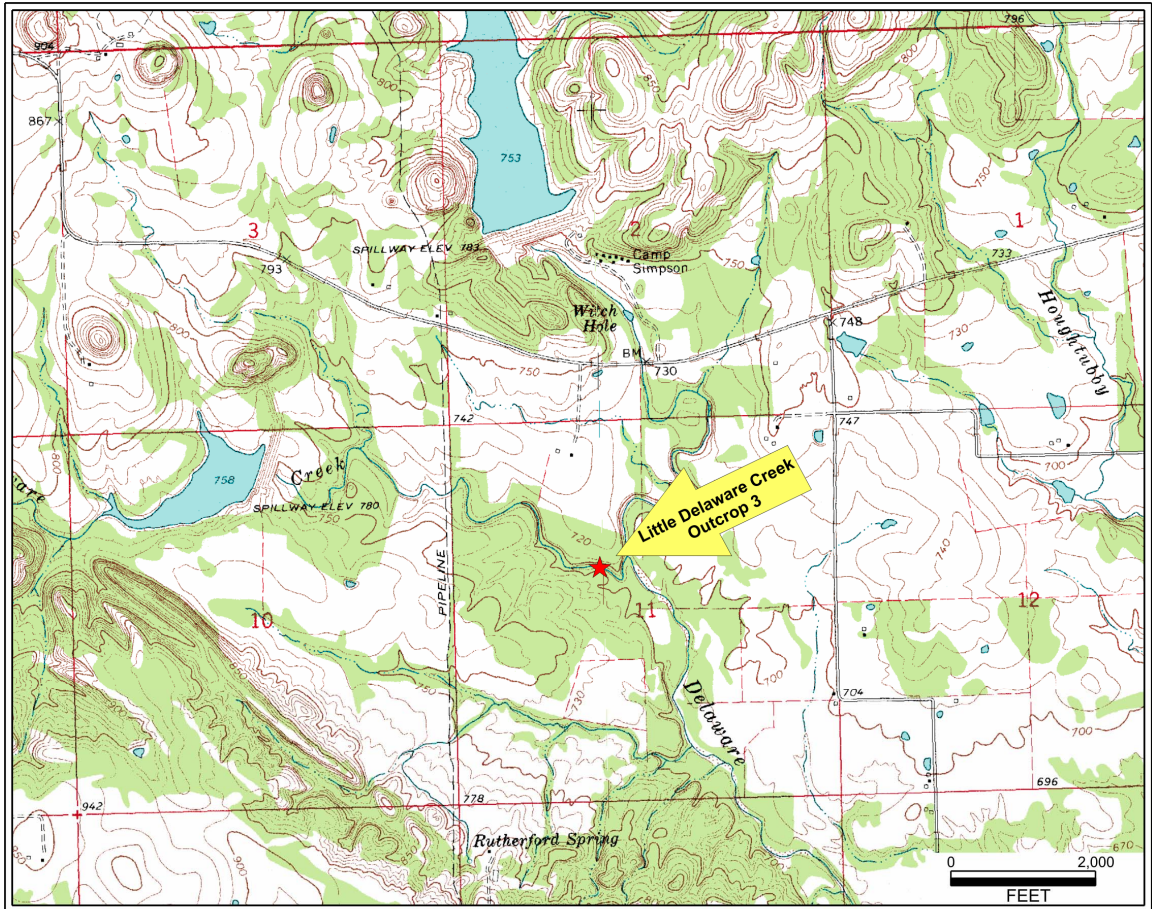
Figure AI.22 Location map for Little Delaware Creek outcrop 3

194

Little Delaware Creek Outcrop 3
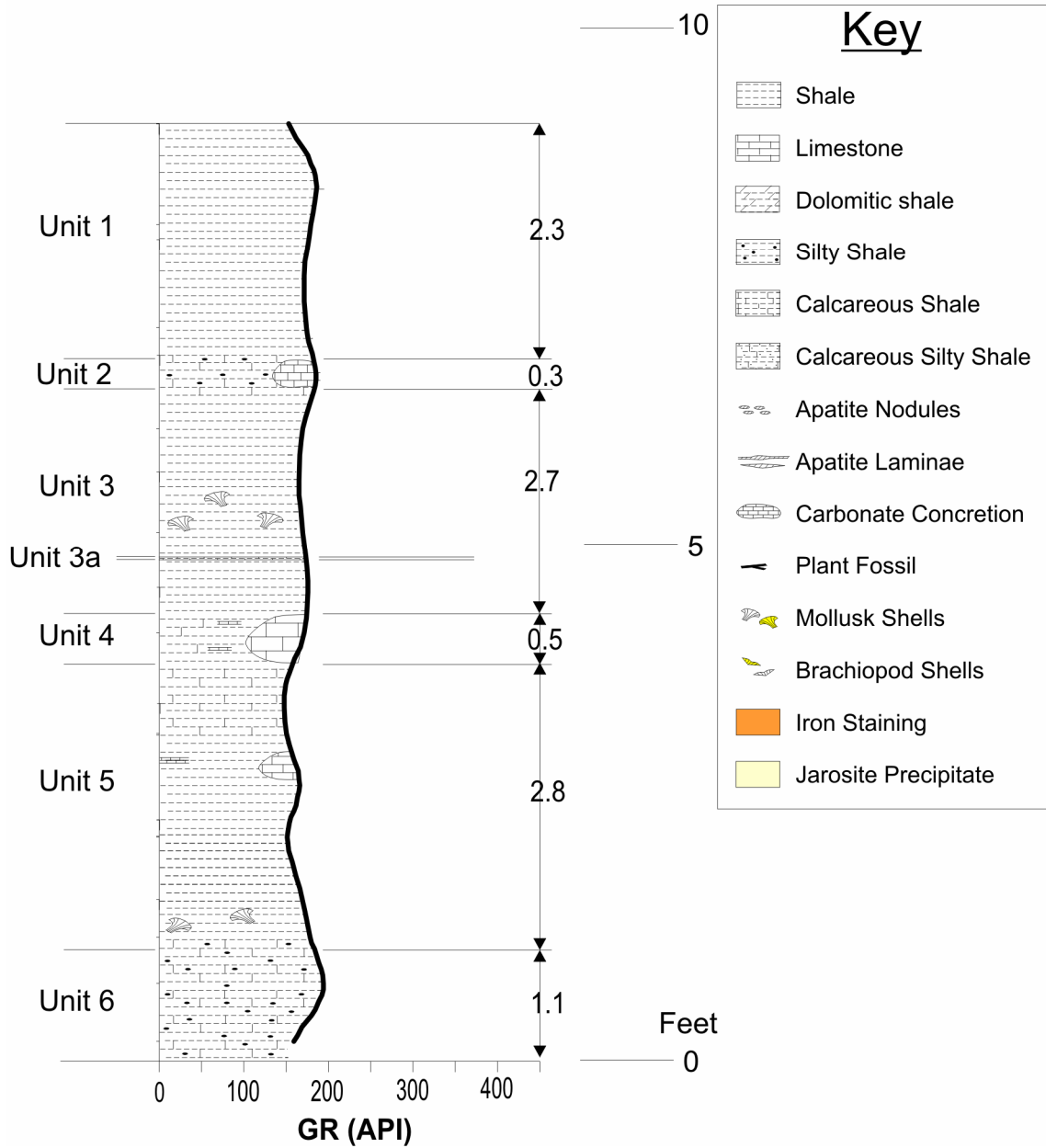
Figure AI.23 Geology strip log for Little Delaware Creek outcrop 3

Figure AI.24 Photograph of Little Delaware Creek outcrop 3

This unit contains a grayish-black, weakly fissile, shale that weathers to a light gray. The shale is slightly resistant, contains no apparent silt, and is non-calcareous. At 3.0 and 4.1 ft apparent mollusk impressions were noted. These impressions often have a thin calcareous sheen covering them.

Unit 3a – 4.23 to 4.3

This unit is a layer of interbedded, thin, irregular laminae of calcareous shale and shaly carbonate. The shaly carbonate laminae are gray to slightly translucent, while calcareous shale laminae are gray.

Unit 4 – 4.8 to 5.3 ft

This unit consists of a grayish-black shale. The shale possibly contains some silt, but it is difficult to determine in hand sample. The unit is calcareous, but does not contain any carbonate layers. Moving laterally, the shale laminae transition into thin carbonate layers and then into a carbonate concretion.

Unit 5 – 5.3 to 8.1 ft

This unit consists of a grayish-black fissile shale. The shale contains little to not apparent silt and is calcareous. At an interval between 6.5 and 6.75 ft shale beds transition laterally into shaly mudstone. This mudstone is similar in composition to carbonate concretions, but does not have the characteristic concretion shape. The same bed transitions laterally the other direction into a carbonate concretion. At 8.0 ft apparent

mollusk impressions were noted. These bivalve impressions often have a thin calcareous layer covering them.

Unit 6 – 8.1 to 9.2 ft

This unit makes up a resistant bench at the base near the water level. The unit consists of a grayish-black shale. The shale is calcareous and silty. The resistant shale is not fissile but blocky in nature.

Outcrop 9 – Little Delaware Creek Outcrop 4 (LDC4)

This outcrop the fourth of four outcrops exposed along the Little Delaware Creek. This small outcrop is exposed on the north bank of the Little Delaware Creek where it empties into Delaware Creek. This outcrop is located to the southwest of Bromide, OK in Section 11, T.2S., R.7E. (Figure AI.25). The coordinate marked location for this section is N 34.39962^o and W 96.54107^o (Datum WGS 84). This outcrop was measured from the top down. The total thickness of this measured section was 7.8 ft. This outcrop is disturbed and tilted in locations due to vegetation. Figures AI.26 and AI.27 below contain a geology strip log and photograph of this outcrop respectively.

Unit 1 – 0.0 to 1.05 ft

This unit consists of a blackish-brown shale. The shale is fairly weathered and it is difficult to determine if fresh surfaces exist. The shale contains no apparent silt and is non-calcareous silt. There are abundant apatite nodules present within the unit. The shale weathers with a fissile to blocky nature.
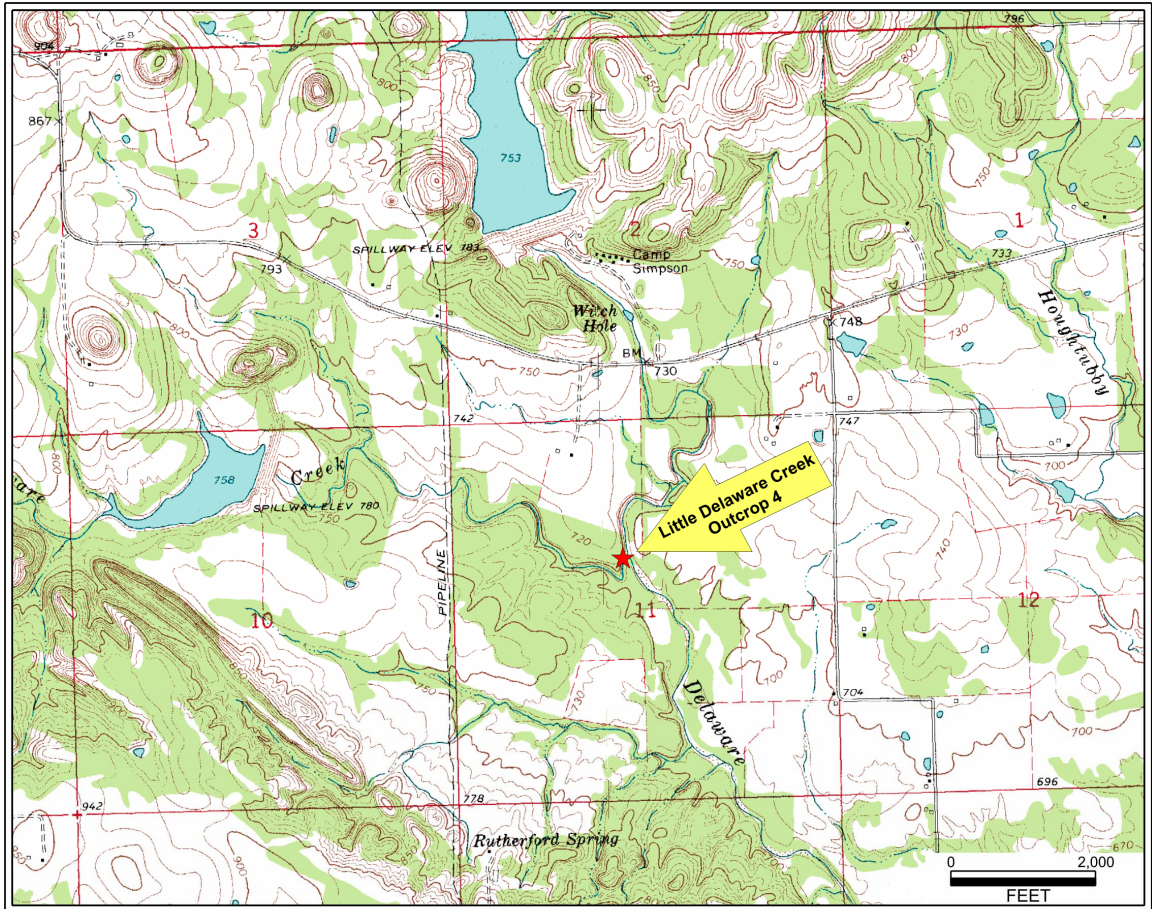
Figure AI.25 Location map for Little Delaware Creek outcrop 4
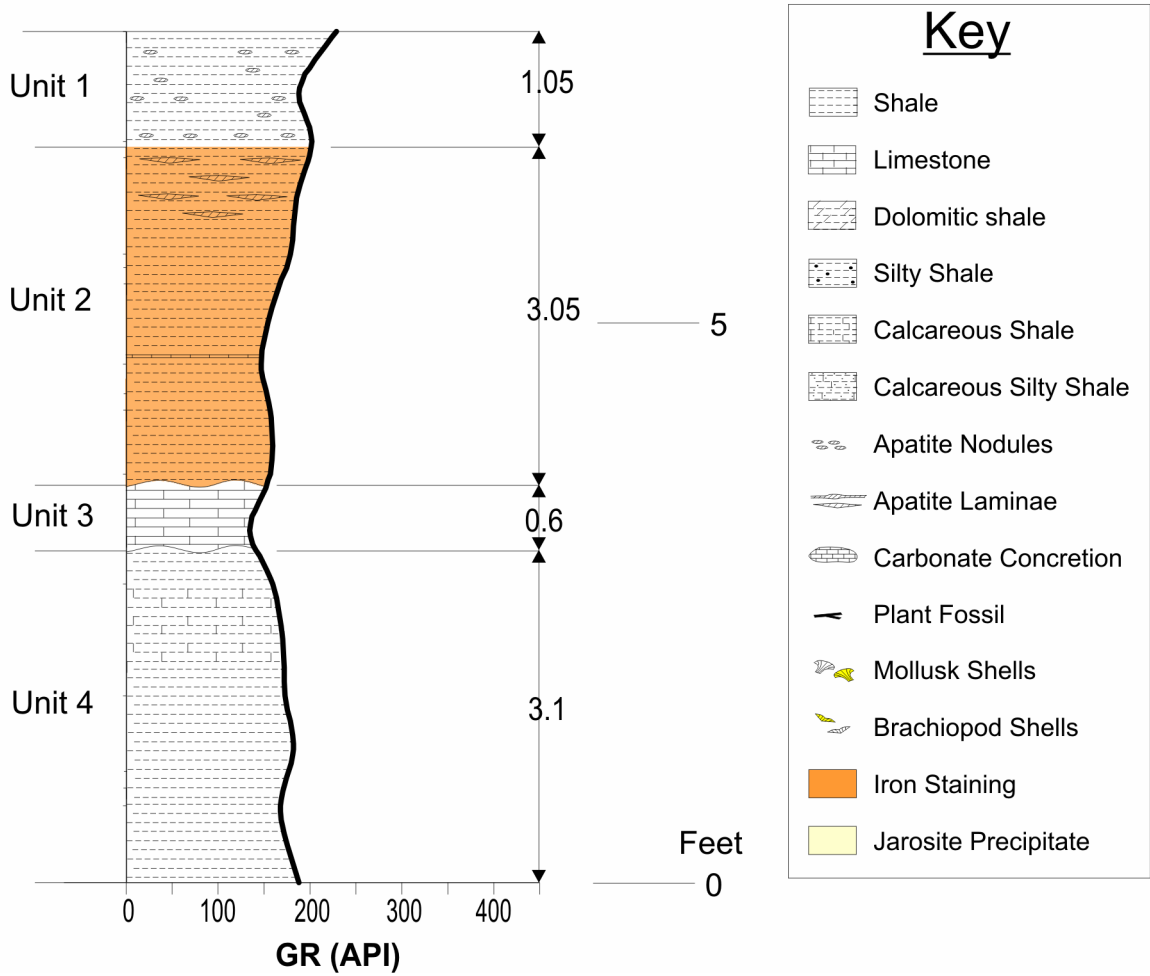
Figure AI.26 Geology strip log for Little Delaware Creek outcrop 4

Figure AI.27 Photograph of Little Delaware Creek outcrop 4

Unit 2 – 1.05 to 4.1 ft

This unit consists of a grayish-black fissile shale that weathers to a light gray. The shale contains no apparent silt and is non-calcareous. Iron staining is common between bedding planes. At an interval between 1.05 and 1.4 ft there are thin lenticular laminations of apatite. These laminates are light gray, resistant, and non-calcareous. At a depth of 3.3 ft, a single thin calcite layer is present. This layer is slightly translucent with irregular bedding planes, and is probably a result of outcrop weathering.

Unit 3 – 4.1 to 4.7 ft

This interval contains a large carbonate bed. The bed is possibly several concretions grown together. The carbonate bed is blackish-gray in color and weathers to a light gray or light brown. The upper and lower boundaries of the concretion are wavy , and do not have a uniform thickness.

Unit 4 – 4.7 to 7.8 ft

This interval consists of a grayish-black shale that weathers to a light gray. The shale is soft, non-resistant, and fissile. At an interval between 5.3 and 5.7 ft the shale is slightly calcareous, but is non-calcareous in the remaining unit.

Outcrop 10 – Pine Top Mountain Outcrop (PT)

The outcrop was first described by Hendricks and Gardner (1947) and then was later visited by Siy (1988) and Suneson and Campbell (1990). The original location given by Hendricks and Gardner (1947) differs from that given by Suneson and Campbell

(1990). Suneson and Campbell's (1990) location differs slightly from the one given here.

This location is an accurate outcrop location, but it is possible that the location is not the

same as that described by Hendricks and Gardner (1947). Their (ibid) location describes

units and thicknesses not observed in this study.

This outcrop is exposed along an intermittent stream about ¾ of a mile east of the

Indian Nation Turnpike on EW1610. This outcrop is located southwest of the town of Ti,

OK and east, northeast of the town of Pine Top, OK. The outcrop is in the NW1/4 NE1/4

of Section 4, T.2N., R.15E. (Figure AI.28). The coordinate location for this outcrop is N

34.67850^o W 95.73162^o (Datum WGS 84).

This outcrop is interpreted to be a slump block of Caney Shale that was latter

upthrusted during the Ouachita Orogeny. The exposed shale in this location is more

brittle and resistant than Caney Shale viewed in outcrops to the west. At first glance the

section appears to contain mainly Woodford Shale lithology. However, after detailed

investigation the outcrop was determined to be Caney on the basis of gamma-ray

response. The use of this outcrop in this research is somewhat problematic, because the

outcrop is no longer in its original stratigraphic position and the lithology of the Caney

and "Mayes" (lower Caney Shale) is different that that viewed at the outcrops at the

eastern Arbuckle Mountains.

The total thickness of the outcrop was 206.8 ft. Because of the large size of this

outcrop, it was divided into 7 sections. These sections are Pine Top Mountain 1 through

7. Each section was measure from the bottom up. Figures AI.29 and AI.30 contain a

geology strip log for this outcrop.
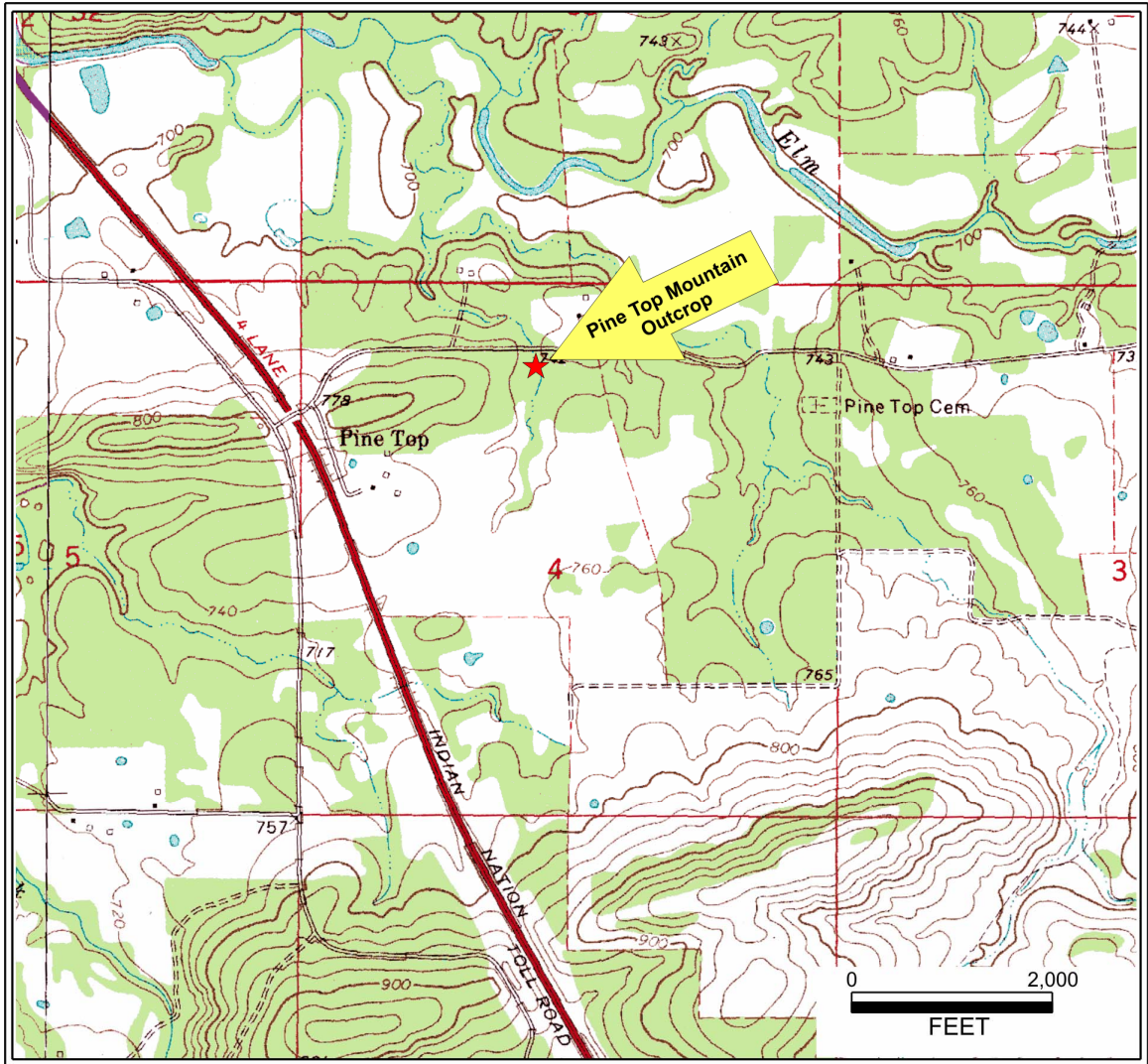
Figure AI.28 Location map for the Pine Top Mountain outcrop

Figure AI.29 Geology strip log for Sections 1, 2, and 3 at the Pine Top Mountain outcrop.

Figure AI.30 Geology strip log for Sections 4, 5, 6, and 7 at the Pine Top Mountain outcrop.

Pine Top Mountain Section 1 (PT1)

The total measured thickness of this section was 29.5 ft. Figure AI.31 below contains a photograph of this outcrop. According to descriptions by Hendricks and Gardner (1947), Siy (1988), and Suneson and Campbell (1990) this section was identified as Woodford Shale. However, the gamma-ray readings for this section were low, 110 to 190 API units; where as the Woodford Shale typically has a gamma-ray reading that averages around 360 API units (Krystyniak, 2005).

0.0 to 29.5 ft

This first section was measured from the base up and is the lowest section stratigraphically. The total thickness of this section is 29.5 ft. This measured section is composed of fissile black shale that weathers brown to blue gray. Shale laminae are on average 3 mm thick. There is no apparent silt with in the section and shale is non-calcareous. A yellow precipitate was noted on the weathered bedding planes between 13.5 ft and 22 ft, and again at the top of the section. The top of the section also had iron staining on the bedding planes. Two carbonate nodules were noted in the section one at 14.9 to 15.6 and the other at 23.5 to 24.0 ft. Carbonate nodules are dark gray in color and weather to a brownish red. Butcher block weathering patterns were common on the nodule surface. An apatite nodule was noted at 13.05 ft.

The beds in the outcrop were nearly vertical. Two strike and dip measurements were taken at the location. These measurements were: N80E 88°S and N79E 71°S. Vegetation and weathering are possibly causing bed rotation in isolated areas. As a result finding suitable locations to measure strike and dip was difficult.

Figure AI.31 Photograph of Pine Top Mountain outcrop Section 1.

The outcrop appears slightly weathered at first glance, however because the beds are nearly vertical, weathered shale particles tend to fall between laminae or are washed off of the outcrop face. As a result the outcrop appears more weathered when the shale is excavated.

Pine Top Mountain Section 2 (PT2)

This section starts at the top of PT1, and was measured to be 42.9 ft thick. The lithologic variability of this section was much higher than other sections at the Pine Top locality. Figure AI.32 below contains a photograph of this outcrop.

Unit 1 – 0.0 to 2.3 ft

The base of the section from 0 to 2.3 ft is composed of a grayish-green shale. This shale was heavily weathered. The contact between this interval and the lower interval appears to be sharp and straight parallel. The shale is finely laminated with laminae thicknesses of approximately 2.5 mm. The interval is non-calcareous with no apparent silt. Apatite nodules were noted at the basil contact.

Unit 2 – 2.3 to 3.0 ft

From 2.3 to 3.0 ft an extremely weathered, brownish-tan, shale was measured. The shale is calcareous and containes no apparent silt.

Unit 3 – 3.0 to 5.6 ft

Figure AI.32 Photograph of Pine Top Mountain outcrop Section 2

At the interval between 3.0 and 5.6 ft a blackish-brown shale was measured. This shale was heavily weathered. The interval contained no apparent silt, and reacted slightly with dilute HCL.

Unit 4 – 5.6 to 6.4 ft

At the interval between 5.6 and 6.4 ft a blackish-gray dolomitic silty mudstone was measured. This unit contains large portions of silt to fine sand and at first glance could be mistaken as a very fine grained sandstone. This unit is more resistant than the surrounding shales and formed a small ridge.

Unit 5 – 6.4 to 8.4 ft

From 6.4 to 8.4 ft a brown shale was measured. This shale is both calcareous and silty, and in outcrop the shale is heavily weathered.

Unit 6 – 8.4 to 16.75 ft

From 8.4 to 16.75 ft a grayish-black shale was measured. This shale is non-calcareous and silty, and in outcrop the shale is heavily to extremely weathered.

Unit 7 – 16.75 to 17.15 ft

The next unit between 16.75 and 17.15 ft consisted of a dolomitic silty mudstone. This interval is very similar to the interval recorded between 5.6 and 6.4 ft. The unit contains a large portion of silt to fine sand and possibly some clays. It is grayish-black in color and weathers to a brown color. The bedding planes for this unit are sharp and

straight uneven. As a result the thickness of the unit increases above the measured area in a lobe like shape. Like the carbonate unit below, this unit is more resistant to erosion and forms a small ridge.

Unit 8 – 17.15 to 26.3 ft

From 17.15 to 26.3 a blackish-gray shale was measured. The shale is fissile to blocky in nature. This shale is silty and non-calcareous, except at the base of the unit where it is slightly calcareous.

Unit 9 – 26.3 to 33.1 ft

At the interval between 26.3 and 33.1 ft a fissile black shale was measured. This shale is more resistant than the shales below and resembles the shales measured in section PT1. The shale contains laminae that are on average 1.5 mm thick, and weathers gray to brown. The shale is silty in the lower portions, but this silt disappears in the upper portions of the unit. From 31.0 to 33.1 ft, there is no apparent silt in the unit and the unit is less resistant to erosion. As a result laminae are less visible in this upper portion.

33.1 to 40.9 ft

From 33.1 to 40.9 ft the section is covered

Unit 10 – 40.9 to 41.7 ft

Above the covered unit from 40.9 to 41.7 ft a papery-black shale is present. This shale is moderately weathered, and weathers to a light gray color.

Unit 11 – 41.7 to 42.9 ft

From 41.7 to 42.9 ft a calcareous shalely sandstone was measured. This unit is brownish-black in color and weathers to a brown. The unit is similar to the mudstone units below, however the unit appears to contain more coarse grains and less calcite. The unit contains beds that are 0.15 to 0.05 ft thick.

Pine Top Mountain Section 3 (PT3)

This is a small section exposed south of the top of PT2. The bottom of PT3 and the Top of PT2 are not directly adjacent. Instead, 8.7 ft of cover occurs between these two subsections. This section is 9.9 ft thick. Figure AI.33 below contains a photograph of this outcrop.

0.0 to 9.9 ft

This subsection has a uniform lithology throughout and is measured to be 9.9 ft thick. It is composed of a heavily weathered fissile shale. The shale is black but weathers to a light gray. This unit contains no apparent silt and is non-calcareous. Shale laminae are on average 3 mm thick. Apatite nodules were recorded at 4.6 and 6 ft.

Pine Top Mountain Section 4 (PT4)

This is a large section exposed south of the top of PT3. The bottom of PT4 and the Top of PT3 are not directly adjacent. Instead, 12.6 ft of cover occurs between these

Figure AI.33 Photograph of Pine Top Mountain outcrop Section 3.

two subsections. This section was measured to be 37.0 ft thick. Figure AI.34 below contains a photograph of this outcrop.

0.0 to 37.0 ft

This subsection has a fairly uniform lithology throughout, and is measured to be 37 ft thick. It is composed of a black fissile shale that weathers to a reddish brown or light grey. Shale laminae are on average 1.5 to 2 mm thick. This unit contains no apparent silt and is non-calcareous. This unit is fairly similar to PT3, but appears to be slightly more resistant. The shale is moderately to heavily weathered and appears more weathered upon excavation. Apatite nodules were recorded at 6.1, 6.5, 9.95, 11.0, 11.8, 14.4, 15.0, 15.8, 16.2, 23.8, 24.7, and 33.6 ft.

Pine Top Mountain Section 5 (PT5)

This subsection starts at the top of PT4 with no cover between the two sections. This section was measured to be 27.0 ft thick. Figure AI.35 below contains a photograph of this outcrop.

0.0 to 27.0 ft

This subsection has a fairly uniform lithology that appears to be the same as PT4. The subsection is 27.7 ft thick, and is composed of a black fissile shale that weathers to a reddish brown or light gray. Shale laminae are on average 1.5 to 3 mm thick. There is no apparent silt and the shale is non-calcareous. The shale is moderately to heavily weathered and appears more weathered upon excavation. Roots from modern vegetation

215

Figure AI.34 Photograph of Pine Top Mountain outcrop Section 4.

Figure AI.35 Photograph of Pine Top Mountain outcrop Section 5.

have tilted some of the shale beds. Apatite nodules were recorded at 4.1, 10.5, 15.0, 15.5, 17.2, and 20.5 ft. Additionally, a carbonate nodule was observed at 2.95 ft.

Pine Top Mountain Section 6 (PT6)

This section starts at the top of PT5 with no cover between the two sections. This section was measured to be 6.0 ft thick. Figure AI.36 below contains a photograph of this outcrop.

0.0 to 6.0 ft

This subsection has a fairly uniform lithology that appears similar to PT5. The subsection is 6 ft thick, and is composed of a black fissile shale that weathers to a light gray. There is no apparent silt in this unit and it is non-calcareous. Shale laminae are on average 2 mm thick. The shale is heavily weathered and appears more weathered upon excavation. An apatite nodule was record at 2.8 ft.

Pine Top Mountain Section 7 (PT7)

This is a small section exposed south of the top of PT6. The bottom of PT7 and the Top of PT6 are not directly adjacent. Instead, approximately 26 ft of cover occurs between these two subsections. The measured thickness of this section was 6.5 ft. Figure AI.37 below contains a photograph of this outcrop.

0.0 to 6.5 ft

Figure AI.36 Photograph of Pine Top Mountain outcrop Section 6.

Figure AI.37 Photograph of Pine Top Mountain outcrop Section 7.

This subsection is approximately 6.5 ft thick; however the thickness is difficult to measure as a result of bed disruption and rotation by vegetation. This subsection has a fairly uniform lithology, and is composed of a grayish-black fissile shale. The shale weathers brown to light gray in color, and iron staining is present on some bedding planes. Weathered laminae are approximately 2 mm thick. There is a large portion of silt to fine sand within the unit, and the unit is non-calcareous. This unit is more resistant in nature than underlying subsections. The resistant nature could be due to the silt and fine sand fraction.

APPENDIX II

THIN SECTION DESCRIPTIONS

Figure AII.1 2.0 ft Richard's Farm Outcrop 1

This unit is characterized as a coarse grained dolomite. The unit is composed

predominantly of a dolomite rhombs with a clay matrix between the grains. Dolomite

appears to be of ferroan dolomite. Rare dolomitized bivalve shells and apatite nodules

can be found within the unit.

Figure AII.2 3.25 ft Richard's Farm Outcrop 1

This unit is characterized as a shaley dolomitic carbonate. The matrix is predominantly

clay with some calcite mud. Most of the grains within the unit are dolomite rhombs.

Some angular silt size quartz and calcite grains are present within the unit. A few large

dolomite replaced bivalves were noted in thin section.
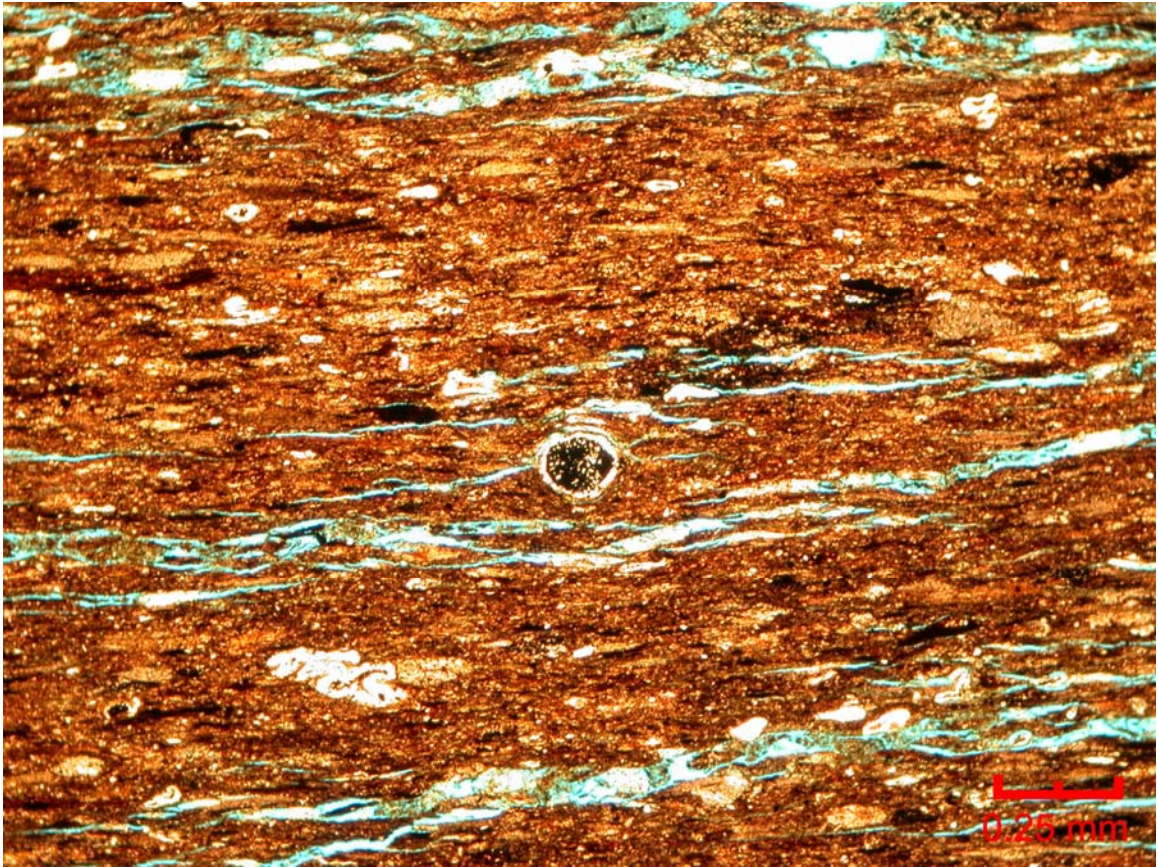
Figure AII.3 0.6 ft Richard's Farm Outcrop 2

This unit is characterized as a slightly laminated to laminated brown shale. Within the

unit <u>Tasmanites</u> cysts are common. Many of these cysts are compacted and replaced with

microquartz. Some quartz replaced cysts contain bitumen in the center and other cysts

are replaced entirely with bitumen. A few cysts are pyritized and were not compacted.

An occasional bivalve fragment was noted in the units. These fragments appeared to be

replaced by dolomite to partially dissolved.
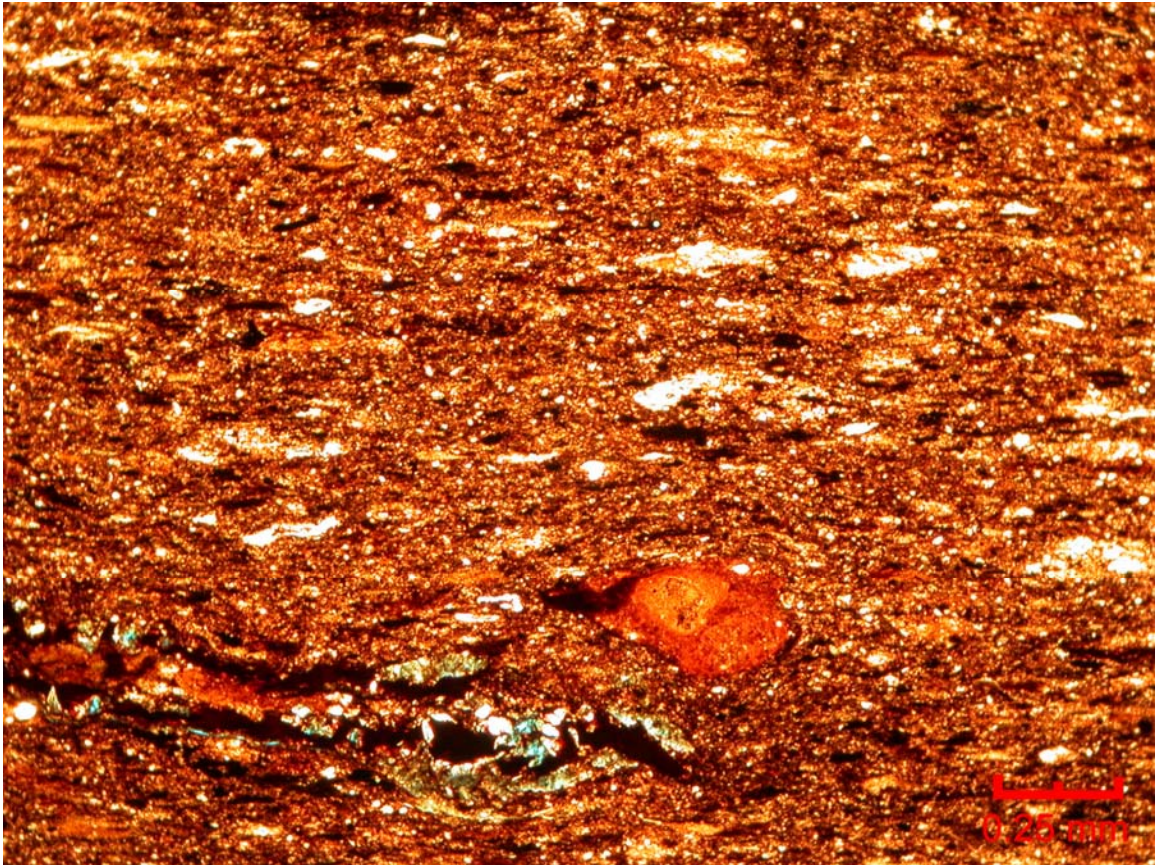
Figure AII.4 2.5 ft Jeff Luke Shale Pit Section 1B

This unit is characterized as a slightly laminated brown shale. Tasmanites cysts were

common in the unit. Most of these cysts were compacted and replaced with microquartz

or bitumen. Some cysts consisted of a microquartz rim with bitumen in the center, and

others were replaced with pyrite and not compacted. Apatite nodules were present in the

unit. Some apatite nodules appeared to contain iron. Glauconite was also present within

the thin section. Silt size angular quartz was present in thin section along with quartz

filled fractures.

Figure AII.5 4.0 ft Jeff Luke Shale Pit Section 2

This unit is characterized as a brown to tan to black shale. The shale is weakly laminated

to laminated. <u>Tasmanites</u> cysts were common in the unit. These cysts were compacted

and replaced with microquartz and/or bitumen. Some cysts appeared to contain clays. A

few non-compacted to partially compacted cysts were present. These cysts were replaced

with pyrite. Possible glauconite pellets appearing in a weak laminae were noted. Apatite

nodules were present in the thin section along with silt size angular quartz. Gypsum was

present along a fracture in the thin section.
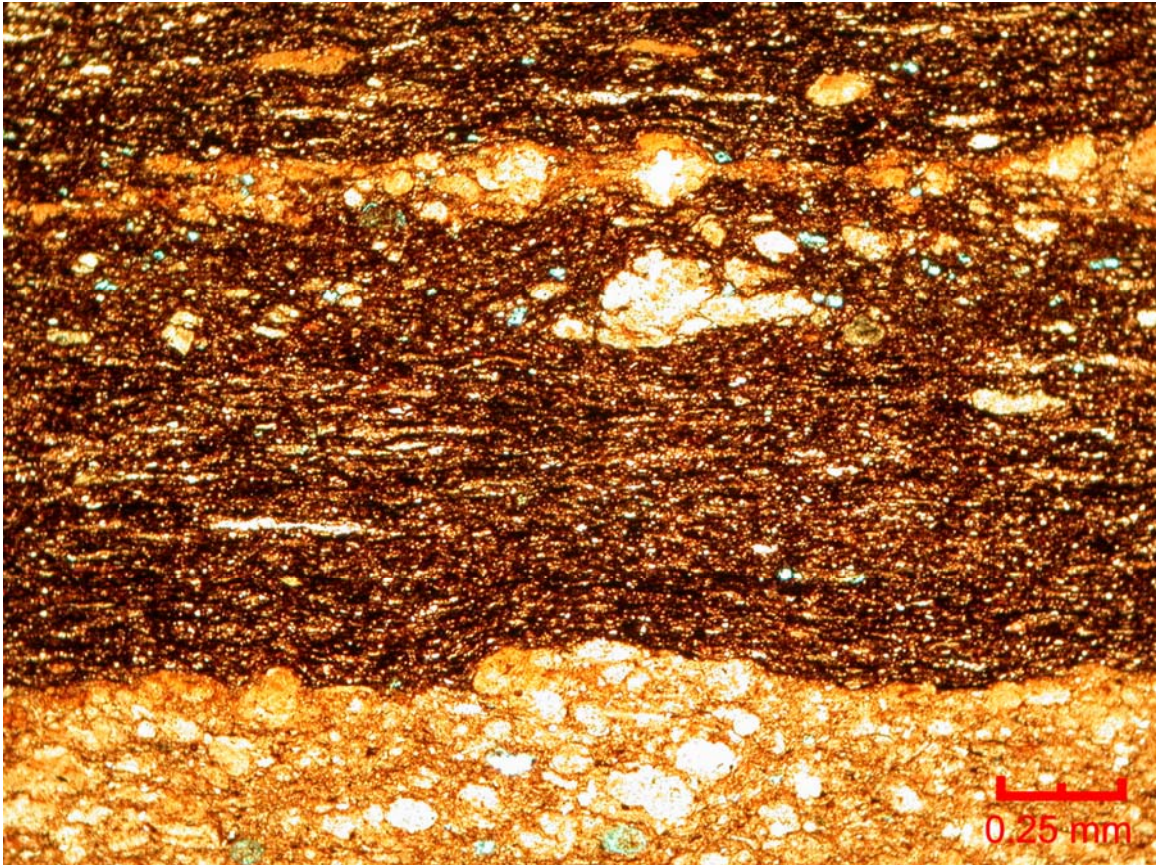
Figure AII.6 8.0 ft Jeff Luke Shale Pit Section 3

This unit is characterized as a brown to black shale with well developed apatite

laminations. These apatite laminates were composed of nodules grouped together with

clay. Some of the apatite was stained with iron oxide. Glauconite pellets were present in

thin section.   These pellets were non-compacted to slightly compacted, and occurred

both with the apatite laminae and separate from the apatite laminae. Silt size angular

quartz grains were present in the thin section along with algal Tasmanites cysts. These

cysts were compacted and replaced with microquartz and/or bitumen.
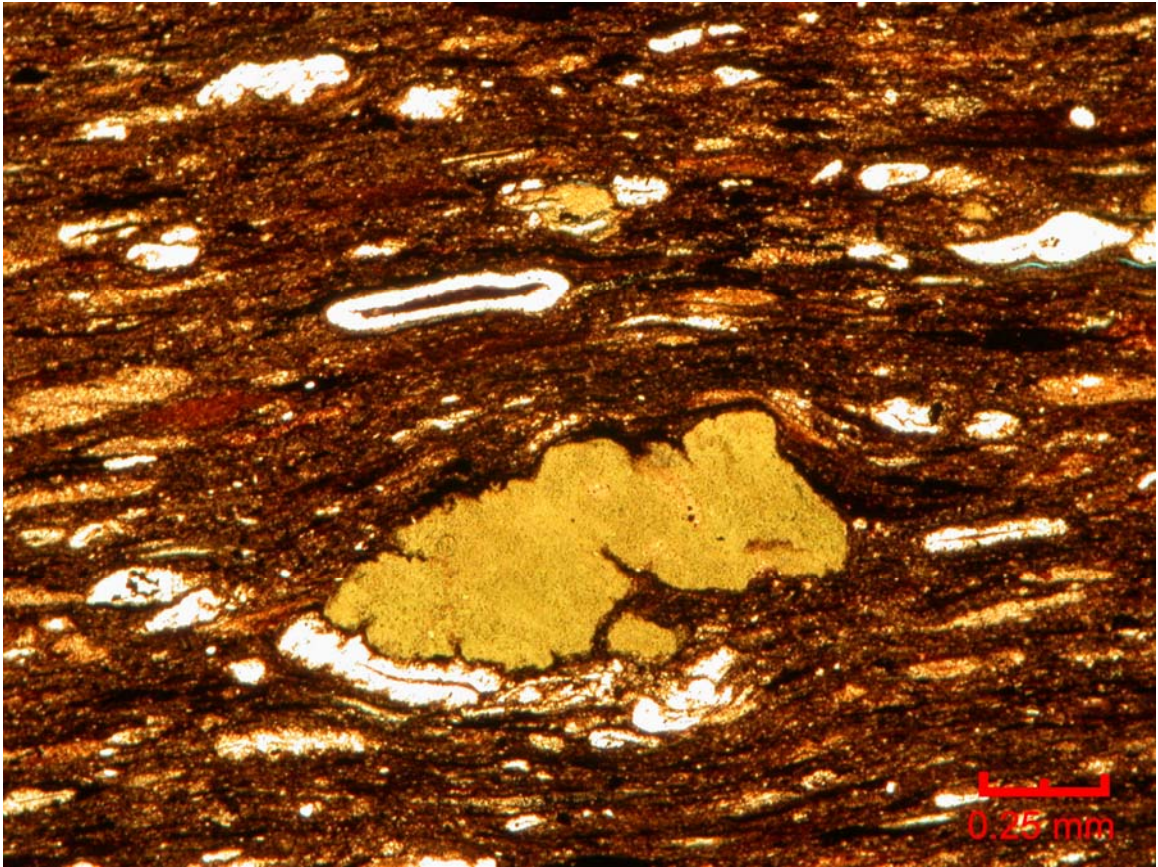
Figure AII.7 1.0 ft Delaware Creek Outcrop

This unit is composed of a laminated brown to black shale. Compacted <u>Tasmanites</u> cysts

were common in the thin section. These cysts were replaced by microquartz and

bitumen. Some cysts had a microquartz rim with bitumen in the center. Apatite and

glauconite nodules were present in the thin section. A few silt size angular quartz grains

were also noted.
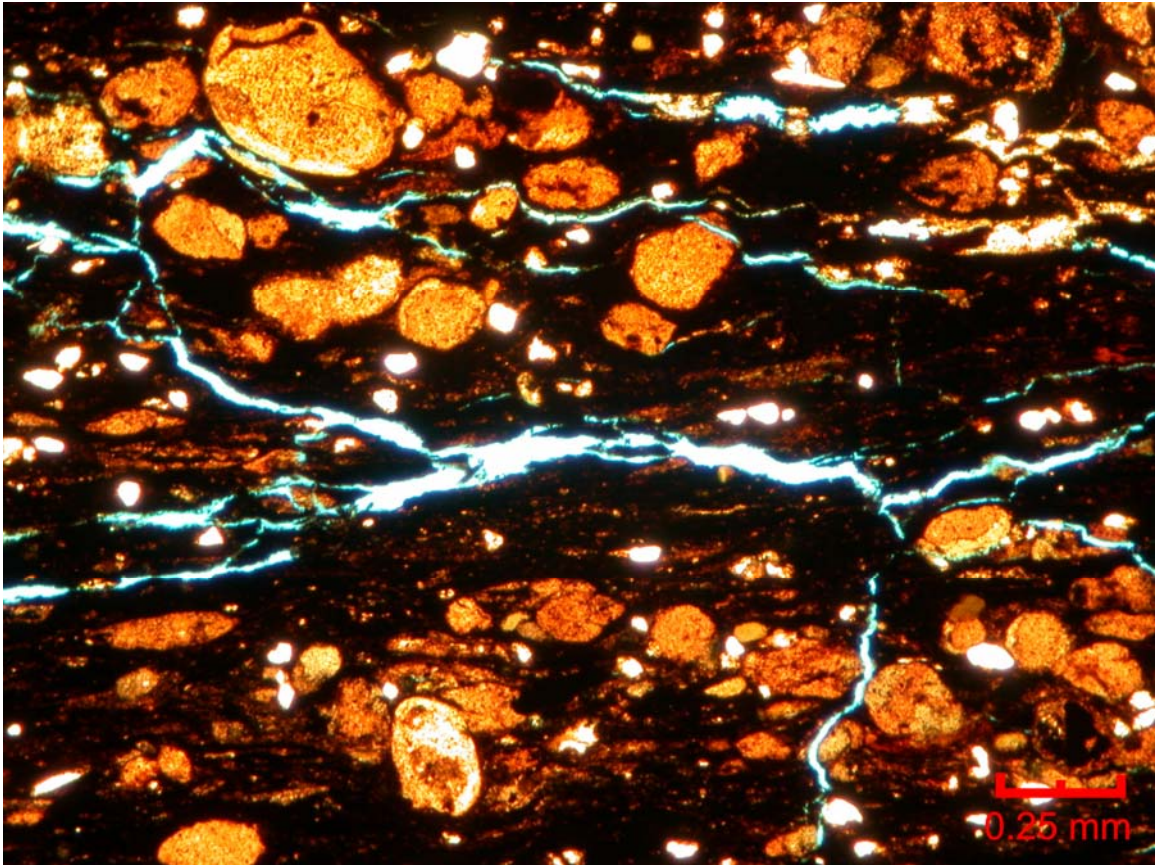
Figure AII.8 4.0 ft Delaware Creek Outcrop

This thin section was composed of a black shale with poorly developed apatite laminae.

Laminations were only a few apatite nodules thick. Fine sand and silt size angular quartz

grains were present in the thin section. This thin section contained the greatest

proportion of detrital quartz. Glauconite was present in the thin section and often

occurred with the apatite. Only a few possible Tasmanites cysts were present in the thin

section and some gypsum was noted to occur in fractures. Pyrite was precipitated

throughout the thin section.
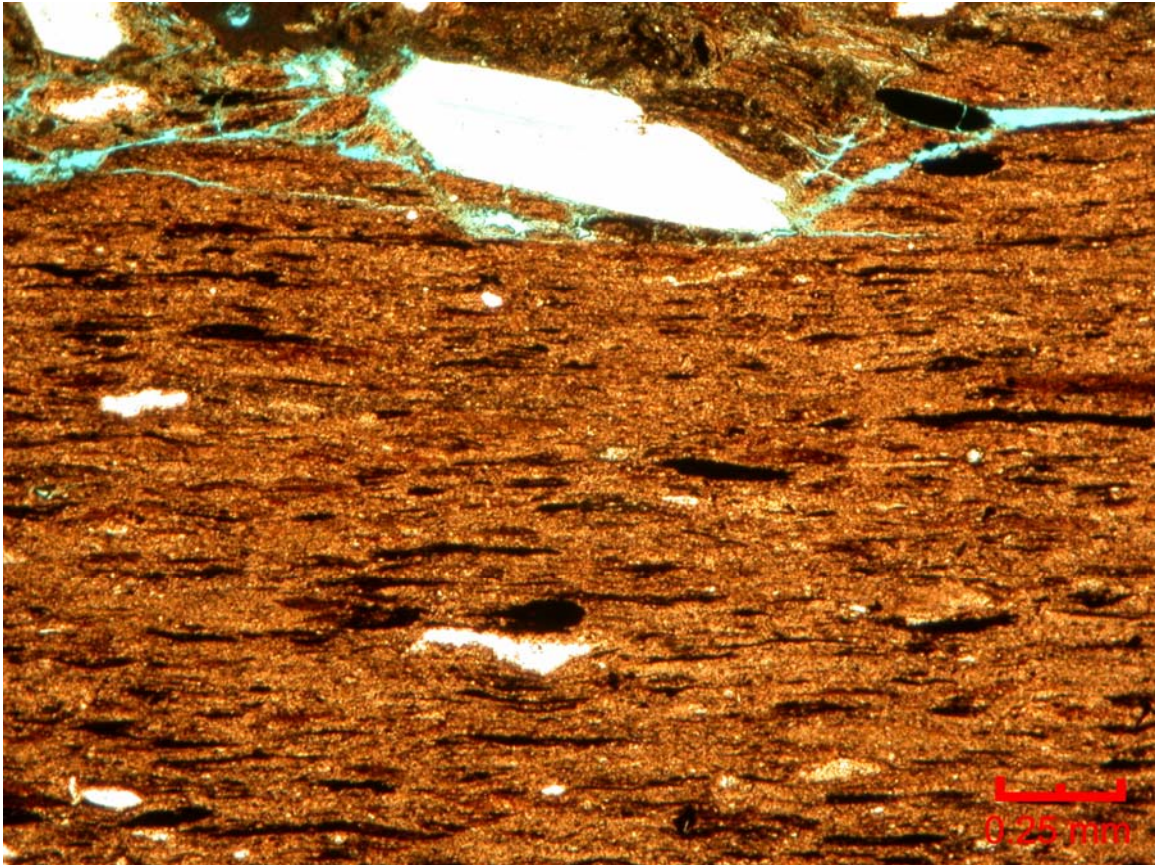
Figure AII.9 11.0 Delaware Creek Outcrop

This thin section consists of a slightly laminated to laminated brown shale. Abundant

Tasmanites cysts make up the thin section. Most of these cysts are compacted and

replaced with bitumen. Some of the Tasmanites cysts are replaced with microquartz.

Pyrite was commonly precipitated in cysts that were non-compacted to slightly

compacted. Gypsum was precipitated in a fracture in the thin section.
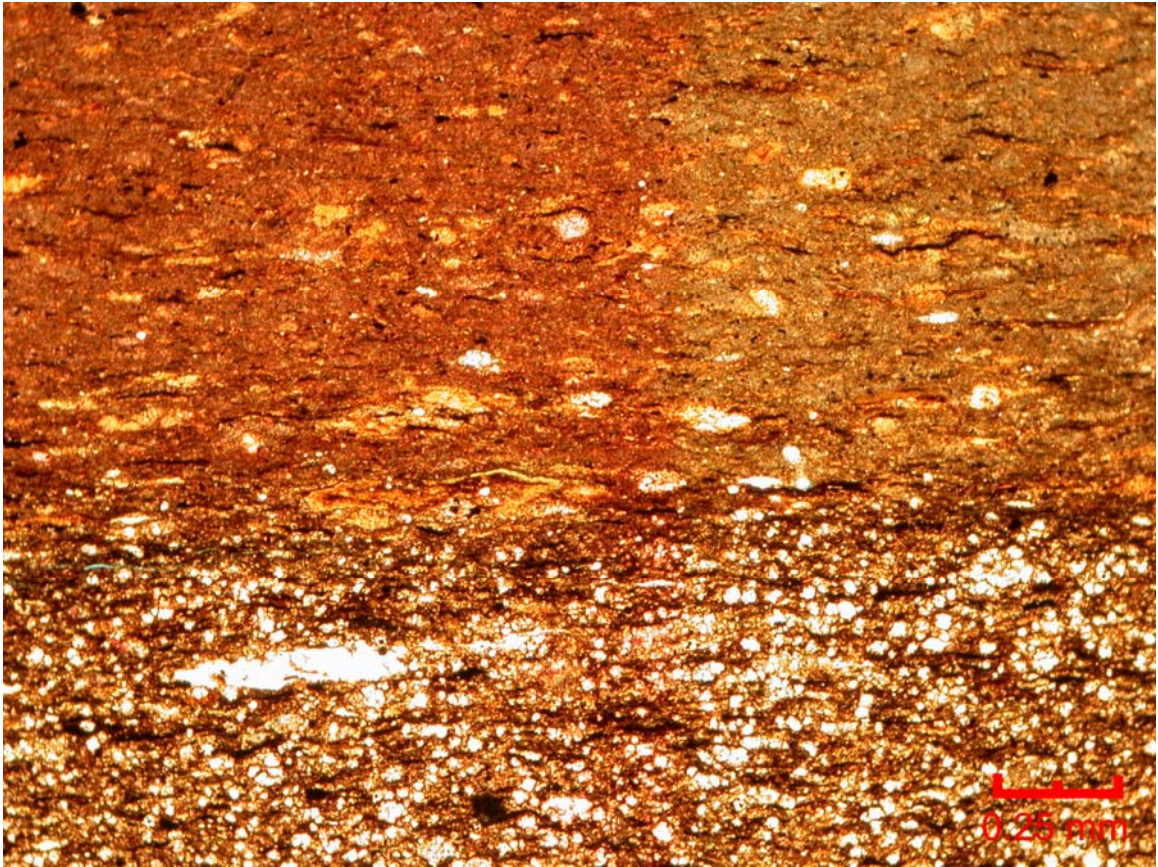
Figure AII.10 12.0 Little Delaware Creek Outcrop 1

This thin section is characterized as a dolomitic calcareous shale. The shale contains

laminations of calcite mud with apatite nodules and clay. In between these laminations

large dolomite rhombs with clay and calcite mud are present. Some <u>Tasmanites</u> cysts are

present within the thin section. These cysts are compressed and replaces with bitumen or

microquartz. Within the laminations containing apatite a few cysts are possibly replaced

by dolomite and calcite. Glauconite is also present in the laminations containing apatite

with on laminae composed predominantly of glauconite and only a few apatite nodules.
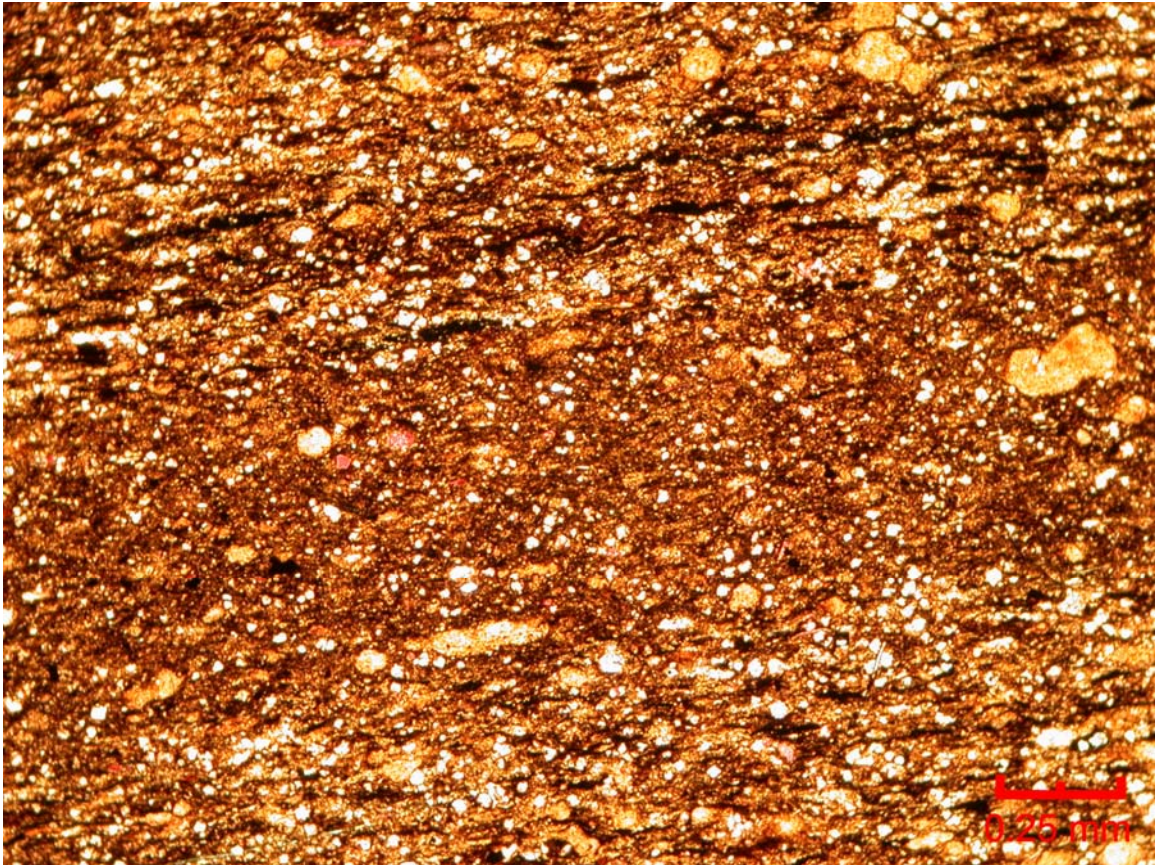
Figure AII.11 3.5 ft Little Delaware Creek Outcrop 2

This shale is characterized as a slightly laminated to laminated brown dolomitic shale.

The thin section contains one poorly developed laminae composed of apatite nodules and

clay. Apatite nodules are present throughout the thin section, but are more concentrated

in or near the poorly developed laminae. Dolomite rhombs are present throughout the

thin section and a few calcite grains were also noted. A few possible <u>Tasmanites</u> cysts

replaced with bitumen were noted. Also, bivalve shell fragments and glauconite nodules

were also viewed in the thin section.
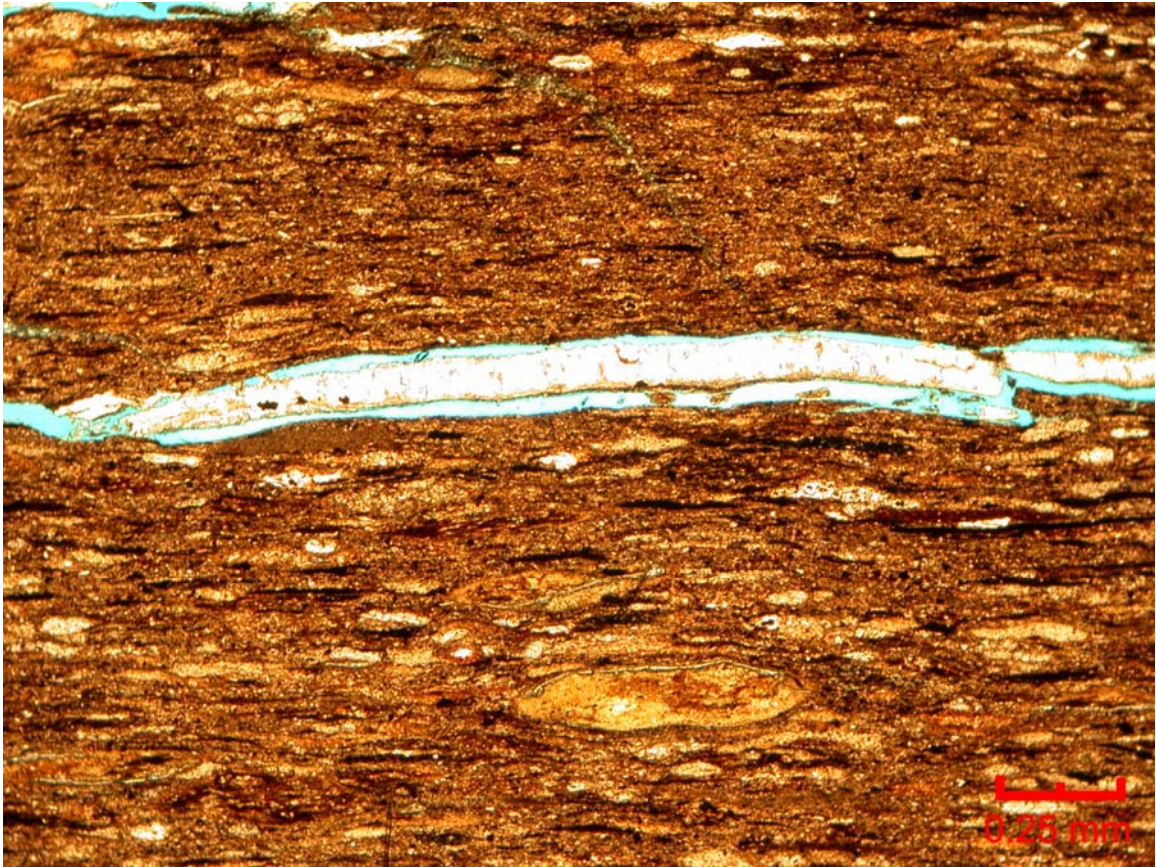
Figure AII.12 11.0 ft Little Delaware Creek Outcrop 2

This unit is characterized as slightly laminated brown shale. The shale contains some

apatite nodules, but the nodules do not occur in laminations. Tasmanites cysts are present

within the thin section. These cysts are generally compacted and replaced by bitumen. A

few of the cysts are replaced with microquartz. Some glauconite was noted in the thin

section. Also, calcite bivalve fragments were noted. These fossil fragments were

partially dissolved away. Some of the fossil fragments and Tasmanites were replaced

with pyrite.

Figure AII.13 8.5 ft Little Delaware Creek Outcrop 3

This unit is characterized as a slightly laminated to laminated shale. The shale is brown

in color and is composed of abundant bivalve shells and apatite nodules. The apatite

nodules appear throughout the thin section, and are moderately developed into laminae in

certain areas. Glauconite was noted to occur with apatite nodules. Some of the bivalve

fossils were partially dissolved away and others were replaced with pyrite. A few

<u>Tasmanites</u> cysts were noted in the thin section. Again these cysts were replaced with

bitumen and microquartz.
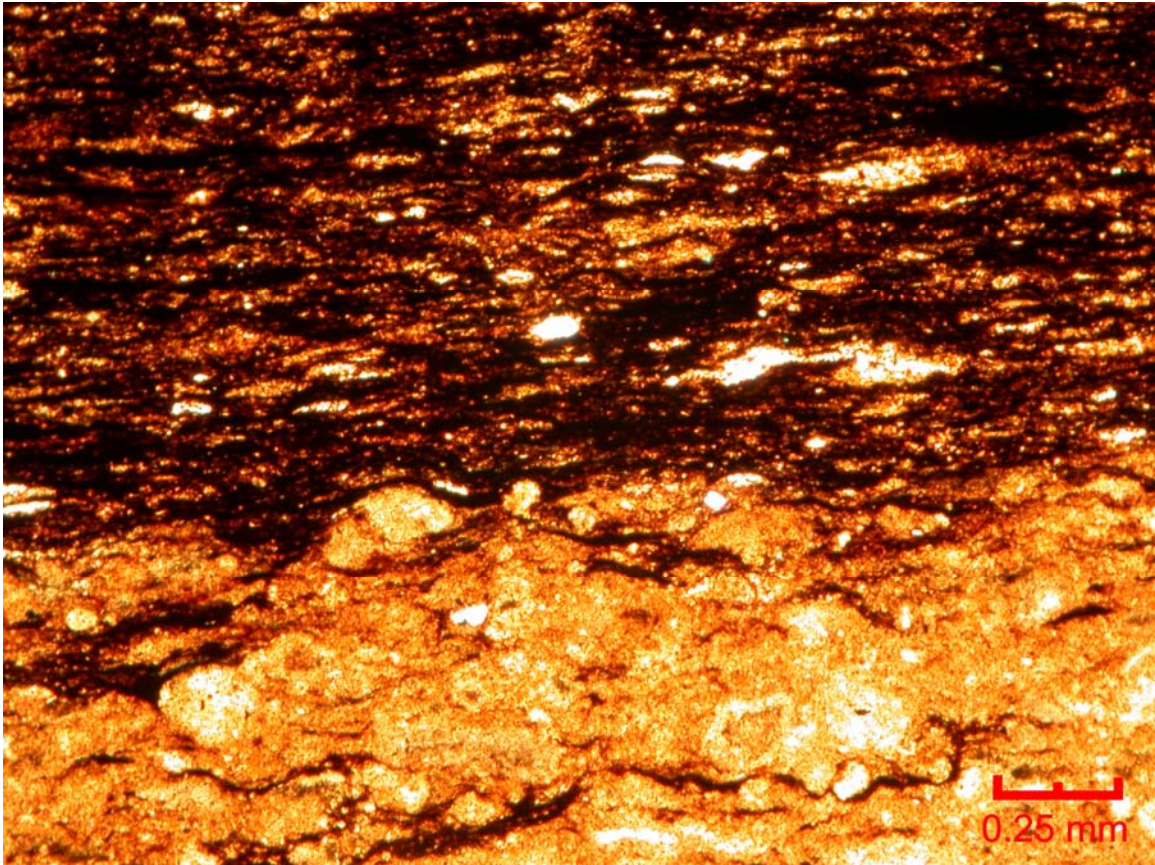
Figure AII.14 0.5 ft Little Delaware Creek Outcrop 4

This shale is characterized as a laminated brown to black shale. The unit contains well

developed apatite laminations composed predominantly of apatite. Glauconite is present

with the apatite laminations. Tasmanites cysts were noted in the thin sections. These

cysts are compacted and replaced with bitumen or quartz. Some silt size subangular

quartz grains were present in the thin section.
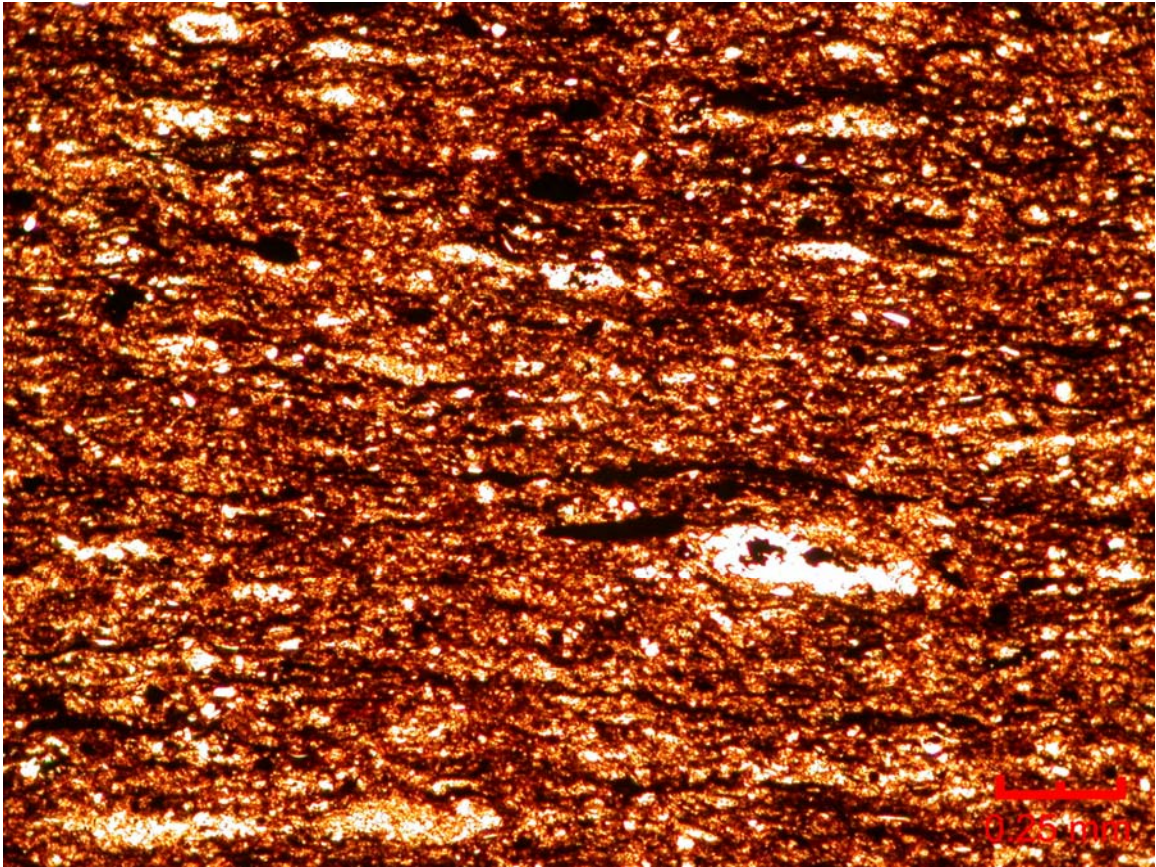
Figure AII.15 24.0 ft Pine Top Mountain Outcrop Section 1

This unit is composed of a non-laminated to weakly laminated brown shale. <u>Tasmanites</u>

cysts were common in the thin section. These cysts were mainly compacted and replaced

with bitumen and microquartz. Some cysts were replaced with pyrite and are non-

compacted to slightly compacted. A few possibly phosphatic shell fragments were noted

in the thin section. This thin section contains silt size subrounded to rounded quartz

grains. These grains are possibly radiolarians.

Figure AII.16 32.5 ft Pine Top Mountain Outcrop Section 2

This unit is characterized as a brown slightly laminated shale. The shale contains

abundant Tasmanites cysts. These cysts are mainly compacted and replaced with

microquartz. Some of the cysts are replaced by bitumen. Thin laminae of apatite cutting

across bedding planes is present in the shale and calcite is precipitated is some of the

shale fractures. The thin section also contained abundant angular to rounded silt size

quartz grains. These grains are possibly a result from ditrital silt deposition and

radiolarians.
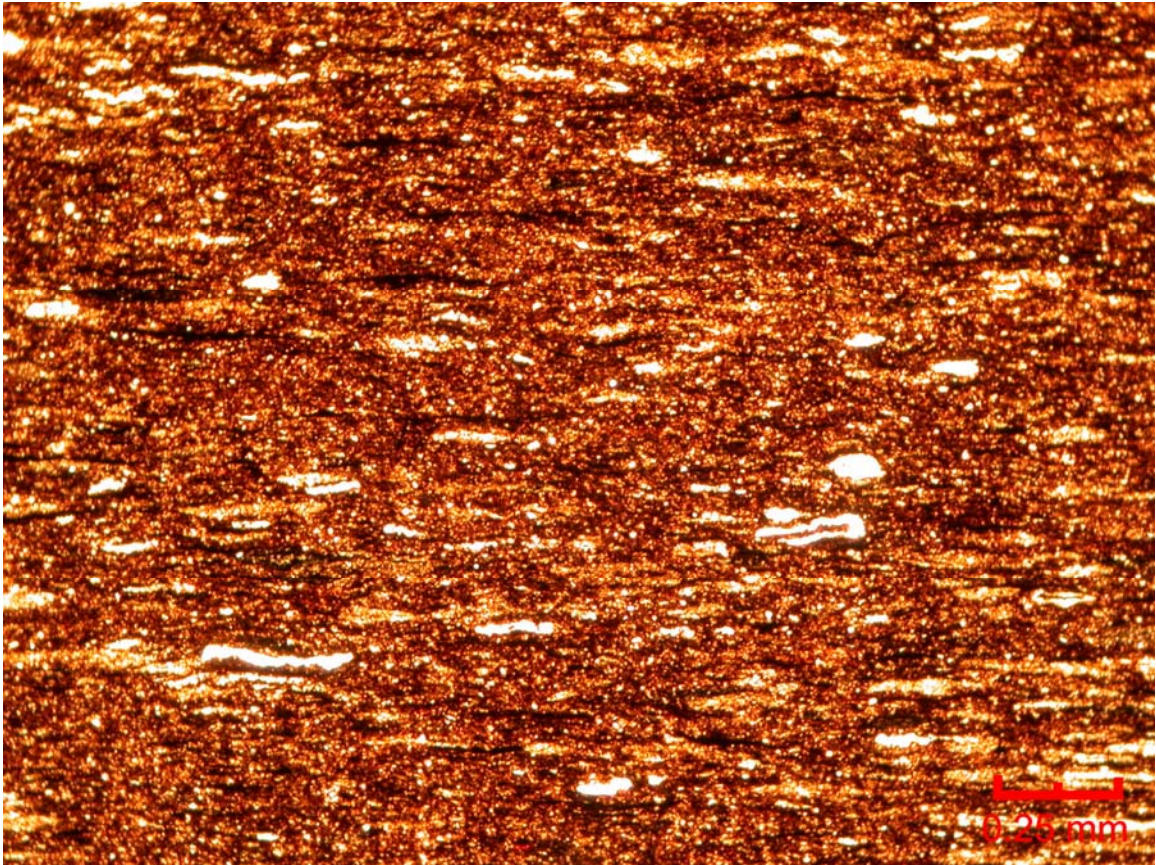
Figure AII.17 6.5 ft Pine Top Mountain Outcrop Section 4

This unit is characterized as a weakly laminated brown shale. The unit contains abundant

Tasmanites cysts. These cysts are commonly replaced with microquartz and bitumen and

are compacted. Some cysts are pyritized and are non-compacted. Pyrite was

interdispersed in the shale matrix. Rounded to subrounded silt size quartz was present in

the thin sections. This quartz possibly originates from radiolarians.
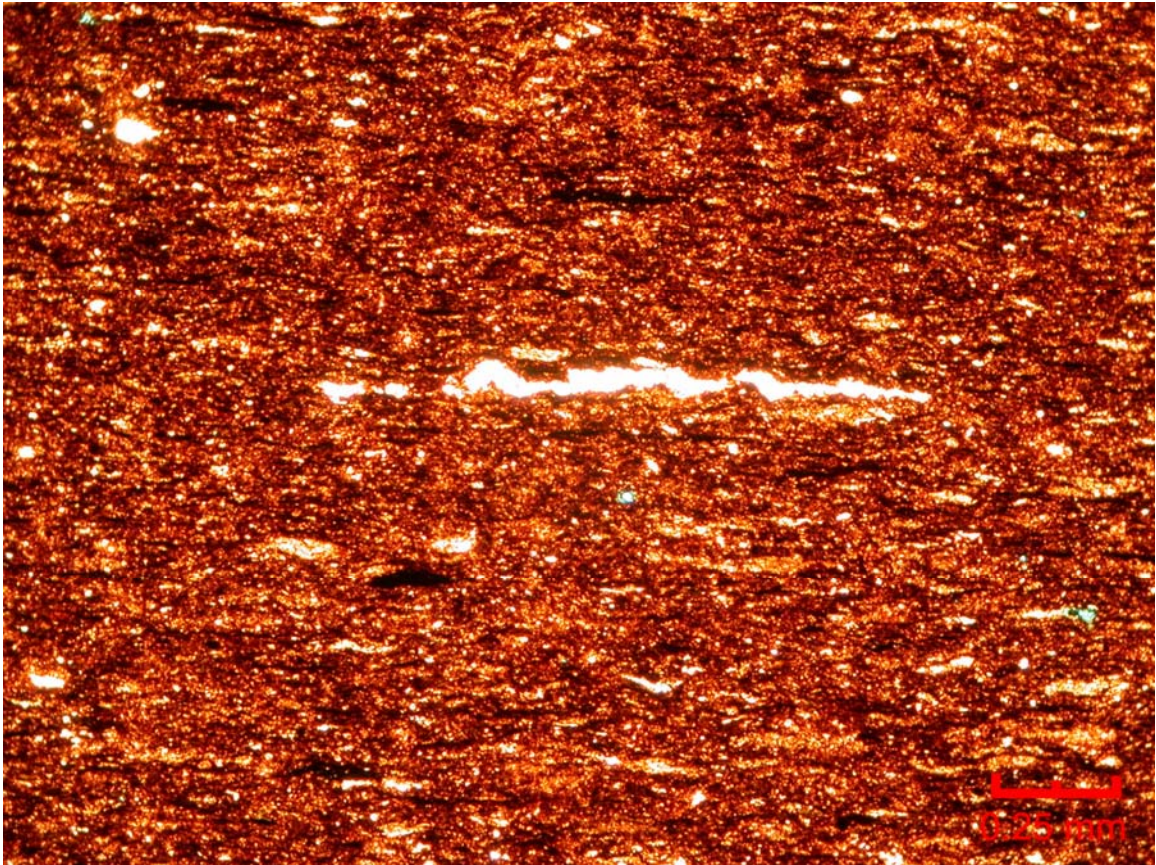
Figure AII.18 11.0 ft Pine Top Mountain Outcrop Section 5

This shale is characterized as a non-laminated to slightly laminated brown shale. The

shale contains compacted <u>Tasmanites</u> cysts. These cysts are replaced with microquartz

and bitumen. Some cysts are replaced by pyrite and are non-compacted to slightly

compacted. Small subrounded to rounded silt size quartz is present in the thin sections.

This quartz result possibly from radiolarians. Some more angular quartz is present that

may be detritial silt.
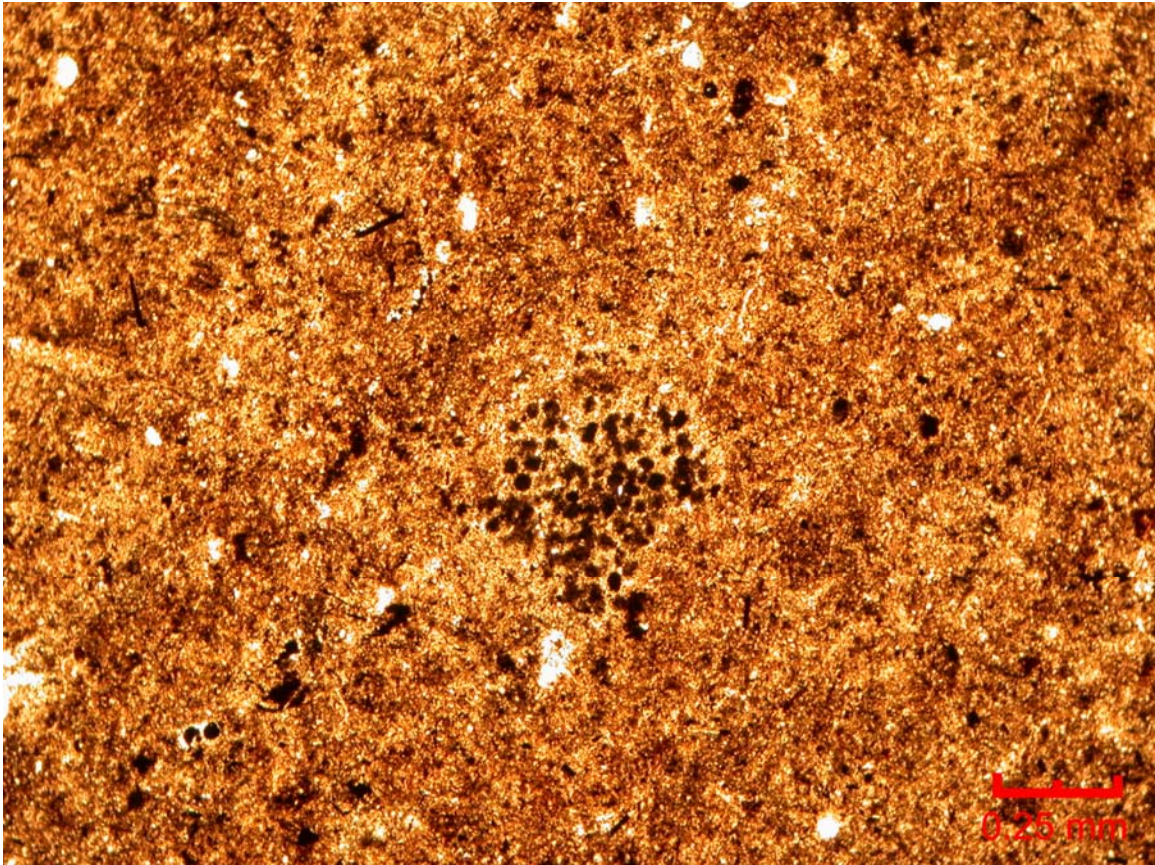
Figure AII.19 6.0 ft Pine Top Mountain Outcrop Section 7

This unit is composed of a tan to brown non-laminated shale. The shale contains

Tasmanites that are compacted and replaced with quartz. Pyrite blebs are common in the

matrix. These pyrite blebs appear in clusters or are separate from other pyrite. Round silt

size quartz grains are present within the matrix. This quartz is possibly derived from

radiolarians.
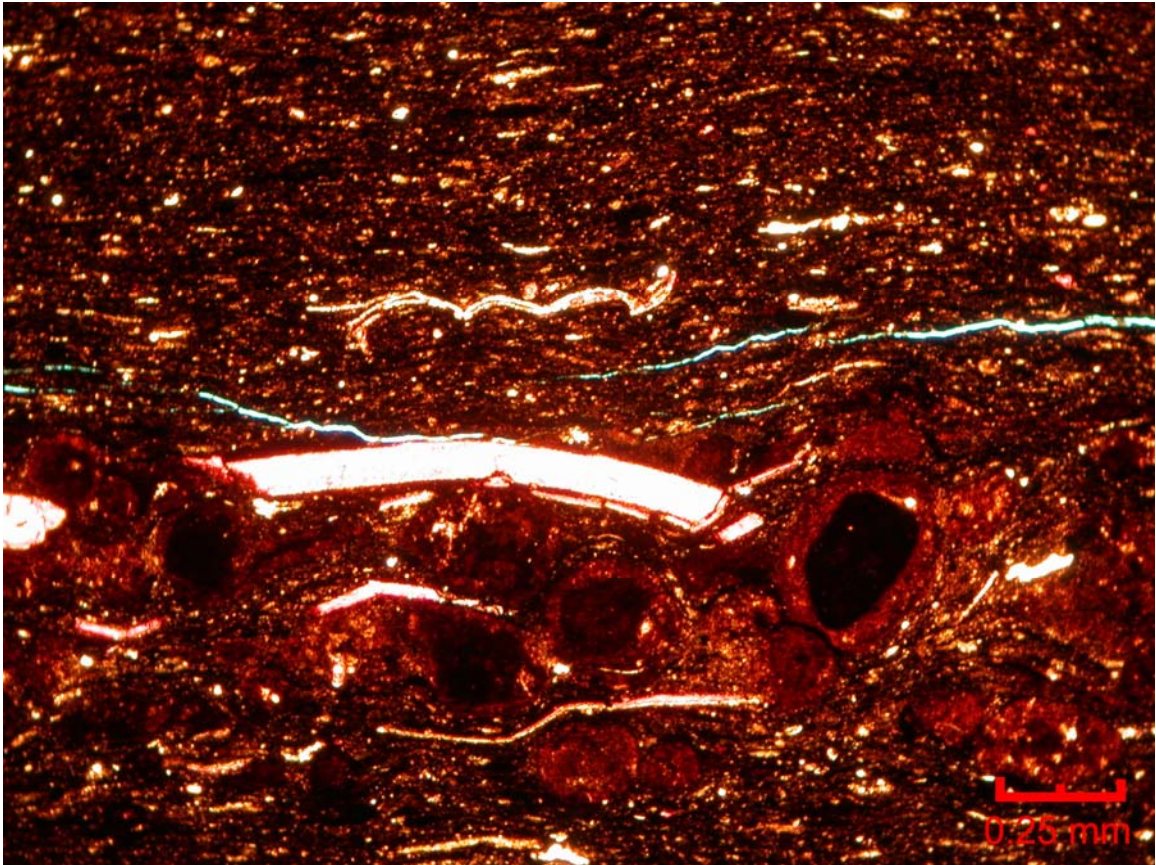
Figure AII.20 5881.5 ft Richardson 2-33

This thin section is characterized as a weakly laminated brown to black shale. The shale contains apatite nodules in weak laminations and large bivalve fragments. Large fossil fragments are predominantly whole with few abraided. Angular to rounded silt size quartz grains are present within the shale and <u>Tasmanites</u> cysts were also noted. The cysts are generally compacted and contain microquartz or bitumen. Some cysts possibly have phosphatic rims.
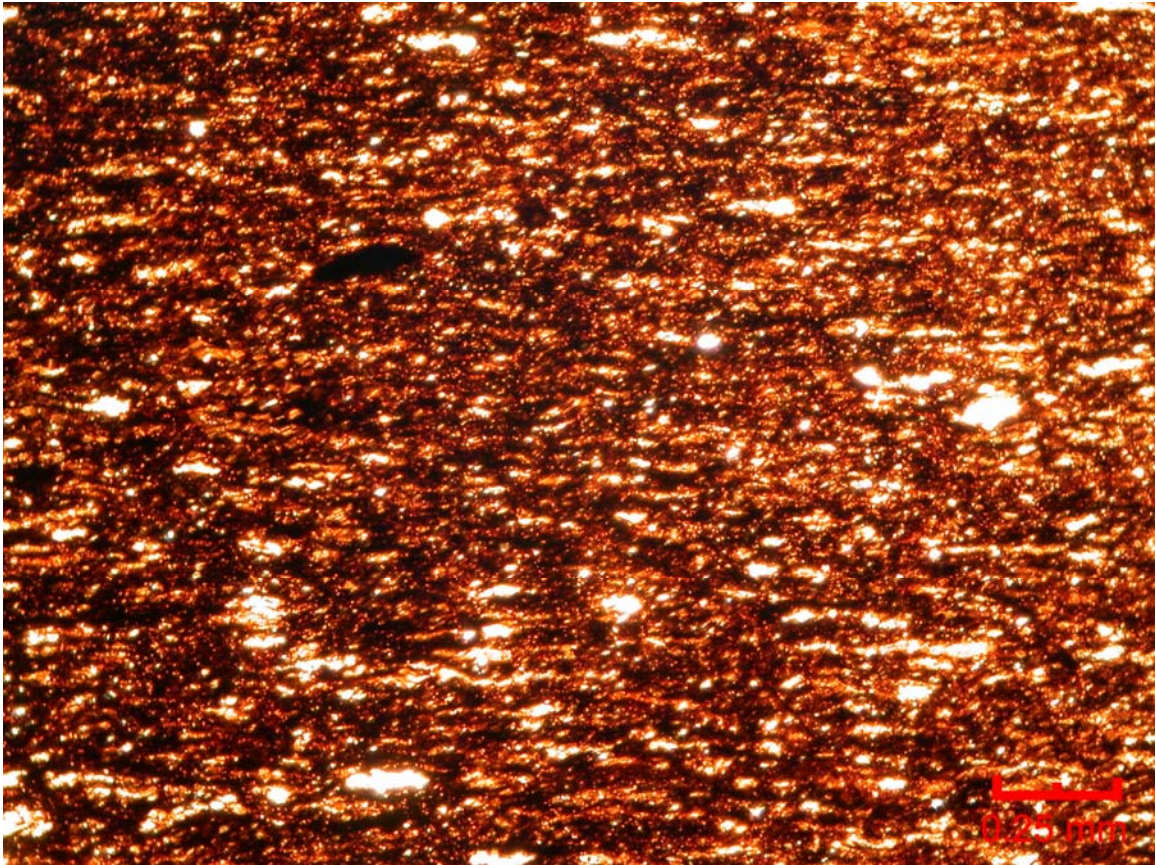
Figure AII.21 5908.0 ft Richardson 2-33

This unit is characterized as a slightly laminated brown shale. <u>Tasmanites</u> cysts are abundant within the shale matrix. These cysts are compacted and predominantly replaced by microquartz. Some cysts are replaced by bitumen. Angular silt size quartz is common in the thin section and a few apatite nodules are present. Some apatite nodules are slightly compacted.
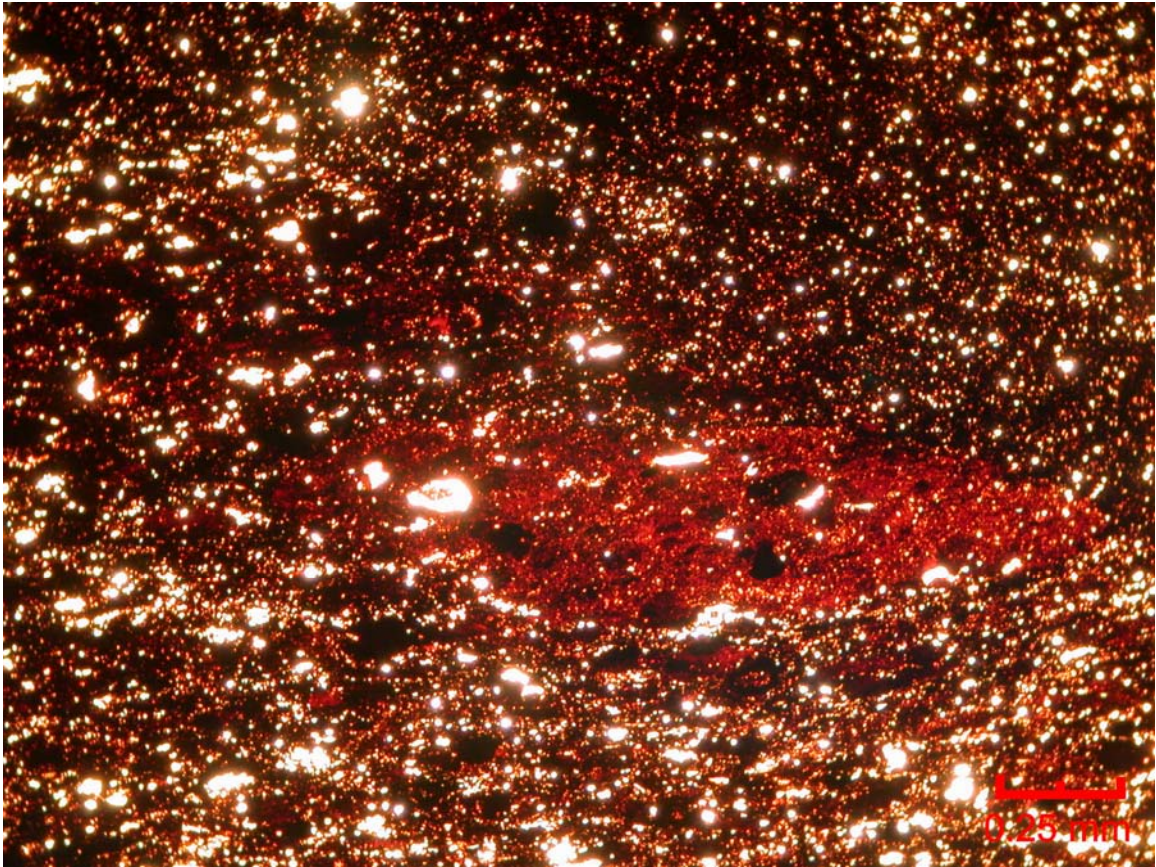
Figure AII.22 5927.0 ft Richardson 2-33

This unit is characterized as a slightly laminated brown shale. <u>Tasmanites</u> cysts are abundant within the shale matrix. These cysts are compacted and predominantly replaced by microquartz. Some cysts are replaced by bitumen. Angular silt size quartz is abundant in the thin section and a few apatite nodules are present. The apatite nodules appear to be iron stained. A few small fragments of mica were possibly present in the thin section.
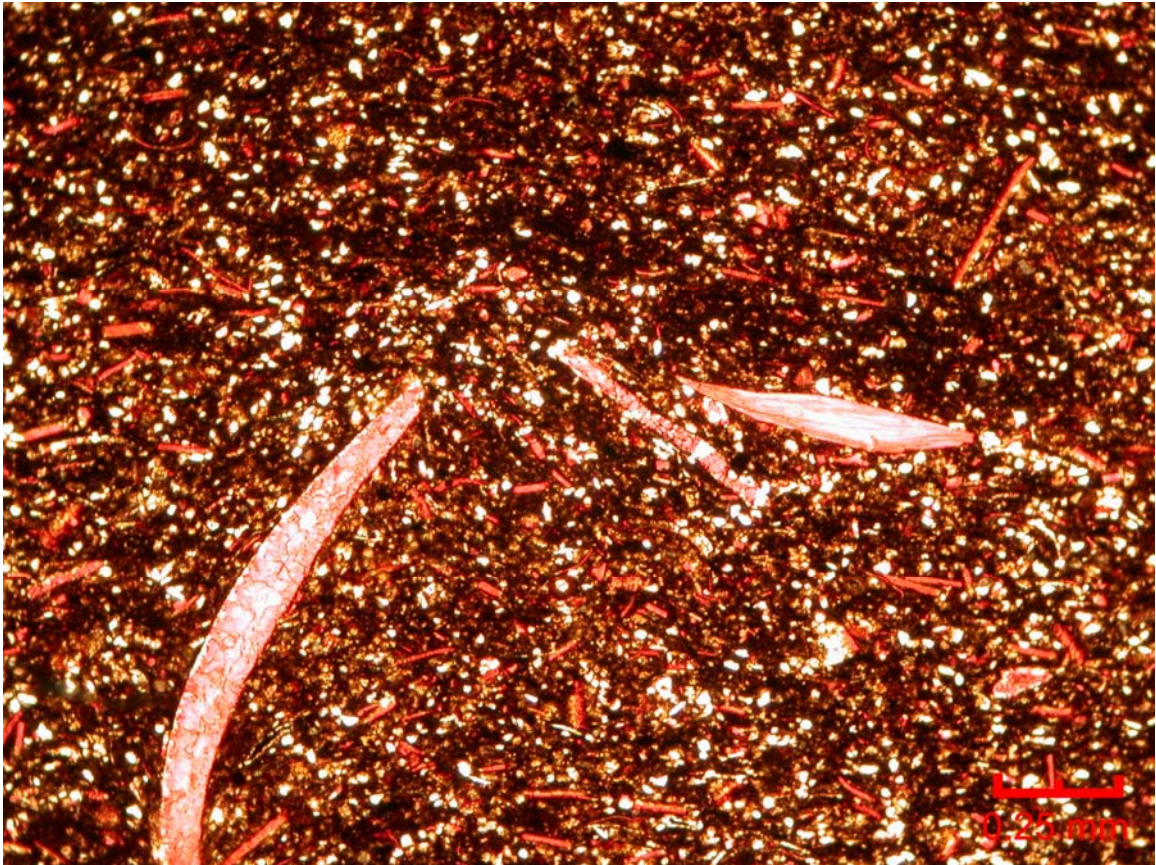
Figure AII.23 5932.0 ft Richardson 2-33

This unit is characterized as a fossiliferous non-laminated shale. The shale contains

abundant bivalve and brachiopod fragments. Many of the fragments are small and

abraided. There are also large whole to slightly abraided fragments in the thin section.

The thin section also contains abundant quartz silt. This silt is angular and does not

appear in identifiable laminations. A shale matrix supports the silt and fossil fragments.

There are a few identifiable Tasmanites cysts present within the thin section. These cysts

are compacted and replaced with microquartz and some bitumen.
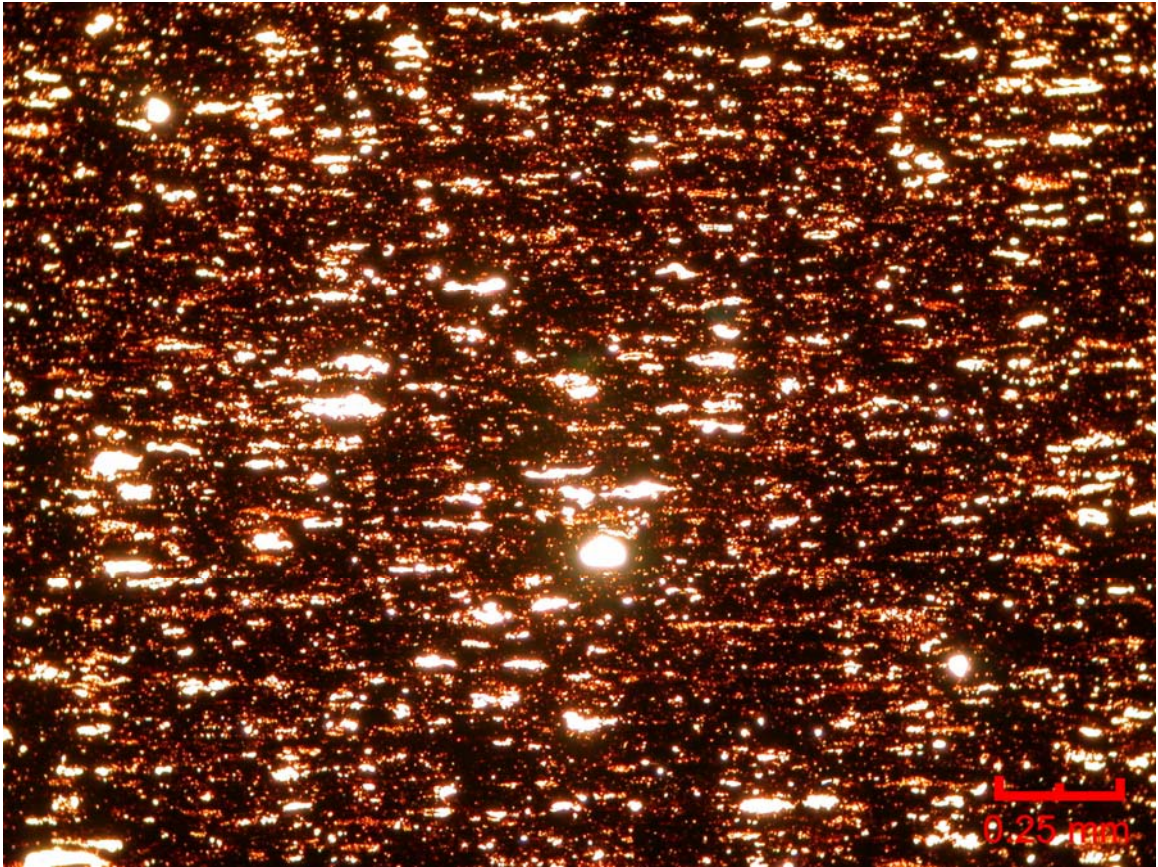
Figure AII.24 5951.0 ft Richardson 2-33

This unit is characterized as a black to brown slightly laminated shale. The shale contains abundant <u>Tasmanites</u> cysts. Most of the cysts are compacted and replaced with microquartz. Some cysts are replaced with bitumen or pyrite. The thin section contains abundant silt size angular quartz and a few carbonated fragments.
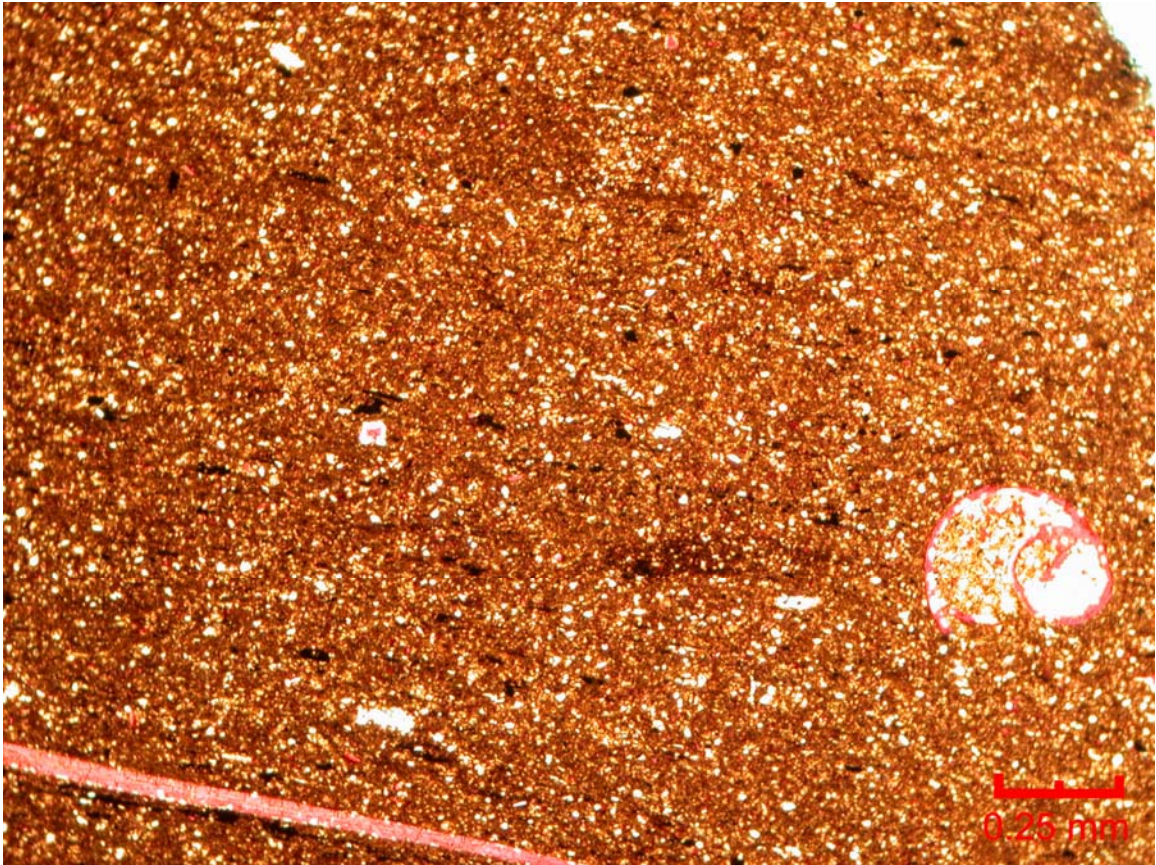
Figure AII.25 5996.0 ft Richardson 2-33

This unit is composed of a non-laminated brown shale. The shale contains large

carbonate fossils. These fossils are generally whole and are of bivalves and gastropods.

The unit also contain abundant small calcite grains. These grains are the same size as the

abundant silt size quartz grains present. A few Tasmanites cysts were present in the thin

section. These cysts are replaced with microquartz and bitumen.
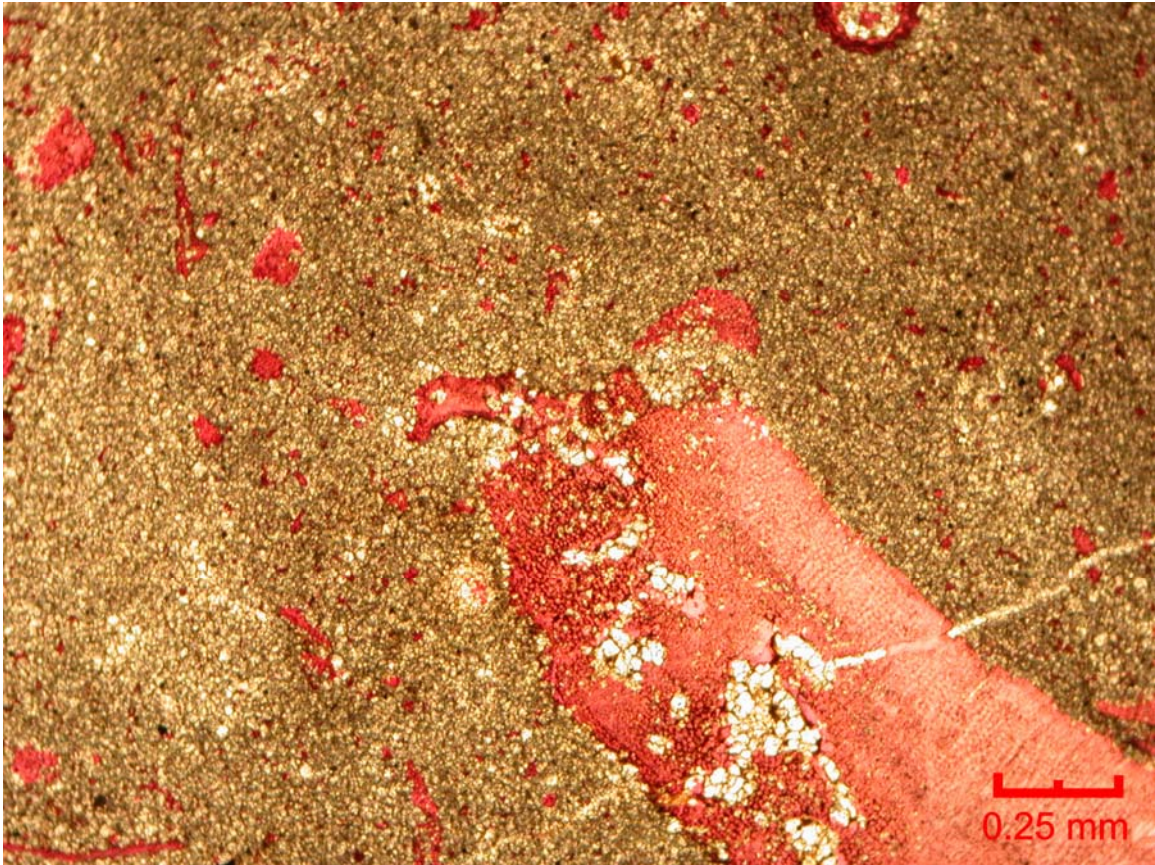
Figure AII.26 6142.0 ft. Richardson 2-33

This unit is characterized as a shaley calcareous dolomite. The section contains abundant

dolomite rhombs mixed with carbonate fossils fragments and micrite. Some of the large

carbonate fossils are partially replaced with dolomite. These fossils are of bivalves,

brachiopods, and echinoderms. There are some dolomitized ghost structures present

within the thin section.

Figure AII.27 6208.0 ft Richardson 2-33

This unit is composed of abundant silt size angular quartz grains in a shale matrix. The

unit is very weakly laminated with some clay rich layers forming irregular discontinuous

laminations. Silt size carbonate grains are also present within the unit. No dolomite was

visible in the thin section. Some fractures were filled with calcite and multiple pyrite

blebs were present.
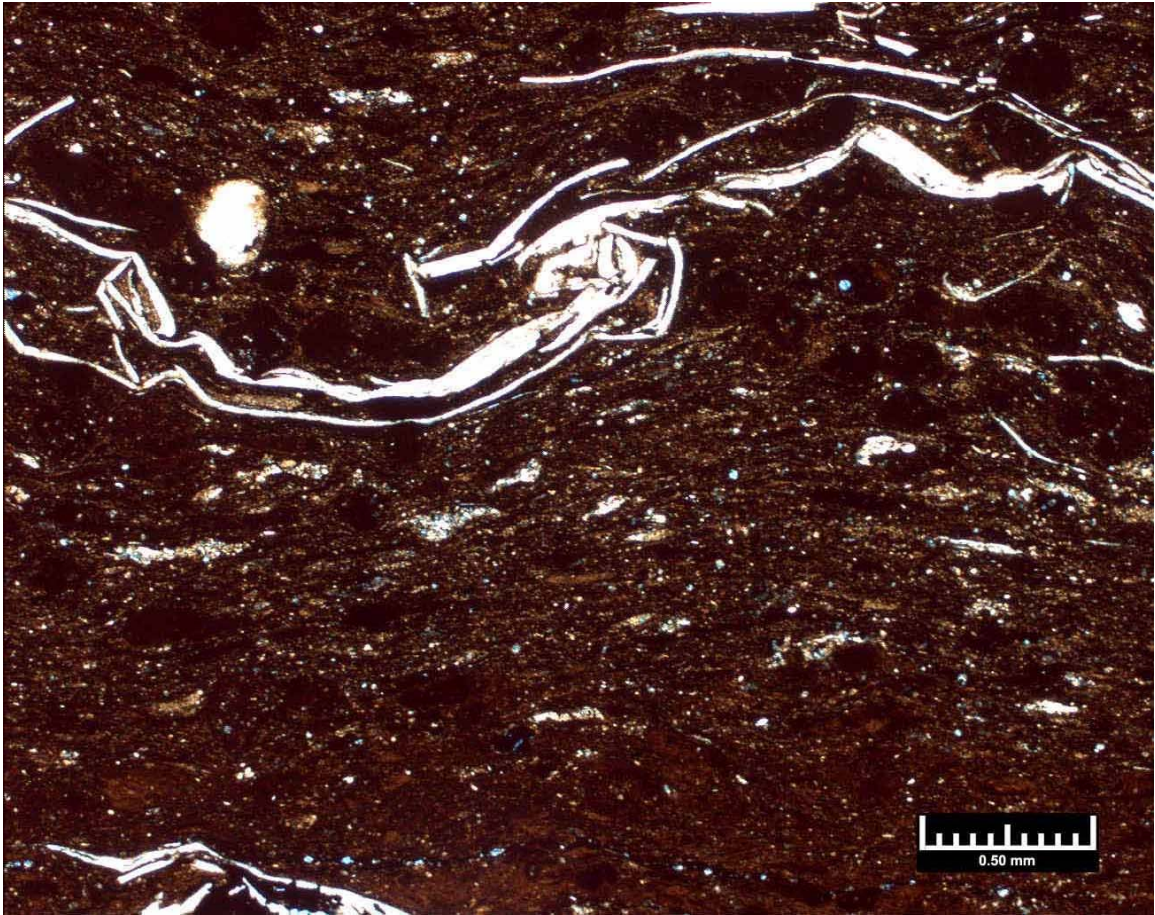
Figure AII.28 6778.0 Rogers Trust 1-24

This shale is characterized as a slightly laminated to laminated brown to black shale.

There are abundant apatite nodules within the thin section. These nodules are grouped

together in weakly developed laminations. Bivalve shell fragments are common within

the thin section along with silt size angular quartz. Tasmanites cysts are present in the

thin section. Most of the cysts are compacted and replaced with microquartz. A single

large non-compacted cyst replaced with quartz is present.
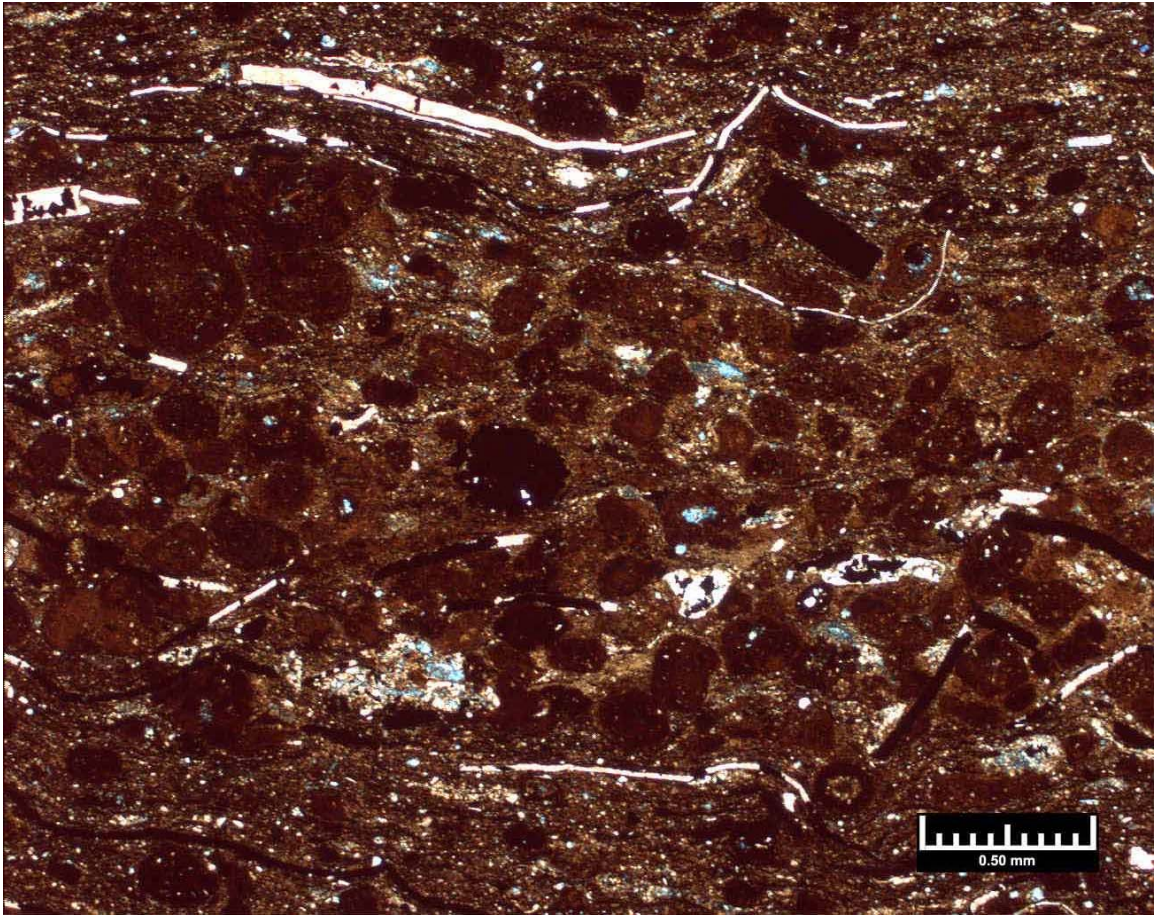
Figure AII.29 6786.0 Rogers Trust 1-24

This shale is characterized as a laminated brown shale. Large scale laminae of apatite nodules and clay grains are present in the thin section. Apatite nodules appear to be possibly iron stained. This unit also contains broken bivalves, and silt size angular quartz. A large rectangular woody fragment is present in the upper right corner of the above thin section. Tasmanites cysts are common in this thin section. Most of the cysts are compacted and replaced with microquartz. A few cyst were replaced with bitumen. Pyrite has replaced some parts of the fossil fragments and cysts in the thin section.
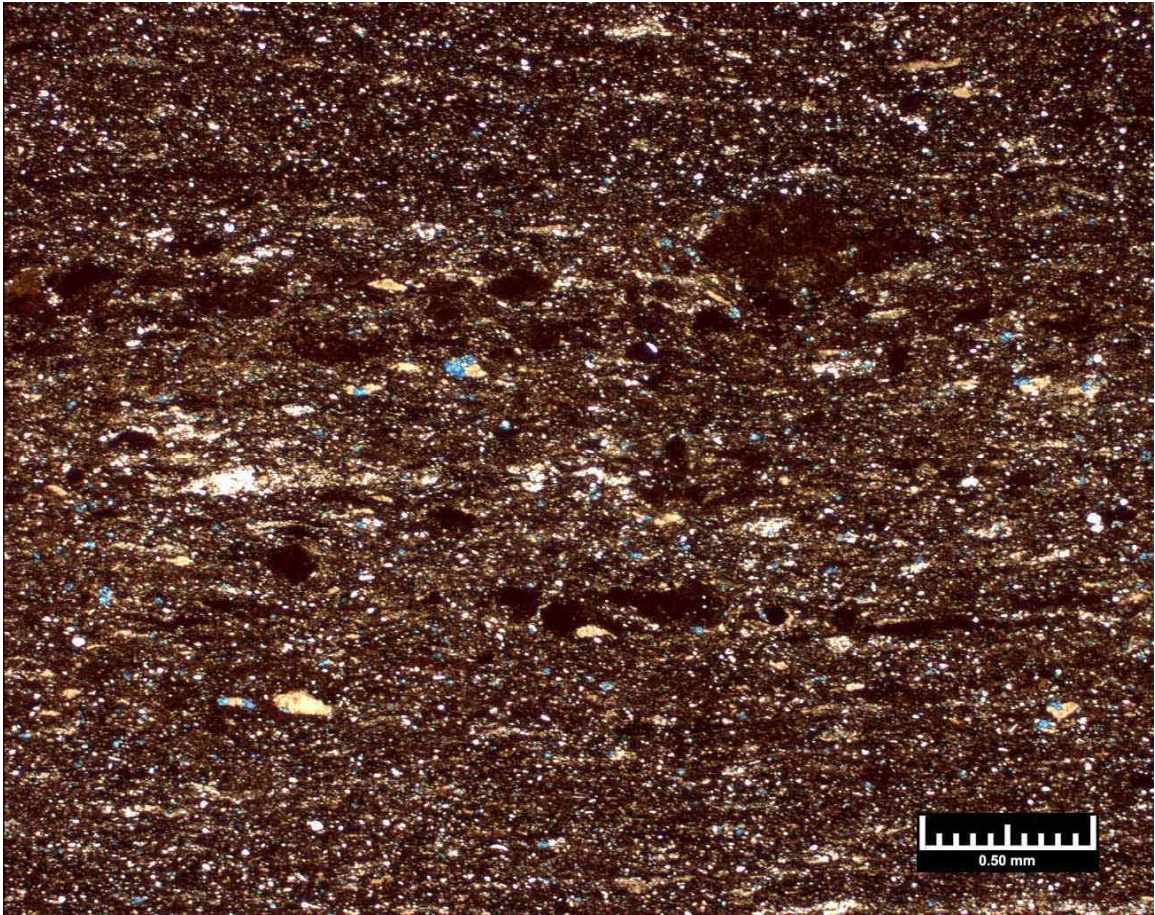
Figure AII.30 6793.0 Rogers Trust 1-24

This unit is characterized as a non-laminated to slightly laminated brown shale. The unit

contains abundant silt size angular quartz. This quartz appears to be spread evenly

throughout the thin section. Some round apatite nodules are in a weak laminae in the thin

section. These nodules are small and poorly developed. A few Tasmanites cysts are

present in the thin section. These cysts are compacted and replaced with microquartz.
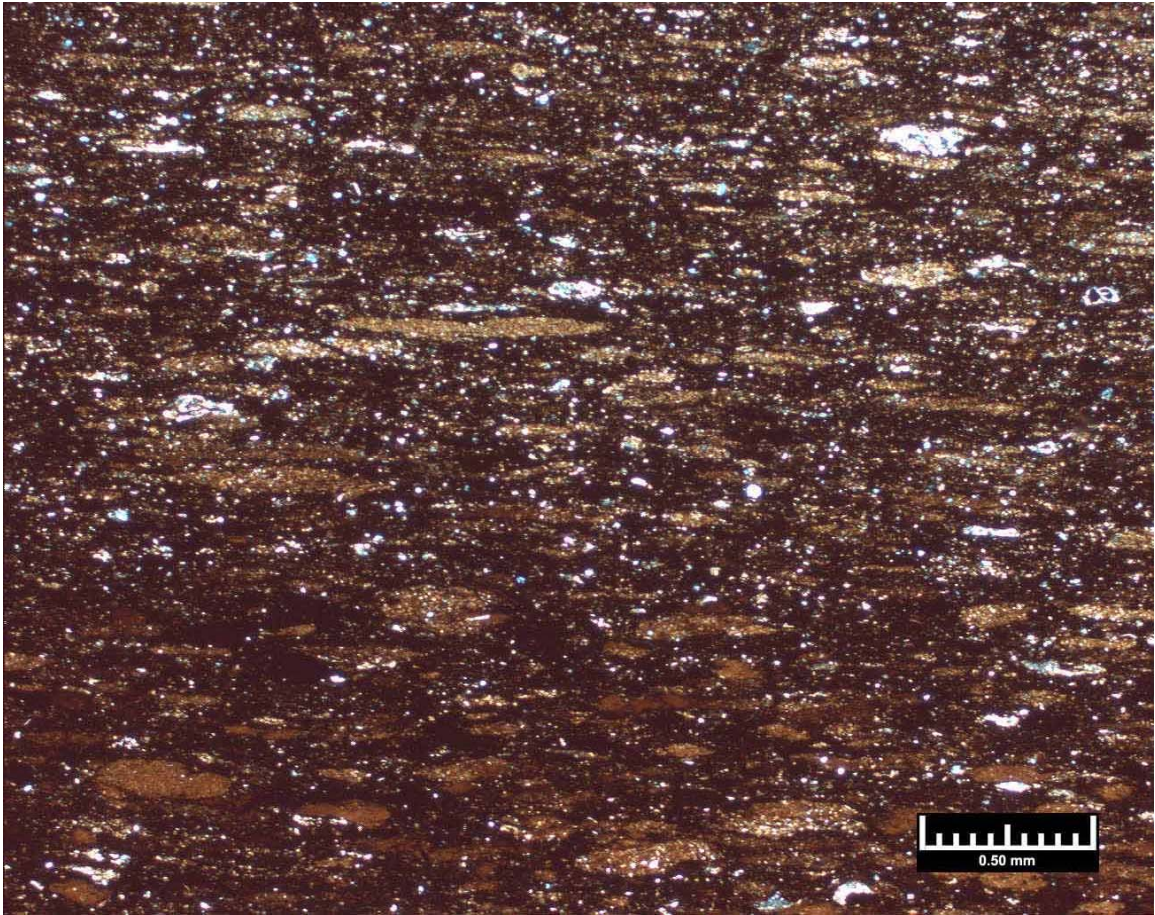
Figure AII.31 6803.0 Rogers Trust 1-24

This shale is characterized as a laminated to slightly laminated brown shale. Apatite nodules are present in the thin section, but do not form laminations. These nodules are compacted and contain a possible component of clay. Tasmanites cysts are common in this thin section. Most of the cysts are compacted and replaced with microquartz. A few cysts were replaced with bitumen. Small angular silt size quartz is common in the thin section.
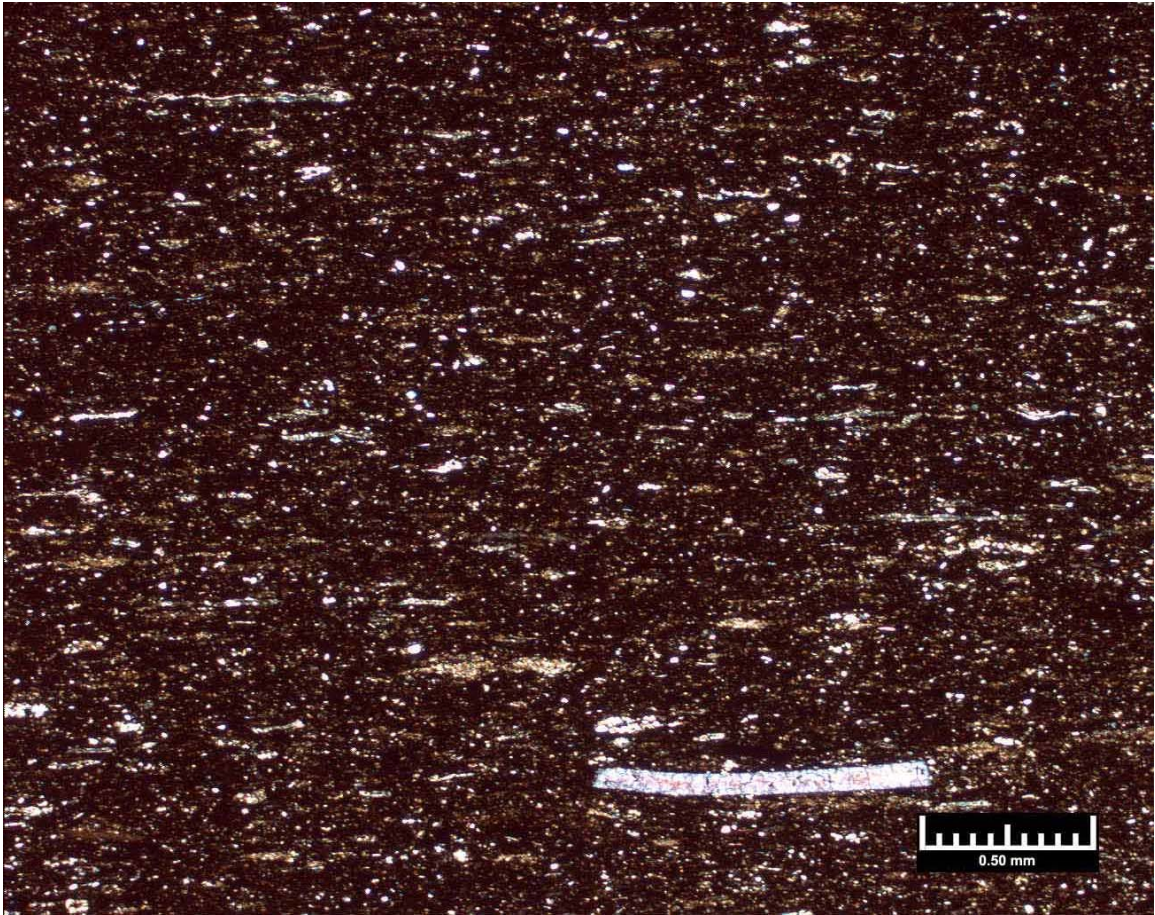
Figure AII.32 6826.0 Rogers Trust 1-24

This shale is characterized as a slightly laminated brown to black shale. There are no apatite nodules within the thin section. Bivalve shell fragments are sparse within the thin section. Silt size angular quartz is common throughout the thin section. As single bivalve fragment is present the picture above. This fragment appears to be recrystallized calcite, but it is difficult to tell. Tasmanites cysts are common in the thin section. Most of the cysts are compacted and replaced with microquartz. Some cysts are possibly replaced with bitumen.
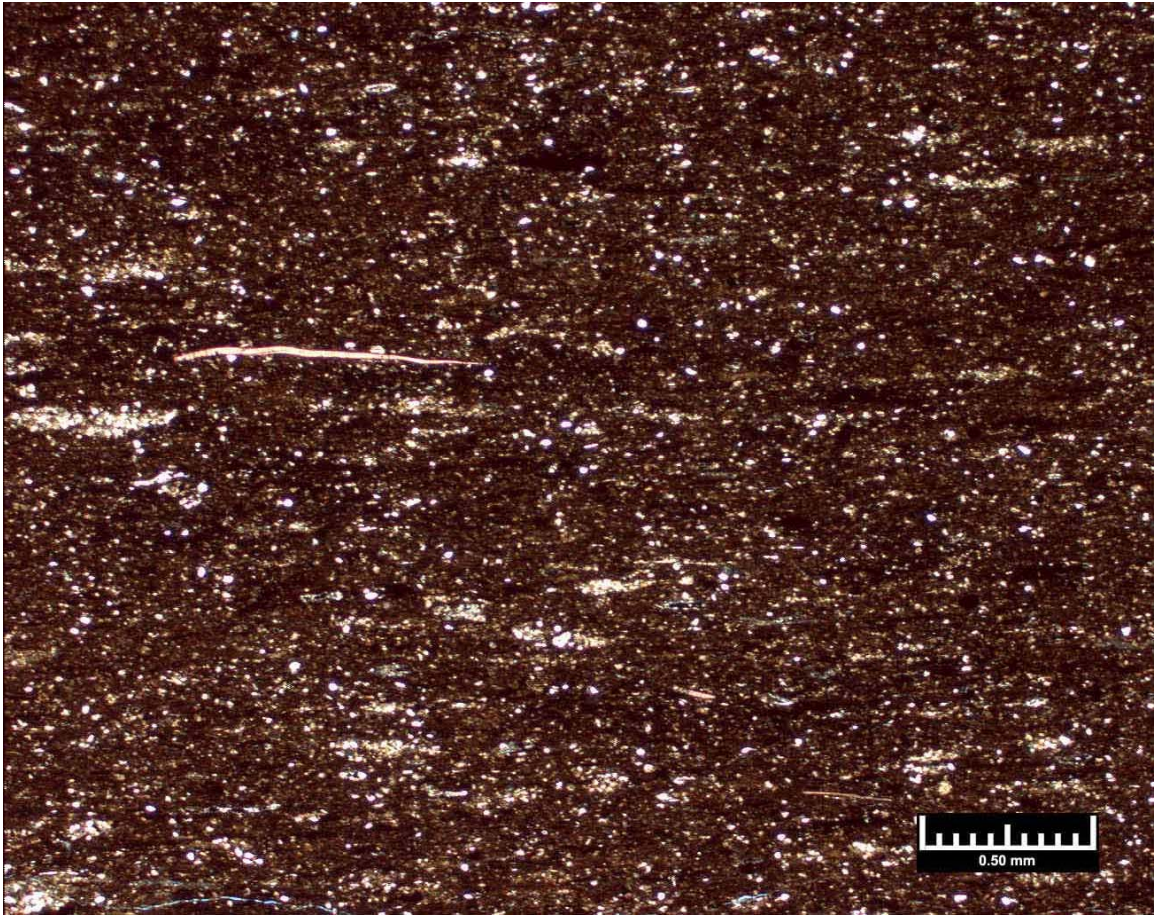
Figure AII.33 6846.0 Rogers Trust 1-24

This shale is characterized as a slightly laminated brown to black shale. Bivalve shell

fragments are sparse within the thin section. Silt size angular to rounded quartz is

common throughout the thin section. Tasmanites cysts are present in the thin section.

Most of the cysts are compacted and replaced with microquartz. Some cysts are possibly

replaced with bitumen. Rare bivalve fragment are present; along with some possible silt

filled burrows.
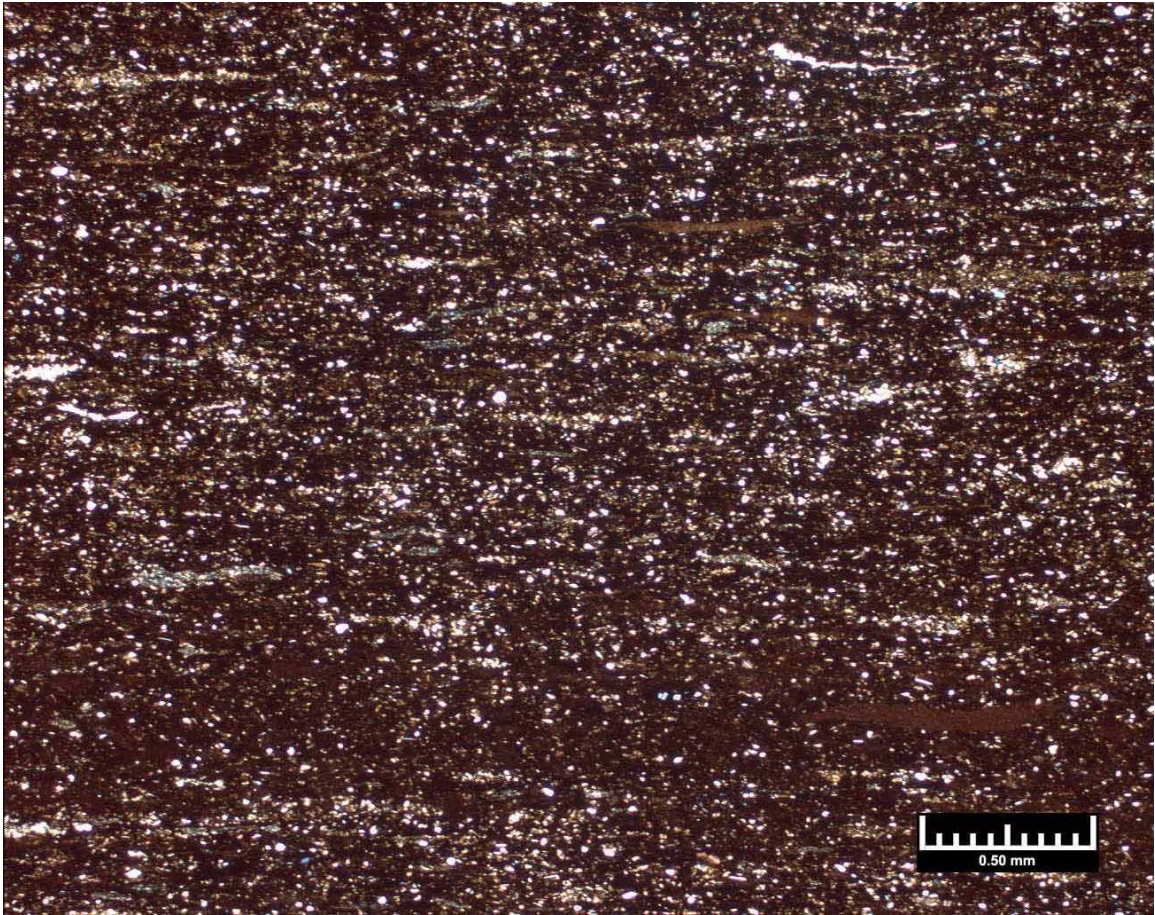
Figure AII.34 6910.0 Rogers Trust 1-24

This shale is characterized as a slightly laminated to non-laminated brown to black shale.

Silt size angular to rounded quartz is common throughout the thin section. Tasmanites

cysts are present in the thin section. Most of the cysts are compacted and replaced with
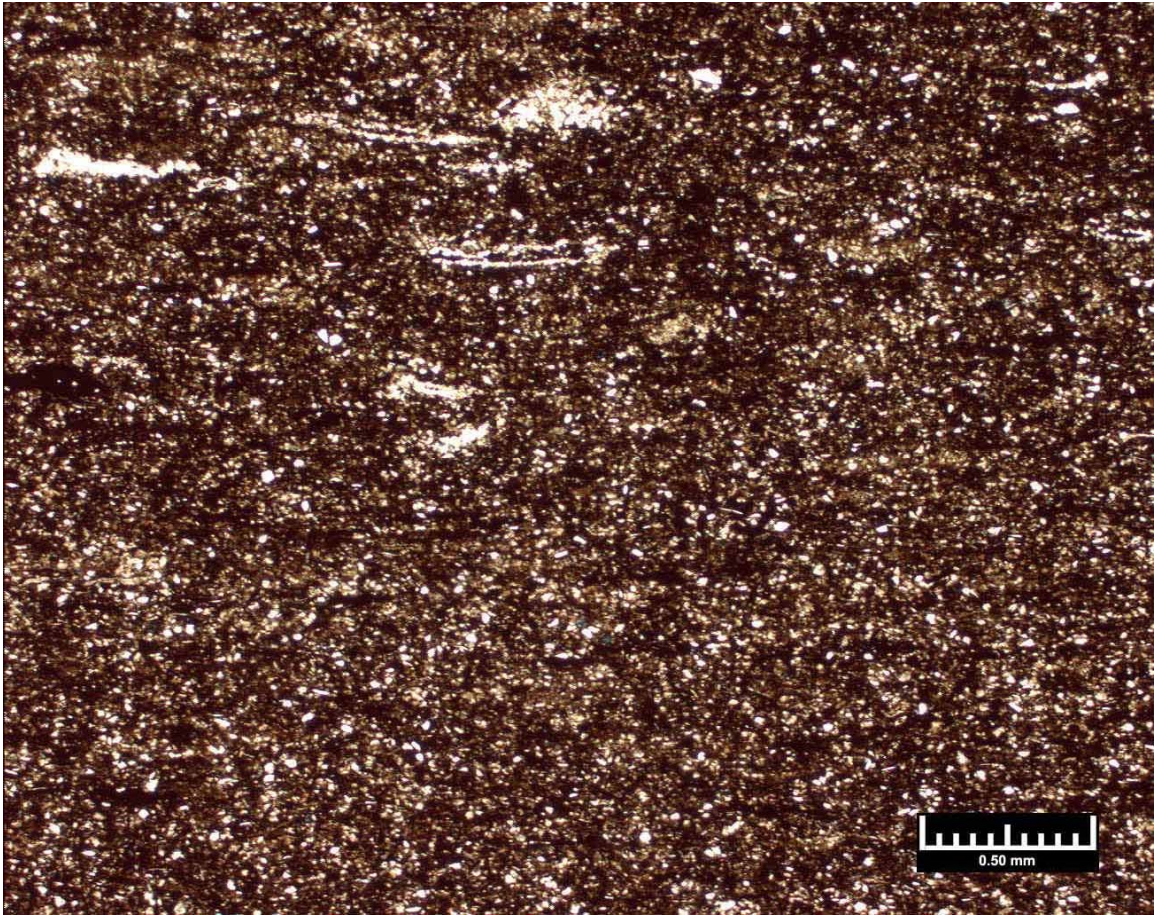
microquartz.

Figure AII.35 7001.0 Rogers Trust 1-24

This shale is characterized as a non-laminated brown shale. Tasmanites cysts are present

in the thin section. Most of the cysts are compacted and replaced with microquartz.

Some cysts have pyrite and or bitumen precipitated in the center. This shale contains

abundant angular to subrounded quartz grains. These grains are scattered evenly

throughout the thin section.
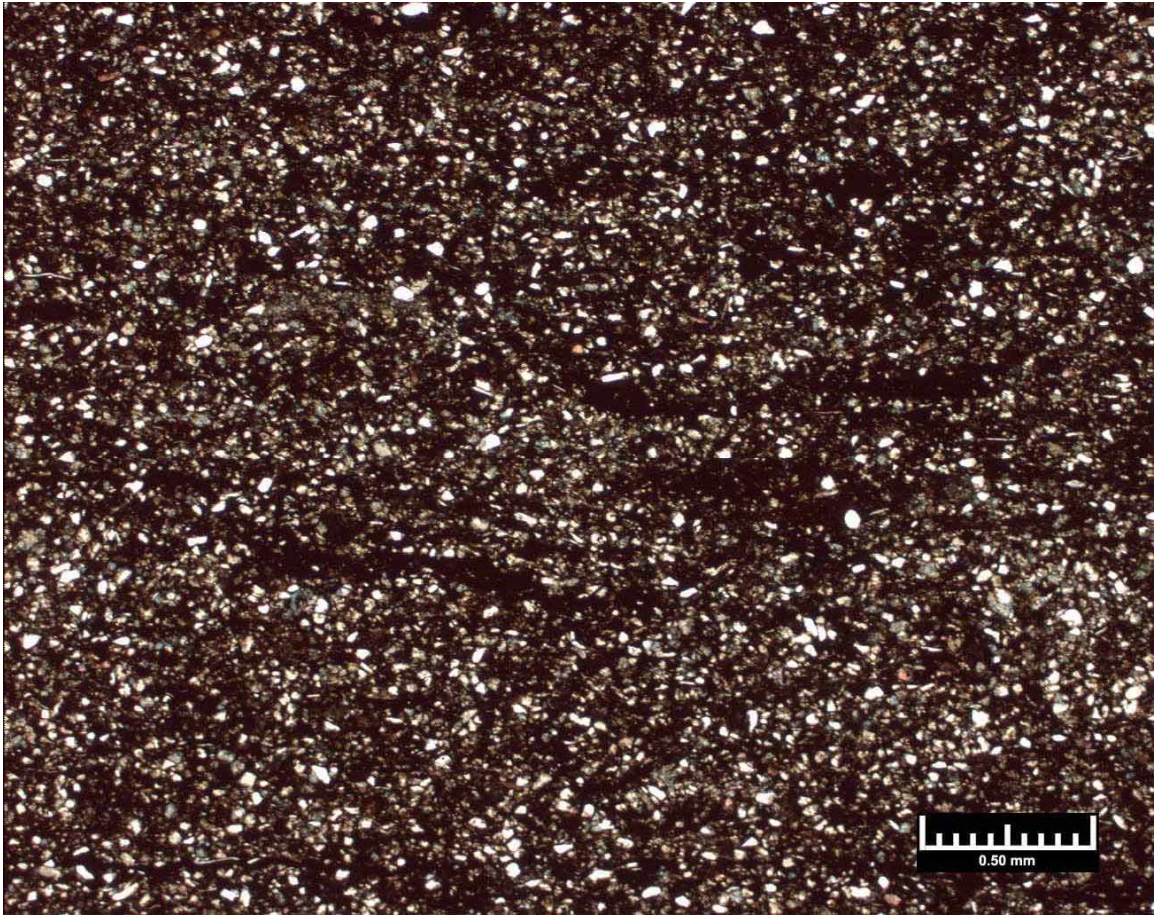
Figure AII.36 7042.0 Rogers Trust 1-24

This shale is characterized as a non-laminated brown to black shale. Tasmanites cysts are

rare in the thin section. Most of the cysts are compacted and replaced with bitumen and

microcquartz. This shale contains abundant angular to subrounded quartz grains. These

grains are scattered evenly throughout the thin section. A few silt size carbonate grains

are also present in the section.
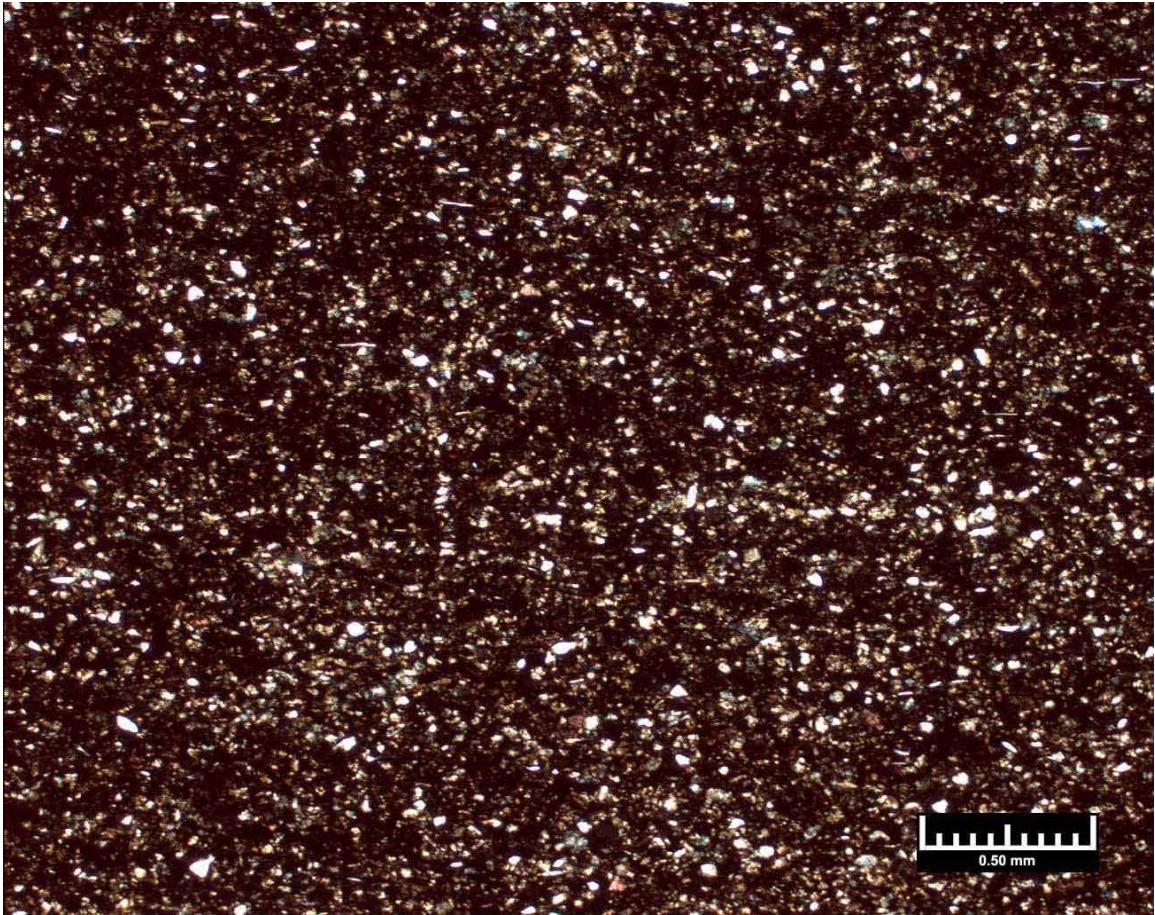
Figure AII.37 7059.0 Rogers Trust 1-24

This shale is characterized as a non-laminated brown to black shale. Tasmanites cysts are rare to absent in the thin section. This shale contains abundant angular to subrounded quartz grains. These grains are scattered evenly throughout the thin section. Silt size carbonate grains are also present in the section. Pyrite is precipitated with some carbonate grains.

258
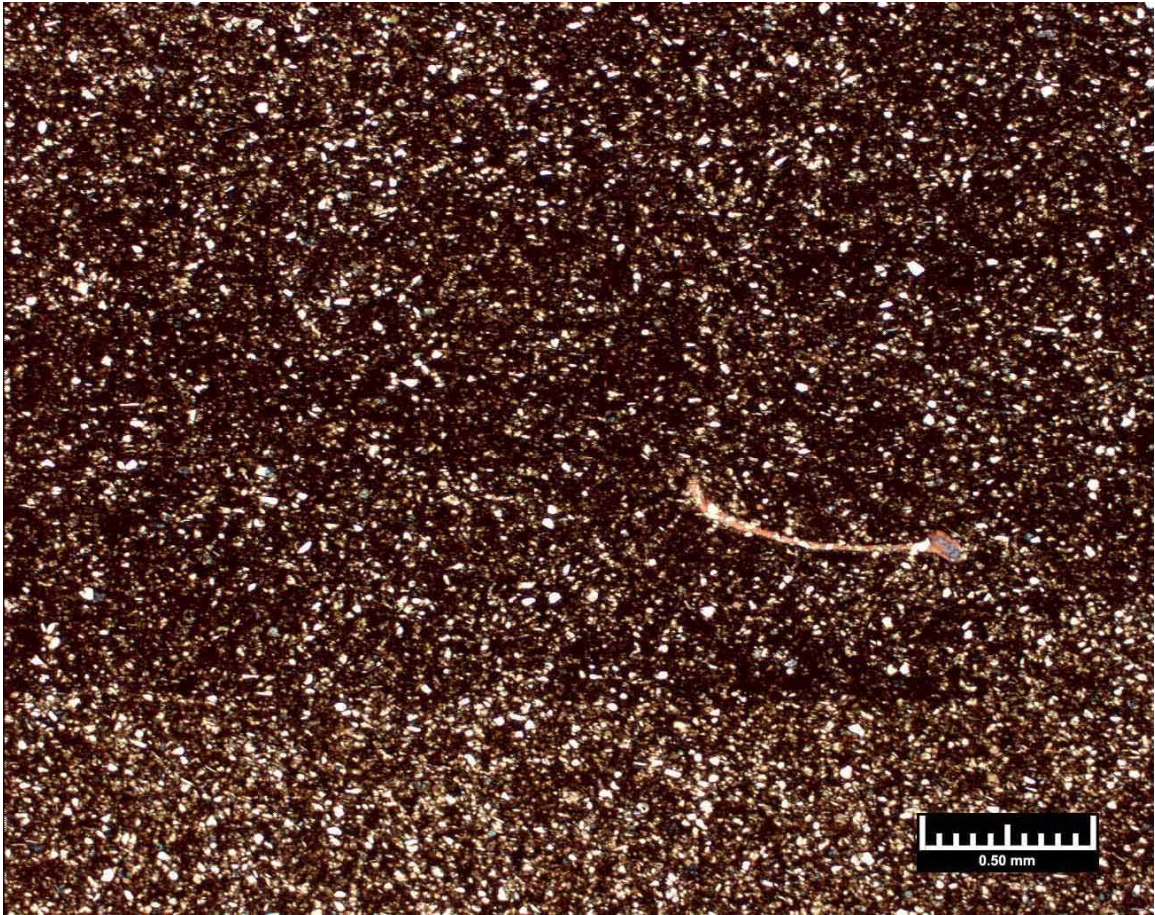
Figure AII.38 7103.0 Rogers Trust 1-24

This thin section is characterized as a slightly laminated brown shale. The shale has

weak laminations created by an increase in grains and a decrease in shale matrix. These

grains consist mainly of silt size angular quartz. Silt size carbonate grains are also

present in the section. A few bivalve shells were noted in the shale matrix.

VITA

Patrick J. Kamann

Candidate for the Degree of

Master of Science

Thesis: SURFACE-TO-SUBSURFACE CORRELATION AND
LITHOSTRATIGRAPHIC FRAMEWORK OF THE CANEY SHALE
(INCLUDING THE "MAYES" FORMATION) IN ATOKA, COAL, HUGHES,
JOHNSTON, PITTSBURG, AND PONTOTOC COUNTIES, OKLAHOMA

Major Field: Geology

Biographical:

Education: Graduated from Cardinal Stritch High School, Oregon, Ohio in May
1998; received a Bachelor of Science degree in Environmental Safety and
Occupational Health Management with a pre-Engineering Emphasis from
the University of Findlay, Findlay, Ohio in December 2001; received a
Master of Science degree in Geology from Wright State University,
Dayton, Ohio in June 2004; completed the requirements for the Master of
Science degree with a major in Geology at Oklahoma State University in
May, 2006

Experience: Employed by Wright State University, Department of Geological
Sciences, as a research assistant; employed by Oklahoma State University,
School of Geology, as a teaching and research assistant; currently
employed as a geologist at Devon Energy.

Professional Memberships: American Association of Petroleum Geologists,
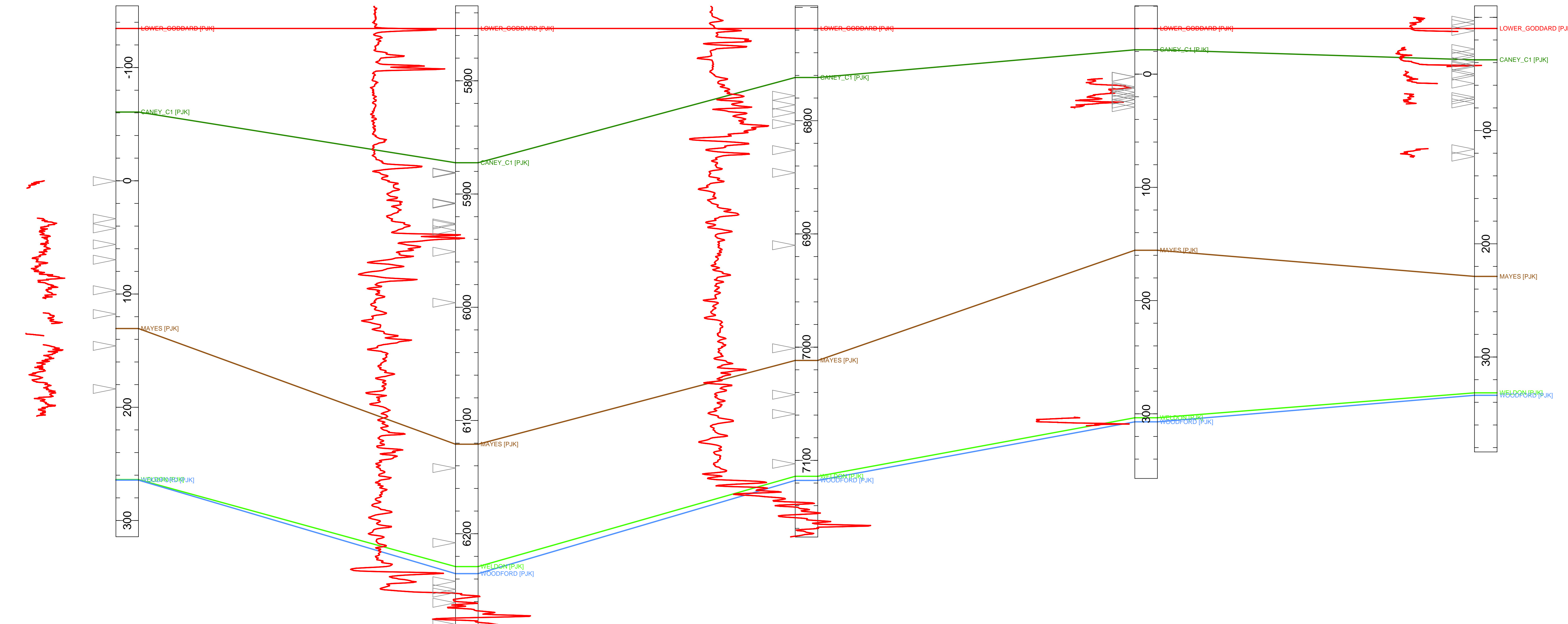Society for Sedimentary Geology

Cross Section of Outcrop Gamma-Ray Scans to the Subsurface

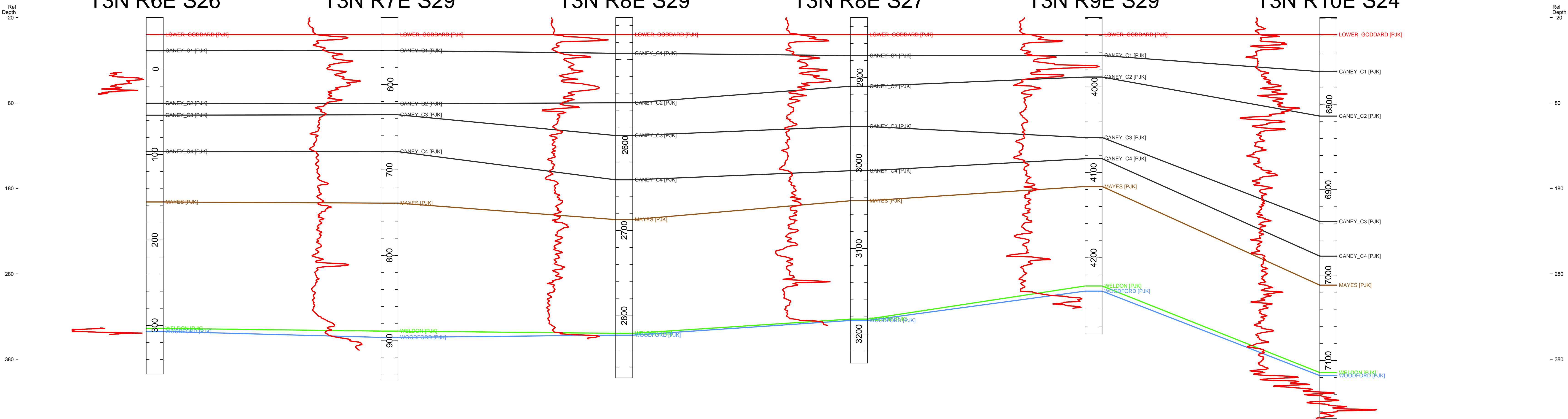Cross Section from the Lawrence Uplift to the Rogers Trust 1-24 Well

Plate 2

Kamann (2006) Thesis

Horizontal Scale = 9553.0
Vertical Scale = 100.0
Vertical Exaggeration = 95.5x

LOG CURVES

GR (GAPI) NATURAL GAMMA

TOPS AND MARKERS

LOWER_GODDARD PJK
CANEY_C1 PJK
CANEY_C2 PJK
CANEY_C3 PJK
CANEY_C4 PJK
MAYES PJK
WELDON PJK
WOODFORD PJK

February 18,2006 4:34 PM

HS=9553

PETRA 2/18/2006 4:34:31 PM (Lawrence Uplift to Rogers Trust CSP)